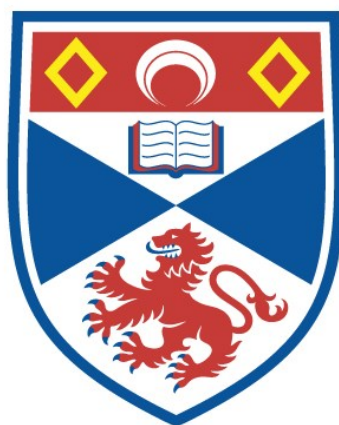


**Exploration of the pharmacodynamic profile of Acelarin,
a novel ProTide drug, in an *in vitro* model of ovarian
cancer**

Jennifer Bré

A thesis submitted for the degree of PhD
at the
University of St Andrews



2019

Full metadata for this item is available in
St Andrews Research Repository
at:

<https://research-repository.st-andrews.ac.uk/>

Identifier to use to cite or link to this thesis:

DOI: <https://doi.org/10.17630/10023-18773>

This item is protected by original copyright

Candidate's declaration

I, Jennifer Bré, do hereby certify that this thesis, submitted for the degree of PhD, which is approximately 39,480 words in length, has been written by me, and that it is the record of work carried out by me, or principally by myself in collaboration with others as acknowledged, and that it has not been submitted in any previous application for any degree.

I was admitted as a research student at the University of St Andrews in January 2016.

I received funding from an organisation or institution and have acknowledged the funder(s) in the full text of my thesis.

Date

Signature of candidate

Supervisor's declaration

I hereby certify that the candidate has fulfilled the conditions of the Resolution and Regulations appropriate for the degree of PhD in the University of St Andrews and that the candidate is qualified to submit this thesis in application for that degree.

Date

Signature of supervisor

Permission for publication

In submitting this thesis to the University of St Andrews we understand that we are giving permission for it to be made available for use in accordance with the regulations of the University Library for the time being in force, subject to any copyright vested in the work not being affected thereby. We also understand, unless exempt by an award of an embargo as requested below, that the title and the abstract will be published, and that a copy of the work may be made and supplied to any bona fide library or research worker, that this thesis will be electronically accessible for personal or research use and that the library has the right to migrate this thesis into new electronic forms as required to ensure continued access to the thesis.

I, Jennifer Bré, confirm that my thesis does not contain any third-party material that requires copyright clearance.

The following is an agreed request by candidate and supervisor regarding the publication of this thesis:

Printed copy

Embargo on all of print copy for a period of 3 years on the following ground(s):

- Publication would preclude future publication

Supporting statement for printed embargo request

We are planning to submit a manuscript for publication that include the data presented in this thesis.

Electronic copy

Embargo on all of electronic copy for a period of 3 years on the following ground(s):

- Publication would preclude future publication

Supporting statement for electronic embargo request

We are planning to submit a manuscript for publication that include the data presented in this thesis.

Title and Abstract

- I require an embargo on the abstract only.

Date

Signature of candidate

Date

Signature of supervisor

Underpinning Research Data or Digital Outputs

Candidate's declaration

I, Jennifer Bré, hereby certify that no requirements to deposit original research data or digital outputs apply to this thesis and that, where appropriate, secondary data used have been referenced in the full text of my thesis.

Date

Signature of candidate

Acknowledgements

I would first like to thank my supervisor Prof David Harrison for his guidance and support throughout the PhD journey. Keep having your hunches! I would also like to thank Dr Paul Reynolds for his assistance and advice.

I am grateful to Peter Mullen for the technical assistance in the lab, the coffees and overall support over the past three years. I also wish to thank Dr In Hwa Um for her expertise in immunohistochemistry, the medical students I supervised and who took part in projects related to my PhD and all the members of labs 248 and 249.

This work would not have been possible without NuCana, from the chemists who develop the ProTides to the people in the office who work to make a difference in people's lives.

A massive thank to all the friends I made along the way, from the school of Medicine and through the Postgraduate society. Their friendship means a lot as they made my experience in St Andrew truly unique. It has been fantastic!

I would also like to thank my friends at home, who always find time to meet when I go back or come visit me in Scotland, and especially Yvan who supported me from the first day at university.

Finally, I am so thankful to my parents, my biggest supporters.

Funding

This work was supported by NHS Lothian and NuCana plc.

Abstract

Although most women with ovarian cancer initially respond to platinum-based therapy, overall survival is poor with only 45% of women alive 5 years after diagnosis. Gemcitabine, a fluoropyrimidine analogue often used when relapse occurs, shows limited additional survival benefit due to intrinsic and acquired resistance. Therefore, chemoresistance remains a burden for the treatment of these patients. Acelarin, a phosphoramidate modification of gemcitabine, is the first anti-cancer ProTide to enter the clinic and is currently in a Phase II trial for ovarian cancer. To date, it is showing clinically significant anti-tumour activity, even in patients who were not responsive to gemcitabine or relapsed. Understanding its mode of action may help to improve its efficacy and determine a biomarker for clinical response. A panel of ovarian cancer cell lines was used to compare the mode of action of Acelarin and gemcitabine. Combination of cisplatin and Acelarin was investigated in PE01 and PE04 cells, sensitive and resistant cell lines derived from a single patient who developed cisplatin resistance. DCK and DCTPP1 were previously identified as potential modulators of cancer cell sensitivity to Acelarin and could be used as predictive biomarkers.

Acelarin and gemcitabine displayed differences in cytotoxicity, delays in cell cycles and DNA damage. PE01 and PE04 cells responded differently to combination, depending on the order of the sequence. The pyrimidine metabolism pathway, through the regulation of nucleotide pools, modulated sensitivity to Acelarin. However, there was no correlation between DCK and DCTPP1 and patients' response from a Phase I cohort treated with Acelarin.

Although similar in structure, Acelarin has a more targeted mechanism of action to induce cell death than gemcitabine. Repair mechanisms associated with platinum-based therapies resistance might potentiate Acelarin cytotoxicity. DCK and DCTPP1 are unlikely to either be of use as predictive biomarkers of clinical response to Acelarin.

Contents

1	Introduction	23
1.1	Ovarian cancer	23
1.1.1	Epidemiology and risk factors	23
1.1.2	Histopathology	26
1.1.3	Molecular pathology	27
1.1.4	Diagnosis and staging	30
1.2	Standard treatments in ovarian cancer	33
1.2.1	Primary surgery	33
1.2.2	Taxanes	34
1.2.3	Platinum-based therapies	35
1.2.4	Topoisomerase I poisons	37
1.2.5	Nucleoside analogues	38
1.3	ProTide technology as a new approach	47
1.3.1	Acelarin, first anti-cancer ProTide	48
1.3.2	Acelarin metabolism	50
1.4	Drug development: from pre-clinical studies to patients	53
1.4.1	Cancer cell lines and cytotoxicity	53
1.4.2	Patient derived xenografts and animal models	56
1.4.3	Combination treatments for ovarian cancer	57
1.5	Identification of biomarkers	59

1.5.1	Loss-of-function screen	59
1.5.2	CRISPR/Cas9 system	60
1.5.3	Digital and quantitative pathology	62
1.6	Hypotheses and aims	64
2	Material and methods	65
2.1	Cell culture	65
2.1.1	Cryopreservation and cell recovery from liquid nitrogen	66
2.1.2	Optimisation of cell number for growth inhibition experiments	66
2.1.3	Cytotoxicity analysis	67
2.2	Hypoxia	69
2.3	Time-lapse	69
2.4	Flow cytometry	69
2.4.1	Samples preparation	69
2.4.2	Staining & analysis	70
2.5	Gene expression alteration	71
2.5.1	Clustered Regularly Interspaced Short Palindromic Repeats (CRISPR)	71
2.5.2	Nucleofection	76
2.5.3	siRNA	77
2.6	Gene expression analysis	78
2.6.1	RNA extraction and purification	78
2.6.2	Reverse transcription	78
2.6.3	Real-Time PCR	79
2.7	Protein expression analysis	80
2.7.1	Protein extraction	80
2.7.2	Quantification: BCA assay	80
2.7.3	SDS polyacrylamide gel electrophoresis	81

2.7.4	Western blot	82
2.7.5	Immunocytochemistry	83
2.8	Comet assay for DNA damage	84
2.8.1	Preparation of samples & slides	84
2.8.2	Electrophoresis conditions	85
2.8.3	Staining & analysis	85
2.9	CalcuSyn	86
2.10	Phase I clinical study	86
2.10.1	Patient cohort and clinical data	86
2.10.2	Immunohistochemistry	87
2.10.3	Image analysis with QuPath	89
2.11	Statistical analysis	90
3	Comparison of Acelarin and gemcitabine effects on ovarian cancer cell lines <i>in vitro</i>	93
3.1	Introduction	93
3.2	Determination of best assay to study cytotoxicity of Acelarin and gemcitabine	94
3.3	Ovarian cell lines display different sensitivity to Acelarin and gemcitabine	99
3.4	Time-lapse showed delayed death of Acelarin-treated cells and cell cycle disruption	104
3.5	Inhibition of RRM1	109
3.6	DNA damage induced by Acelarin and gemcitabine	110
3.7	Discussion	113
4	Combination of Acelarin and cisplatin in ovarian cancer	119
4.1	Introduction	119
4.2	Validation of CalcuSyn method	121

4.3	Sequential treatments with Acelarin-cisplatin combination in ovarian cell lines	126
4.4	Discussion	133
5	Identification of predictive biomarkers for Acelarin	140
5.1	Introduction	140
5.2	Pyrimidine metabolism pathway modulates sensitivity to Acelarin and gemcitabine	142
5.2.1	Validation of candidate genes DCK and DCTPP1 <i>in vitro</i>	142
5.2.2	DCK and DCTPP1 in Acelarin Phase I cohort	151
5.2.3	Case studies	155
5.3	Candidate approach for biomarker: activation of Acelarin	157
5.4	Discussion	160
6	General discussion	168
6.1	Discussion	168
6.2	Future work	176
7	Appendices	179
8	Publication	194
	References	208

List of Figures

1.1	Histology of epithelial ovarian cancers	25
1.2	Pathway molecular pathology	29
1.3	Mode of action of cisplatin	35
1.4	Structure of deoxycytidine and its analogue gemcitabine.	39
1.5	Mode of action gemcitabine	42
1.6	Factors involved in resistance to cancer	46
1.7	Structure of a ProTide	47
1.8	Acelarin (NUC-1031) overcomes resistance associated with gemcitabine	48
1.9	Putative activation of ProTide	51
1.10	CRISPR/Cas9 is a bacterial adaptive immune system	60
1.11	The principle of CRISPR/Cas9-targeted genome editing	62
2.1	Design oligos for CRISPR	71
2.2	PCR gel to validate the ligation of the sgRNA with the vector	74
2.3	Kill curve for puromycin selection	76
2.4	Identification of cancer cells	91
2.5	Annotation and segmentation of an image on QuPath	92
2.6	Segmentation to exclude non-tumour cells within a region of interest . .	92
3.1	Comparison of two methods to assess optimal cell density	95
3.2	Analysis of cell confluence with Celigo	97

3.3	Effect of Acelarin treatment on growth of a panel of ovarian cell lines	99
3.4	Effect of oxygen condition on A2780 cells sensitivity to treatment with Acelarin or gemcitabine	100
3.5	Effect of oxygen condition on CAOV3 cells sensitivity to treatment with Acelarin or gemcitabine	101
3.6	Effect of oxygen condition on SKOV3 cells sensitivity to treatment with Acelarin or gemcitabine	102
3.7	Time lapse of A2780 cells treated with gemcitabine or Acelarin	105
3.8	Effect of gemcitabine or Acelarin on the cell cycle of A2780	107
3.9	Effect of gemcitabine or Acelarin on the cell cycle of SKOV3	108
3.10	Effect of gemcitabine and Acelarin on RRM1 expression	109
3.11	Aspect of the comets in A2780 cells	111
3.12	γ H2AX and comet assay to assess DNA damage induced by Acelarin and gemcitabine	112
4.1	Dose response of SKOV3 cells to different chemotherapies	123
4.2	Effect of sulforaphane and cisplatin combination in SKOV3 cells	124
4.3	Effect of Fluvastatin and cisplatin combination in SKOV3 cells	125
4.4	Dose response of Acelarin and cisplatin in PE01 and PE04 cells	126
4.5	Effect of Acelarin (2 h) and cisplatin (4 h) combination in PE01 and PE04 cells	130
4.6	Effect of Acelarin (2 h) and cisplatin (24 h) combination in PE01 and PE04 cells	131
4.7	Effect of cisplatin (4 h) and Acelarin (2 h) combination in PE01 and PE04 cells	132
5.1	Roles of DCK and DCTPP1 in pyrimidine metabolism pathway	141

5.2	Effect of DCK knockdown on sensitivity of A2780 cells to Acelarin and gemcitabine	143
5.3	Effect of DCTPP1 knockdown on sensitivity of A2780 cells to Acelarin	144
5.4	Effect of DCTPP1 knockdown on sensitivity of A2780 cells to Acelarin and gemcitabine	144
5.5	GFP signal as positive control of nucleofection	147
5.6	Effect of DCK-DCTPP1 double knockdown on sensitivity of A2780 cells to Acelarin and gemcitabine	147
5.7	Effect of DCK-DCTPP1 double knockdown on sensitivity of A2780 cells to Acelarin and gemcitabine	148
5.8	DCK expression and localisation in response to gemcitabine and Acelarin treatment	148
5.9	RRM1 expression in DCK knockdown cells	149
5.10	Effect of dCMP/dCTP pool on sensitivity to Acelarin and gemcitabine	150
5.11	Comparison of Allred score for DCK and DCTPP1	154
5.12	DCK expression in patients with partial response	155
5.13	DCK and DCTPP1 expression in tumour tissues	156
5.14	Endogenous expression of candidates in ovarian cell lines	158
5.15	Effect of HINT1 knockdown on sensitivity of A2780 cells to Acelarin . .	159
5.16	Allred score of HINT1 in patients	159
5.17	Pyrimidine metabolism pathway	163
7.1	Verification of sgRNA inserts in pLentiCRISPRv2 and px333 plasmids .	180
7.2	Comparison of cell confluence of A2780 cells with Celigo and SRB . . .	181
7.3	Comparison of cell confluence of CAOV3 cells with Celigo and SRB . .	181
7.4	Comparison of cell confluence of OVCAR3 cells with Celigo and SRB .	182
7.5	Comparison of cell confluence of OVCAR4 cells with Celigo and SRB .	182

7.6	Comparison of cell confluence of PE04 cells with Celigo and SRB . . .	183
7.7	Comparison of cell confluence of PE06 cells with Celigo and SRB . . .	183
7.8	Comparison of cell confluence of SKOV3 cells with Celigo and SRB . .	184
7.9	Effect of simultaneous treatment with Acelarin-cisplatin combination on PE01 and PE04 cells	185
7.10	Repeats of drug combinations Acelarin-cisplatin in PE01 cells (1) . . .	186
7.11	Repeats of drug combinations Acelarin-cisplatin in PE01 cells (2) . . .	187
7.12	Repeats of drug combinations Acelarin-cisplatin in PE01 cells (3) . . .	187
7.13	Repeats of drug combinations Acelarin-cisplatin in PE04 cells (1) . . .	188
7.14	Repeats of drug combinations Acelarin-cisplatin in PE4 cells (2)	188
7.15	Repeats of drug combinations Acelarin-cisplatin in PE04 cells (3) . . .	189
7.16	DCK knockdown in A2780 ovarian cancer cell line	190
7.17	DCTPP1 knockdown in A2780 ovarian cancer cell line	190
7.18	Allred score ratio of DCK and DCTPP1	191
7.19	HINT1 expression in ovarian cancer	192
7.20	Ethics approval	193

List of Tables

1.1	FIGO staging classification for cancer of the ovary, fallopian tube, and peritoneum.	32
2.1	Molecular signature of cell lines	66
2.2	Drug concentrations used for cytotoxicity assays	68
2.3	sgRNA used for CRISPR knockdown	72
2.4	Primers used for RT-qPCR	79
2.5	Antibodies used for western blot analysis	83
3.1	Cell density optimisation	98
3.2	IC ₅₀ values for cells treated with Acelarin and gemcitabine in normoxia and hypoxia	103
4.1	Interpretation of CI values from CalcuSyn software	122
5.1	Patients information from phase I clinical study.	153
7.1	DCK and DCTPP1 Allred scores with RECIST and gemcitabine information	184

Abbreviations

BCA: Bicinchoninic Acid

BRCA1/2: Breast Cancer 1 and 2

CES2: Carboxylesterase 2

CI: Combination index

CDA: Cytidine deaminase

CRISPR: Clustered Regularly Interspaced Short Palindromic Repeat

DCK: Deoxycytidine kinase

DCTPP1: Deoxycytidine pyrophosphatase 1

dCyd: Deoxycytidine

dFdC: 2',2'-difluoro-2-deoxycytidine (gemcitabine)

dCMP: Deoxycytidine monophosphate

dFdCDP: 2',2'-difluoro-2-deoxycytidine diphosphate

dFdCTP: 2',2'-difluoro-2-deoxycytidine triphosphate

dFdU: 5-fluorodeoxyuridine

DMEM: Dulbecco's modified Eagle medium

DMSO: Dimethyl sulfoxide

DSB: Double strand break

EDTA: Ethylenediaminetetraacetic acid

FA: Fraction affected

GAPDH: Glyceraldehyde-3-Phosphate Dehydrogenase

GeCKO: Genome-scale CRISPR Knock Out

hENT1: human Equilibrative Nucleotide Transporter 1
HGSOC: high-grade serous ovarian cancer
HRP: Horse Peroxidase
IC₅₀: Inhibitory Concentration 50
IHC: Immunohistochemistry
LGSOC: low-grade serous ovarian cancer
NHEJ: Non-Homologous End Joining
OD: Optical density
PI3K: Phosphoinositide 3 kinase
PBS: Phosphate Buffered Saline
PCR: Polymerase chain reaction
PFA: Paraformaldehyde
PVDF: Polyvinylidene fluoride
RNAi: Ribonucleic acid interference
RPMI: Roswell Park Memorial Institute medium
RR: Ribonucleotide reductase
RRM1: Ribonucleotide reductase subunit M1
RRM2: Ribonucleotide reductase subunit M2
RT-qPCR: Reverse transcriptase q-PCR
SDS: Sodium dodecyl sulfate
sgRNA: Single guide RNA
siRNA: Small interference RNA
SRB: Sulforhodamine B
TCA: Trichloroacetic acid

1 | Introduction

1.1 Ovarian cancer

1.1.1 Epidemiology and risk factors

Ovarian cancer is the seventh most common cancer among women worldwide, and is associated with one of the highest mortality rate of all gynaecologic cancers. It accounts for 2.5% of all malignancies among females and 5% of cancer deaths (Howlader et al., 2017), because of low survival rates largely driven by late stage diagnoses and resistance development to standard treatments. In 2018, more than 295,000 women were diagnosed with ovarian cancer and 185,000 died from this disease (Bray et al., 2018). The lifetime incidence is 1 in 75 and mortality is 1 in 100 (Howlader et al., 2016). The median age of patients at diagnosis is 63 years, with over 80% of ovarian cancers occurring after age 45 years (Permeth-Wey and Sellers, 2009). Over the past decade, minimal improvement in mortality has been observed as the 5-year survival rate is about 45% (Ries et al., 2006; Torre et al., 2018). Survival is reported to be over 90% in patients who are diagnosed when the tumour is localised in the ovaries, but decreases to 25% when it has already metastasised. Therefore, improving prevention and early detection is a priority, in addition to finding effective therapies that will overcome the limitations encountered with the standard treatments.

The risk of developing ovarian cancer is increased by several factors that include age, hormonal profile and genetic factors. Epidemiological studies have established the correlation between hormonal and reproductive factors. Casagrande and colleagues first described the hypothesis of the "incessant ovulation"; the number of ovulatory cycles increases the rate of cellular division associated with the repair of the surface epithelium after each ovulation (Casagrande et al., 1979). Consequently, spontaneous mutations are increased, mostly in TP53 gene (Bast et al., 2009; Permuth-Wey and Sellers, 2009), and this promotes carcinogenesis. It is also associated with an early age at menarche and late age at menopause as it increases the period of ovulation. On the contrary, other physiological aspects can reduce the risk of ovarian cancer. Both pregnancy and lactation cause anovulation, hence parous women are estimated to have a 30-60% lower risk for ovarian cancer compared with nulliparous women (Booth et al., 1989; Reid et al., 2017). Furthermore, each additional pregnancy is estimated to lower the risk by approximately 15% more (Whittemore et al., 1992). Oral contraception is also well established as a protection against ovarian cancer, and is estimated to reduce the risk by at least 5% per year, with about a 50% reduction in risk for long-term use of 10 years or greater (Jelovac and Armstrong, 2011).

The strongest risk factor is a family history of breast or ovarian cancer, which accounts for 10% of the patients with ovarian cancer (Rubin et al., 1998). Lifetime risk is also increased with the most significant known genetic risk factors for ovarian cancer, germline BRCA1 and BRCA2 mutations, which are found in up to 13% of patients (Zhang et al., 2011; Alsop et al., 2012). Located on chromosomes 17q and 13q, respectively, their gene products are involved in DNA repair (King et al., 2003). Inheritance of a deleterious mutation in one of those genes is associated with 27% to 44% increase of risk of ovarian cancer (Ford et al., 1994; Antoniou et al., 2003). Women with a BRCA1 mutation are more susceptible to develop cancer at about 45

years old, whereas it is more likely to occur at 60 years old for carriers of a BRCA2 mutation (Russo et al., 2009). Besides BRCA genes, patients with germline mutations in other genes involved in DNA repair, such as CHEK2, MRE11A, RAD50, ATM and TP53, might also increase the risk of developing ovarian cancer (Walsh et al., 2011). In addition, hereditary non-polyposis colorectal cancer syndrome (HNPCC), also known as Lynch syndrome II, may account for at least 2% of cases (Bonadona et al., 2011), mostly endometrioid carcinomas (Prat, 2012). The syndrome is characterised by inheritance of a germline mutation in genes of the DNA mismatch repair system (Lynch et al., 2009).

Other risk factors for ovarian cancer are environmental (diet, obesity, smoking) and ethnic variation, correlated with genetic inheritance (Schulz et al., 2004; Jordan et al., 2006; Permuth-Wey and Sellers, 2009; Torre et al., 2018).

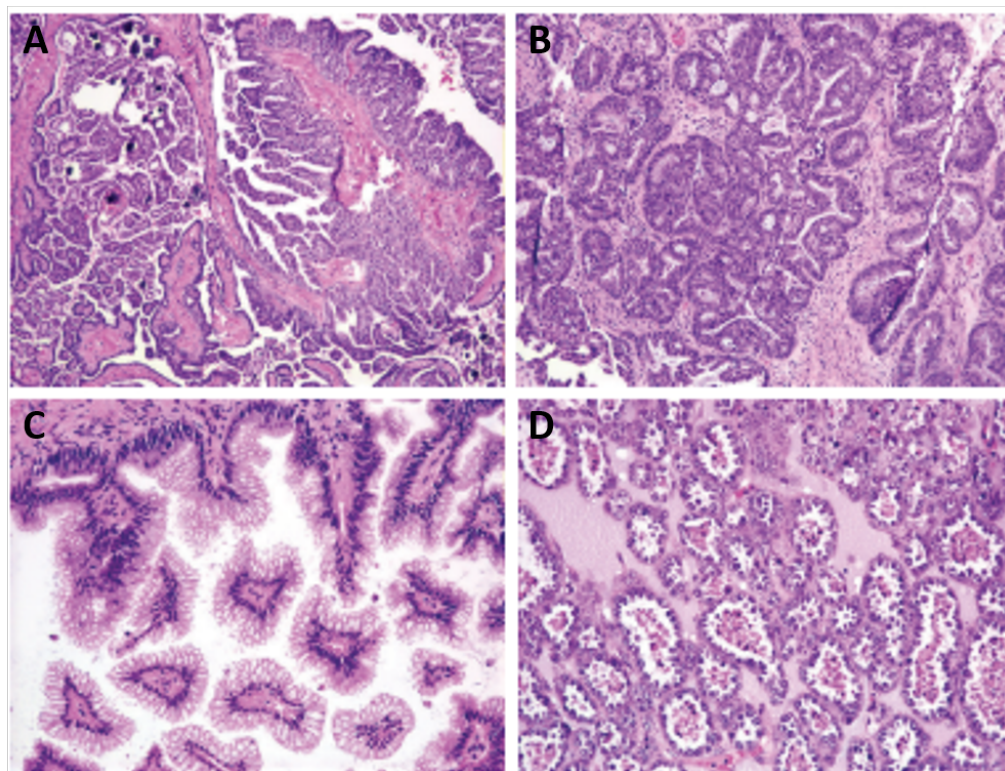


Figure 1.1: Histology of epithelial ovarian cancers. (A) Serous, (B) endometrioid, (C) mucinous and (D) clear cell histotypes (adapted from Karst et al., 2010).

1.1.2 Histopathology

Although traditionally referred to as a single entity, ovarian cancer is a heterogeneous disease composed of a diverse group of tumours. Most of them originate from one of three cell types: epithelial cells, stromal cells and germ cells. The epithelial tumours, also known as carcinomas, constitute the predominant and most lethal form, as they account for 90% of the malignant ovarian tumours. They are comprised of five main histotypes: high-grade serous (HGSOC) (70%), endometrioid (10%), clear cell (10%), mucinous (3%) and low-grade serous (LGSOC) (<5%) (Prat, 2012). The low-grade serous carcinomas appear to arise from a serous borderline tumour in many cases (Della Pepa et al., 2015). Other subtypes include epithelial tumours lacking any specific differentiation classified as transitional, undifferentiated and mixed (Chen et al., 2003; McCluggage, 2011). The distinct histotypes differ with regard to their cellular origin, pathogenesis, molecular alterations, gene expression, prognosis and response to chemotherapeutic regimes.

The origin and pathogenesis of ovarian cancer are poorly understood. The traditional view of ovarian carcinogenesis was that the different tumours all derived from the ovarian surface epithelium and that subsequent metaplastic changes led to the development of the different cell types (Karst and Drapkin, 2010; Kurman and Shih, 2010). However, the normal ovary has no constituents that look like these tumours. Morphologically, endometrioid tumours resemble the endometrium, mucinous tumours look like the endocervical epithelium or, more frequently, intestinal epithelium, and finally clear cell tumours are formed by cell that relate to those of vaginal rests (Fig.1.1) (Chen et al., 2003; Kurman and Shih, 2010). The main sites of origin of high grade serous cancers are debated, with a hypothesis being that it originates from the fallopian tubes

rather than the ovaries. This is supported by a histopathological study that showed most HGSOC samples had little resemblance to the ovarian epithelial surface and ovarian tissue, but recapitulated the histological features of Müllerian epithelium that is present in the fallopian tube (Piek et al., 2001). As the tumour develops, cancer cells acquire a proliferative capacity and spread to the ovarian surface and may establish tumour formation and transformation to HGSOC (Klotz and Wimberger, 2017).

Clear cell and endometrioid carcinomas are often detected at an early stage, when still confined to the ovary and therefore are of good prognosis. Contrastingly, 88% of the serous tumours are diagnosed at stage III and IV, when they have already spread through the organism and this is associated with poor survival (McCluggage, 2011). The different tumours are usually classified into two groups on the basis of clinical, cellular, and molecular characteristics. Type I tumours, low-grade serous, mucinous, endometrioid and clear cell carcinomas, are thought to derive from borderline tumours. They are usually detected at early stage (I or II), they grow slowly and resist conventional chemotherapy. On the other hand, high-grade serous tumours form the type II, with an aggressive phenotype, rapid proliferation and are diagnosed at an advanced stage (III or IV) but they are initially responsive to chemotherapy (Shih and Kurman, 2004; Koshiyama et al., 2014).

1.1.3 Molecular pathology

At a molecular level, ovarian cancers derived from several genetic mutations, dysregulations and altered patterns of gene expression can be specific to the different histotypes.

Within type I tumours, low-grade serous and mucinous are associated with frequent mutations of the oncogenes BRAF and KRAS (mutated in more than 20% of

the cases) (Bast et al., 2009). It has been shown that endometrioid tumours arise from endometriosis with somatic mutations of the β -catenin and PTEN genes in 20% of the cases (Bell, 2005). Clear cell carcinomas can have mutations in PTEN and PI3K (Kuo et al., 2009). There is also activation of the PI3K signalling pathway in approximately 70% of ovarian cancers, which is associated with resistance to cytotoxic chemotherapy and inhibition of apoptosis (Kurman and Shih, 2008; Bast et al., 2009).

While low-grade serous carcinomas arise from RAS-signaling-related pathways, tumorigenesis of high-grade serous is RAS-signaling-independent (Della Pepa et al., 2015) and KRAS and BRAF are wild type in these tumours (Singer et al., 2002, 2003). On the contrary, TP53 is specific to HGSOC as it was found highly mutated (73%) in these tumours and it correlates with metastatic potential (Havrilesky et al., 2003); but no mutations were detected in LGSOC (Wong et al., 2010). Similarly to TP53, BRCA1 and BRCA2 are wild type in type I tumours but mutated in 22% of HGSOC, due to a combination of germline and somatic mutations (The Cancer Genome Atlas Research, 2011; Romero and Bast, 2012). Upon DNA damage, the tumour suppressor p53 is activated and induces a cell cycle arrest in order to enable cells to repair their DNA. If the damage is beyond repair, then they undergo apoptosis. Mutations in this gene prevent the physiological regulation of the cells and promote proliferation and genomic instability (Ahmed et al., 2010). BRCA1 and BRCA2 are involved at a later stage, during the DNA repair processes. Both proteins function in homologous recombination (HR), which uses the undamaged sister chromatid as a template to repair the double-strand breaks that occurred on the other chromatid. HR appears to be the major mechanism to protect the integrity of the genome in proliferating cells (Roy et al., n.d.). The Cancer Genome Atlas Project, which analysed more than 300 high-grade serous cancers, detected a high prevalence of mutations and promoter methylation in putative DNA repair genes including homologous recombination components.

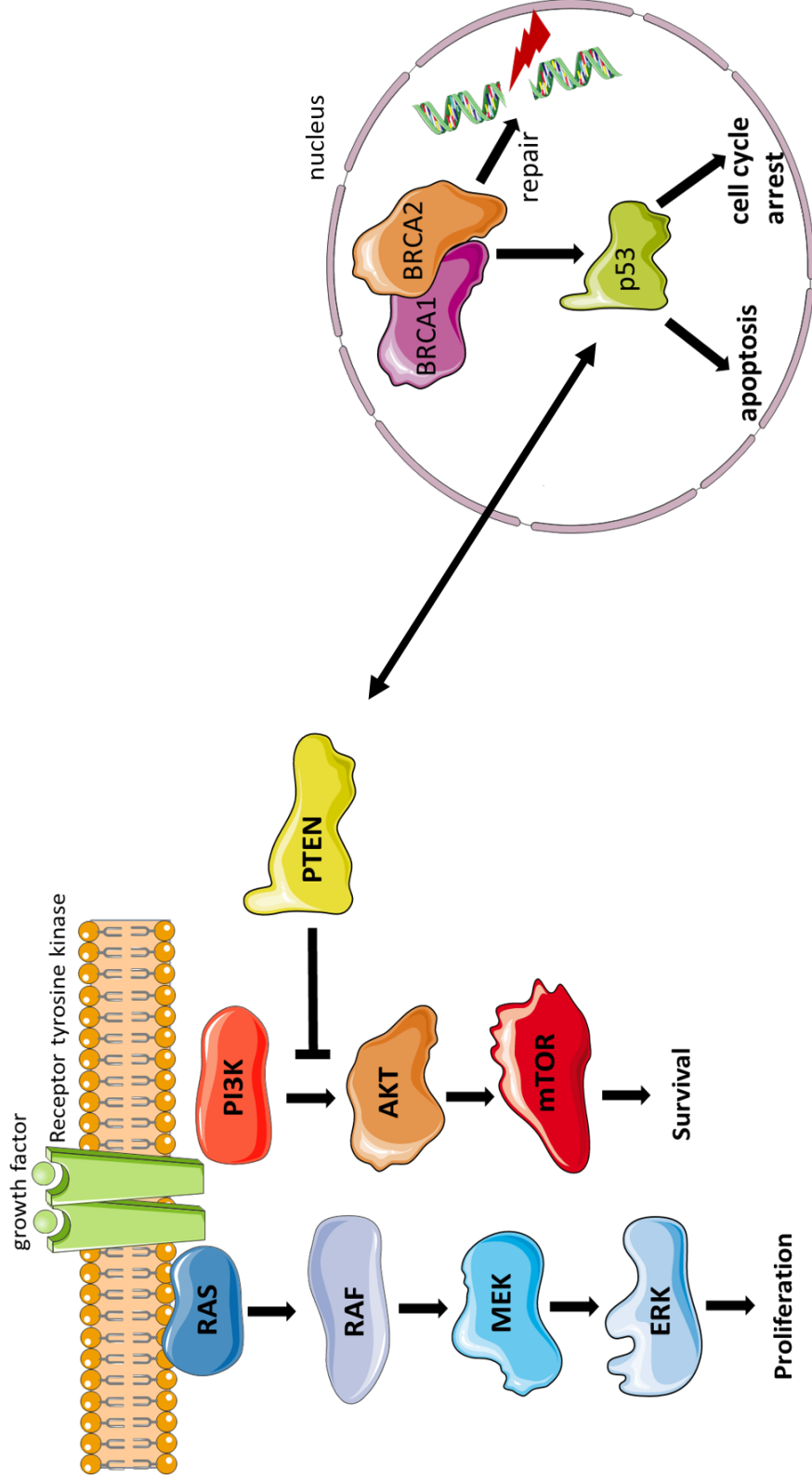


Figure 1.2: Pathway molecular pathology. Upon binding of growth factors to receptor tyrosine kinases, there is activation of the Ras/Raf/MAPK and PI3K/Akt/mTOR signalling cascades which are tightly regulated in normal cells but also play a pivotal role in the pathogenesis of various cancers, including ovarian. Mutations of Ras pathway leads to the expression of constitutively active Ras proteins which promote cell proliferation while activation of PI3K/Akt/mTOR signalling pathway contributes to cell survival. These pathways are often mutated in type I ovarian cancer. HGSOC mostly display mutations in BRCA1/BRCA2 and p53, which are involved in the repair of DNA damage and regulation of cell cycle and apoptosis. PTEN and p53 interact with each other, thus acting as a regulated switch between survival and death in normal cells.

1.1.4 Diagnosis and staging

Contrary to other types of cancer such as breast or testis which can have detectable signs, the symptoms of ovarian cancer might be initially missed because they are not specific and often thought to be due to normal changes associated with ageing and menopause. They can also suggest the presence of upper abdominal disease or occasionally pelvic pain due to ovarian torsion (Cannistra, 2004; Bankhead et al., 2008). Consequently, an early detection is difficult and diagnosis frequently occurs at late stage when cancer has already spread. The ovarian cancer is frequently nicknamed the “silent killer” (Goff et al., 2000; Karst and Drapkin, 2010; Jelovac and Armstrong, 2011).

Detection screening includes physical examination of the patient (pelvic and recto-vaginal examination), and radiographic imaging (transvaginal ultrasonography, abdominal ultrasonography, MRI, CT and/or PET scans). Another method which is minimally invasive and cost effective is the CA-125 blood test (Bast et al., 1981). Most widely used marker for the disease screening (Longuespée et al., 2012), it is a high molecular weight transmembrane glycoprotein expressed in 80% of ovarian cancers but in less than 1% of healthy women (Yin and Lloyd, 2001). In patients with ovarian cancer, CA-125 is shed and circulates in serum, where it can be detected. Although it is considered as a useful biomarker, some precautions remain when interpreting the results, given that CA-125 levels are increased in only 50% of stage I ovarian cancers and can also be increased by a range of benign conditions (pelvic inflammatory disease, endometriosis, uterine fibroid, and ovarian cysts) thus making false positive results concerning ovarian cancer (Matulonis et al., 2016). Furthermore, it has been shown that CA-125, combined with transvaginal ultrasonography, appeared to be only sensitive in detecting ovarian cancer at an advanced stage (Dorum et al., 1996; Olivier et al., 2005).

In case of suspicion of ovarian cancer, an exploratory laparotomy is performed for histologic confirmation and staging. Staging of ovarian epithelial tumours is performed according to the Tissue, Node and Metastasis (TNM) staging system, guidelines established by the American Joint Committee on Cancer. It is comparable to an alternative staging system approved by the International Federation of Gynaecology and Obstetrics (FIGO) (Table1.1). Although ovarian carcinoma is often considered clinically as one disease, the understanding of the underlying pathogenesis and molecular events have greatly improved, in parallel of a realisation that the different tumour subtypes have a different natural behaviour and prognosis. At present, treatments are mainly based upon tumour stage and grade rather than type. However, some tumour types such as clear cell, endometrioid, mucinous and low grade serous carcinomas are considered relatively resistant to traditional chemotherapeutic regimes. Given these factors and that ongoing trials are investigating the efficacy of different agents in some of these tumour subtypes, it is clear that accurate pathological typing of ovarian carcinomas is becoming more important and may be critical in directing therapy in the future.

Stage I: Tumour confined to ovaries or fallopian tube(s)	T1-N0-M0
IA: Tumor limited to 1 ovary (capsule intact) or fallopian tube; no tumor on ovarian or fallopian tube surface; no malignant cells in the ascites or peritoneal washings	T1a- N0- M0
IB: Tumor limited to both ovaries (capsules intact) or fallopian tubes; no tumor on ovarian or fallopian tube surface; no malignant cells in the ascites or peritoneal washings	T1b- N0- M0
IC: Tumor limited to 1 or both ovaries or fallopian tubes, with any of the following:	
IC1: Surgical spill	T1c1- N0- M0
IC2: Capsule ruptured before surgery or tumor on ovarian or fallopian tube surface	T1c2- N0- M0
IC3: Malignant cells in the ascites or peritoneal washings	T1c3- N0- M0
Stage II: Tumor involves 1 or both ovaries or fallopian tubes with pelvic extension (below pelvic brim) or peritoneal cancer	T2- N0- M0
IIA: Extension and/or implants on uterus and/or fallopian tubes and/or ovaries	T2a- N0- M0
IIB: Extension to other pelvic intraperitoneal tissues	T2b- N0- M0
Stage III: Tumor involves 1 or both ovaries or fallopian tubes, or peritoneal cancer, with cytologically or histologically confirmed spread to the peritoneum outside the pelvis and/or metastasis to the retroperitoneal lymph nodes	T1/T2- N1- M0
IIIA1: Positive retroperitoneal lymph nodes only (cytologically or histologically proven):	
IIIA1(i) Metastasis up to 10 mm in greatest dimension	
IIIA1(ii) Metastasis more than 10 mm in greatest dimension	
IIIA2: Microscopic extrapelvic (above the pelvic brim) peritoneal involvement with or without positive retroperitoneal lymph nodes	T3a2- N0/N1- M0
IIB: Macroscopic peritoneal metastasis beyond the pelvis up to 2 cm in greatest dimension, with or without metastasis to the retroperitoneal lymph nodes	T3b- N0/N1- M0
IIC: Macroscopic peritoneal metastasis beyond the pelvis more than 2 cm in greatest dimension, with or without metastasis to the retroperitoneal lymph nodes (includes extension of tumor to capsule of liver and spleen without parenchymal involvement of either organ)	T3c- N0/N1- M0
Stage IV: Distant metastasis excluding peritoneal metastases	
Stage IVA: Pleural effusion with positive cytology	
Stage IVB: Parenchymal metastases and metastases to extra- abdominal organs (including inguinal lymph nodes and lymph nodes outside of the abdominal cavity)	Any T, any N, M1

Table 1.1: FIGO staging classification for cancer of the ovary, fallopian tube, and peritoneum (source Berek et al. (2018)). Regional lymph nodes (N): N0: No regional lymph node metastasis; N1: Regional lymph node metastasis. Distant metastasis (M): M0: No distant metastasis; M1: Distant metastasis (excluding peritoneal metastasis).

1.2 Standard treatments in ovarian cancer

1.2.1 Primary surgery

Surgery is necessary for diagnosis, staging and reduction of tumour bulk. It is one of the few malignancies in which primary cytoreductive surgery is carried out, even if complete resection cannot be achieved. It is considered as optimal cytoreduction when no macroscopic tumour is left before chemotherapy, or suboptimal if it has been reduced to more than 1 cm (Matulonis et al., 2016). It can also be performed after neoadjuvant chemotherapy when optimal cytoreduction is not considered feasible at initial diagnosis. Meta-analyses of retrospective studies have shown that the post-operative residual tumour size is considered as a main prognostic factor in advanced epithelial ovarian cancer (Chi et al., 2006; du Bois et al., 2009). The extent of surgery is determined by the stage of cancer; a patient diagnosed at a low-risk stage I tumour might undergo unilateral oophorectomy only, whereas a bilateral oophorectomy is more likely to be performed in the case of a more advanced cancer. Following the primary surgery, patients receive a combination of platinum- and taxane-based chemotherapy (Hainsworth et al., 1997; Lorusso et al., 2006; Rose, 2016). Although many tumours are initially responsive to this treatment, more than 70% of patients will be affected by disease recurrence and will require a second-line chemotherapy (Romero and Bast, 2012; Pignata et al., 2017).

1.2.2 Taxanes

In the 1960s, bark extracts from the Pacific Yew Tree *Taxus brevifolia* were discovered to have anticancer activity. In 1971, Wani and colleagues identified taxol as the active agent (Wani et al., 1971). Taxol was later renamed paclitaxel when the pharmaceutical company Bristol-Myers Squibb trademarked the name “Taxol” (Walsh and Goodman, 1999, 2002). Scarcity of supply, in addition of a relative insolubility of the compound, limited experimentation on these extracts and synthetic approaches to paclitaxel production remained a challenge for about 20 years. It led to the development of docetaxel, a semi-synthetic analogue of paclitaxel, extracted from the renewable and more readily available needles of the European yew tree *Taxus baccata* (Guénard et al., 1993). In 1994, Holton and his group succeeded the first total synthesis of paclitaxel (Holton et al., 1994).

Paclitaxel is a spindle poison, as are other compounds such as colchicine and vinca alkaloids. They interrupt cell division by affecting the microtubules, essential proteins in the mitotic process. This leads to a variety of effects on dividing cells with defects in mitotic spindle assembly and chromosome segregation, cell cycle arrest in G2/M phase and apoptosis (Spratlin and Sawyer, 2007). Tubulin is normally present in cells in a dynamic equilibrium between tubulin dimers and microtubules. Unlike vinca alkaloids, which inhibits microtubules polymerisation (Brabander et al., 1981), paclitaxel binds to their beta-tubulin subunits and promotes polymerisation and stabilisation. This causes an accumulation of disorganised microtubules, resistant to disassembly by physiological stimuli such as cold or calcium treatment (Clarke and Rivory, 1999). Paclitaxel is widely use as treatment in a range of cancers such as ovarian (Einzig et al., 1992; Sarosy et al., 1992), breast (Reichman et al., 1993) and lung

(Schiller et al., 2002).

1.2.3 Platinum-based therapies

The clinical benefits of platinum compounds as anti-cancer agent have been recognised for over 30 years. They are used in a wide variety of solid tumours such as testicular, head and neck, colorectal, non-small cell lung, and bladder (Prestayko et al., 1979; Lebwohl and Canetta, 1998) and are part of the first-line treatment for ovarian cancer (du Bois et al., 2003; Ozols et al., 2003). Cisplatin, also called cis-diamminedichloroplatinum(II), was the first of the family. The cytotoxicity of cisplatin resides in its ability to react with the N7 site of purine bases in DNA (Rabik and Dolan, 2007) and form mainly intrastrand crosslinks; with additional interstrand crosslinks (Fig.1.3). All crosslinks result in contortion of the DNA and DNA lesions, in addition of activation of signalling pathway such as ATR, p53 and MAPK, that lead to apoptosis (Siddik, 2003).

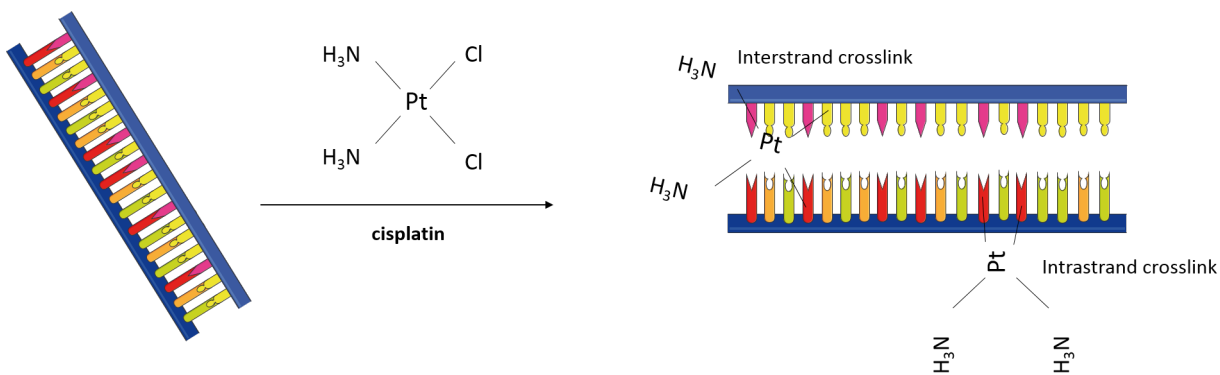


Figure 1.3: Mode of action of cisplatin. Cisplatin is activated through a series of aquation reaction which involve the replacement of the cis-chloro ligands of cisplatin with water molecules. It can then interact with nucleophilic N7-sites of purine bases (A or G); upon binding cisplatin forms intrastrand and interstrand crosslinks. This affects the conformation of DNA and induces DNA damage, leading to cell death.

Cisplatin is responsible for severe toxic effects in some patients such as nephrotoxicity, neurotoxicity and ototoxicity (Lokich and Anderson, 1998) which limits the dose that can be administered and an alternative with less side effect was sought. Carboplatin and oxaliplatin were part of the second-generation platinum compounds and were developed with the specific aim of reducing the side effects of cisplatin while retaining its anticancer properties. Oxaliplatin is used in colorectal cancer whereas both cisplatin and carboplatin are used in the treatment of ovarian cancer (Chibaudel et al., 2013). Although carboplatin has fewer side effects than its precursor cisplatin, with its main toxicity being myelosuppression, it is also less potent, which might be due to differences in rates of adduct formation with DNA (Harrap, 1985). As the active form of carboplatin is similar to that of cisplatin, they share a mechanism of action, form identical lesions on DNA and are cross-resistant (Galluzzi et al., 2012). Resistance mechanisms include decreased cytoplasmic accumulation of cisplatin and carboplatin due either to decreased influx or increased efflux, increased levels of glutathione or glutathione-S-transferase activity, increased levels of cytoplasmic metallothioneins, and enhanced DNA repair (Johnson et al., 1997; Rabik and Dolan, 2007).

The BRCA1 and BRCA2 proteins play a critical role in DNA damage repair, notably the homologous recombination (HR) repair pathway, and their mutation status may be a potential predictor for platinum resistance in ovarian cancer (Swisher et al., 2008; Dhillon et al., 2011). BRCA-null tumours have impaired repair of platinum induced DNA crosslinking and are preferentially sensitive to treatment with platinum-based chemotherapy. It has been shown that reversion mutations in BRCA2, which restore its function, is a mechanism of resistance to platinum-based chemotherapy (Sakai et al., 2008, 2009).

Despite an initial response to these drugs, relapse occurs for more than 70% of the patients. Patients who experience relapse during the course of treatment or less than six months after the last platinum treatment are categorised as platinum-refractory and resistant. If it occurs after six months, they are considered platinum-sensitive. This determines the next line of treatment they will receive. For platinum-sensitive patients, the use of platinum-based combinations such as carboplatin-paclitaxel or carboplatin-gemcitabine is associated to a better outcome compared with non-platinum or platinum administered as monotherapy (ICON and AGO, 2003; Pfisterer et al., 2006).

1.2.4 Topoisomerase I poisons

Nuclear DNA topoisomerase I (TOP1) is an ubiquitous and essential human enzyme. Its function is to relax supercoiled DNA in order to remove helical constraints that can otherwise hinder DNA replication and transcription, thereby blocking cell growth. The introduction of DNA single-strand breaks by TOP1 enables the rotation of the intact DNA strand around the break and facilitate DNA relaxation. The cleavage intermediate is referred to as a cleavage complex because TOP1 cleaves DNA by forming a covalent bond to the 3' DNA terminus that it generates. Once the DNA is relaxed, religation occurs by reversion of TOP1 covalent binding. Under normal conditions, the cleavage complex is transient and religation is favoured over cleavage. However, they can be stabilised by topoisomerase inhibitors such as camptothecin. The trapping of the cleavage complex by inhibitors results in DNA damage. Topotecan is a derivative of camptothecin and a Food and Drug Administration (FDA) approved drug for treatment of ovarian cancer (Pommier, 2006). It is indicated for the treatment of recurrent or persistent ovarian cancer after failure of initial or subsequent chemotherapy (Herzog, 2002).

1.2.5 Nucleoside analogues

The development of nucleoside analogues is at the origin of the main treatments for patients with cancer or viral infections. This family of therapeutic compounds was expanded in the past decades, with the addition of more than 30 new molecules (De Clercq, 2012; De Clercq and Li, 2016). Nucleoside and nucleotides analogues are involved in cellular processes such as DNA or RNA synthesis, cell signalling and metabolism. Chemically modified to mimic their physiological counterparts, they go through the same metabolic pathways and act as antimetabolites (Jordheim et al., 2013). Cellular uptake by the mean of a transporter and intracellular phosphorylation are required in order for the nucleosides analogues to be activated into their active nucleotide analogue form. Only then, they inhibit DNA synthesis upon incorporation during replication, this leading to chain termination and inhibition of cancer cell growth. Some of these analogues also interact and inhibit essential enzymes such as ribonucleotide reductase and thymidylate synthase, which are involved in the synthesis of endogenous nucleotides. It results in reduction of the pool of nucleotides available and enhance even more incorporation of the analogues into DNA (Galmarini et al., 2001). The main nucleoside analogues currently in use are sofosbuvir, used in the treatment of the Hepatitis C virus (Keating, 2014); cytosine arabinoside, extensively used in the treatment of acute leukaemia, and gemcitabine which is one of the standard treatment in solid tumours (Mini et al., 2006).

Gemcitabine

Gemcitabine (2'-deoxy-2',2'-difluorocytidine, dFdC) is a deoxycytidine analogue with two fluorine substituted for the two hydrogen atoms in the 2' position of the deoxyribose

sugar (Fig.1.4). Originally investigated as an antiviral agent, it was developed as an anticancer drug on the basis of its impressive *in vitro* and *in vivo* antitumoral activity. Evidence of its efficacy to inhibit cancer cell growth was obtained in a range of solid and haematological cancer cell lines as well as human tumour xenografts in mice (Hertel et al., 1990; Boven et al., 1993; Ruiz Van Haperen et al., 1994). It is now used as a single agent for the treatment of pancreatic cancer (Kamisawa et al., 2016), and it also has a well-proven activity in platinum/paclitaxel resistant ovarian cancer patients (Lund et al., 1994; D'Agostino et al., 2003).

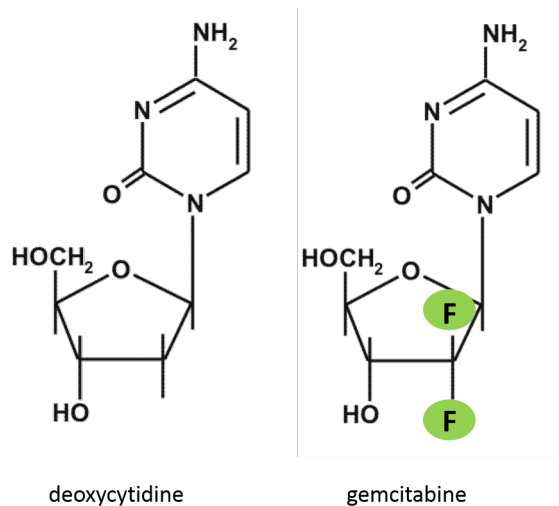


Figure 1.4: Structure of deoxycytidine and its analogue gemcitabine. Gemcitabine contains two fluorine substituted for the two hydrogen atoms in the 2' position of the deoxyribose sugar.

Human nucleoside transporter carrier (hNT) mediate the transport of physiologic nucleosides through the plasma membrane and are major routes of entry for a variety of nucleoside analogues used in cancer treatment due to their hydrophilic nature. There are two classes of hNTs with different mechanisms of transport: equilibrative nucleoside transporters (ENTs, Solute carrier 29 family) and concentrative nucleoside

transporters (CNTs, Solute carrier 28 family) (Spratlin et al., 2004). Although they are structurally unrelated transporters, they have overlapping substrate specificities. It was demonstrated that the majority of gemcitabine uptake is mediated by hENT1 and, to a lesser extent, by hENT2, hCNT1 and hCNT3 (Mackey et al., 1998; Ritzel et al., 2001). While all ENTs are considered to be ubiquitously expressed across most tissue types, they have a high protein expression in ovary (Boswell-Casteel and Hays, 2017). Human NTs accept only dephosphorylated compounds; therefore, gemcitabine is in a pro-drug form and undergoes intracellular phosphorylation. dFdC is initially phosphorylated by the deoxycytidine kinase (DCK) to its monophosphate form dFdCMP and subsequently phosphorylated by pyrimidine kinases to di- and tri-phosphate dFdCDP and dFdCTP. The latter one is the active antimetabolite that is incorporated in the C sites of the newly synthesised DNA strand during replication. An additional endogenous nucleotide is added alongside and masks dFdCTP, preventing DNA repair by base pair excision. This process inhibits DNA polymerase and induces the termination of chain elongation (Lorusso et al., 2006). This leads to a cytostatic effect, with a block in G1 phase of the cell cycle and may involve DNA mismatch sensors. Failure to repair the DNA subsequently triggers apoptosis and inhibits tumour growth (Jordheim et al., 2013; Slusarczyk et al., 2014).

Another cytotoxic mechanism of gemcitabine is through the inhibition of RRM1 and RRM2, subunits of ribonucleotide reductase (RR) by dFdCDP, the diphosphate form of gemcitabine. RR is a key enzyme of the *de novo* pathway for maintenance of the deoxyribonucleotide triphosphate (dNTPs) pools which replicating cells are heavily dependent on (Galmarini et al., 2001). This inhibition self-potentiates gemcitabine activity by decreasing intracellular concentrations of normal dNTPs (particularly dCTP), therefore, there is a higher probability that dFdCTP will be incorporated into DNA (Fig.1.5). dFdCMP upon conversion to dFdUMP may serve as either a substrate or an

inhibitor of the enzyme thymidylate synthase (TS) (Honeywell et al., 2015). Inhibition of TS could result in the depletion of the endogenous nucleotide thymidine monophosphate (dTMP) pools and block tumour cells growth. Over time, the concentration of the three faulty nucleotide increases in the tumour cells. When the level of faulty nucleotides analogues accumulated at the different DNA replication sites is beyond repair, it triggers apoptosis and tumours then stabilise or decrease in size.

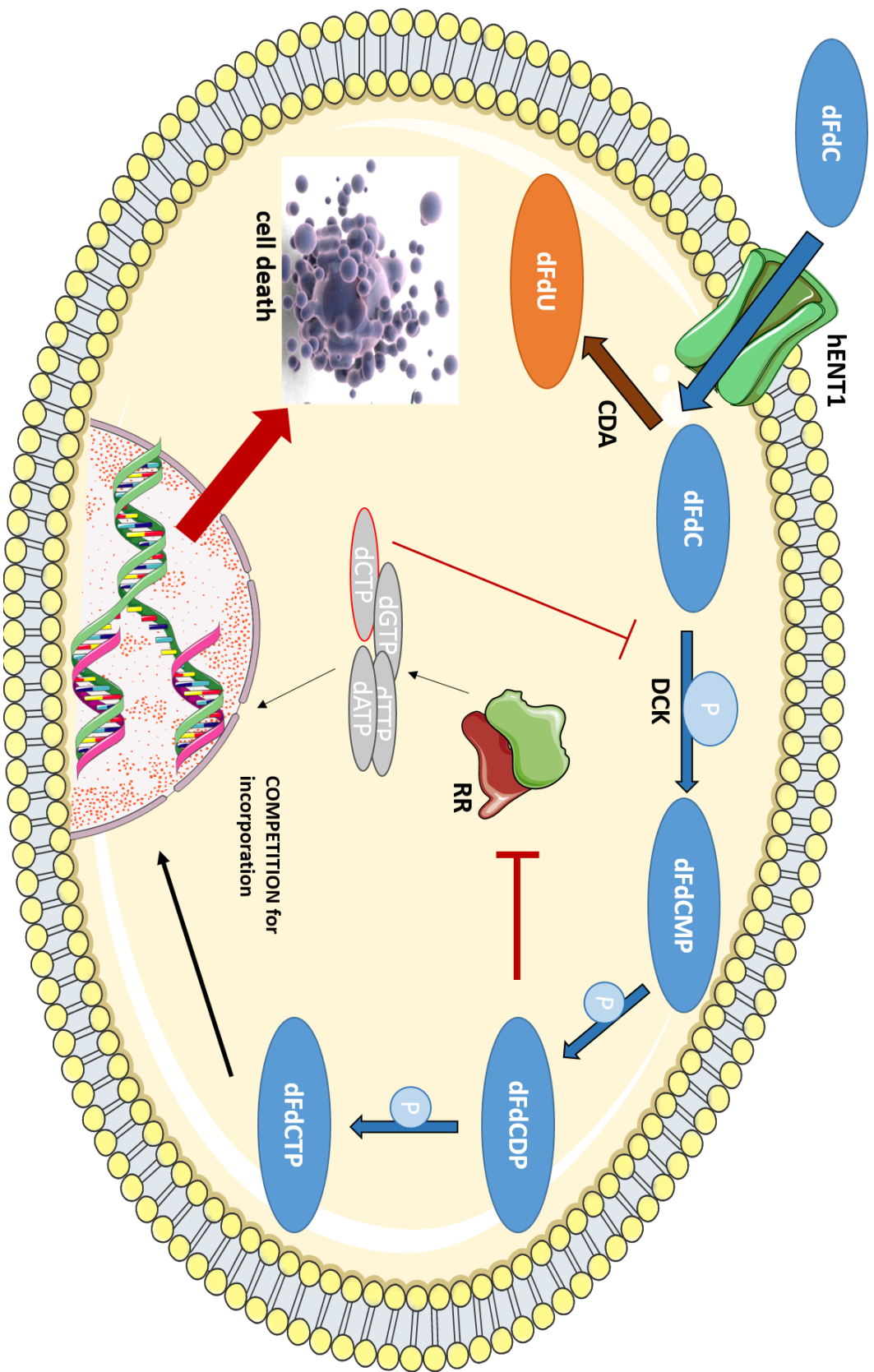


Figure 1.5: Mode of action of gemcitabine. Intracellular uptake of gemcitabine (dFdC) is mediated by hENT1 membrane transporter. It is activated by phosphorylation by DCK into dFdCMP which in turn is phosphorylated into dFdCDP which inhibits the ribonucleotide reductase. This results in reduction of intracellular pool of dNTP. dFdCDP is also phosphorylated into the active metabolite dFdCTP, that competes with endogenous dCTP for incorporation into DNA during replication. Inhibition of DNA synthesis by dFdCTP leads to apoptosis. However, the majority of gemcitabine is rapidly inactivated by deamination into dFdU. Endogenous dCTP pool is also responsible for regulation of DCK and can inhibit the enzyme.

Although nucleoside analogues, and particularly gemcitabine, represented a great breakthrough for cancer treatment, they show limited efficacy and patients develop resistance with time. Understanding the underlying resistance mechanisms is crucial for the development of novel agents that could circumvent these and therefore be administered to patients with relapsing or refractory disease. The main mechanisms result from molecular and cellular changes and are related to the metabolism of gemcitabine. Although little research on gemcitabine has been done in ovarian cancer tissues, several factors have been identified and well studied over the years in pancreatic cancer as it remains the main treatment.

Several studies have shown that a lack of hENT1 transporter is associated with resistance to gemcitabine *in vitro*, despite the presence of other transporters (Mackey et al., 1998; Achiwa et al., 2004). Spratlin and colleagues reported hENT1 as a potential predictive marker to select patients for treatment with gemcitabine, based on the protein expression in a small cohort of patients (Spratlin et al., 2004). Its significance was confirmed by two other research studies performed in larger cohorts (Giovannetti et al., 2006; Eto et al., 2013).

The deoxycytidine kinase (DCK) activates gemcitabine in a rate-limiting step by phosphorylating the pro-drug. *In vitro* investigations have established that a lack of DCK results in resistance to gemcitabine in different types of cancer cell lines, including ovarian, pancreatic, gastric and colorectal (Ruiz Van Haperen et al., 1994; Saiki et al., 2012). However, the prognostic value of DCK in patients is controversial as some studies found a correlation between DCK expression and overall survival after treatment with gemcitabine (Sebastiani et al., 2006; Maréchal et al., 2010, 2012), whereas others have not (Giovannetti et al., 2006; Farrell et al., 2016).

Inactivation of gemcitabine may result from rapid deamination by cytidine deaminase (CDA) to its di-fluoro-deoxyuridine (dFdU) metabolite (Fig.1.5) (Heinemann et al., 1988, 1992). dFdU has several postulated intracellular roles including regulating the transport, accumulation and cytotoxicity of gemcitabine, as well as being cytotoxic itself (Veltkamp et al., 2008; Rudin et al., 2011; Hodge et al., 2011).

Other factors of resistance to gemcitabine include ribonucleotide reductase subunits expression. The ribonucleotide reductase is responsible for the conversion of ribonucleotide diphosphate into deoxyribonucleotide diphosphate, which is a rate limiting step for DNA synthesis and repair. Gemcitabine inhibits RRM1 and RRM2, thereby reducing the endogenous pool of nucleotide and self-potentiating its cytotoxic effect. Minami and colleagues investigated mechanisms underlying the gemcitabine resistance in pancreatic cell line. They found RRM1 overexpression to be associated with resistance and that this could be reverse by inhibiting RRM1 activity (Minami et al., 2015).

Several studies have investigated the relationship of two or more of the factors together. Maréchal and colleagues measured the proteins levels of hENT1, DCK and RRM1 by immunohistochemistry in 434 patients who had resected pancreatic cancers and investigated their relationship with patients' overall survival time. Among this cohort, 243 patients were administered gemcitabine while the others received non gemcitabine regimens or did not receive treatment. They found that levels of hENT1, RRM1, and DCK were not associated with survival time for patients who did not receive adjuvant treatment. On the contrary, high levels of hENT1 and DCK were significantly associated with longer survival time among patients who were treated with gemcitabine (Maréchal et al., 2012). In another publication, hENT1 and RRM1 were investigated in biliary tract cancer, as potential predictive biomarkers for gemcitabine

as first line therapy. The study was conducted by immunohistochemistry on 44 patients previously treated with gemcitabine. Results showed that patients with clinical benefits from the treatment had high levels of hENT1 and low levels of RRM1 (Deng et al., 2014). Nakano and colleagues went further and investigated the relationship between the different factors of resistance to gemcitabine and established a ratio of expression levels of hENT1, DCK, RRM1, RRM2 and gemcitabine resistance (Nakano et al., 2007). The first report of expression of these genes in ovarian cancer was performed by Ferrandina and colleagues, in a small cohort of patients (n=25). Although they did not find correlation with clinical outcome, probably due to the small sampling, they suggest that gene expression was associated with more aggressive histotypes such as serous carcinomas. Furthermore, preliminary data suggested the importance of RRM2 in resistance to gemcitabine in ovarian cancer and this is warrant of further investigation in a larger cohort (Ferrandina et al., 2010). Similar findings about RRM2 were described in a study of 229 patients who had pancreatic cancer and received gemcitabine (Farrell et al., 2016).

The different resistance mechanisms to chemotherapy described in this section are among several others that also include epigenetics regulation that can silence tumour suppressor, the target of the drug can be altered or else there can be cell death inhibition (Fig.1.6) (Norouzi-Barough et al., 2018). Hypoxia is also known to be implicated in resistance to therapy. Rapid cancer cell proliferation, combined with structural and functional abnormalities in tumour blood vessels, result in regions within solid tumours that have significantly reduced oxygen availability compared to healthy tissues. Oxygen and nutrients are essential for solid tumour growth, and when sufficient oxygen is not provided growth arrest or necrosis occur in the unvascularised tumour core. Therefore, angiogenesis is required to keep the growing tumour oxygenated and this is associated with an increased risk of metastasis. The transcriptional activity of hypoxia-inducible

factor 1 α (HIF1 α) is the best understood mechanism of how cancer cells adapt to a hypoxic environment. HIF1 α plays a role in reprogramming cancer cells by regulating the expression of multiple genes involved in angiogenesis, and regulating the metabolism of glucose and as well as promoting cancer cell invasion. Reflecting these major roles, there is compelling evidence that hypoxia can compromise clinical outcomes in human cancer (Wilson Hay, 2011).

The knowledge accumulated over the years about the mechanisms of action of standard chemotherapy is of great value for the development of new compounds, which may overcome some of the resistance mechanisms, by acting independently of membrane transporters or activating kinases and therefore, less susceptible to degradation. A better understanding of the mechanisms of these new drugs will also contribute to the development of synergistic combinations with compounds that have different and/or complementary mechanisms of action.

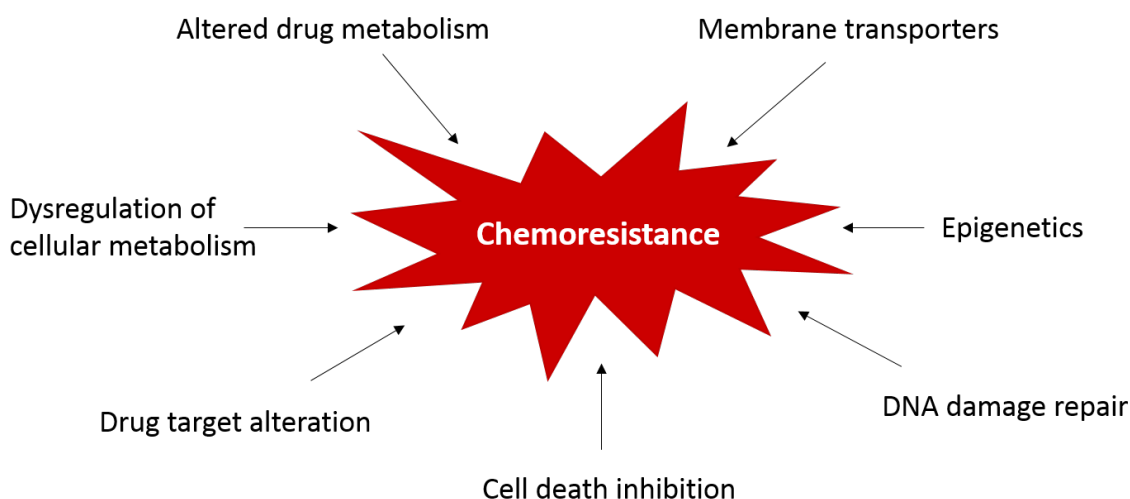


Figure 1.6: Factors involved in resistance to cancer. Different mechanisms can promote direct or indirect drug resistance in human cancer cells. These mechanisms can act independently or in combination and through various signal transduction pathways, therefore making it a complex issue to overcome.

1.3 ProTide technology as a new approach

In 1992, Chris McGuigan and his group created the ProTide technology, a pro-drug approach designed for the intracellular delivery of nucleoside analogue monophosphates (McGuigan et al., 1992). Synthesised as a lipophilic pro-drug, the nucleoside monophosphate passes through the cellular membrane by passive diffusion and, following enzymatic cleavage, the free mono-phosphate is released at high intracellular concentrations. The structure of the pro-drug consists of an aryl, an ester and an amino acid moiety to mask the negative charges of the nucleoside monophosphate (Fig.1.7). The ProTide approach has been successfully applied to several anti-viral nucleosides including abacavir and sofosbuvir (Derudas et al., 2010) and anti-cancer nucleosides Acelarin, NUC-3373 and NUC-7738.

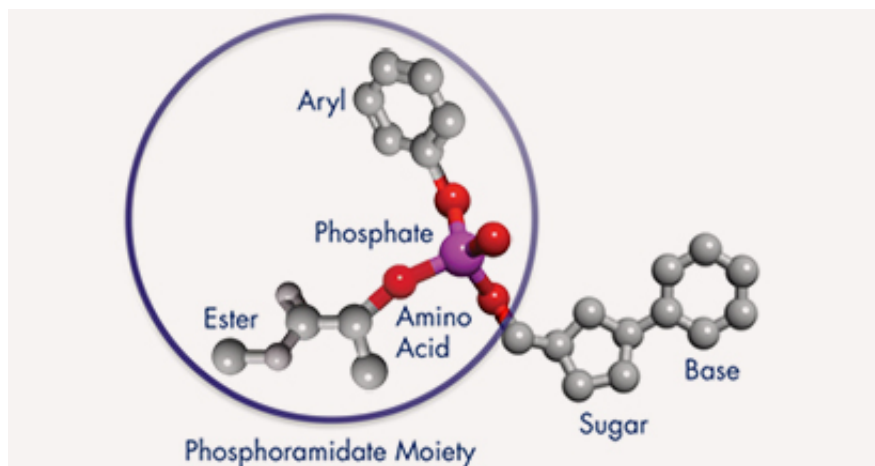


Figure 1.7: Structure of a ProTide (source: Nucana). A protected phosphate was added onto a nucleoside analogue scaffold, thereby creating a new chemical compound. The phosphoramidate moiety is composed of the phosphate, protected by an aryl, an ester and an amino acid. The properties of the ProTide vary with the individual components of the phosphoramidate moiety.

1.3.1 Acelarin, first anti-cancer ProTide

Acelarin, also called NUC-1031, is a phosphoramidate transformation of gemcitabine developed by Nucana plc, and the first anti-cancer ProTide to enter the clinic. Pre-activated analogue of gemcitabine, it circumvents hENT1-mediated transmembrane transport due to its increased lipophilicity. Once inside the cell, the phosphoramidate protective group is cleaved off by esterases and phosphoramidases, releasing dFdCMP which is then rapidly converted to dFdCDP and dFdCTP, bypassing the rate-limiting step of phosphorylation by DCK (Fig.1.8). Furthermore, Acelarin avoids CDA-mediated catabolism, thus preventing dFdU accumulation.

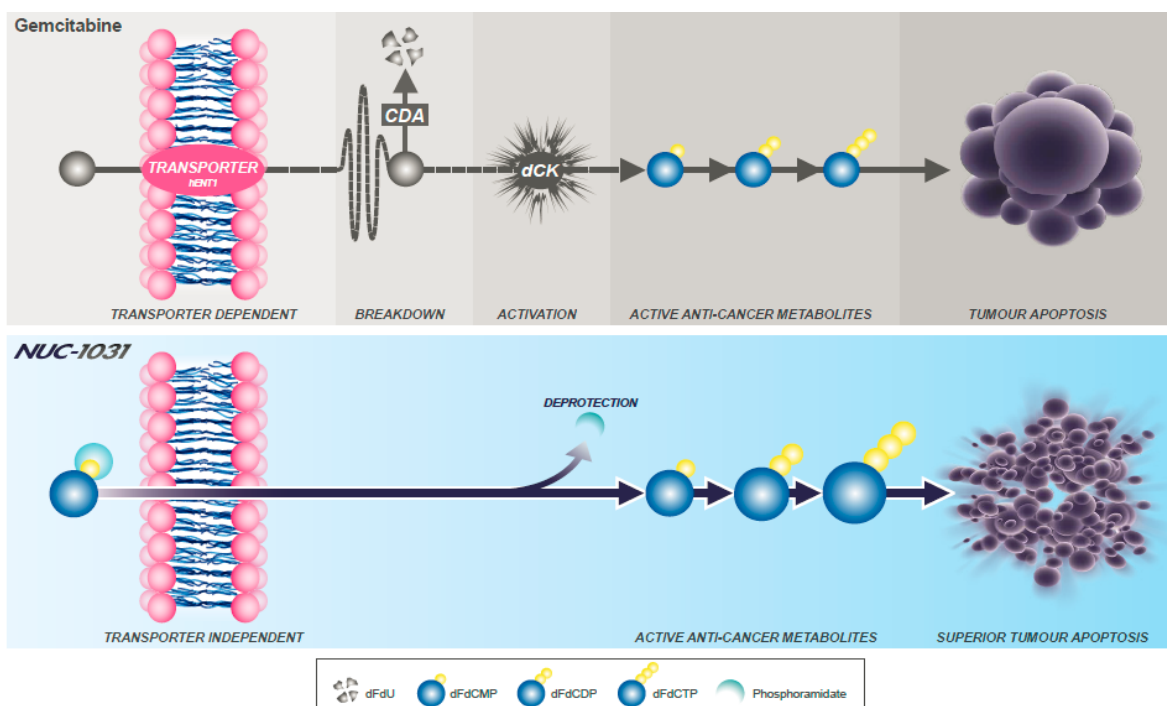


Figure 1.8: Acelarin (NUC-1031) overcomes resistance associated with gemcitabine (source: Nucana) Cellular uptake of Acelarin is independent from hENT1 transporter and once in the cell, it is protected from deactivation by the CDA. Unlike gemcitabine, it does not require activation by DCK as it already bears a phosphate group. Once the phosphoramidate group is removed, Acelarin is phosphorylated into its triphosphate active form (dFdCTP), which is incorporated in DNA during synthesis and this leads to tumour apoptosis.

Pre-clinical data show that Acelarin has superior efficacy, improved safety and overcome the key cancer cell resistance pathways encountered with gemcitabine (Slusarczyk et al., 2014). As Acelarin releases higher levels of the active agent and has the capacity to resist degradation, this results in superior efficacy and reduced toxicity (Slusarczyk et al., 2014). A statistically significant reduction in pancreatic tumour volume after treatment with Acelarin in tumour xenograft models was observed, compared with gemcitabine and control (McGuigan et al., 2011).

Acelarin is currently in phase II and phase III clinical trials for ovarian and pancreatic cancer respectively and the results look promising. In phase I only, Acelarin achieved clinical activity across multiple tumour types when all the patients had advanced, progressive solid tumours that were resistant or refractory to conventional chemotherapy, including gemcitabine (Blagden et al., 2018). The standard protocol in clinic is to administrate gemcitabine intravenously over 30min to the patients on day 1, 8 and 15 of a 4 weeks cycle. The study design of phase I for Acelarin clinical trial consisted of a 10min intravenous injection, administered on days 1, 8 and 15 of a 4 weeks cycle (Ghazaly, Rizzuto, Gabra, Habib, Leonard, Wasan, McGuigan and Blagden, 2014; Blagden et al., 2018). Blood samples were taken from patients prior to, and up to 24 hours following, treatment with Acelarin. Plasma and peripheral blood mononuclear cells (PBMCs) were separated from blood for pharmacokinetic analyses. PBMCs were assayed for dFdCMP, dFdCDP and dFdCTP using a liquid chromatography-tandem mass spectrometry (LC-MS/MS) method. Plasma and urine samples were assayed for Acelarin, dFdC and dFdU (Ghazaly, Rizzuto, Gabra, Habib, Leonard, Wasan, McGuigan and Blagden, 2014; Blagden et al., 2015). Acelarin has already demonstrated clinically significant anti-tumour activity, even in patients with prior gemcitabine exposure and some who were not responsive to gemcitabine. The pharmacokinetic studies showed a higher intracellular concentration of the active metabolite dFdCTP and a longer half-

life than gemcitabine. The intracellular concentration of dFdCTP throughout the 24 h period following administration of Acelarin was higher than reported for gemcitabine at its maximal concentration at 2h. Therefore, this suggests that tumour cells are exposed to considerably higher levels of the active metabolite dFdCTP when patients are treated with Acelarin, compared to gemcitabine. The phase III is randomised and designed to compare Acelarin and gemcitabine in patients with metastatic pancreatic cancers. More than 150 patients have been enrolled and it will be used to assess the efficacy of Acelarin over gemcitabine in a large cohort (Palmer et al., 2018).

1.3.2 Acelarin metabolism

The ProTide activation has not been fully elucidated yet but, like actors involved in gemcitabine metabolism, looking for activation of Acelarin could help determine biomarkers to define which patients would be likely to benefit from treatment. The novelty of Acelarin is the phosphoramidate moiety attached to a gemcitabine molecule that helps bypass the need of a transporter and deliver a pre-activated compound inside the cells. It is hypothesised that the initial step of metabolism consists of the cleavage of the ester moiety by an esterase-type enzyme to form the intermediate (Fig.1.9A), followed by an intramolecular attack of the carboxylate anion on the phosphorus centre, resulting in a spontaneous cyclisation and elimination of the aryl moiety (Fig.1.9B). This cycle being likely unstable, it would be hydrolysed (Fig.1.9C). Finally, the cleavage of the PN bond, mediated by intracellular phosphoramidase-type enzyme, releases the corresponding monophosphate (Fig.1.9D) (Saboulard et al., 1999; Jordheim et al., 2013). Carboxylesterase and phosphoramidase enzymes are likely to be involved in the activation of Acelarin. Based on the literature, Cathepsin A (CatA), carboxylesterase 2 (CES2) and Histidine triad nucleoside binding protein 1 (HINT1) are suggested to have

a role in the metabolism of ProTide compounds. The general knowledge about ProTide activation comes from studies based on the anti-viral compounds. Recent publications from the group who developed Acelarin showed carboxypeptidase Y and HINT1 to be involved in the activation of 6-substituted-5-fluorouridine ProTides (Shah et al., 2017; Slusarczyk et al., 2018).

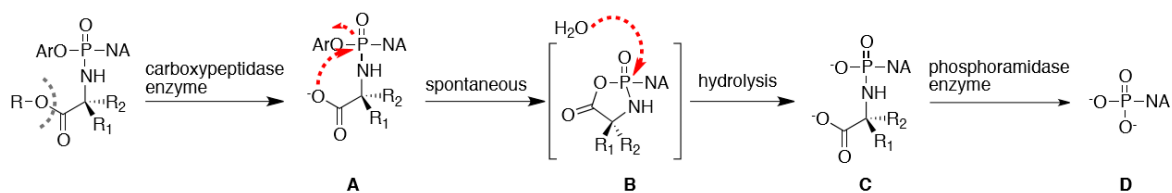


Figure 1.9: Putative activation of ProTide (source: Nucana). The intracellular activation of phosphoramidates is considered to be based on two enzymatic cleavages: the hydrolysis of the amino acid ester moiety by carboxypeptidases, and the P-N bond cleavage as the step that would release the corresponding nucleoside analogue monophosphate.

Cathepsin A, also called Carboxypeptidase A, hydrolyses peptides bonds in peptides and proteins and also esters in carboxy terminal end. It is known to be involved in the first step of metabolism of antiviral phosphoramidate pro-drugs, such as sofosbuvir, another ProTide (Murakami et al., 2010), as well as GS-9191 and GS-7340 respectively targeting papillomavirus and HIV (Birkus et al., 2007, 2011). Carboxylesterases (CES1, CES2 and CES3) are members of a family of α/β -fold serine hydrolases that mediate drug metabolism of compounds with ester, thioester, and amide linkages (Redinbo and Potter, 2005) and are known to hydrolyse several drugs. Pratt and colleagues investigated the hydrolysis of a pro-drug of gemcitabine, whether CES2 is responsible for this activation and whether cellular CES expression confers pro-drug sensitivity. The study was performed in several cancer lines and was correlated with pro-drug anti-proliferative response due to CES2 expression (Pratt et al., 2013). CES2 is known to be decreased in patients with advanced stage of ovarian cancer (Cai et al., 2009) and

this could potentially contribute to resistance to Acelarin.

HINT1 belongs to the highly conserved histidine triad superfamily that is ubiquitously expressed in diverse species including mammalian tissues. Its physiological function is based on its hydrolase activity towards purine nucleotide phosphoramidates substrates, cleaving them between nucleoside 5'-monophosphate and an amine leaving group (Bieganowski et al., 2002; Chou et al., 2006). It was demonstrated that a phosphoramidate ProTide of 2'-C- β - methylguanosine, an inhibitor of dengue virus 2, incorporates a HINT1 hydrolysable tryptamine phosphoramidate (Okon et al., 2017). Furthermore, Congiatu and colleagues reported enzyme-substrate interactions between purine analogues and HINT1. They concluded that the nature of the amino acid moiety seemed to affect the binding of the Protide to HINT1 and that even though pyrimidine based derivatives displayed a lower affinity, they could potentially act as substrate of Hint proteins (Congiatu et al., 2007). In addition, HINT1 is also considered as a tumour suppressor; it is involved in the regulation of apoptotic pathways by inducing an up-regulation of p53 expression (Li et al., 2008).

The ProTides have several potential advantages compared to currently available chemotherapies: ability to overcome the key resistance pathways; greater efficacy; broader clinical utility and improved tolerability. Acelarin may be of particular benefit to patients with resistance mechanisms to gemcitabine and be more effective or better tolerated.

1.4 Drug development: from pre-clinical studies to patients

In the process of drug development, it is crucial to monitor and ensure that the new chemotherapeutic drugs are potent and have an appropriate safety profile prior to administration to the patients. The first step consists of pre-clinical studies; with initial determination of the cytotoxicity by evaluating the half-maximal inhibitory concentration (IC_{50}) in human cancer-derived cell lines. Fundamental models, these cell lines are derived from cancer cells from patients. They are immortalised and can divide and grow over time, under certain conditions in a laboratory. Once the ability to inhibit cancer growth is proven, the pharmacokinetic and pharmacodynamic properties are evaluated in animals. This is performed in order to assess the safety profile of the compounds. After the safe dose for first-in-man study has been determined, the study may go on to clinical trial in patients. The process takes years and each step is carefully controlled in order to get approval by the Food and Drug Administration and European Medicines Agency.

1.4.1 Cancer cell lines and cytotoxicity

Cancer cell lines are powerful tools, used to screen for new potential anti-cancer drugs as well as help determine biomarkers that will assess efficacy of the compounds. Garnett and colleagues looked at more than 600 cancer cell lines to capture the high degree of genomic diversity in cancer and to identify rare mutant subsets with altered drug sensitivity (Garnett, 2012). A number of ovarian cell lines have been derived from patients and represent a panel of models to study the different aspects of the disease

and represent the different tumours types. Most cell lines have been used for decades but unfortunately, records of their creation are often missing, making it difficult to trace the exact histological origin of each cell line. Recent studies have established their genomic profiles and have enabled assumption of the subtype they are more likely to be derived from. Interestingly, the profile of SKOV3 and A2780 cell lines, which are present in 60% of the work published on ovarian cancer on PubMed, do not correspond to the main type of cancer (HGSOC) (Domcke et al., 2013), responsible for the most part of ovarian cancer and the most lethal. A2780 cells present a TP53 wild-type and mutations in PI3K and PTEN, which is more likely to be endometrioid or clear cell carcinomas (Beaufort et al., 2014). Although these cancers are known to be more likely resistant to traditional chemotherapies, A2780 cell line is sensitive to all of them (Caltová and Červinka, 2012; Beaufort et al., 2014). Despite not being representative of the most common type of cancer, A2780 is an excellent model to study drug resistance. It has been exposed to increasing concentrations of different main agents until cells became resistant (Lengyel et al., 2014) and nowadays, there is model to study resistance to gemcitabine (AG6000), cisplatin (ADDP), paclitaxel (A2780/PTX) and topotecan (A2780TR).

Cytotoxicity is one of the golden standards to assess drug potency in pre-clinical studies and new drugs are often compared to current compounds to determine their efficacy (Florento et al., 2012). However, a primary difficulty with *in vitro* studies comes from poor definition of study endpoints. Most of the currently used cytotoxicity assays are based on cell death analysis and/or inhibition of cell proliferation, without precise determination of changes in cell biology. Such studies are imprecise, as the induction of apoptosis is dependent on the dose of the compound being tested. Also, a recurring problem is the validation of a good test, as it has been demonstrated that a given compound may display IC_{50} inconsistencies between different cytotoxicity assays

(He et al., 2016; Damiani et al., 2019). Other assays commonly used *in vitro* include anti-proliferation of cancer cells (cellular enzymes and proteins, DNA synthesis, cellular ATP and membrane integrity), cell migration and invasion, angiogenesis, antioxidant and oxidative stress markers, cellular senescence, techniques to detect gene mutations and chromosomal alterations and assays for monitoring energy metabolism in cancer cells.

Molecules which exhibit nanomolar rather than micromolar IC_{50} values are highly sought after by researchers, based on the extrapolation that such high potency predicts clinical efficacy. A range of factors might contradict this assumption, such as the lack of aqueous solubility, poor bioavailability, and metabolic instability which could reduce efficacy in humans (Wong et al., 2012). On the other hand, drug concentrations or doses found in pre-clinical studies are often much higher than what can be achieved in patients, either above the maximally tolerated dose or much higher than the clinically relevant exposures. For these reasons, more and more emphasis is put on research related to the compounds mechanisms of action, rather than only determination of the degree of cell growth inhibition. Yet, for the purpose of high-throughput screening (HTS), cell-death related cytotoxicity remains a fast, easy and inexpensive way to determine drug potency.

Regarding Acelarin, the ProTide approach was applied to gemcitabine to overcome resistance mechanisms associated with it and during the initial screening, several parameters were taken into account. The IC_{50} of Acelarin was better than gemcitabine only in two of the four cell lines tested, but other parameters such as metabolic stability when incubated with human hepatocytes and liver microsomes made it a better candidate than another candidate compound which had a similar IC_{50} (Slusarczyk et al., 2014). Furthermore, it has been shown to be more potent on pancreatic xenograft than

in cancer cell lines *in vitro*. Ultimately, the effect of any candidate drugs on animal models of cancer is a better predictor of human drug efficacy than any *in vitro* assays.

1.4.2 Patient derived xenografts and animal models

Tumour xenografts have been widely used to investigate ovarian cancer growth, metastasis, and chemotherapy response in live animal for pre-clinical studies, as they often represent human tumours more accurately than *in vitro* systems. Human cancer cells are injected into immunocompromised mice to enable the cells to engraft without being eliminated by the immune system, and will grow as tumour. This can be done ectopically (subcutaneous) or orthotopically, using intraperitoneal (IP) and intra-ovarian bursa methods (Bobbs et al., 2015). Garcia-Cremades and colleagues characterised the effect of gemcitabine administered as single agent or in combination with carboplatin on ovarian xenografts in mice. The analysis of the pharmacokinetic and pharmacodynamic properties showed that their study may provide a robust pre-clinical model that could be used for translational approaches (Garcia-Cremades et al., 2017).

While A2780 cell line and chemotherapy-resistant derivatives are commonly used in xenograft studies as they allow for validation of therapies and studies of drug resistance (Shaw et al., 2004; Bobbs et al., 2015), the use of an established cancer cell line can result in a population that is not truly representative of the original tumour and will therefore produce a different response to therapy compared to those seen in patients (Hasan et al., 2015). Patient-derived xenograft (PDX) was developed in order to improve the model. In contrast to the cell lines and their xenografts, patient's tumour tissue excised at the time of surgery is immediately transplanted into immunodeficient mice. Unlike xenografts formed from cell lines, PDXs recapitulate aspects of ovarian cancer like metastasis and ascites formation. PDX models have been ap-

plied to pre-clinical drug testing and biomarker identification established from cancers including melanoma, breast, pancreatic, lung, colorectal, and ovarian (Boone et al., 2015; Hernandez et al., 2016). However, xenograft models from both cancer cells or PDX are conducted in immunocompromised mice, therefore the contribution of the full immune system in chemotherapy response and tumour growth inhibition is missing. A new study just showed that it is possible to tolerise murine fetuses to human tumour cells (Basel et al., 2018) and this could improve the animal model to make them more relevant.

1.4.3 Combination treatments for ovarian cancer

Once the pre-clinical studies have been successful, the next stage is to start clinical trials in patients. The first step is to assess the safety profile and anti-tumour activity in patients and define the recommended Phase II dose. With the limited effect of a single drug and the inherent and acquired resistances, combination of two or more drugs is a cornerstone in the treatment of cancer. This is used to achieve an improved therapeutic result by exploiting the chances for better efficacy, decreased toxicity, and reduced development of drug resistance (Bijnsdorp et al., 2011; Fouquier and Guedj, 2015). Based on the knowledge of the biology of each compound, combination studies can be initially investigated in cancer cell lines, then in human xenograft used in appropriate animal models and finally in patients.

The first line of chemotherapy following debulking surgery is often carboplatin with paclitaxel for six cycles. During the first clinical study, 410 women with advanced ovarian cancer were randomly assigned to receive $75\text{mg}/\text{m}^2$ of cisplatin with $135\text{ mg}/\text{m}^2$ paclitaxel over a period of 24 h or with cyclophosphamide (McGuire et al., 1996). Incorporating paclitaxel in the first line therapy significantly improved

the progression-free survival (18 vs 13 months) and overall survival (38 vs 24 months) and it became a standard treatment for ovarian cancer. Long-term follow-up confirmed the efficacy established during this first study (Piccart et al., 2000, 2003). With the development of carboplatin, which exhibited less toxic effect than cisplatin, new trials happened to successfully establish the profile of carboplatin-paclitaxel (du Bois et al., 2003; Ozols et al., 2003).

When patients experience relapse of refractory disease, gemcitabine is often used as second line treatment as it has a well-proven activity in platinum-paclitaxel resistance ovarian cancer patients and does not present with cross-resistance with platinum compounds. The combination of gemcitabine with cisplatin has been extensively studied in several solid tumours, after evidence of synergism between the two drugs in ovarian cancer cell line A2780 and its cisplatin resistant derivative were established (Bergman et al., 1996, 2000). Successful clinical trials with cisplatin-gemcitabine combination in patients with platinum-resistant ovarian cancer were reported. In the study conducted by Rose, eleven of the thirty-six patients with platinum-resistance had a partial clinical responses and four had a complete response, with median survival of 12 months (Rose et al., 2003); similar results were reported by another group (Nagourney et al., 2003). In addition, recent studies have shown the clinical activity and tolerability of bevacizumab-gemcitabine combination in platinum-resistant recurrent ovarian cancer (Bevis et al., 2011; Komiyama et al., 2018; Takasaki et al., 2018).

1.5 Identification of biomarkers

Traditionally, cancer drugs were identified mainly through empirical approaches (Chabner and Roberts, 2005). This has led to a generation of chemotherapeutic agents relatively nonspecific in targeting cancer cells, and that often benefit only a minority of patients, because of both intrinsic and acquired drug resistance. Therefore, there is a need to develop a more personalised approach to cancer treatment, for which patients can be pre-selected for specific therapies.

1.5.1 Loss-of-function screen

Over the last decade, the development of genomic technology has revolutionised modern biological research and drug discovery and development. Functional genomic approaches are performed on a global scale and have enabled a better understanding of molecular mechanisms underlying cancer development, biomarker discovery, drug target identification and drug resistance (Chen et al., 2009). Among the array of new high-throughput technologies (DNA sequencing, single-nucleotide polymorphism genotyping, comparative genomic hybridisation, proteomics and gene expression micro-arrays), the loss-of-function genetic screens are widely used to identify genes and cellular signalling pathways involved in drug resistance, as well as potential drug target (Berns et al., 2004). Before the development of CRISPR/Cas9 system, most large-scale knockdown screens were achieved using RNA interference (RNAi) gene expression silencing technology (Ito et al., 2005; Root et al., 2006). A RNAi library is introduced into cells, which are then treated with a drug of interest. The differential abundance of RNAi reagents between treated and non-treated cells is compared, to identify genes conferring resistance or sensitivity to the drug. A growing concern with using RNAi was

the off-target effects, one siRNA can potentially bind mRNAs with limited sequence complementarity and consequently repress hundreds of transcripts (Sigoillot and King, 2011). CRISPR/Cas9 system offers new alternatives to RNAi strategy to inactivate gene expression more efficiently and libraries as for RNAi are available for genome functional screens (Sanjana et al., 2014; Shalem et al., 2014).

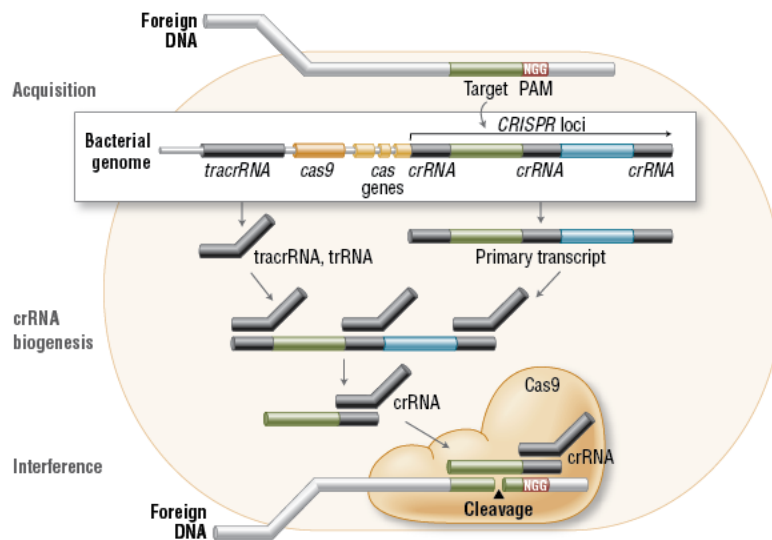


Figure 1.10: CRISPR/Cas9 is a bacterial adaptive immune system (source: NEB). CRISPR locus consists of a transactivating CRISPR RNA (*tracrRNA*), Cas genes and a CRISPR RNA (*crRNA*). Upon recognition and integration of foreign DNA into the *crRNA* region, a *tracrRNA* and a precursor CRISPR RNA (*precrRNA*) are generated and they interact to form a complex processed, this is the *crRNA* biogenesis. The resulting *tracrRNA*-*crRNA* recruits Cas9 protein and guide it to the sequence complementary to the *crRNA* on the foreign DNA to induce a cleavage.

1.5.2 CRISPR/Cas9 system

CRISPR (Clustered Regularly-Interspaced Short Palindromic Repeats)/Cas9 is a RNA-guided DNA endonuclease system. Originally discovered in bacteria and archeobacteria, which use it as an adaptive immune system to protect themselves from infection by viruses (Rath et al., 2015), it is now a powerful tool in gene-editing technology. It

enables to knockdown specific gene expression in an irreversible manner with higher efficacy than the other techniques, including RNAi. It is composed of a short non-coding guide RNA (gRNA), that matches a desired target gene, and Cas9 (CRISPR-associated protein 9), an endonuclease that causes double-strand DNA break.

The exogenous nucleic acid is integrated into the CRISPR locus. Then, a transactivating small RNA (tracrRNA) binds repeat sequences of CRISPR RNAs (crRNAs). These are transcribed from this CRISPR locus, thus forming an RNA duplex that is processed in a mature tracrRNA-crRNA. The crRNA acts as a guide for the Cas9 to cleave this nucleic acid by inducing a specific double strand DNA break (Fig.1.10) (Reis et al., 2014). Two mechanisms can be involved in the repair of double strand breaks. The non-homologous end joining (NHEJ) can generate insertion/deletion (indels), this may disrupt the translational reading frame of a coding sequence, thus causing gene disruption and inactivation. The second one is homology-directed repair (HDR) which can be used to introduce specific point mutations or to insert desired sequences through recombination of the target locus with exogenously supplied DNA donor templates.

CRISPR/Cas9 system was modified and a simplified two-components system has been developed by combining trRNA and crRNA into a single synthetic single guide RNA (sgRNA) (Mali et al., 2013). A lentiviral vector has been engineered to deliver Cas9, a single guide RNA, and a puromycin selection marker into target cells (plentiCRISPR) (Fig.1.11); making this system amenable to adaptation for genome editing (Jinek et al., 2012; Hendel et al., 2015).

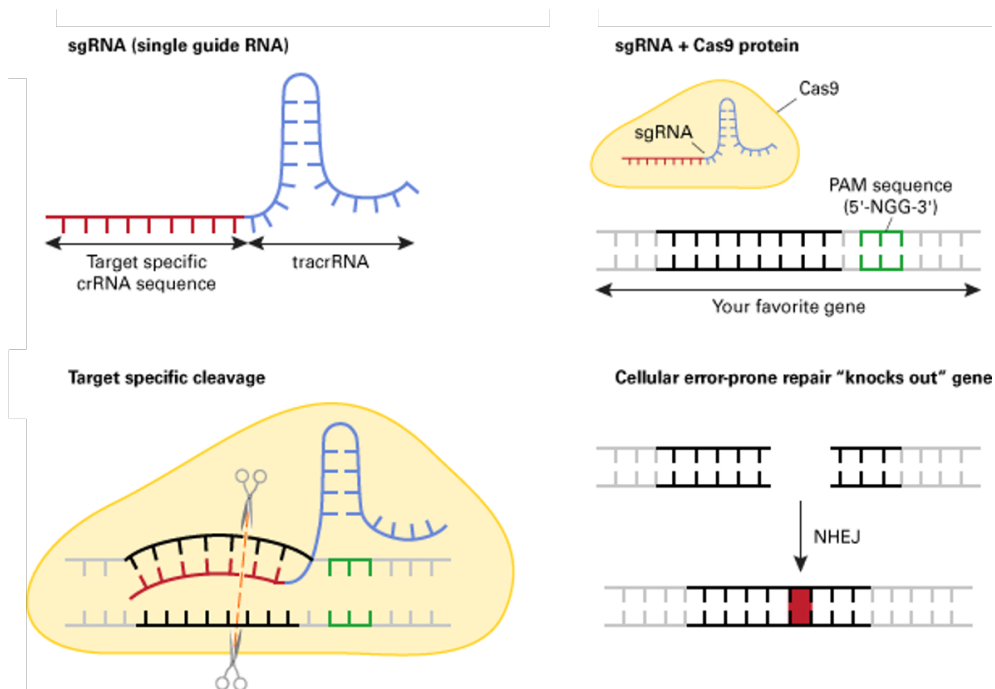


Figure 1.11: The principle of CRISPR/Cas9-targeted genome editing (source: Clontech). A single guide RNA (sgRNA) with a specific sequence that is complementary to a genomic target, is associated with a nuclease called Cas9 protein. This complex binds its DNA target site, adjacent to a PAM sequence. A cleavage is induced, which results in a DNA double strand break. The NHEJ (Non-Homologous End Joining) DNA repair system is activated but cellular prone-error repair introduces insertion or deletion mutations, disrupting the target gene which is then knockdown.

1.5.3 Digital and quantitative pathology

Biomarker research was routinely based on immunohistochemistry (IHC) applied to tissue biopsies and manually scored by a pathologist. The characterisation of the appropriate tumour areas within a complex tissue section requires a trained eye and the visual interpretation of the expression patterns and intensities in tumour cells and surrounding tissues is subject to personal interpretation. This represents laborious and expensive work and despite the existence of robust guidelines, the assessment of IHC expression patterns of tissue is subject to poor inter-laboratory, inter-observer and

intra-observer reproducibility (Varga et al., 2012; Polley et al., 2013). This variability is slowing the progress of biomarker discovery and delivery of precision medicine. Therefore, this method is no longer sufficient to support large-scale tissue biomarker trials, and cannot ensure the reproducible and objective analysis essential for reliable clinical correlation and candidate biomarker selection.

The implementation of whole slide scanning has led to a rapid development of digital pathology in the last few years. Image analysis with automated digital algorithms allows the accurate recognition of tumour and non-tumour cells within sections, in addition of a reproducible IHC scoring of relevant biomarkers, less subjective than manual scoring (Bankhead et al., 2018). Furthermore, the development of artificial intelligence, machine learning and deep learning technologies promise great improvement in the diagnosis of cancer and biomarker discovery (Harder et al., 2018).

1.6 Hypotheses and aims

Inherent and acquired resistance of chemotherapy agents remain a major issue in cancer management and there is a need for development of new treatment for ovarian cancer. Acelarin is a new compound designed to overcome the main resistance mechanisms associated with gemcitabine, however little is known about its molecular mechanisms of action.

The first aim of this thesis was to compare both Acelarin and gemcitabine in cancer cell lines to unravel the underlying mechanisms of Acelarin that lead to cell death. An array of cell biology techniques were used to compare both drugs and their effect on cancer cells over time.

The second aim was to study the interaction of Acelarin with cisplatin in an *in vitro* model of ovarian cancer to identify which sequence would be most beneficial for the patients, based on their sensitivity to platinum treatments. Different sequences of treatments were considered.

The last aim was to determine any potential biomarkers involved in resistance to Acelarin by using two different approaches. A genome-wide CRISPR/Cas9 knockdown screen was previously performed in a pancreatic cell line to determine factors modulating sensitivity to Acelarin and two candidates involved in the pyrimidine synthesis were discovered. As part of this thesis, the loss of their expression was investigated in an ovarian cancer cell line. The second method was a more specific candidate gene approach based on the metabolism of Acelarin. The clinical relevance of the different candidates was investigated in tissue biopsies from patients enrolled in the phase I cohort for Acelarin.

2 | Material and methods

2.1 Cell culture

A panel of eight adherent ovarian cell lines was used for this study: A2780, CAOV3, OVCAR3, OVCAR4, PE01, PE04, PE06 and SKOV3. Cells were a kind gift from Dr Simon Langdon, from the Division of Pathology Unit in University of Edinburgh. Short tandem repeat (STR) profiling was carried out previously to ensure the quality and integrity of their genotype, as well as mycoplasma test. STR typing was carried out in November 2009 using the AmpFLSTR Identifiler PCR amplification kit (Applied Biosystems, Warrington, UK), confirming that matched pairs were from the same patient and matched previous profiles. The mutation status for the main genes involved in ovarian cancer are displayed in Table 2.1.

Cells were cultured in RPMI-1640 media (Gibco®), Cat. no. 61870044) supplemented with 10% heat-inactivated fetal calf serum (FCS) and penicillin/streptomycin (100IU/mL). They were grown as monolayer cultures in a humidified atmosphere of 5% CO₂, at temperature of 37°C. When cell number achieved about 80% confluence, they were trypsinised: media was removed and cells were washed once with PBS before being incubated with trypsin (Gibco®), Cat. no. 25300) for a few minutes at 37°C. Trypsin was neutralised by addition of media and cells were spun down at 435 x g for 5 min. The pellets were re-suspended in normal culture media and transferred into flasks, at an appropriate dilution.

Cell line	TP53	BRCA1	BRCA2	PI3KCA	KRAS	BRAF	PTEN
A2780	WT	WT	mut	mut	WT	WT	mut
CAOV3	mut	WT	WT	WT	WT	WT	WT
OVCAR3	mut	WT	WT	WT	WT	WT	WT
OVCAR4	mut	WT	WT	WT	WT	WT	WT
PE01	mut	WT	mut	WT	WT	WT	WT
PE04	mut	WT	mut*	WT	WT	WT	WT
PE06	mut	WT	mut*	WT	WT	WT	WT
SKOV3	mut	WT	WT	mut	WT	WT	WT

Table 2.1: Molecular signature of cell lines (sources: (Ikediobi et al., 2006; Sakai et al., 2009; Beaufort et al., 2014)). Information on the mutation status for the main genes known for ovarian cancer for the different cell lines. WT : wild-type, mut: mutation. PE01, PE04 and PE06 cell lines were derived from the same patient; mut* : a secondary BRCA2 mutation occurred that was not present in PE01 cells.

2.1.1 Cryopreservation and cell recovery from liquid nitrogen

Cells were harvested following the usual protocol. Cell pellets were re-suspended in 4 mL of freeze mixture-heat-inactivated FCS/10% DMSO and aliquoted into cryopreservation vials. All cells were frozen and stored in liquid nitrogen. Cell recovery was performed by thawing the freeze mixture with warm culture media. This was transferred into a universal and media was added up to a volume of 25 mL. Cells were spun down at 435 x g for 5 min, re-suspended in media and transferred into a flask for culture routine.

2.1.2 Optimisation of cell number for growth inhibition experiments

Cell numbers were optimised for all cell lines, using a Celigo Scanning microscope (Nexcelom, USA). Cells were plated at different densities in 200 μ L RPMI-1640 (100 to 1000 cells/well or 500 to 5000 cells/well) in 96-well culture plates (in 6 replicates) and then scanned every day with Celigo, using ‘confluence with image based auto focus’ and

‘best contrast’ software options. In addition, a Sulforhodamine B assay was performed on the last day (Day 6).

2.1.3 Cytotoxicity analysis

All experiments in terms of drug treatment utilised the following protocol. Cells were harvested in RPMI-1640 supplemented with 10% FCS and penicillin/streptomycin, seeded according to their optimal initial numbers in a 96-well tray, in a volume of 200 μ L media per well, and let to grow in a humidified atmosphere of 5% CO₂ at 37°C for 48 h prior to drug treatment.

Acelarin ((2'-deoxy-2',2'-difluoro-D-cytidine-5'-O-[phenyl(benzyloxy-L-alanyl)] phosphate) provided by NuCana plc), gemcitabine ((4-amino-1-[(2R,4R,5R)-3,3-difluoro-4-hydroxy-5-(hydroxymethyl)oxolan-2-yl]pyrimidin-2-one); Sigma-Aldrich), sulforaphane (Sigma-Aldrich) and fluvastatin (Sigma-Aldrich) were re-suspended in 0.1% DMSO and kept at a concentration stock of 10 mM, at -20°C. Cisplatin (1 mg/mL, TevaUK) was kept at 4°C. The vials were put in the incubator at 37°C for a couple of minutes. Acelarin and gemcitabine were diluted 1:10 in pre-warmed RPMI-1640 to get a concentration of 10 μ M, final concentration of cisplatin, fluvastatin and sulforaphane was 100 μ M. This stock solution was used for any further dilution required for experiments and was made-up fresh every time. Deoxycytidine (Sigma-Aldrich) was re-suspended at a stock concentration of 10 mM in distilled water, and stored at -20°C.

Cells were treated with a range of concentrations for each drug (Table 2.2), for different periods of time as specified in the results section. After treatment, media was then removed and replaced with drug-free media. At 96 h post-treatment, cells were fixed by 25% cold trichloroacetic acid (50 μ L/well) and incubated for 1 h at 4°C. Plates

were washed 10 times with running tap water and dried at 50°C. Cells were stained with sulforhodamine B dye (0.4% solution in 1% acetic acid, 50 μ L/well) for 30 min, washed 4 times with 1% acetic acid and dried again at 50°C. The dye was dissolved in 150 μ L Tris buffer solution (10 mM, pH 10.5) for at least 1 h prior reading. The optical density (OD) was recorded using a Biohit BP800 Microplate reader at 540 nm.

OD value for each concentration was normalised to the control. The half-maximal inhibitory concentration (IC_{50}) was calculated using GraphPad Prism software. Concentration values were put in the X-axis and transformed into logarithm: $X = \text{Log}(X)$. IC_{50} values for each drug were obtained by using the ‘Fit curve with non-linear regression: log(inhibitor) vs normalised response’.

Acelarin	gemcitabine	cisplatin	sulforaphane	fluvastatin
5 nM	5 nM	0.5 μ M	0.5 μ M	0.5 μ M
10 nM	10 nM	1 μ M	1 μ M	1 μ M
25 nM	25 nM	2 μ M	2 μ M	2 μ M
50 nM	50 nM	4 μ M	4 μ M	4 μ M
75 nM	75 nM	8 μ M	8 μ M	8 μ M
100 nM	100 nM	12 μ M	12 μ M	12 μ M
150 nM	150 nM	16 μ M	16 μ M	16 μ M
250 nM	250 nM	20 μ M	20 μ M	20 μ M
500 nM	500 nM		25 μ M	25 μ M
750 nM				

Table 2.2: Drug concentrations used for cytotoxicity assays. The range of concentrations for each drug was determined based on cell sensitivity tested in the lab and information found in the literature. The control was composed of drug-free media with 0.1% DMSO.

2.2 Hypoxia

Cells were kept in a humidified hypoxic chamber (H35 Hypoxystation, Don Whitley Scientific) at 37°C, 5% CO₂ and 0.5% O₂. In order to become hypoxic, they were put in the chamber at least 24 h prior any treatment or experiment.

2.3 Time-lapse

Cells were grown as per usual condition, in 25cm² flasks and left for 24 h. Flasks were put under the CytoMate Camera for 24 h prior to any treatment. The light of the camera induced heat, causing condensation to form on the top of the flask. This needed to be removed before recording any experimental data.

Cells were treated following the usual protocol, using IC₅₀ for Acelarin and gemcitabine as well as a control drug-free media, for 2 h. A picture was recorded every 7.5 min, allowing to follow the fate of the cells over several days. Data collected included a movie as well as a graph representing the percentage of cell coverage over the duration of the movie (96 h).

2.4 Flow cytometry

2.4.1 Samples preparation

Cells were seeded in 6 cm petri dishes and grown as per usual before treatment with IC₅₀ of Acelarin and gemcitabine, as well as a control drug-free media, for 2 h. Media

was removed after 2 h and cells left to grow until they were harvested, at different time points (2 h, 24 h, 48 h, 72 h and 96 h). 30 min before each time point, 4 μ L of a 10 mM BrdU stock (Invitrogen B23151) was added to the media to achieve a 10 μ M solution and cells were incubated for 30 min at 37°C. Cells were trypsinized and spun down at 435 x g for 5 min, washed in 5 ml PBS and centrifuged again at 435 x g for 5 min. 1 mL of ice-cold 70% ethanol was added to the samples while vortexing. Samples were stored at 4°C until ready to stain and analyse on the flow cytometer.

2.4.2 Staining & analysis

1.5 mL of pepsin (0.4 mg/mL in 100 mM HCl - Sigma: P6887) was added to each sample in order to digest the proteins and incubated at 37°C for 45 min with frequent mixing. Samples were centrifuged at 510 x g for 4 min and supernatant was discarded. 2 mL of 2N HCl / 0.5% Triton X-100 was added and incubated for 30 min at room temperature. Samples were centrifuged at 510 x g for 4 min prior being washed with 2 mL of 0.1 M Sodium Tetraborate solution, pH8.5, followed by two centrifugations at 510 x g for 4 min with a PBS wash in between. Hydrochloric acid is used to denature DNA so that anti-BrdU antibody can bind to BrdU, while Tetraborate solution neutralized the effect of HCL.

2 mL of PBS / 0.5% BSA / 0.5% Tween 20 solution containing mouse anti-BrdU (Beckton Dickinson; clone B44; 347580) at a dilution of 1:100 was added for 30 min at room temperature, followed by 2 centrifugations at 510 x g for 4 min with a PBS wash in between. 2 mL of PBS / 0.5% BSA / 0.5% Tween 20 solution containing anti-mouse FITC (Alexa Fluor 488; Invitrogen #A11001) at a dilution of 1:200 was added to the cells for 30 min at room temperature in the dark, followed by 2 centrifugations at 510 x g for 4 min with a PBS wash in between. 100 μ L of RNase A (0.1 mg/mL - Qiagen

103130) was added to the samples, as well as 400 μL of Propidium Iodide (50 $\mu\text{g}/\text{mL}$ - Sigma P4864).

Tubes were wrapped in tinfoil and stored on ice in the dark until ready to analyse on the flow cytometer. Samples were run on a BD FACSJazz™, the 488nm laser was used for measuring forward scatter, side scatter, and PI fluorescence (685/35 bandpass filter). Data analysis was done using FlowJo software V10.

2.5 Gene expression alteration

2.5.1 Clustered Regularly Interspaced Short Palindromic Repeats (CRISPR)

Cloning

sgRNA were chosen from a genome-scale CRISPR-Cas9 knockout (GeCKO) library and their length is 20mer (Fig.2.1). A 5' phosphorylation was added to the customised sgRNA oligonucleotides (Table 2.3) (Invitrogen). Upon arrival, they were re-suspended at 1 nmol/ μL with milliQ water. Annealing solution was prepared with 1 μL of diluted forward oligo, 1 μL of diluted reverse oligo (0.1 nmol/ μL), 10x NEB buffer 2 and MiliQ water. It was first incubated for 5 min at 95°C, then for a further 10 min at 70°C in a water bath and samples were left in water to cool down to room temperature.



Figure 2.1: Design oligos for CRISPR. When designing the primers, a short sequence CACCG was added at the beginning and for the reverse primer a AAAC before and a C after the 20 mer.

Name	Sequence
sgScr	5'-CACCGCCTAAGGTTAAGTCGCCCTC-3' (forward) 5'-AAACGAGGGCGACTTAACCTTAGGC-3' (reverse)
sgDCKa	5'-CACCGAAGGTAAAAGACCATCGTTC-3' (forward) 5'-AAACGAACGATGGTCTTTTACCTTC-3' (reverse)
sgDCTPP1a	5'-CACCGCAGCCCGGAGCCCACGCTCG-3' (forward) 5'-AAACCGAGCGTGGGCTCCGGGCTGC-3' (reverse)
sgDCTPP1b	5'-CACCGCCTAGTCAGTGGAAAACCGA-3' (forward) 5'-AAACTCGGTTTTTCCACTGACTAGGC-3' (reverse)
sgDCTPP1c	5'-CACCGTGCTTACATGTCCTCGAGCG-3' (forward) 5'-AAACCGCTCGAGGACATGTAAGCAC-3' (reverse)
sgDCTPP1d	5'-CACCGGGGAACAGTTCCATCAGCCT-3' (forward) 5'-AAACAGGCTGATGGAACTGTTCCCC-3' (reverse)
sgDCTPP1e	5'-CACCGGTTCCGCAGCAAACCTCAGCA-3' (forward) 5'-AAACTGCTGAGTTTGCTGCGGAACC-3' (reverse)
sgDCTPP1f	5'-CACCGGCGACGCTACCCAGCCCATC-3' (forward) 5'-AAACGATGGGCTGGGTAGCGTCGCGC-3' (reverse)
sgHINT1a	5'-CACCGCCTGGTGGCGACACGATCTT-3' (forward) 5'-AAACAAGATCGTGTCGCCACCAGGC-3' (reverse)
sgHINT1b	5'-CACCGGGTATCACCAGAAAATGTGT-3' (forward) 5'-AAACGATTTCTGTGGCAGAAGATGC-3' (reverse)

Table 2.3: sgRNA used for CRISPR knockdown

LentiCRISPRv2 (Addgene, Plasmid #52961) was used to as vector to transduced target cells with sgRNA of interest. A solution composed of pLentiCRISPRv2, FastDigest Esp3I (BsmBI) (Fermentas/ Life Technologies FD0454), 10X FastDigest buffer, CIP (NEB), 100 mM DTT (freshly prepared) and distilled water was incubated at 37°C for 30 min. Both control and digested vectors were supplemented with 6X DNA loading buffer (New England Biosciences, UK), loaded on a 0.8% agarose gel TAE with ethidium bromide and run at 40V for 45 min. Under a UV light, bands appeared on the gel. The larger band in the digested sample (12.8kb) was excised and weighted before being extracted using a QIAquick Gel Extraction Kit (28704) and eluted in 50 μ L of EB (Tris-HCl pH8.5).

Ligation of sgRNA with the vector was done using a Roche Rapid Ligation Kit (11635379001 Roche) and following the protocol furnished with it. A ligation mix with no sgRNA oligo was prepared as a control for self-ligation. Ligation reactions were incubated at 16°C overnight. The plasmids obtained were kept at -20°C.

Plasmids were amplified by transformation into competent bacteria STBL3 (C737303). Bacteria were thawed on ice, 5 μ L of ligation mix was added to them and they were incubated on ice for 30 min. A heat shock was performed at 42°C for 45 sec prior to another incubation of 2 min on ice. LB was added to the mix and this was incubated on a shaker at 37°C for 60min. 200 μ L was plated on 10cm petri dishes containing LB agar with ampicillin (100 μ g/mL), a selective antibiotic, and incubated at 37°C overnight. 3 single colonies per condition were picked to be cultured in LB carb (100 μ g/mL carbenicillin) for 16h overnight in a shaking incubator at 37°C. Stocks of cultures were made by adding 750 μ L bacteria to 250 μ L 80% glycerol and froze down at -80°C for future use. Miniprep to collect and purify DNA from bacteria was performed using a Qiagen Miniprep kit (27104), following manufacturer's protocol. The purified DNA was

quantified with NanoDrop 2000 micro-volume spectrophotometer (Thermo Scientific).

A double digestion was done, in order to verify if the colonies carried the correct insert (sgRNA) in pLentiCRISPRv2, using NdeI and EcoRI restrictive enzyme (New England Biolabs, UK)s. The plasmid was incubated for 30 min at 37°C with the enzymes, or without for the negative control and the final products were ran on a 2% agarose gel with ethidium bromide. The gel was analysed in a BioRad machine with UV light (Fig.2.2). Samples were sent for sequencing to verify the insert was correct and not mutated.

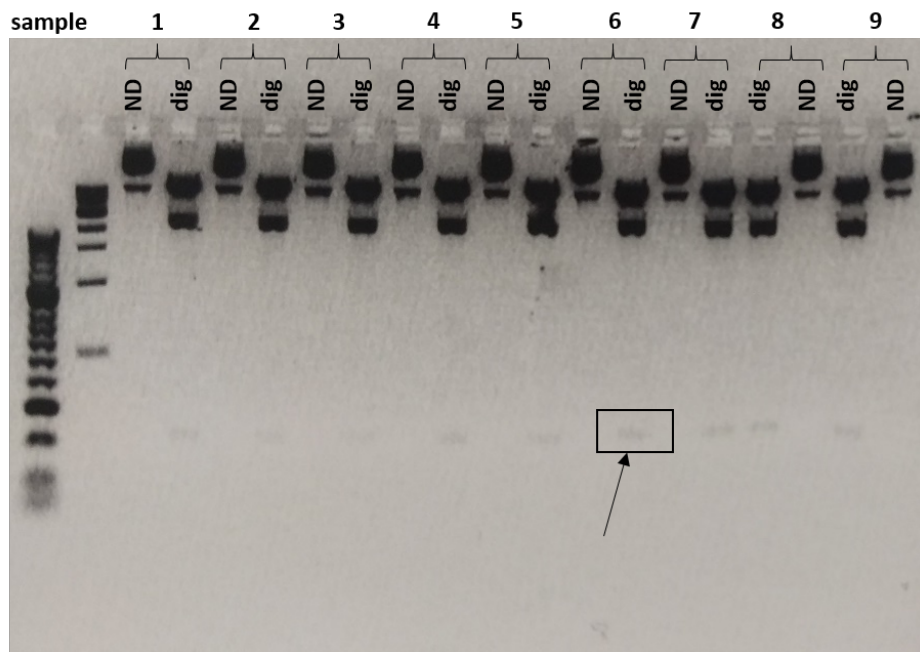


Figure 2.2: PCR gel to validate the ligation of the sgRNA with the vector. Two conditions were carried out for each sample: a non digested control and a plasmid incubated with enzymes of restriction NdeI and EcoRI. If the sgRNA was correctly ligated with the vector, 3 bands can be seen on the gel: one at 10,347bp, one at 2,299bp and a smaller one at 154bp (black arrow and box).

Transduction into cancer cell lines

pLentiCRISPRv2: $4 \cdot 10^6$ HEK293T cells were seeded with 10 mL DMEM supplemented media in 10 cm dishes for lentivirus production. The following day, transfection reagent Mirus LT1 (MIR2300) was mixed with 1.5 mL Opti-MEM® Reduced Serum Medium (Life Technologies™, cat. no. 31985062) and left for 20 min at RT. Packaging plasmids (pVSVg and psPAX2) and 4 µg of plasmid were mixed together, the DNA mixture was added to Opti-MEM® + Mirus LT1 reagent and left for 30 min at RT. The transfection mix was spread drop by drop all over the HEK293T cells.

Plates were placed in the viral incubator overnight. 24 h after incubation with the transfection mix, media was replaced with 4 mL of fresh DMEM. The smaller volume is meant to increase the concentration of viruses. At 48 h, the media was changed again but the 4 mL was collected and stored in the fridge at 4°C in a sealed box. Cells to be transduced were seeded at a density of 5×10^5 cells/dish. At day 5, 72 h and 48 h viral media were pooled together and filtered through a 10 mL sterile syringe connected to a 0.45 µm filter (SE2M230104). About 8 mL was collected in a tube containing 2 µL Polybrene, to help attach the viruses to the cells. They were incubated for 4 h with the filtered media in the viral incubator. Media was removed and replaced with 10 mL of RPMI-1640 for 72 h.

Puromycin kill curve and selection

Plasmid contained a gene coding for resistance to puromycin and only cells that had integrated it into their DNA survived the puromycin selection. The optimal concentration of puromycin to use is cell dependent and needed to be determined. Cells were trypsinised and seeded with different concentrations of puromycin (0 to 4 µg/mL) to de-

termine the minimum dose to kill them all when they do not have any gene of resistance to the antibiotic (Fig.2.3).

Transduced cells were trypsinised and plated in flasks with puromycin (2 $\mu\text{g}/\text{mL}$). 4 days later, only puromycin-resistant cells remained and media was replaced with fresh, puromycin-free media. Those were stable genetically modified cell lines and knockdown expression of the protein of interest was assessed by western blot.

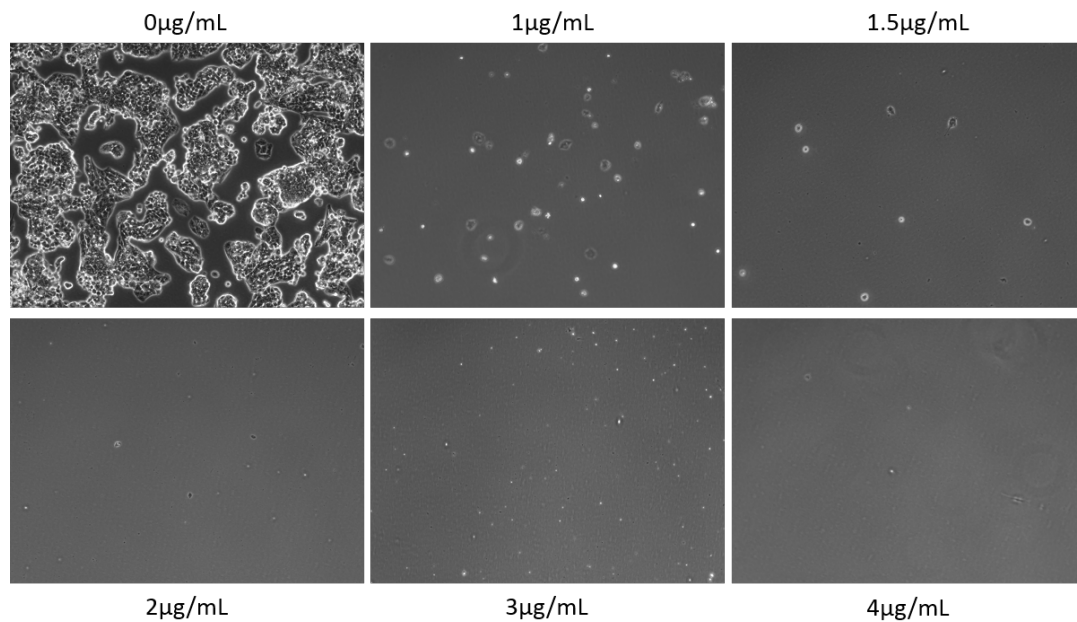


Figure 2.3: Kill curve for puromycin selection. Cells were trypsinised, plated with different concentration of puromycin and left in the incubator for 4 days. 2 $\mu\text{g}/\text{mL}$ proved to be the efficient concentration that killed all non transfected cells and was used for further selection experiments.

2.5.2 Nucleofection

Nucleofection was performed using Amaxa® Cell Line Nucleofector® kit L for A2780 (VACA-1003; VACA-1005) with a Nucleofector® Device (Lonza). Cells were trypsinised, and counted to have 10^6 cells and spun down at 435 x g for 5 min. Supernatant was

removed cell pellets re-suspended in Nucleofector Solution. This was combined with plasmids containing sgDCK-sgDCTPP1 or sgScr-sgScr insert. These had been cloned and verified by Awa Sarr (Appendix 7.1).

The cell/DNA suspension was transferred into a cuvette and placed into the device and the L-10 program was used. Once the program was finished, 500 μ L of media was immediately added to the cuvette and the sample was transferred into prepared 6 well-plates containing pre-warmed media. A control sample with a plasmid containing a gene coding for GFP was done to assess the efficiency of the nucleofection.

2.5.3 siRNA

SMARTpool ON-TARGETplus siRNA for HINT1, Cathepsin A, CES2 and non-target control were ordered from Horizon Discovery. The oligos were re-suspended in 250 μ L RNase-free water to obtain a 20 μ M stock. The reconstituted oligos were aliquoted and stored at -20°C. The cells were transfected using DharmaFECT 1 Transfection Reagent (Horizon Discovery, T-2001-03), as per the manufacturer's protocol. The cells were cultured in RPMI supplemented with 10% FBS and the reagents were diluted in Opti-MEM® Reduced Serum Medium. Double transfection was performed, meaning that the transfection protocol was repeated again after 24 h. After 48 h of transfection with 25 nM of siRNA, protein lysates were carried out, as previously described, to assess the efficacy of the siRNA. Otherwise, cells were treated with Acelarin or gemcitabine as per usual.

2.6 Gene expression analysis

2.6.1 RNA extraction and purification

Total RNA were collected from cells grown in 6 wells-plates, using Mini RNAeasy kit (Qiagen 74104). Media was discarded and cells washed in excess PBS. Plates were put on ice and all liquid was removed. 350 μ L of RLT buffer (with 1:100 β -mercaptoethanol) was added to the dishes and cells were scraped and allowed to lyse for 5 min. Lysates were transferred into sterile micro-centrifuge tubes and vortexed for 1 min. 350 μ L of 70% ETOH was added to each lysate, which were mixed well by pipetting up and down. Samples were transferred to an 'RNeasy Spin Column' placed inside a 2 mL tube and centrifuged at 9700 x g for 15 sec. Successive washes with 700 μ L RW1 and RPE Buffer/ETOH were done before elution with 30 μ L of RNase-free water to collect the purified RNA. Samples were kept on ice and quantified with NanoDrop before being stored at -80°C.

2.6.2 Reverse transcription

Reverse transcription of 1 μ g RNA for each sample was performed with Qiagen QuantiTect Reverse Transcription kit (205311). RNA were kept on ice all the time to minimize the risk of degradation. Samples were incubated with gDNA Wipeout Buffer for 2 min at 42°C to eliminate genomic DNA, before addition of a master mix composed of 5X RT Buffer, RT Primer Mix, and Reverse Transcriptase. This was incubated for another 15 min at 42°C, and 3 min at 95°C to inactivate the enzyme. Reactions were stored at -20°C. cDNA obtained was quantified with Nanodrop and diluted to obtain a final

concentration of 100 ng/ μ L.

Name	Sequence
β - Glucuronidase	5'-CGTGGTTGGAGAGCTCATTTGGAA-3' (forward) 5'-ATTCCCCAGCACTCTCGTCGGT-3' (reverse)
HINT1	5'-CCTTGCTTTCCATGACATTTCCC-3' (forward) 5'-CATTCACCACCATTTCGATAACC-3' (reverse)
HINT2	5'-TGTGACTGATGGGAATGAAGTG-3' (forward) 5'-TTAGGAATGACCAGGAAGTGC-3' (reverse)
HINT3	5'-CCAGCAGCAACTCATCATTATC-3' (forward) 5'-GGAAATGGAACAGAATGGTG-3' (reverse)
Cathepsin A	5'-GGAATCTGATTGCCAATGTG-3' (forward) 5'-GGAAAGAGGCGGAAGAAATC-3' (reverse)
CES2	5'-AGTGGAGTCAGAGTTTCTTAGC-3' (forward) 5'-AGTGGAGTCAGAGTTTCTTAGC-3' (reverse)

Table 2.4: Primers used for RT-qPCR

2.6.3 Real-Time PCR

Gene expression was assessed using Quantitect SYBR Green (204074) and a Rotorgene instrument (Qiagen). A mix of Rotor-gene SYBR Green, forward and reverse primers (Table 2.4), and RNase free-water was distributed in PCR tubes, as indicated on

manufacturer's protocol. 100 ng of cDNA was added to each reaction. The protocol used on the instrument was: initial activation step for 5 min at 95°C, followed by 40 cycles of denaturation for 5 sec at 95°C – annealing/extension for 10 sec at 60°C.

2.7 Protein expression analysis

2.7.1 Protein extraction

Cells were plated into 10cm petri dishes and incubated until sufficiently confluent or for a pre-specified period after treatment. Cells were washed once with cold PBS, dislodged and lysed on ice with a scraper and using the lysis buffer RIPA [50 mM Tris-HCl (pH 7.5), 5 mM EGTA (pH 8.5) 150 mM NaCl, 1% Triton X-100], complemented with proteases inhibitors (Roche 11836153001; Sigma-Aldrich; P5726; Sigma-Aldrich; P0044). Lysates were collected into Eppendorf tubes and passed 6 times through a 29-gauge syringe needle. The disrupted-cell suspension were centrifuged at 16200 x g for 6 min. Supernatants were transferred to microcentrifuge tubes and stored at -80°C.

2.7.2 Quantification: BCA assay

A 2 mg/mL protein standard BSA (Pierce™ 23209) was used to create an 8-point standard curve, with concentrations varying from 0 mg/mL to 2 mg/mL. Protein concentration was determined using the Bicinchoninic Acid assay (Pierce™ 23225). Samples were diluted 1:5 with distilled water to avoid saturation of the reaction. BCA solution was made by adding 1 volume of Copper Sulphate solution to 50 volumes of Bicinchoninic Acid solution and mixed thoroughly to give a green-coloured solution. 1

mL of this solution was added to each sample and then incubated for 15 min at 60°C, in a water bath. The solution turned purple proportionally to the amount of protein.

200 µL of each sample, including the standard curve, was pipetted in duplicate into a 96-well plate for analysis. Absorbance of the sample solution was measured at 540 nm using the microplate reader. Protein concentration was calculated using the standard curve generated from known the BSA standard. Aliquots of protein lysates were prepared with loading buffer 5X (75 mg Tris, 0.75g SDS, 3.75 ml mercaptoethanol, 7.5 ml glycerol, 250 µL-bromophenol blue saturated solution, and distilled water making up to 25 ml), denatured at 95°C for 5 min and stored at -80°C until analysis.

2.7.3 SDS polyacrylamide gel electrophoresis

Denaturing sodium dodecyl sulphate polyacrylamide gel electrophoresis (SDS-PAGE) was used to separate the proteins. 12% gels were made, using the vertical electrophoresis system (PROTEAN® II, BioRad). Proteins with high molecular weight are at the top of the gel and the smallest, migrating faster, are located at the bottom.

The system is composed of two gels; the bottom one is the resolving gel, and it is made with acrylamide/bis-acrylamide 37:1 (Sigma A6050), 1M Tris-HCl pH 8.85, 10% SDS, distilled water and finally TEMED and 10% APS, added only at the end as they are responsible for the polymerisation. This was set up in a gel caster and overlaid with isopropanol in order to flatten the gel without letting it dry. Once the gel had polymerised, the isopropanol was removed and the stacking gel was poured on the top (acrylamide/bis-acrylamide 37:1, 0.375M Tris, pH6.8, 10% SDS, distilled water, 10% APS and TEMED).

Up to 50 µg of proteins were loaded on the gel as well as 15 µL of Chameleon Duo

Pre-stained protein ladder [P/N 928-60000]. Gels were run in a buffer containing Tris Base, glycine, 10% SDS and distilled water at 80V whilst the samples were migrating in the stacking gel and 140V when in the resolving gel.

2.7.4 Western blot

After the SDS-PAGE, proteins were transferred on a pre-activated PVDF membrane in a transfer buffer (Tris base, glycine and distilled water) at 30V, 4°C overnight. Membrane was activated by soaking in pure methanol for a few seconds. Efficiency of the transfer was checked by incubating the membranes with a Ponceau solution (P7170). Membranes were blocked with Li-Cor Odyssey blocking buffer (diluted 50:50 in PBS - 927-40003), for 1 h at room temperature before probing overnight at 4°C with primary antibodies of interest (Table 2.5), made up in Li-Cor Odyssey buffer (diluted 50:50 in PBS).

Membranes were washed with PBS - 0.1% Tween 20 (PBST), 3 times 5 min, before incubation for 1 h at room temperature with fluorescently-labelled secondary antibodies in Li-Cor Odyssey blocking buffer (diluted 50:50 in PBS) containing 0.01% SDS. Protein of interest and loading control proteins were usually labelled with green (800 nm) and red (680 nm) secondary antibodies, respectively. By combining a mouse and a rabbit primary antibodies along with their respective secondary antibodies, this allows to have dual-labelled western blots. Membranes were washed 3 times 5 min with PBST and 3 times 5 min with PBS to remove all traces of non-bonded secondary antibodies and get a better signal when scanning. Images were obtained with a Li-Cor Odyssey scanner and analysed with Image Studio Lite software.

Antibody	Dilution	Source	Manufacturer	Cat number
Actin	1:10 000	Mouse	NEB	3700S
GAPDH	1:10 000	Rabbit	Sigma, UK	PLA0125
DCK	1:1000	Rabbit	Gentex, USA	GTX102800
DCTPP1	1:500	Mouse	Santa Cruz, San Diego	398501
HINT1	1:1000	Rabbit	Abcam, UK	109319
RRM1	1:1000	Rabbit	Proteintech, EU	10526-1-AP
2nd anti-mouse	1:10 000	Goat	Licor-Odyssey	926-32210
2nd anti-rabbit	1:10 000	Donkey	Licor-Odyssey	926-68071

Table 2.5: Antibodies used for western blot analysis

2.7.5 Immunocytochemistry

Cytospins

A2780 cells were cultured and treated with Acelarin and gemcitabine as per usual. At 72 h, they were trypsinised, spun down, re-suspended at a concentration of 10^6 cells/ml in RPMI media. Adhesive slides were prepared with cytospin gaskets (EZ Single Cytofunnel™ A78710003). 200 μ L cell suspension was added to each gasket, which were placed in a cytospin, set to run for 6 min as 800 gsm. Fresh 4% PFA in PBS was immediately applied to slides for 30 min for fixation, in the fume hood, followed by 3 washes of 5 min in PBS. Slides were stored in PBS at 4°C until analysis.

Immunoperoxidase

Cells were permeabilised with 100 μ L 0.1% Triton X-100 in PBS for 5 min, then washed with PBS Tween 0.1% 3 times for 5 min. Aldehyde sites were blocked with 100 μ L 0.1M glycine in PBS and slides were washed with PBS Tween 0.1% 3 times for 5 min. They were then incubated with 2% FBS/PBS for 10 min to avoid nonspecific binding of the primary antibody. DCK antibody was diluted 1/200 in 2% FBS/PBS and incubated for 30 min, followed by 3 washes of 5 min each in PBS Tween 0.1%. Slides were incubated with 2 drops of Dako anti rabbit HRP (K4003) for 30 min, followed by 3 washes of 5 min each in PBS Tween 0.1%. One drop of DAB chromogen (Dako K3468) was added to 1 mL of DAB substrate buffer (1:50 dilution), put on the slides for 10 min, then rinsed with running tap water for 1 min. They were dipped in haematoxylin for 10 sec to stain the nuclei, rinsed with running tap water for 1 min and incubated with Scots tap water for 1 min. Slides were mounted with DPX (SEA-1304-00A) in the fume hood and let to dry overnight. They were scanned with Leica SCN 400 scanner using 40x magnification.

2.8 Comet assay for DNA damage

2.8.1 Preparation of samples & slides

A2780 cells were plated and treated as usual. Samples were collected at different time points (2 h, 24 h, 48 h, 72 h). Negative control (untreated cells) as well as positive (cells treated with 10 μ M of H₂O₂ 10 min prior to collection) were included. Cells were trypsinized and kept in ice-cold PBS, cell density was adjusted to 5x10⁴ cells/mL and

samples were kept at -80°C until experiment was carried out.

1% low melting point agarose (LMPA) was dissolved and kept at 40°C in water bath. Microscopic slides were dipped in the agarose and let air-dry to a thin film. 100 μL of cells was mixed with 900 μL of 1% LMPA at 40°C . Cell suspension was mixed and 100 μL was deposited onto a pre-coated slide and covered with a coverslip to spread the sample evenly. Once the gel was set, coverslips were removed and the slides were submerged in neutral lysis solution [2% sarkosyl, 0.5 M Na_2EDTA , 0.5 mg/mL proteinase K (pH 8.0)], at 37°C for 1 h in the dark.

2.8.2 Electrophoresis conditions

Slides were put in electrophoresis buffer [90 mM Tris buffer, 90 mM boric acid, 2 mM Na_2EDTA (pH 8.0)] for 30 min at RT, this step was repeated twice. They were then put in an electrophoresis chamber filled with more buffer. Electrophoresis was run for 25 min at 20V. After that, slides were rinsed and neutralised in distilled water in a coplin jar.

2.8.3 Staining & analysis

100 μL of a 10 $\mu\text{g}/\text{mL}$ stock solution of propidium iodide was pipetted directly onto the slide and incubated for 20 min in the dark. Slides were rinsed with 400 mL distilled water to remove excess stain. Images were taken with an epifluorescence microscope (Leica DM5500) and analysed with Image J and its plug-in OpenComet (Gyori et al., 2014).

2.9 CalcuSyn

CalcuSyn is a software used to assess the efficacy of drug combination studies *in vitro*. Drugs were used alone and combined together and SRB was done as per usual at 96 h post-treatment and OD values were analysed with CalcuSyn in order to determine potential effects of the drugs on the cells. The combination index (CI) was calculated for each combination by using the Chou–Talalay equation: $CI = (D)_1 / (D_x)_1 + (D)_2 / (D_x)_2$, where $(D_x)_1$ and $(D_x)_2$ are the concentrations required for drug 1 $(D)_1$ and drug 2 $(D)_2$ alone that gives x% inhibition, whereas D_1 and D_2 in the numerators are the concentrations of drug 1 and drug 2 in combination that also inhibits x%. This takes into account both the potency (median-effect dose or IC_{50}) and the shape of the dose–effect curve. The combination index quantitatively depicts synergism ($CI < 1$), additive effect ($CI = 1$), or antagonism ($CI > 1$). Data were collected and analysed with two undergraduate students under my supervision, Ka Wing Chu and Sarah Puthur.

2.10 Phase I clinical study

2.10.1 Patient cohort and clinical data

Patients with advanced solid tumours had been recruited for a phase I, dose-escalation clinical study to assess the safety and anti-tumour activity of Acelarin. It was conducted at the National Institute for Health Research / Wellcome Trust Imperial Clinical Research Facility, Hammersmith Hospital, from October 2012 to June 2015. Patients were 18 years or older and diagnosed with cancer that was refractory to standard therapy, or for which no standard therapy existed. Other criteria included adequate organ function,

a life expectancy of at least 12 weeks, no history of allergic reactions to gemcitabine, no symptomatic central nervous system or leptomeningeal metastases, or another active cancer. The study protocol was approved by the Medicines and Healthcare products Regulatory Agency, the West London Research Ethics Committee 12/LO/1100 and local review boards. The study was registered on clinicaltrials.gov (NCT01621854) (Blagden et al., 2018). The use of the tissues came under the ethical approval MD9202 (Appendix 7.20).

Whole section slides from a pan-cancer Phase I cohort were also obtained where all biopsies were taken prior to Acelarin treatment. Corresponding clinical data was also obtained from clinical records including tumour diagnosis, sex, and details on previous chemotherapy, and response if any to Acelarin. All data was rendered patient non-identifiable prior to receipt.

Tumours were assessed by CT scan or MRI after cycles 2, 4 and 6 and compared with those conducted prior to starting the study, using RECIST 1.1 criteria (Eisenhauer et al. 2008). Duration of response was calculated from date of first response until RECIST or symptomatic disease progression.

2.10.2 Immunohistochemistry

Tissues had previously been fixed in 10% formalin and processed according to the routine histopathology standard operating procedure to generate formalin-fixed paraffin-embedded (FFPE) tissue blocks. 3 μm sections were then cut from the FFPE blocks to be stained by immunohistochemistry.

Sections were deparaffinised by incubating them in xylene three times for 5 min followed by 2 min of each of those steps: 100% (twice), 80%, 50% alcohol and wash in

running tap water in order to rehydrate the tissues. Meanwhile, an antigen retrieval solution was prepared by adding 18 mL 0.1M Citric Acid to 82 mL 0.1 M Sodium Citrate and top up to 1 L with Elga water. This was pre-heated in Instant Pot® electric pressure cooker for 1 min. The slides were then boiled in this solution, inside the Instant Pot®, for an additional minute and cooled down in running tap water.

They were washed for 5 min with 0.1% PBST and incubated with 3% hydrogen peroxide (Sigma H1009) for 5 min to remove any active endogenous peroxidase in the cells, which might react with DAB stain at a later stage of the protocol. The slides were washed again in 0.1% PBST prior to incubation with blocking solution (Dako X0909) for 10 min. Blocking solution was removed and slides were incubated with primary antibodies (DCK 1:500 and DCTPP1 1:250), diluted with Dako antibody diluent (S0809) and placed in a humidity chamber with moist tissue for 30 min. After that, the slides were washed twice in 0.1% PBST for 5 min, and incubated for another 30 min with HRP conjugated secondary antibody, using anti-rabbit (Dako K4003) and anti-mouse (Dako K4001) antibodies for DCK and DCTPP1 respectively. The slides were washed twice in 0.1% PBST for 5 min. One drop of DAB chromogen was added to 1 mL of DAB substrate buffer (1:50 dilution), and this was used to cover each slide for 10 min, until a brown colour developed.

To stain nuclei, slides were immersed in haematoxylin for 10 sec, washed in running tap water for 2 min, transferred into Scott's tap water for 1 min until the tissue sections turned blue and washed again in running tap water for 2 min. After that, they were dehydrated in 50%, 80%, 100% (twice) alcohol for 2 min each and cleared in xylene 3 times for 5 min each. Slides were mounted with DPX in the fume hood and let to dry overnight. They were scanned with Leica SCN 400 scanner using 20x and 40x magnification.

2.10.3 Image analysis with QuPath

Manual annotation of cancer cells

This phase I cohort consisted of biopsies from fourteen different organs, meaning a consequent histological heterogeneity between samples (Fig.2.4A-D). However, cancer cells display similar characteristics and were identified by morphological features, such as hyperchromatism, disorganised arrangement of cells, pleomorphism and mucus-bounded appearance (Fig.2.4E). Region of interest (ROI) were manually annotated (Fig.2.5A) by Tsz Huen Chan, an undergraduate student under my supervision, and confirmed by an experienced biomedical scientist (In Hwa Um) and a pathologist (David Harrison). To limit misleading results, some areas were excluded from annotation, such as presence of artefacts due to poor focus and areas of where diagnosis of cells was indeterminate.

Computer segmentation and exclusion of lymphocytes from analysis

Cancer cells were detected within annotated regions of interests using QuPath's tool and nuclei were identified based on their H&E staining. QuPath categorised intensity of positivity in nuclei and perinuclear area (2 μm around the nuclei), into four different categories: negative, cells have no expression of protein of interest; 1+ mild intensity associated with relatively low expression of protein; 2+ cells have a relatively higher expression than 1+; 3+ cells have high protein expression (Fig.2.5B). To ensure consistency in the analysis of all samples, intensity thresholds were kept the same in the parameter settings.

Invasion was often associated with an inflammatory response. In order to prevent false positive analysis by the software, parameters were adjusted to exclude cells with

nuclei of 10 μm or less, suspected to be lymphocytes, retaining the large nuclei cells, more likely to be cancer cells (Fig.2.6).

2.11 Statistical analysis

Statistical analysis were done using GraphPad Prism V.7 (GraphPad Software). The Mann-Whitney non parametric U test was used when at least four replicates were available; $p < 0.05$ was considered statistically significant.

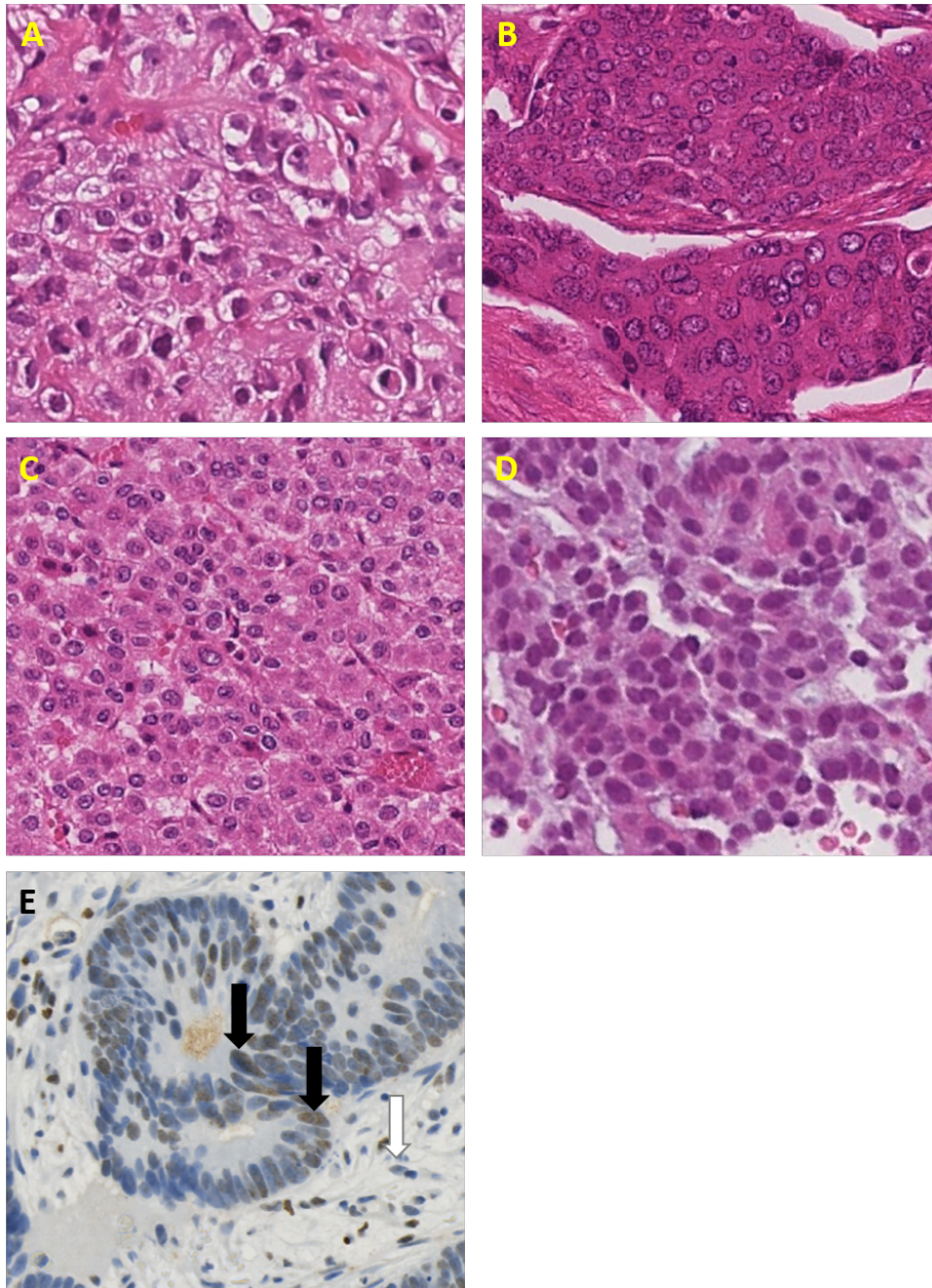


Figure 2.4: Identification of cancer cells. Despite the histological heterogeneity between different tissues, cancer cells display similar features in all of them and were identified based on the following criteria: pleomorphic, hyperchromatic cells with enlarged nuclei and irregular arrangement. (A) Lung adenocarcinoma, (B) Ovarian cancer, (C) Adrenal carcinoma, (D) Breast cancer. (E) Tissue section of colorectal cancer, nuclei are in blue and DCK in brown. Black arrows point to characteristic tumour cells, which display hyperchromatism, disorganised arrangement and enlarged nuclei. White arrow shows a lymphocyte in the stroma, which also contains fibroblasts and blood vessels.

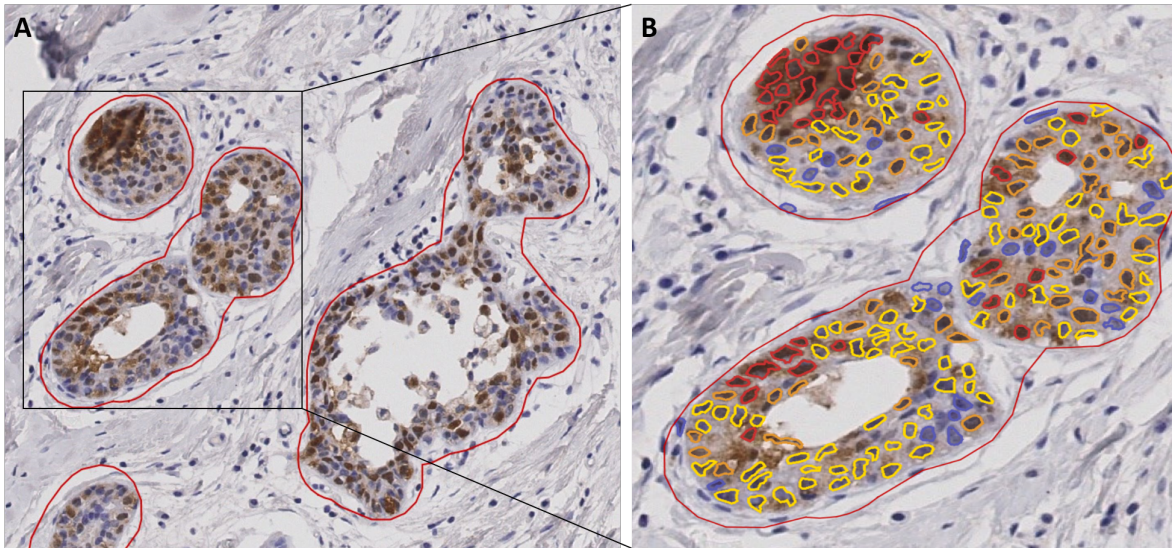


Figure 2.5: Annotation and segmentation of an image on QuPath. (A) Cancer cells are enclosed in the red lines and only expression of those will be included in the analysis performed by the software. (B) Colour code is associated with intensity of DCTPP1 staining: blue – negative; yellow – mild; orange – moderate; red – high expression.

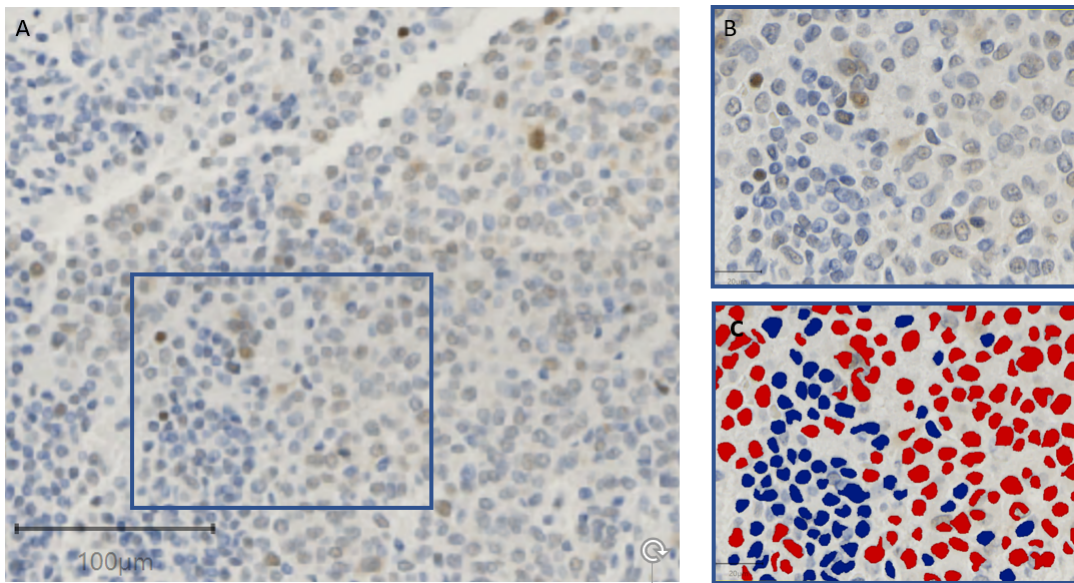


Figure 2.6: Segmentation to exclude non-tumour cells within a region of interest. (A) Tissue section of lung adenocarcinoma stained for DCTPP1 expression. (B) Highlighted and enlarged area from A. (C) Lymphocytes (blue) have smaller nuclei than tumour cells (red) and were recognised by the software and excluded from Allred score calculation.

3 | Comparison of Acelarin and gemcitabine effects on ovarian cancer cell lines *in vitro*

3.1 Introduction

Acelarin is the first anti-cancer ProTide to enter the clinic. It was designed to overcome the resistance associated with gemcitabine in patients with cancer. The inactive nucleoside analogue pro-drug, gemcitabine, is converted to dFdCMP and protected by the addition of specific combination of an aryl, ester and amino acid grouping. Pre-clinical data showed that Acelarin incorporation is independent of hENT1 trans-membrane transporter and, once inside the cell, dFdCMP is rapidly converted to dFdCDP and dFdCTP, bypassing the rate-limiting step of DCK phosphorylation. Furthermore, Acelarin avoids CDA-mediated catabolism, thus preventing dFdU accumulation (Slusarczyk et al., 2014; Mehellou et al., 2017).

Acelarin has already demonstrated clinically significant anti-tumour activity, even in patients who were not responsive to gemcitabine or subsequently relapsed. The pharmacokinetic studies showed a higher intracellular concentration of the active metabolite dFdCTP and a longer half-life than gemcitabine (Blagden et al., 2018). This suggests that tumour cells are exposed to considerably higher levels of the active

metabolite dFdCTP when patients are treated with Acelarin, compared to gemcitabine.

Despite the promising results in the clinic, little is known about the cytotoxic mechanisms of Acelarin. We hypothesised that because it bypasses mechanisms of gemcitabine that generate toxic metabolites, its mode of action might be more targeted. The aim of this chapter was to investigate whether there were differences in response of cells treated with Acelarin and gemcitabine *in vitro*.

3.2 Determination of best assay to study cytotoxicity of Acelarin and gemcitabine

Cytotoxicity of Acelarin was assessed in a panel of eight ovarian cell lines derived from primary tumours of different patients, with the exception of PE01, PE04 and PE06 cell lines which were derived from a single patient, but at different stages of her cancer. Since all cell lines have different characteristics, such as size and doubling time, the starting cell number needed to be empirically established by a cell growth experiment. Also, as cytotoxicity experiments were done over six days, it was essential to ensure that the cells remained sub-confluent and in an optimal growth phase for the entire duration of the experiment. The experiment was designed as such that cells were initially left to settle for 48 h before treatment, thus allowing a 24 h pre-incubation in hypoxic conditions when required before starting any experiment (see Materials and Methods, section 2). Traditionally, cytotoxicity assays are performed over 48 to 96 h post-treatment with drugs. For this work, cell death was investigated as an end point to determine concentration of drug to use. However, the main focus was to compare the mechanisms that led to apoptosis between Acelarin and gemcitabine and a longer time point was chosen in order to be able to detect these effects.

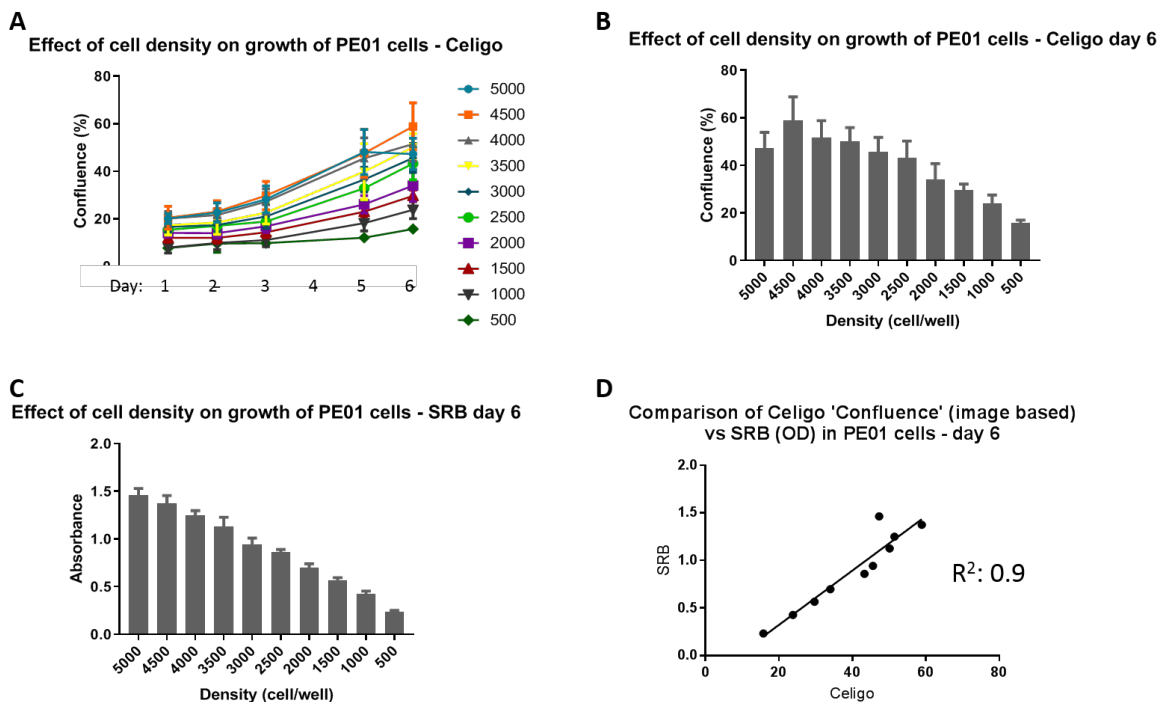


Figure 3.1: Comparison of two methods to assess optimal cell density. The effect of cell density on growth of PE01 cells (confluence) was assessed during several days with Celigo (A), up to day 6 (B) (no data for day 4). (C) Effect of cell density on growth on the last day determined with SRB assay. (D) Comparison of data obtained from Celigo and SRB at day 6, $R^2=0.9$, then the results obtained from the two sets of data are similar.

Celigo is a cell imaging cytometer, useful for the determination of the growth characteristics of cell lines. With the bright field imaging, image segmentation and analysis tools, cell growth can be analysed with the cell number or confluence algorithms. It was previously determined in the group that confluence was directly correlated to cell number and was chosen as a preferred parameter as it is quicker to scan the different wells for general confluence than specific cell number. The Sulforhodamine B (SRB) assay is widely used for cytotoxicity screening *in vitro* (Vichai and Kirtikara, 2006; Kasinski et al., 2015; Orellana and Kasinski, 2016). This method relies on the property of SRB, which binds stoichiometrically to proteins. Thus, the amount of dye extracted from stained cells can be used as a proxy for cell mass, which can then be extrapolated to measure cell proliferation (Skehan et al., 1990). The growth of cells over time can be

easily assessed by Celigo, as a given plate can be scanned on several consecutive days whereas SRB, as an end point assay, requires to sacrifice a plate everyday in order to obtain similar amount of data as Celigo. Both methods have different advantages and were compared whilst doing cell growth optimisation.

Cells were plated at increasing density, plates were scanned with Celigo and growth curves were generated for each density over the six days (Fig.3.1A). On day 6, SRB was performed on these plates (Fig.3.1C) and OD values collected were compared with results from Celigo (day 6) (Fig.3.1D). The coefficient of determination R^2 varied for each cell line, higher than 0.9 for most of them, with the exception of CAOV3 cells ($R^2 = 0.7868$) (Appendix 7.2-8). This means that the results obtained from Celigo and SRB were consistent with each other for all the cell lines other than CAOV3.

For each well, the image focus was automatically determined by Celigo using ‘Image based Focus’. The resolution and phase-contrast of the images depend on the cell line features and this can affect cell recognition by the segmentation tool. PE01 cells, which form clusters with sharp edges (Fig.3.2A), were accurately detected (Fig.3.2B), whereas analysis of the CAVO3 cell line was more challenging due to particular morphology features of the cell line. Although the well was covered with cells (Fig.3.2C), a significant amount of cells were not recognised by the imaging software (Fig.3.2D) and were excluded from the calculations. Therefore, the image interpretation by Celigo failed to accurately assess the confluence of CAOV3 cells.

The optimal number of cells to plate for each cell line, to ensure they were still in a growth phase at day 6, was established based on the results of the SRB assay of the cell growth experiment (Table 3.1). This initial experiment was also carried out to validate both SRB and Celigo methods and determine which one to use for all further cytotoxicity analysis. Often, the most important parameter when carrying out

cytotoxicity assay with drug compounds, is cell survival at the end of the experiment, rather than the growth process of cells. As SRB and Celigo gave comparable results for all cell lines but one, and the trend of cell growth was not needed, SRB was chosen to assay all cytotoxicity experiments.

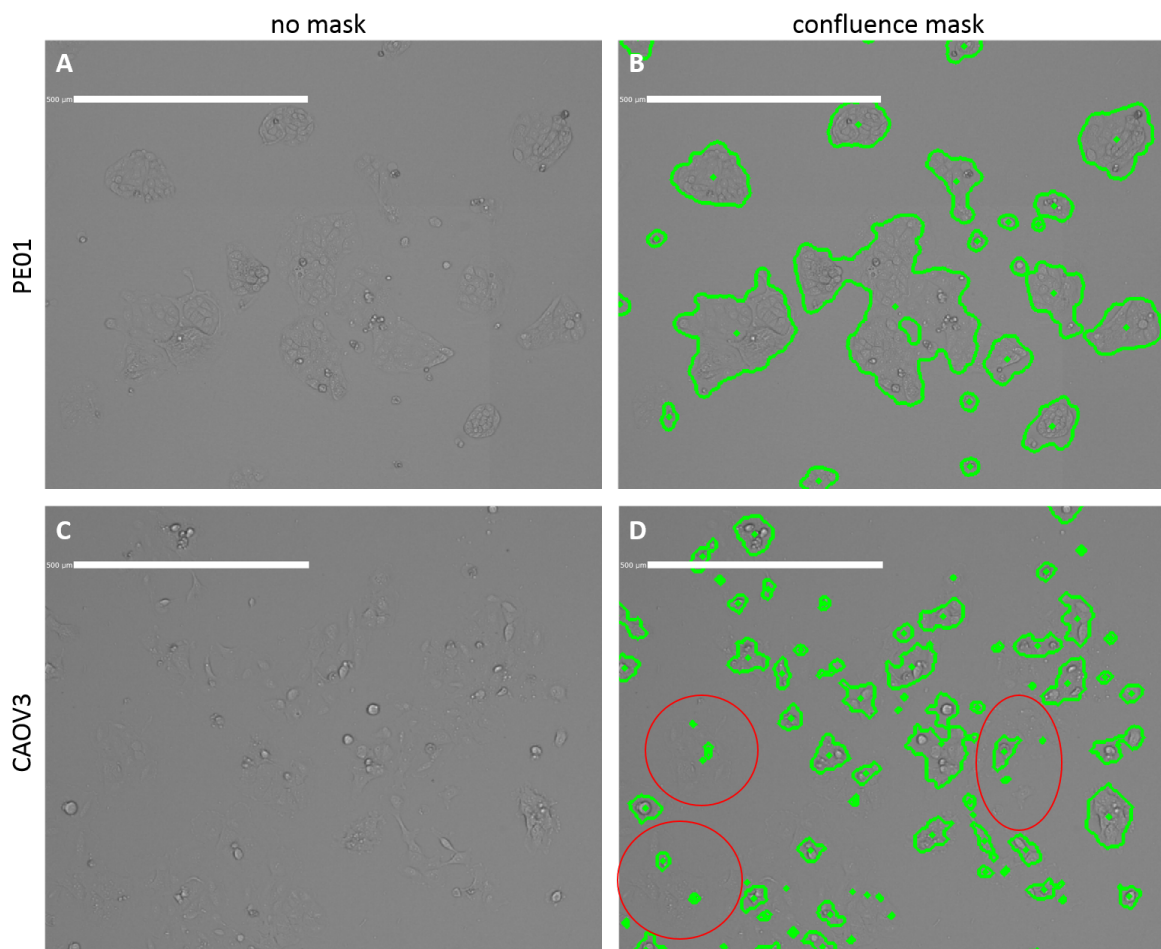


Figure 3.2: Analysis of cell confluence with Celigo. Bright field images of PE01 (A) and CAO3 (C) cells, scanned with Celigo. Confluence mask was applied to those images in order to analyse the confluence in individual whole well of a 96-well plate (B&D). In red circles, cells that were not detected by the segmentation tool of the software.

Cell line	A2780	CAOV3	OVCAR3	OVCAR4	PE01	PE04	PE06	SKOV3
N ^o of cells	750	4000	3000	3000	6000	6000	6000	250

Table 3.1: Optimal number of cells to plate per well in a 96 wells-plate for each ovarian cell line studied. Cell growth can be affected when using a different batch of serum despite the percentage being the same (10%). Some growth curves had to be repeated, and optimal cell number may be different from the values displayed in the graphs comparing SRB and Celigo.

To assess the cell lines sensitivity to Acelarin, cells were grown for 48 h before being treated for 24 h with different concentrations of Acelarin, from 5 to 500 nM, and SRB was performed at 96 h post-treatment, as described in the Materials and Methods (section 2.1.3). This was performed for the eight ovarian cell lines, both in normoxia (21% O₂) and hypoxia (0.5% O₂).

IC₅₀ values ranged from 74 nM to 516 nM in normoxia (Fig.3.3A) and from 53 nM to 538 nM in hypoxia (Fig.3.3B). SKOV3 and OVCAR4 cells were resistant to Acelarin in both conditions. The oxygen level did not affect the sensitivity of A2780 cells, as the IC₅₀ were similar: 75 nM in normoxia and 53 nM in hypoxia. Most cell lines became slightly less sensitive to Acelarin when deprived of oxygen. The most drastic effect was seen in CAOV3 cells which were sensitive in normoxia but became resistant to Acelarin in hypoxia, with a 8.74-fold increase of IC₅₀ (74 nM vs over 500 nM).

Among the initial eight cell lines, three were chosen for future work, due to their characteristic sensitivity to Acelarin: A2780, CAOV3 and SKOV3. A2780 was sensitive in both normoxia and hypoxia, CAOV3 was sensitive in normoxia but resistant in hypoxia and SKOV3 was completely resistant to Acelarin when treated for 24 h with this range of concentrations.

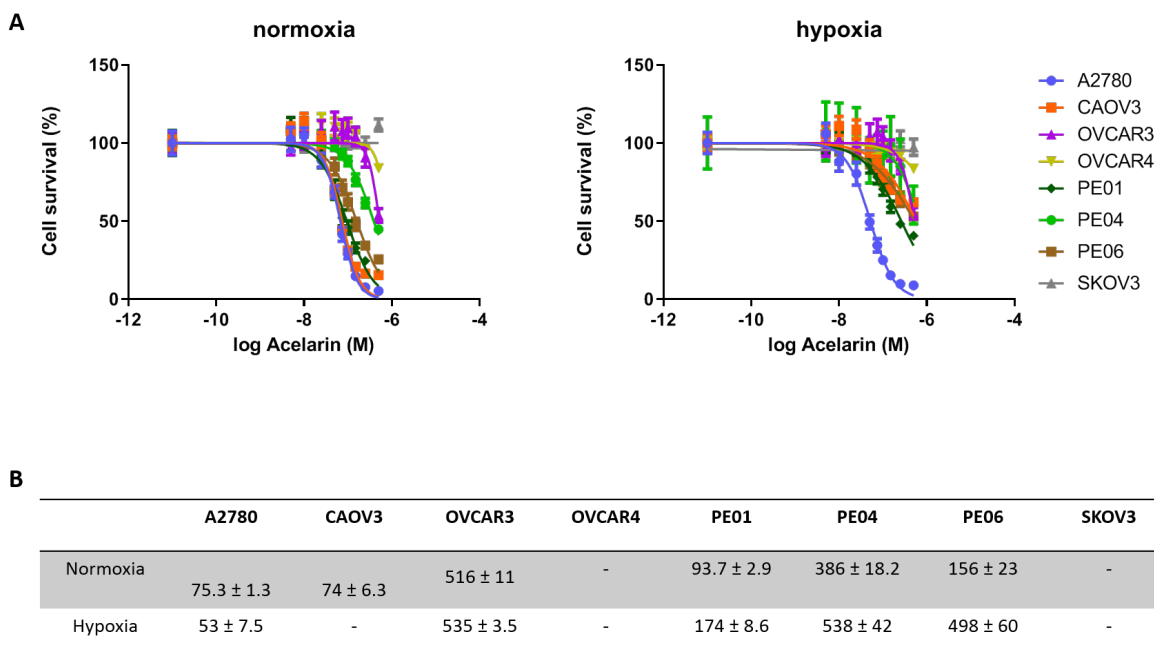


Figure 3.3: Effect of Acelarin treatment on growth of a panel of ovarian cell lines. Eight ovarian cell lines were treated with a range of different concentrations of Acelarin for 24 h and cytotoxicity was assessed 96 h post-treatment. (A) Each graph represents a condition based on the level of oxygen: normoxia and hypoxia. Data are expressed as the mean \pm SEM of three independent experiments. (B) Data for IC₅₀ are reported as mean \pm SEM.

3.3 Ovarian cell lines have different sensitivity to Acelarin and gemcitabine

A 24 h treatment was thought to not be physiologically relevant as cells would be exposed to a constant flow of drug, whereas in the human body it would have already been metabolised for hours. The effect of shorter treatment of Acelarin and gemcitabine, both in normoxia and hypoxia, was assessed in the three cell lines. Cells were treated with Acelarin or gemcitabine for 1 h, 2 h, 6 h, as well as 24 h for comparison.

A2780 cells were more sensitive to gemcitabine than to Acelarin, with a 8.1-fold difference in IC₅₀ at 2 h (76 nM vs 616 nM), and up to 10.5-fold difference at 24 h in

normoxia (6 nM vs 63 nM) (Fig.3.4A-B). The difference was smaller in hypoxia but still significant: 65 nM vs 442 nM at 2 h and 13 nM vs 51 nM at 24 h (Fig.3.4C-D). Similar results were observed in CAOV3 cells, which were up to 112-fold more sensitive to gemcitabine than Acelarin in normoxia (0.75 nM vs 84 nM) (Fig.3.5).

Unlike Acelarin which did not inhibit growth within 24 h, SKOV3 cells treated with gemcitabine were more sensitive and this was confirmed both in normoxia (IC_{50} : 500 nM for 1 h treatment) and hypoxia (IC_{50} : 200 nM for 24 h treatment) (Fig.3.6).

These data suggest that Acelarin and gemcitabine induce cytotoxicity differently and Acelarin does not display the known high cytotoxic effects of gemcitabine *in vitro*.

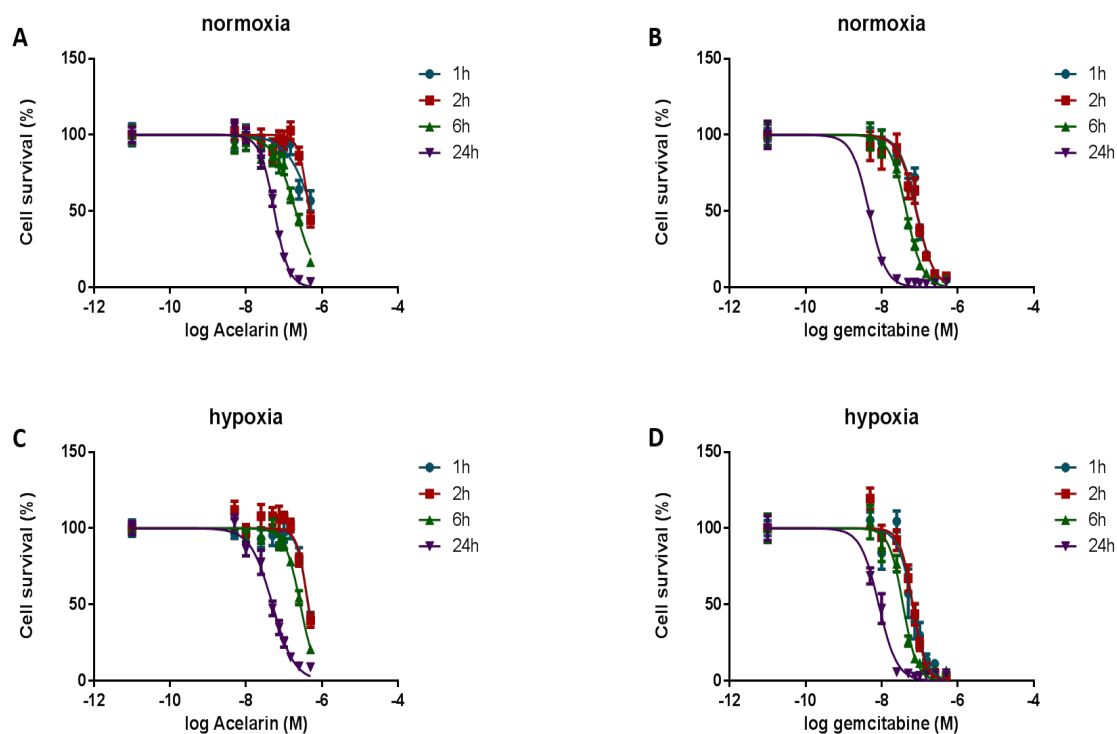


Figure 3.4: Effect of oxygen condition on A2780 cells sensitivity to treatment with Acelarin or gemcitabine. Cells were treated for the time indicated and SRB was performed at 96 h post-treatment. Each graph represents a different condition, normoxia (A, B) and hypoxia (C, D); Acelarin (A, C) and gemcitabine (B, D). Data are expressed as the mean \pm SEM of three independent experiments. Cells treated with Acelarin vs gemcitabine in normoxia: $p < 0.01$. Cells treated with Acelarin vs gemcitabine in 0.5% O_2 : $p < 0.005$, Mann-Whitney test.

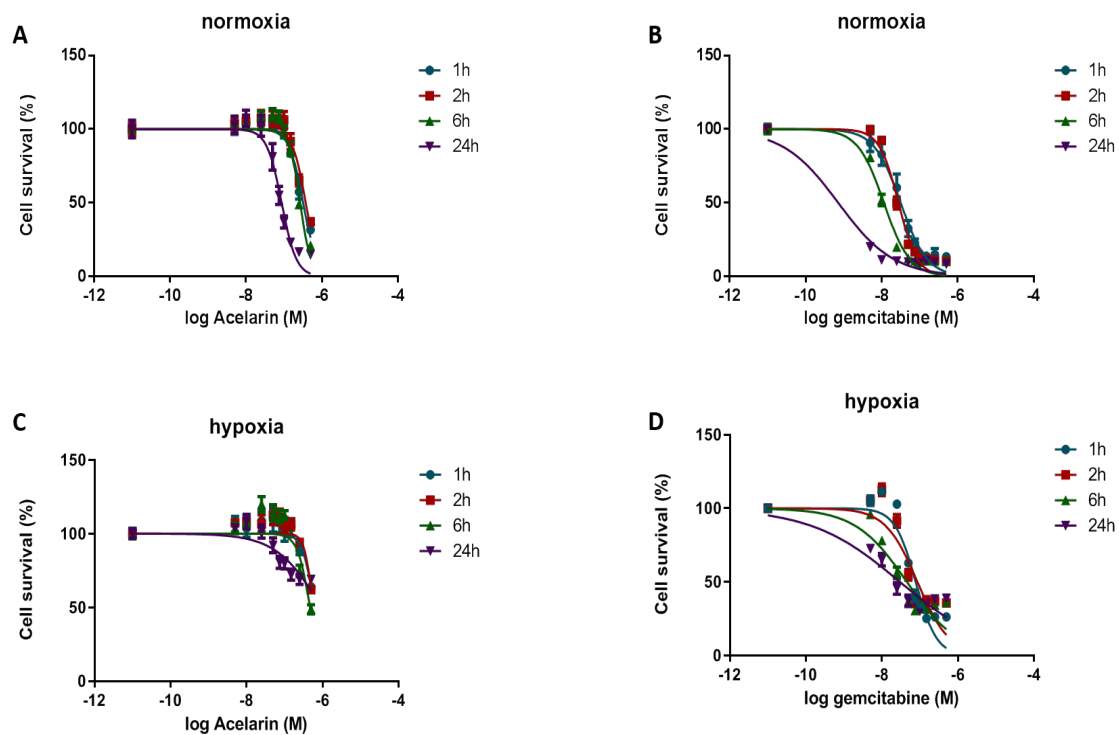


Figure 3.5: Effect of oxygen condition on CAOV3 cells sensitivity to treatment with Acelarin or gemcitabine. Cells were treated for the time indicated and SRB was performed at 96 h post-treatment. Each graph represents a different condition, normoxia (A, B) and hypoxia (C, D); Acelarin (A, C) and gemcitabine (B, D). Data are expressed as the mean \pm SEM of at least two independent experiments. Cells treated with Acelarin vs gemcitabine in normoxia: $p < 0.005$. Cells treated with Acelarin vs gemcitabine in 0.5% O_2 : $p < 0.005$, Mann-Whitney test.

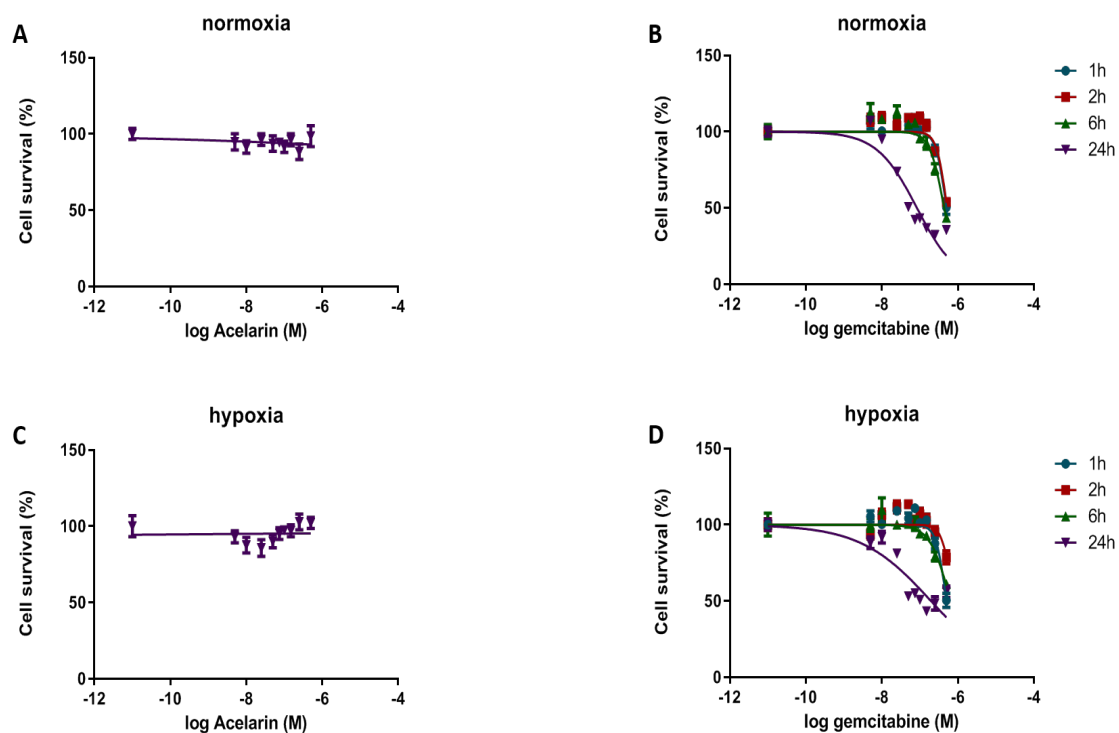


Figure 3.6: Effect of oxygen condition on SKOV3 cells sensitivity to treatment with Acelarin or gemcitabine. Cells were treated for the time indicated and SRB was performed at 96 h post-treatment. Each graph represents a different condition, normoxia (A, B) and hypoxia (C, D); Acelarin (A, C) and gemcitabine (B, D). Data are expressed as the mean \pm SEM of at least two independent experiments. Cells treated with Acelarin vs gemcitabine in normoxia: $p < 0.005$. Cells treated with Acelarin vs gemcitabine in 0.5% O_2 : $p < 0.005$, Mann-Whitney test.

Cell line	Exposure (h)	Normoxia		Hypoxia	
		Acelarin	gemcitabine	Acelarin	gemcitabine
A2780	1	-	84.5 ±2.5	434 ±52	98 ±3
	2	616 ±4	75.7 ±7.1	442 ±82.5	64.7 ±6.8
	6	239 ±75	44.2±1	271 ±38.5	37.2 ±2.8
	24	63 ±8.6	5.7±1.8	51 ±16	13 ±7
CAOV3	1	312 ±6	32 ±16	-	78 ±4.3
	2	385 ±38	28 ±3	-	86.3 ±10
	6	261 ±20	11.4 ±42	-	48 ±2
	24	84.1 ±12.9	0.75 ±0.15	-	27.4 ±1
SKOV3	1	-	498±53	-	-
	2	-	519 ±18	-	-
	6	-	436 ±12.6	-	588 ±32
	24	-	84 ±6	-	196 ±15.8

Table 3.2: IC₅₀ values (nM) obtained for A2780, CAOV3 and SKOV3 cells exposed to Acelarin or gemcitabine in normoxia and hypoxia. Data are reported as mean ± SD; - : no IC₅₀ could be calculated.

3.4 Time-lapse showed delayed death of Acelarin-treated cells and cell cycle disruption

To further investigate these differences, a time-lapse was performed on A2780 cells to observe morphological modifications and induction of apoptosis as a result of treatment with Acelarin or gemcitabine. They were treated at the IC_{50} concentration of Acelarin or gemcitabine for 2 h and images were recorded for 96 h. In addition to the time-lapse, data obtained comprised a graph representing percentage of cell coverage over time.

Untreated cells had a regular growth over the time period and reached 68% cell coverage after 4 days. After 48 h, cells treated with Acelarin reached 30% confluence and most showed a 24 h delay-period before undergoing to apoptosis, compared to cells treated with gemcitabine which started to die from 48 h post-treatment (Fig.3.7). During this 24 h period, morphological modifications were visible for Acelarin treated cells as some displayed a more elongation shape, contrasting with their usual round phenotype.

This led to question what may be the underlying mechanisms of Acelarin. Gemcitabine is known to induce a blockage in S phase of the cell cycle after 24 h (Cappella et al., 2001; Mini et al., 2006). The effect of both Acelarin and gemcitabine on the cell cycle of A2780 and SKOV3 cell lines was investigated, at different time points (2 h, 24 h, 48 h, 72 h and 96 h). For this, bromodeoxyuridine (BrdU), a thymine analogue incorporated into newly synthesised DNA, was used. Labelling cells with BrdU, combined with total DNA staining by propidium iodide and analysis by flow cytometry offers the most accurate measure of cells in the various stages of the cell cycle.

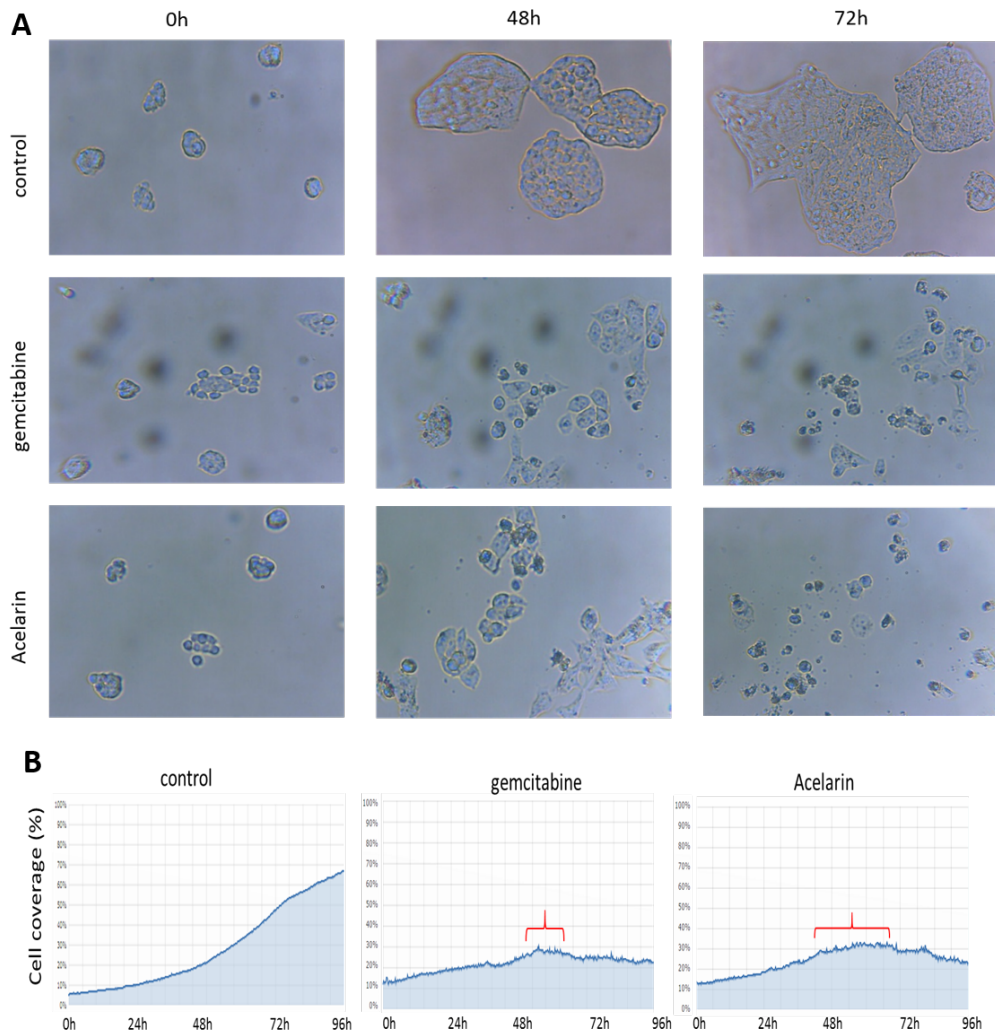


Figure 3.7: Time lapse of A2780 cells treated with gemcitabine or Acelarin. Cells were treated with IC₅₀ of gemcitabine or Acelarin or no drug for 2 h, and washed with drug-free media. (A) Snapshots of cells were taken every few minutes and this for 96 h. (B) Percentage of cell coverage in the photos (n=2). Red brackets represent the phase during which cells do not divide nor die.

There was no effect of the drugs on the cell cycle of A2780 cells at the end of the 2 h treatment (Fig.3.8). At 24 h, most cells treated with gemcitabine or Acelarin underwent a blockage in S phase compared to control cells (62.1% and 57.85% vs 36.85%). At 48 h, there were more cells treated with Acelarin in S phase, compared to control cells (50.65% vs 36.55%), whereas those treated with gemcitabine went back to normal cycle (40.05% and 36.55%). Interestingly, the main difference observed at 72 h was the

proportion of cells in G2/M phase: 18.95% for Acelarin, against 12.6% for gemcitabine and 8.13% for control. No effect of the drugs was observed on the cell cycle of SKOV3 cells, suggesting that a minimum level of active metabolites incorporated into DNA is required (Fig.3.9).

Taken together, these data suggest that Acelarin and gemcitabine display important differences in the timing of *in vitro* cytotoxicity and that the effects of Acelarin persist for longer in sensitive cells, compared to gemcitabine.

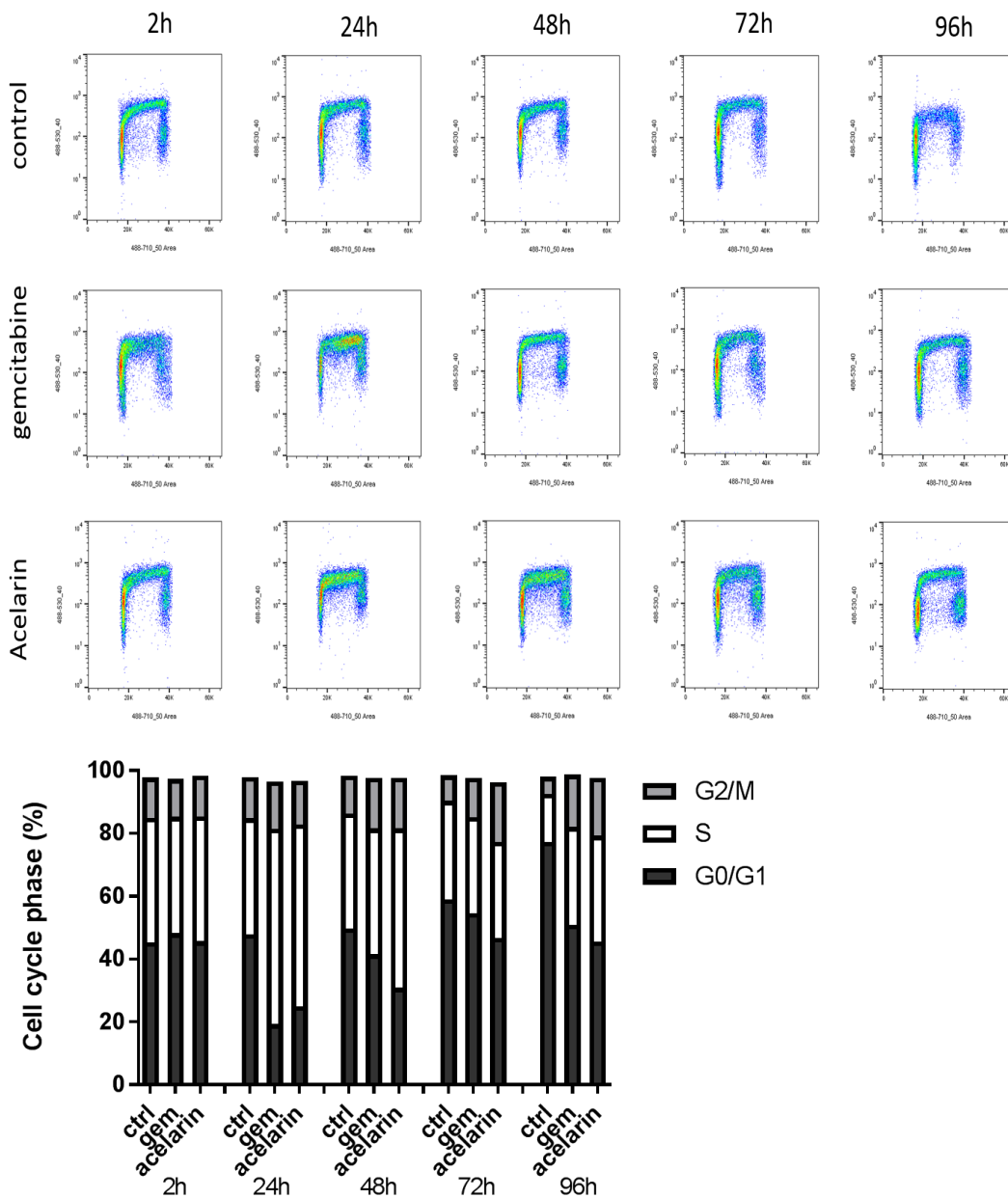


Figure 3.8: Effect of gemcitabine or Acelarin on the cell cycle of A2780. Cells were treated with IC₅₀ of gemcitabine or Acelarin for 2 h, and washed with drug-free media, samples were collected at different time points. 10 μ M BrdU was added in the media 30 min before collection. Three biological replicates were done and data presented are of one representative experiment.

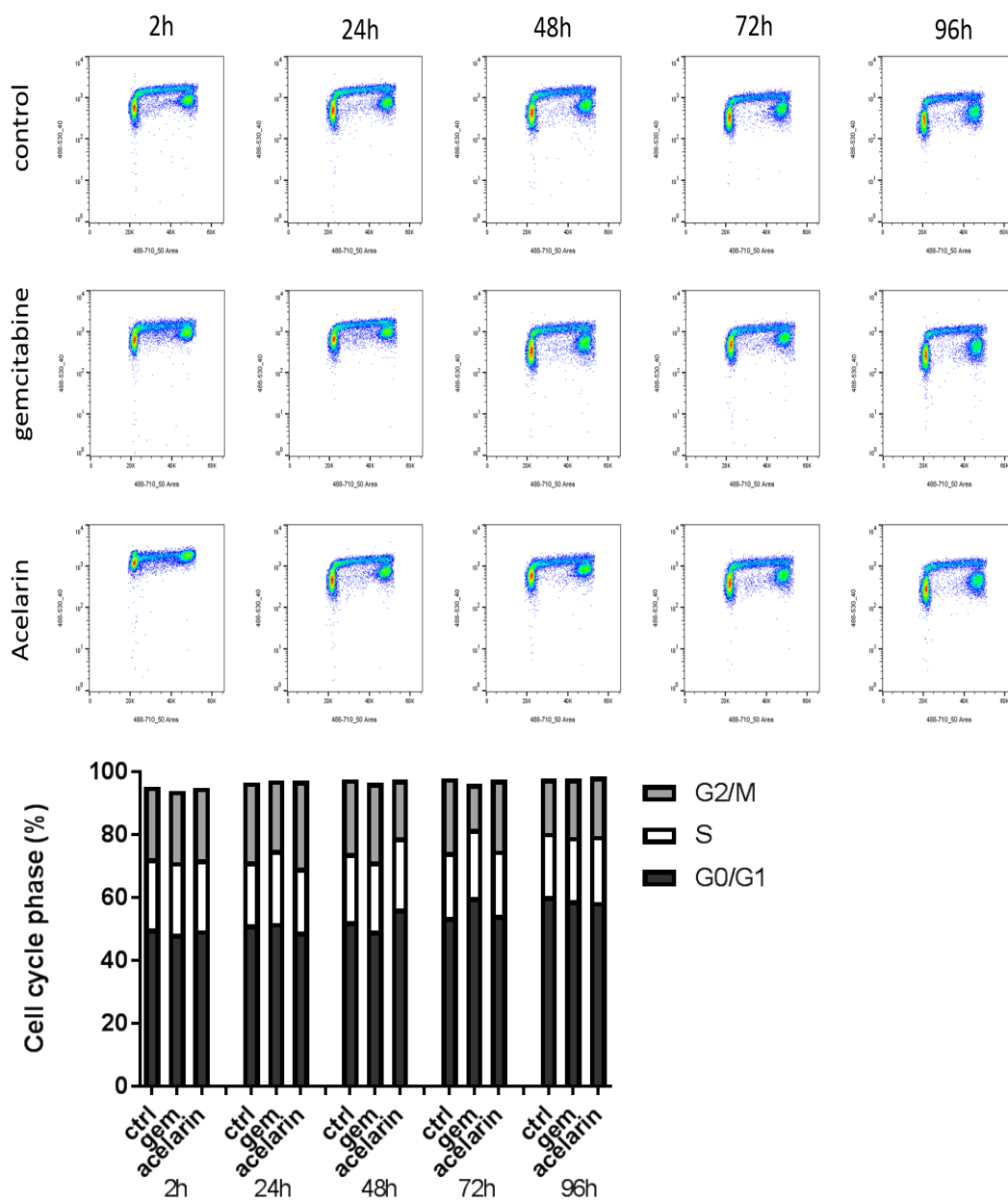


Figure 3.9: Effect of gemcitabine or Acelarin on the cell cycle of SKOV3. Cells were treated with same concentrations of gemcitabine or Acelarin as A2780 for 2 h, and washed with drug-free media, samples were collected at different time points. 10 μ M BrdU was added in the media 30 min before collection. Two biological replicates were done and data presented are of one representative experiment.

3.5 Inhibition of RRM1

Gemcitabine intermediate metabolite dFdCDP inhibits the enzyme ribonucleotide reductase (RR), which is responsible for catalysing the reaction that generates the deoxyribonucleotides required for DNA synthesis and repair. It has been shown that dFdCDP covalently modifies RRM1 in the active site in cancer cell lines and this modification leads to a conformational change (Chen et al., 2011).

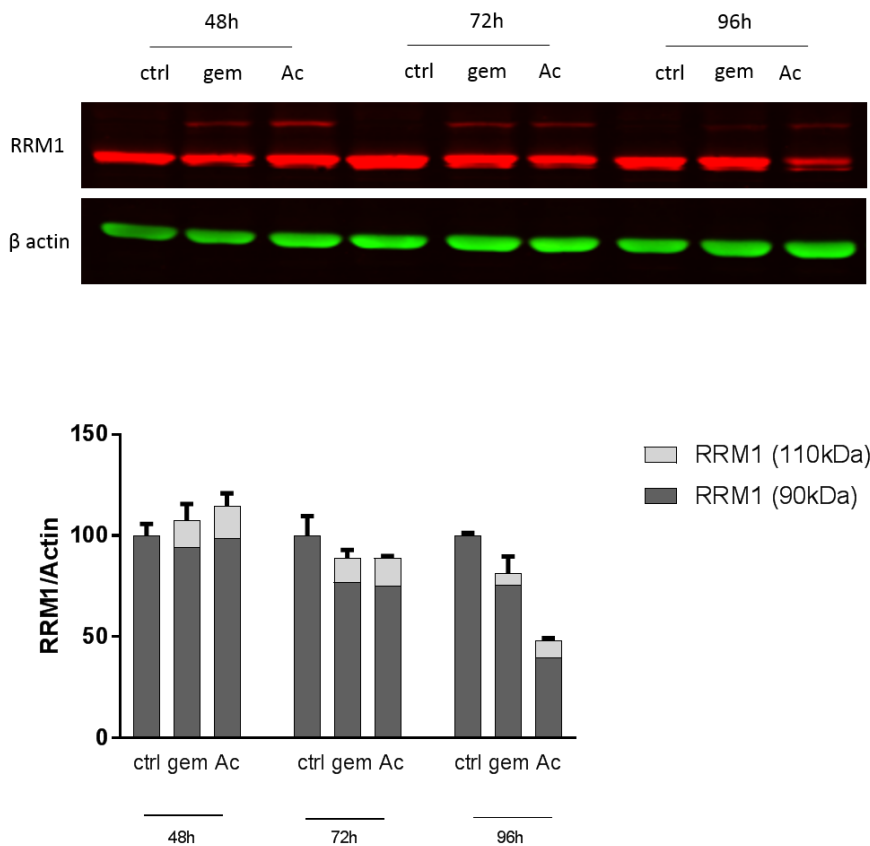


Figure 3.10: Effect of gemcitabine and Acelarin on RRM1 expression. A2780 cells were treated with IC_{50} of Acelarin or gemcitabine for 2 h, protein lysates were collected at indicated times and analysed by immunoblotting with the appropriate antibodies. Expression of RRM1 is relative to β -actin for each sample; error bars represent mean \pm SD (n=3).

The effect of Acelarin and gemcitabine on RRM1 was assessed by western blot in A2780 cells at different time points. From 48 h to 96 h, cells treated with either gemcitabine or Acelarin displayed an extra band at 110 kDa, in addition to the expected band at 90 kDa (Fig.3.10). No change in expression of totale RRM1 (90 + 110 kDa protein) was visible before 96 h. At that time point, RRM1 expression was decreased in treated cells compared to control cells, by about 20% for gemcitabine and up to 52% in cells treated with Acelarin.

3.6 DNA damage induced by Acelarin and gemcitabine

After showing that gemcitabine and Acelarin exhibit some difference in their mode of action, DNA damage induced by both drugs was investigated to find a possible explanation in the difference in timing of cytotoxicity. Gemcitabine induces DNA double-strand breaks that lead to apoptosis (Miyagawa, 2008; Jones et al., 2014). When DNA damage forms double stranded breaks (DSBs), histone H2AX is phosphorylated (γ H2AX) by kinases such as Ataxia telangiectasia mutated (ATM) and RAD3-related (ATR), members of the phosphatidylinositol 3-kinase pathway. γ H2AX, is the first step in recruiting and localising DNA repair proteins (Kuo and Yang, 2008). The presence of γ H2AX is used as a surrogate for cell death by drugs that create DNA double-strand breaks (Banáth and Olive, 2003; Nikolova et al., 2014; Ji et al., 2017).

Another method to observe DNA damage is the Comet assay, which can be used to measure DNA damage in individual eukaryotic cells. Combined with fluorescence microscopy, it allows visualisation of migration of DNA strands from individual agarose-embedded cells, and can therefore assess heterogeneity of DNA damage within a mixed population of cells. The more DNA is damaged, the longer the tail of the comet will

be (Fig. 3.11) (Olive et al., 1991; Olive and Banáth, 2006; Lovell and Omori, 2008).

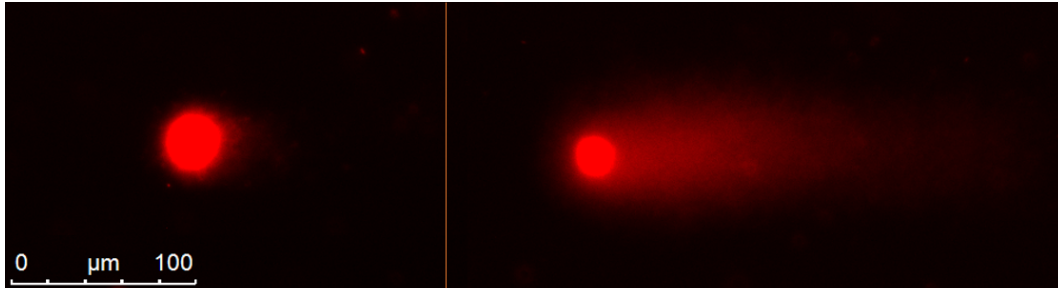


Figure 3.11: Aspect of the comets in A2780 cells. Neutral comet assay was performed to visualise DNA double strand-breaks. The left cell is a control, untreated. DNA is condensed in the "head" as there are no DNA damages. The cell on the right was exposed to H_2O_2 , which caused double strand-breaks and the un-winded DNA migrated during electrophoresis, in what is called the "tail". The longer the tail, the more damage has occurred.

Both expression of $\gamma H2AX$ and comet assay were determined at different time points in A2780 cells treated with Acelarin or gemcitabine. At 24 h post-treatment, there was no significant difference in expression of $\gamma H2AX$ between control, gemcitabine and Acelarin treated cells. After 48 h, both gemcitabine and Acelarin induced a 4-fold increase of $\gamma H2AX$ expression compared to the control. Cells treated with gemcitabine displayed a minor increase of $\gamma H2AX$ expression compared to control: 6.7-fold at 72 h and 5.3-fold at 96 h, whereas in cells treated with Acelarin, it went up to 12.4-fold higher than control at 72 h and 8.6-fold at 96 h (Fig.3.12A).

The comet assay did not demonstrate visible differences in term of DNA damage induced by Acelarin or gemcitabine compared to control, possibly because of significant heterogeneity and variation between experiments (Fig.3.12B).

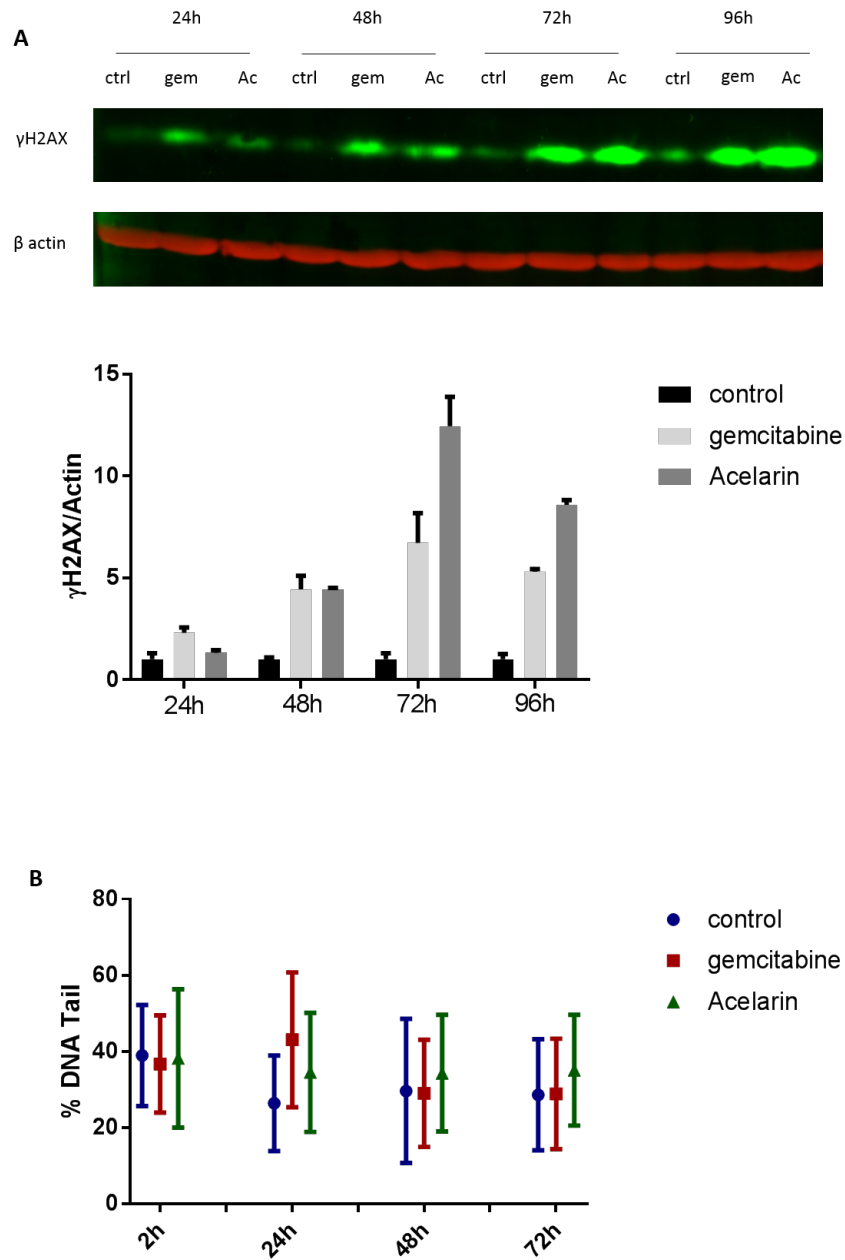


Figure 3.12: γ H2AX and comet assay to assess DNA damage induced by Acelarin and gemcitabine. A2780 cells were treated with IC_{50} of Acelarin or gemcitabine for 2 h, (A) protein lysates were collected at indicated times and analysed by immunoblotting with the appropriate antibodies. Expression of γ H2AX is relative to β -actin for each sample. (B) Quantification of DNA in the tail of the comet; error bars represent mean \pm SD (n=3).

3.7 Discussion

The differences in IC_{50} and morphology, differential delays in cell cycles, and DNA damage observed between treatment with Acelarin and gemcitabine strongly support the idea that, although similar in structure, the compounds have different time courses and therefore possibly different mode of action to induce cell death. Acelarin is showing promising anti-tumoral activity that is superior to gemcitabine *in vivo*. In patients, gemcitabine is known to be quickly inactivated and metabolised in dFdU which is then accumulated in the liver (Beumer et al., 2008; Veltkamp et al., 2008), whereas at 24 h, Acelarin still achieves levels of dFdCTP higher than reported for gemcitabine at its maximal concentration at 2 h (Blagden et al., 2018).

In the conditions of this *in vitro* study, Acelarin was less cytotoxic, with IC_{50} higher than those of gemcitabine in three ovarian cell lines. Both drugs act as cytostatic compounds meaning they inhibit cancer cell growth which, but as IC_{50} was based on survival (compared to untreated control) at the end of the experiment, the results reflect both anti-proliferative and toxic effects. This was confirmed with the time-lapse where cells exposed to gemcitabine or Acelarin underwent growth inhibition from 48 h followed by apoptosis a few hours later whereas control cells kept proliferating as normal. The relatively crude *in vitro* assays of cell death and growth inhibition do not distinguish between targeted toxicity of both Acelarin and gemcitabine (that is incorporation into DNA), versus the toxic effects of metabolites generated from gemcitabine.

The experiments were conducted only in cancer cell lines, which offer the advantages of being easily grown, relatively inexpensive, and amenable to high-throughput testing of therapeutic agents (Ferreira et al., 2013; Goodspeed et al., 2016). However, a main issue with cancer cell lines as a model is the absence of their physiological en-

vironment may be critical, as the enzymatic inactivation of gemcitabine is limited, and normal routes of elimination, such as hepatic detoxification and excretion via urine, are not represented. In order to mimic the hypoxic state of the tumour core, cells were incubated in a hypoxic environment. Because of the fast growing pace of the tumour cells, blood supply is limited, gene expression is altered and this affects cell sensitivity to chemotherapy. Strese and colleagues investigated the effect of hypoxia in a range of cancer cell lines with several anti-cancer compounds and they observed different responses from increased sensitivity to resistance (Strese et al., 2013). In the context of this work, the three cell lines A2780, CAOV3 and SKOV3 were more resistant to Acelarin and gemcitabine in hypoxia than normoxia but one of the reason may be that the growth is slowed down, therefore cells are less prone to incorporate active metabolites. Another study showed that HIF1 α (hypoxic gene) is responsible for metabolic alterations that increase the dCTP pool, which competes with dFdCTP for incorporation into DNA and causes resistance to gemcitabine (Shukla et al., 2017). Cells were less sensitive to both Acelarin and gemcitabine in absence of oxygen, but there was no significant difference between the two compounds.

Both gemcitabine and Acelarin induced cell cycle arrest, with a majority of cells blocked during replication in S phase at 24 h post-treatment. Whilst cells treated with gemcitabine started to revert back to normal cell cycle after 48 h, a higher proportion of cells treated with Acelarin was retained in S phase at 48 h and in G2/M phase at 72 h, compared to control or cells treated with gemcitabine. This corroborates with the changes in morphology observed during the time-lapse where cells appeared bigger due to increase in DNA and protein content following replication. In parallel their growth was slowed by exposure to the drug as the protein content determined at the different time points for western blot was lower compared to control untreated, this indicates that both Acelarin and gemcitabine had an inhibitory effect on cell growth.

This morphological modification also explains the 24 h period during which cells neither divided nor died, until they underwent apoptosis at 72 h for those treated with Acelarin. On the contrary, cells treated with gemcitabine started to die 48 h post-treatment. Carpinelli and colleagues, reported similar observations in C6 rat glioma cells treated with gemcitabine. They did not observe apoptosis at the end of the 24 h treatment, whereas there was approximately 30% of apoptotic cells at 48 h and about 45% at 72 h post-treatment (Carpinelli et al., 2006). Data from time-lapse and cell cycle study suggest that the cytotoxic effects of gemcitabine appear sooner than Acelarin and might be due to other factors than incorporation of dFdCTP in DNA during synthesis only. This could be mediated through the stabilisation of top1 cleavage complexes. Gemcitabine is a known topoisomerase I poison and this is responsible for double-strand break DNA damage (Pourquier et al., 2002; Gmeiner et al., 2003). Acelarin has a more prolonged effect and can potentially induce more accumulation of damage over time.

DNA damage caused by Acelarin and gemcitabine was investigated. γ H2AX foci are commonly detected and can be quantified by immunofluorescence, western blot or flow cytometry (Toyooka et al., 2011; Khan et al., 2018). The advantage of immunofluorescence or flow cytometry is that it is possible to count cells with DNA damage or to sort cells based on their γ H2AX expression (Ewald et al., 2008; Johansson et al., 2017). Here we chose to use western blot and to combine it with a comet assay to detect DNA damage in single cells. Gemcitabine caused DNA damage with an up-regulation of γ H2AX expression up to 4-fold from 48 h and not higher than 6.7, compared to the control. By contrast, Acelarin induced an increase of γ H2AX expression which is 1.85 and 1.62 times greater than gemcitabine at 72 h and 96 h, respectively. This suggests that, in the long term, Acelarin causes more DNA damage and maybe increases the likelihood of apoptosis. On the contrary, gemcitabine is toxic

for the cells, not only due to incorporation of its active metabolite dFdCTP but also because it is degraded by CDA, which generates the toxic metabolite dFdU (Veltkamp et al., 2008). One of the advantages of the comet assay is to be a quick and sensitive method for measuring DNA strand breaks in eukaryotic cells. It can be carried out in single cells and a large number of samples can be evaluated. On the other hand, a main limitation is the variability, that makes the analysis difficult. The minimum recommended sample size is fifty individual comets but this may not be adequate if there is significant heterogeneity in DNA damage within a population (Olive et al., 1991; Olive and Banáth, 2006).

Another limitation is the requirement for a viable single-cell suspension. If samples contain predominantly necrotic or apoptotic cells, accurate information on the presence of specific lesions cannot be obtained as these cells are not visible (Collins, 2004). At 72 h and 96 h, damaged cells underwent apoptosis and therefore, were not likely to be included in the analysis. These different reasons could explain why the results obtained were not conclusive. For early time points, when cells are damaged but not in an irreversible manner, a larger number of samples is required to reduce the factor of heterogeneity in DNA damage. It is also important to keep in mind that interpretation of such experiments is complicated by the fact that there is no simple relationship between the amount of DNA damage caused by a specific chemical and the biological impact of that damage. Each drug can differ in terms of the number of DNA breaks that are associated with a given biological effect.

Ribonucleotide Reductase M1 (RRM1) is the regulatory subunit of the holoenzyme that catalyses the conversion of ribonucleotides to deoxyribonucleotides. Indispensable in cell proliferation and DNA repair, it also has been used as a biomarker of therapeutic efficacy of gemcitabine. Although the mechanistic of RRM1 inhibition

by dFdCDP remains unclear, it was found that a novel 110 kDa band, along with the 90 kDa native RRM1 band, appeared in cells treated with gemcitabine (Chen et al., 2011). In A2780 cells treated with gemcitabine or Acelarin, this conformational change of RRM1 protein was observed with the appearance of the 110 kDa band which was absent from the control. This suggests that Acelarin does act similarly to gemcitabine in the sense that dFdCDP inhibits RRM1, which then decreases the pool of dCTP available for the cells to replicate and potentiate the nucleoside analogues' effect as previously described by Heinemann and colleagues. Interestingly, there was a decrease of protein expression at 96 h which was more important in cells treated with Acelarin compared to gemcitabine. Later time points such as 120 h and 144 h would be useful to verify if the decrease of expression is consistent and specific to Acelarin. This is another difference between the two drugs that could explain why Acelarin's effects are more sustained than gemcitabine. RRM1 is ubiquitous whereas RRM2 is cell cycle dependant. Effect of both drugs on expression of RRM2 should also be investigated to determine how Acelarin might affect it and if there is a link with the cell cycle delay.

This thesis focused on the different pharmacodynamics between Acelarin and gemcitabine. Apart from drug interactions and toxicity that cannot be predicted *in vitro*, a number of biological factors, such as pharmacokinetics including metabolism, drug distribution and degradation, were not taken into account in this study. Higher levels of dFdCTP released by Acelarin compared to gemcitabine could lead to a more prolonged incorporation into newly synthesised DNA and ultimately mean an increased cytotoxic effect. In the context of this cancer model, a higher concentration of Acelarin was used to reach a similar cell death outcome as gemcitabine, whereas it is more potent in patients. It would be interesting to analyse the levels of intracellular metabolites dFdCTP present in the cells, as well as incorporated into DNA, by mass spectrometry. This was not possible because of capacity issues on the mass spectrometry instrument

and problems of metabolite stability.

All the evidence presented in this chapter suggest that Acelarin has a more targeted mode of action than gemcitabine, which could predict why patients in initial studies have fewer side effects and more sustained duration of action.

4 | Combination of Acelarin and cisplatin in ovarian cancer

4.1 Introduction

Combination therapies have become the norm for the treatment of cancer. They are used to achieve an improved therapeutic result by exploiting the chances for better efficacy, decreased toxicity, and reduced development of drug resistance (Foucquier and Guedj, 2015). Understanding the mechanism of action of a given drug can help to decide which other compound(s) to combine it with. Yet, it is not always possible to predict with certainty how they will react together. Furthermore, the sequence of drug administration is also an important factor, in order to achieve the maximal beneficial effect with minimal toxicity.

Positive effects of gemcitabine-carboplatin and gemcitabine-cisplatin combination therapies in ovarian cancer have been reported *in vitro* and in clinical trials (Bergman et al., 1996; Moorsel, 1999; Moufarij, 2003; Eisenhauer et al., 2014; Ulker et al., 2015). The standard regimen consists of gemcitabine intravenously administered over 30min followed by cisplatin or carboplatin for 1 h (Rose et al., 2003; Eltabbakh et al., 2016). Acelarin is already showing promising results *in vivo* (Blagden et al., 2018), and clinical studies of Acelarin in combination with other agents, are currently ongoing in patients with ovarian and biliary cancers.

In this chapter, we aimed to determine the effectiveness of Acelarin-cisplatin combination in an *in vitro* model of ovarian cancer. In patients with platinum-sensitive ovarian cancer, treatment with platinum-based compounds, the platinum binds to DNA (known as platinum-DNA adducts), causing lesions and leading to cell death. However, in patients with platinum-resistant ovarian cancer, the cancer cells have a higher tolerance for DNA damage and are able to repair following platinum treatment (Johnson et al., 1997; Olaussen et al., 2006). It was hypothesised that cisplatin treatment in platinum-resistant cancer cells may act as a sensitiser to further damage with Acelarin by incorporation of dFdCTP into DNA. Cancer cells undergo a higher level of repair following platinum treatment and should therefore incorporate an increased number of faulty nucleotides into DNA when the cells are subsequently treated with Acelarin. The increased incorporation of faulty nucleotides should push the cell towards apoptotic pathways and cell death.

PE01 and PE04 are cell lines derived from a single patient with poorly differentiated ovarian serous adenocarcinoma, at different stages of treatment. PE01 was derived from the peritoneal ascites when the patient was still clinically responsive to cisplatin at the first relapse. PE04 was derived from ascites after the patient developed clinical resistance to cisplatin (Langdon et al., 1988). PE01 cell line has a germline BRCA2 mutation (Sakai et al., 2009) which makes the cells sensitive to platinum treatment. On the contrary, a second mutation has occurred in PE04 cells which restored the wild-type amino acid sequence and rendered them resistant to platinum-based chemotherapy (Sakai et al., 2009; Cooke et al., 2011).

4.2 Validation of CalcuSyn method

Synergy and antagonism are defined by, respectively, greater or lesser effects for drugs in combination than the simple effect of each drug individually. However, translating them into a valid methodology is a delicate issue that generally begins with the formal definition of additivity. Indeed, effect of drug A + drug B being greater than effect of drug A or drug B alone does not necessarily mean synergy, it can simply be an additive effect. The Chou-Talalay method (Chou and Talalay, 1983; Chou and Talalay, 1984) was developed in order to design a consistent system to determine synergism, as prior to that, there used to be several different methods and none supported the others (Goldin and Nathan, 1957; Greco et al., 1995). They introduced the concept of “combination index” (CI) to quantitatively depict synergism ($CI < 1$), additive effect ($CI = 1$), and antagonism ($CI > 1$). A combination index (CI) is calculated from drug cytotoxicity or growth inhibition curves (Bijnsdorp et al., 2011). First released in 1997, CalcuSyn software greatly facilitated its applications and is now used to appraise the therapeutic effects of drug combination (Chou, 2010). The classification of the combination index (CI) is represented in Table 4.1. The CI value of between 0.9 and 1.1 represent additivity. The CI value less than 0.9 represents synergism while the value above 1.1 means antagonism.

Two different studies used CalcuSyn to determine the therapeutic effect of drug combinations involving cisplatin in a panel of ovarian cell lines. Hunakova et al. showed that combination of cisplatin and sulforaphane is synergistic in A2780 and antagonistic in SKOV3 cells (Hunakova et al., 2014). The other study, conducted by Taylor-Harding and colleagues, showed synergistic cytotoxicity of fluvastatin and cisplatin in SKOV3 and CAOV3 cell lines (Taylor-Harding et al., 2010). The effect of combination of those

two drugs with cisplatin was investigated in SKOV3 cells, in order to validate the CalcuSyn method.

Combination Index	Description
<0.1	Very strong synergism
0.1-0.3	Strong synergism
0.3-0.7	Synergism
0.7-0.85	Moderate synergism
0.85-0.90	Slight synergism
0.90-1.10	Nearly additive
1.10-1.20	Slight antagonism
1.20-1.45	Moderate antagonism
1.45-3.3	Antagonism
3.3-10	Strong antagonism
>10	Very strong antagonism

Table 4.1: Interpretation of CI values from CalcuSyn software (Chou, 2006).

First, IC_{50} for each drug was assessed in SKOV3 cells. In both Taylor-Harding's and Hunakova's investigations, cells were treated with single agent or co-treated with drugs combination for 72 h before cytotoxicity was evaluated. In our study, cells were treated for 24 h with increasing concentrations of the different drugs and SRB was performed at 96 h post-treatment, as per usual protocol (section 2.1.3). They displayed an IC_{50} of 3.4 μ M for cisplatin, 7.7 μ M for sulforaphane, and 8.7 μ M when treated with fluvastatin for 4 days (Fig.4.1). There was no effect of fluvastatin after 24 h treatment.

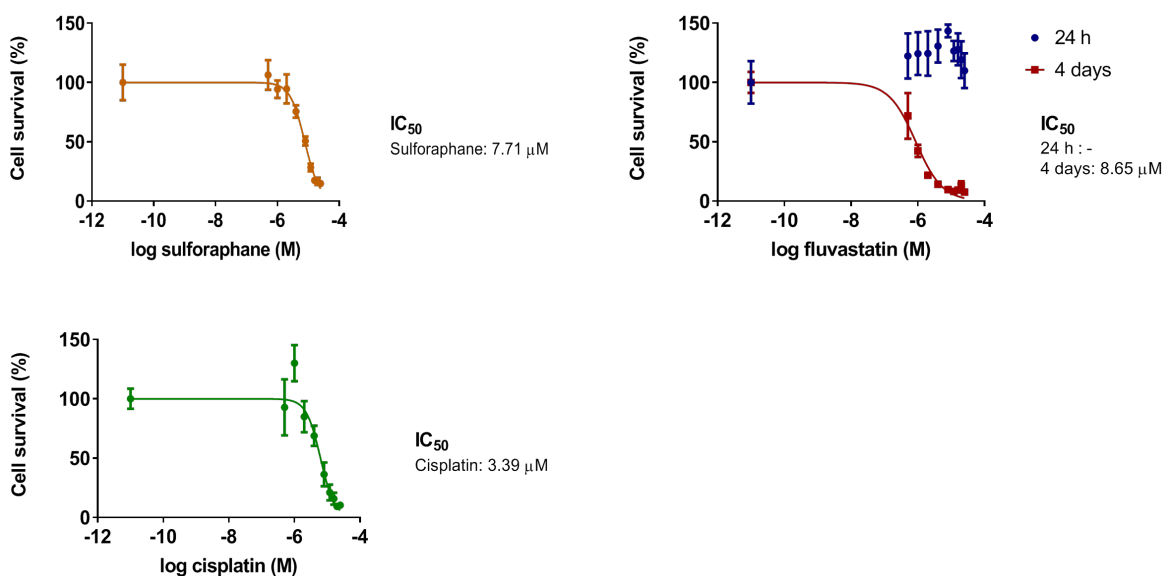


Figure 4.1: Dose response of SKOV3 to different chemotherapies. Cells were treated for 24 h with sulforaphane, fluvastatin or cisplatin as well as 4 days for fluvastatin and SRB was performed at 96 h post-treatment. IC_{50} for each cell line was determined from the average data collected with SRB assay. Data are expressed as the mean \pm SD.

Then, cells were co-treated for 24 h with either 1 μ M or 1.5 μ M of cisplatin as a fixed dose and a range of concentrations of sulforaphane (2 to 12 μ M). The fraction affected (FA) was calculated based on the values obtained from the cytotoxicity assay at 96 h post-treatment, as follow: $FA = 1 - (\%growth/100)$. The FA curve is another

way used by CalcuSyn to depict a growth inhibition curve, it indicates the effect of each separate agent and the combination (Bijnsdorp et al., 2011). Each FA values were entered in CalcuSyn and the combination index for each condition was calculated. In this experiment, the CI values for all combinations were higher than 1.1 (Fig.4.2), meaning that the different combinations were antagonistic. However, the cell survival data displayed no different effect of 1 μ M cisplatin combined with 2 μ M sulforaphane, than for cisplatin alone (63% \pm 6.7 vs 51% \pm 3.2), similar observations were made for combination of 1.5 μ M cisplatin with different concentration of sulforaphane.

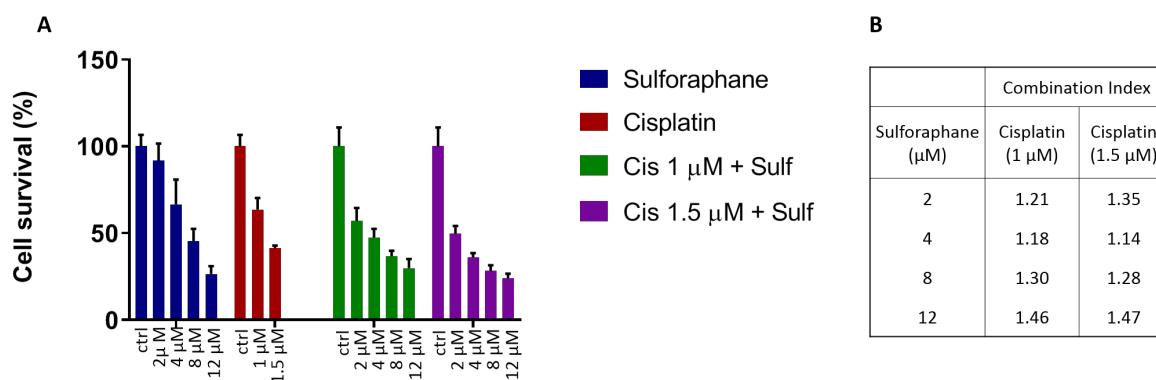


Figure 4.2: Effect of sulforaphane and cisplatin combination in SKOV3 cells. (A) Cells were treated for 24 h with combination of both drugs and SRB was performed at 96 h post-treatment. Data are expressed as the mean \pm SD. (B) Combination index (CI) values calculated by CalcuSyn from relative viability (SRB assay).

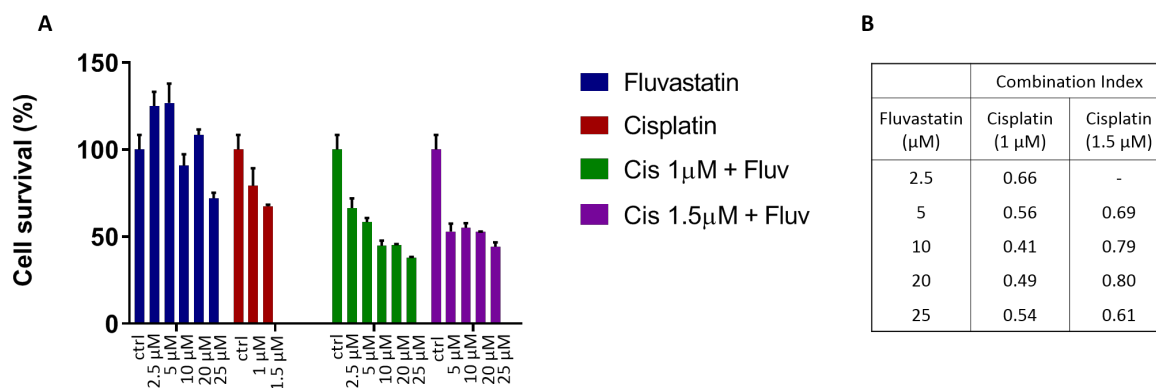


Figure 4.3: Effect of Fluvastatin and cisplatin combination in SKOV3 cells. (A) Cells were treated for 24 h with combination of both drugs and SRB was performed at 96 h post-treatment. are expressed as the mean \pm SD. (B) Combination index (CI) values calculated by CalcuSyn from relative viability (SRB assay). There was no experiment carried out for the combination 1.5 μ M cisplatin with 2.5 μ M fluvastatin.

Similar experiment was carried out by co-treating cells with 1 μ M or 1.5 μ M of cisplatin and different concentrations of fluvastatin (2.5 to 25 μ M) for 24 h. As result, all the CI values were lower than 0.8 for combination of fluvastatin with 1 and 1.5 μ M of cisplatin, which corresponded to the cell survival data (Fig.4.3).

According to the CI values, sulforaphane-cisplatin combination showed to be antagonistic in SKOV3 cells and fluvastatin-cisplatin combination was synergistic. The results obtained were in concordance with the studies this experiment was based on. As no growth inhibition data for the sulforaphane-cisplatin combination in Hunakovas's study were available, there was no comparison possible to explain the divergence between the lack of cell survival difference and antagonistic combination index observed in this chapter. Therefore, based on the CI values the CalcuSyn method was validated and used to determine the efficacy of Acelarin-cisplatin combination in ovarian cell lines.

4.3 Sequential treatments with Acelarin-cisplatin combination in ovarian cell lines

Previous experiments, performed by Ateeb Khan, showed no synergy in PE01 and PE04 cells treated simultaneously with Acelarin and cisplatin for 24 h (Appendix 7.9). Hence, it was hypothesised that, as in a clinical setting, cells should be exposed to both drugs in specific sequence, to bring them into a state more susceptible to the cytotoxic effects of the chemotherapies. Effect of sequence of Acelarin-cisplatin combination was evaluated in PE01 and PE04 cell lines.

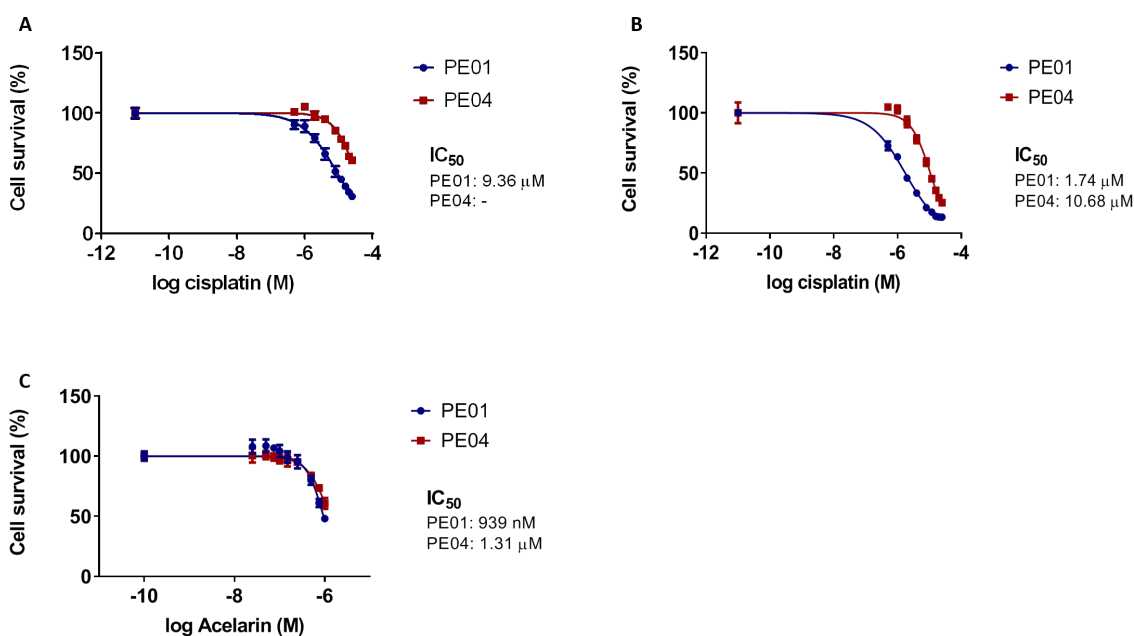


Figure 4.4: Dose response of Acelarin and cisplatin in PE01 and PE04 cells. Cells were treated for 4 h (A) or 24 h (B) cisplatin or 2 h Acelarin (C) and SRB was performed at 96 h post-treatment. IC_{50} were determined from the average data collected with SRB assays. Two biological replicates were done for each condition. Data are expressed as the mean \pm SD.

Cytotoxicity assays for IC_{50} were performed by treating cells with either Acelarin for 2 h, or cisplatin for 4 h and 24 h (Fig.4.4). PE01 cells were slightly more sensitive to Acelarin than PE04 cells (IC_{50} of 939 nM and 1.3 μ M, respectively). As expected, PE01 cell line was more sensitive to cisplatin than PE04, with an IC_{50} of 9.4 μ M for PE01 cells at 4 h, whereas it could not be calculated for PE04 cells, with only 30% cell death at 20 μ M. When cells were exposed to cisplatin for 24 h, IC_{50} was 1.74 μ M and 10.7 μ M for PE01 and PE04 cells, respectively.

The following experimental design was used for all the sequential experiments:

- (1) Cells treated with only Acelarin or cisplatin for the defined time, this was used as single agent control.
- (2) Cells treated with 1 or 12 μ M of cisplatin and varying concentrations of Acelarin (75, 250 and 500 nM).
- (3) Cells treated with 75 or 250 nM of Acelarin and varying concentrations of cisplatin (1, 4, 12 and 20 μ M).

The first drug combination sequence consisted of a 2 h treatment with Acelarin, after which media was removed, and followed by a 4 h treatment with cisplatin. At the end of the sequential treatment, cells were washed out and let to grow until 96 h post-treatment, when cytotoxicity was assessed.

The growth of PE01 cells was inhibited by 15 to 25% compared to the control when cells were treated with increasing concentrations of Acelarin (75 to 500 nM), and up to 45% when treated with 20 μ M of cisplatin (Fig.4.5A). The different combinations of 1 μ M cisplatin with Acelarin exhibited strong antagonism as no cytotoxicity was detected. Combination of 12 μ M cisplatin with 75 nM Acelarin inhibited cell growth by 30%, whereas it was about 25 and 15% with respective drugs alone. This resulted in a lower CI value, at the limit of slight synergism and additivity. On the contrary,

when cells were treated with higher concentration of Acelarin and 12 μM cisplatin, it displayed antagonism, although the cell survival data showed no difference between the combination and cisplatin alone. When cells were treated with 75 nM of Acelarin and 1 or 4 μM of cisplatin, the percentage of survival for cells exposed to Acelarin and cisplatin together was similar to that of 75 nM Acelarin alone. At high concentrations of cisplatin, the cell survival was similar to that of cisplatin alone. This suggests that although both drugs do not antagonise each other, the growth inhibition of the combination is mainly due to the effect of one or the other but there is no synergistic effect. This is represented by CI values of 1.08 to 1.09 (Fig.4.5B).

In this experiment, CI values were not available for PE04 cell line as 4 h treatment with cisplatin alone did not have an effect on growth of the cells. However, it is visible that percentage of cell survival was higher in cells treated with the different combination compared to when treated with only Acelarin (Fig.4.5C).

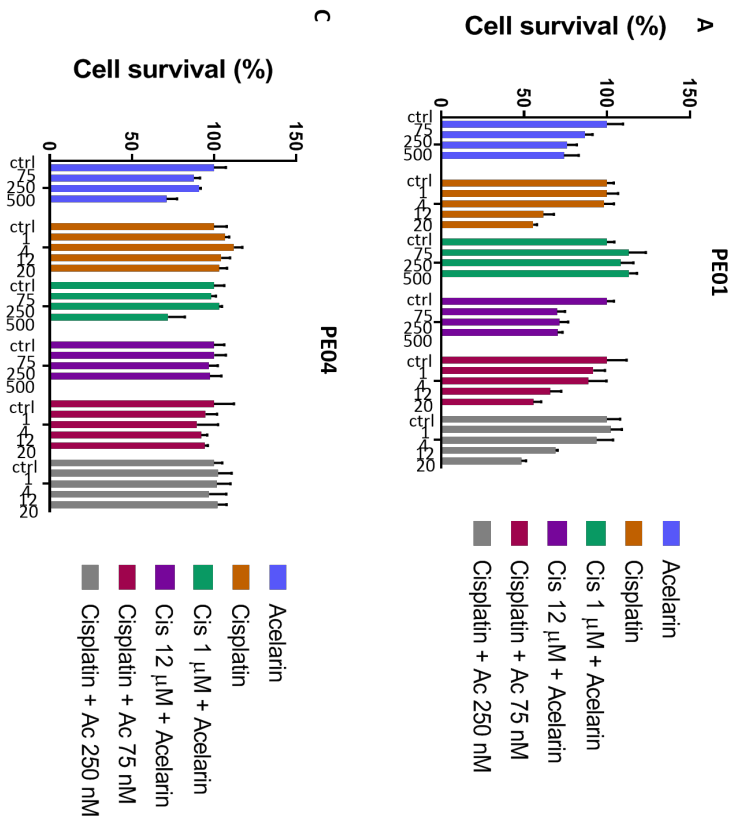
For the second sequence, cells were treated with Acelarin for 2 h, followed by a 24 h treatment with cisplatin. At the end of the sequential treatment, cells were washed out and let to grow until 96 h post-treatment, when cytotoxicity was assessed. Longer exposure to increasing concentrations of cisplatin as a single agent (1 to 20 μM) induced a more important growth inhibition, from 40 to 91% for PE01 and 9 to 70% for PE04 cells. As in the previous experiment, PE01 cells treated with 1 μM and different concentrations of Acelarin displayed a cell growth more important than when treated with Acelarin alone (64% cell survival for 1 μM /500 nM vs 31% for 500 nM Acelarin) (Fig.4.6A). With higher concentration of cisplatin such as 12 μM , the CI values reflected additivity only. A difference was observed with the 75 nM Acelarin combinations which were antagonistic (Fig.4.6B), especially 1 μM /75 nM and 4 μM /75 nM (39% cell survival for 4 μM /75 nM vs 32% for 4 μM cisplatin), whereas

it was additive with shorter treatment of cisplatin. Any combination of treatment with Acelarin first followed by cisplatin resulted in antagonism for PE04 (Fig.4.6C-D).

Independently of the length of cisplatin exposure, pre-incubation with Acelarin prior to treatment with cisplatin resulted only in antagonism in PE04. Different patterns were observed between the different exposure time to cisplatin for the sensitive cell line PE01. When short exposure to cisplatin, there was less antagonism in combination with 75 nM Acelarin. On the contrary, when cells were treated with cisplatin for 24 h, they seemed to be more sensitive to the combinations with Acelarin and 12 μ M cisplatin, compared to the others.

The last experiment consisted of a 4 h treatment with cisplatin followed by 2 h treatment with Acelarin and cytotoxicity assessed at 96 h post-treatment. All CI values for PE01 cell line indicated antagonism (Fig.4.7A-B). The strongest antagonism detected was when cells treated with 1 μ M cisplatin followed by 75 nM Acelarin. Cell death was 20% more important with cisplatin alone than in combination with Acelarin.

Interestingly, an effect was observed for PE04 cells treated with 1 μ M cisplatin and different concentration of Acelarin. When cells were treated with 75 nM Acelarin and 1 μ M or 4 μ M cisplatin, cell survival was reduced by about 10% compared to Acelarin alone at 75 nM (Fig.4.7C). This was never noticed when PE04 cells were pre-treated with Acelarin before cisplatin. CI values could not be obtained since the cell line was resistant to cisplatin treatment (Fig.4.7D). The effect of 4 μ M cisplatin with different concentrations of Acelarin was further investigated (Fig.4.7E-F). Both cell survival and CI values indicate a possible synergy between 4 μ M cisplatin with 250 and 500 nM Acelarin.



B

	Combination Index		Combination Index	
	Acelarin (nM)	Cisplatin (1 μM)	Cisplatin (12 μM)	Acelarin (250 nM)
75	-	0.94	1	-
250	-	1.31	4	5.25
500	-	1.70	12	1.21
			20	1.05

Figure 4.5: Effect of Acelarin (2 h) and cisplatin (4 h) combination in PE01 and PE04 cells. Cells were treated for 2 h with Acelarin, followed by 4 h cisplatin. Concentration of Acelarin are in nM and cisplatin in μM . Graphs represent cell survival from the average data collected with SRB assays for PE01 (A) and PE04 cells (C), data are expressed as the mean \pm SD. (B) Combination index (CI) values calculated by CalcuSyn from relative viability (SRB assay). At least two biological replicates were done for each condition.

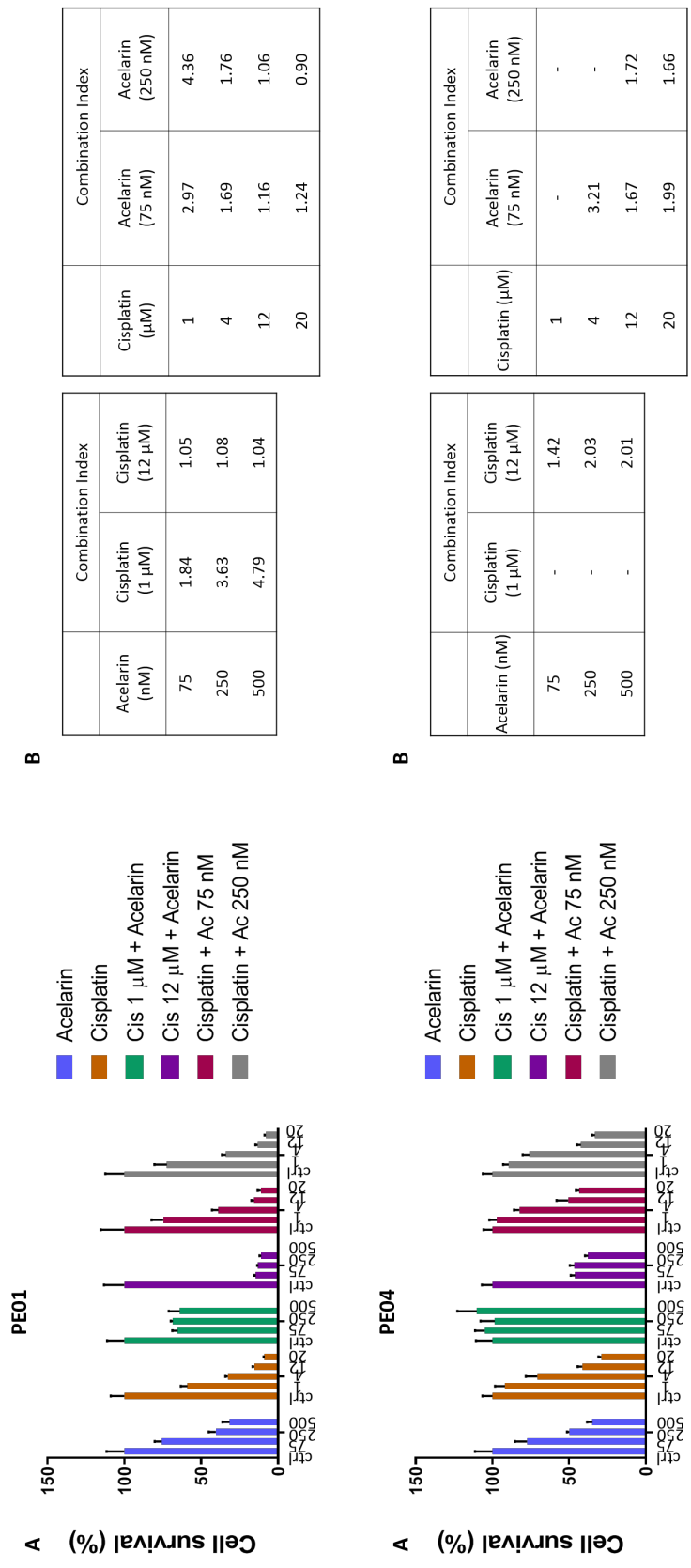


Figure 4.6: Effect of Acelarlin (2 h) and cisplatin (24 h) combination in PE01 and PE04 cells. Cells were treated for 2 h with Acelarlin, followed by 24 h cisplatin. Concentration of Acelarlin are in nM and cisplatin in μM . Graphs represent cell survival from the average data collected with SRB assays for PE01 (A) and PE04 cells (C), data are expressed as the mean \pm SD. (B-D) Combination index (CI) values calculated by CalcuSyn from relative viability (SRB assay). Two biological replicates were done for each condition.

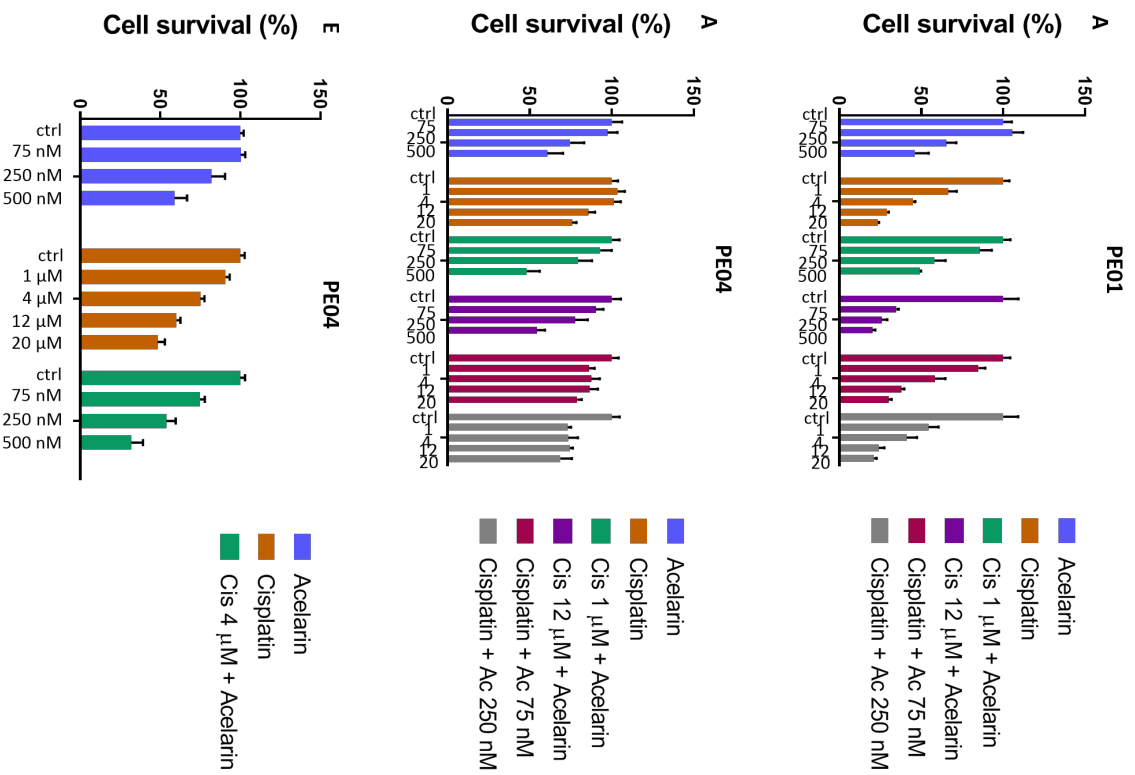


Figure 4.7: Effect of cisplatin (4 h) and Acelarlin (2 h) combination in PE01 and PE04 cells. Cells were treated for 4 h cisplatin followed by 2 h with Acelarlin. Graphs represent cell survival from the average data collected with SRB assays for PE01 (A) and PE04 cells (C&E). Data are expressed as the mean ± SD. (B, D, F) Combination index (CI) values calculated by CalcuSyn from relative viability (SRB assay). At least two biological replicates were done for each condition.

4.4 Discussion

Drug combination therapy is a standard in cancer treatment; however, it is difficult to find the best combination possible and many parameters must be taken into account, such as sequence and timing. For decades, there was no consensus on a method to determine the efficacy of combination studies. The Chou-Talalay method (Chou and Talalay, 1983; Chou and Talalay, 1984) was developed to resolve this issue. In order to eliminate subjectivity and permit automated data analysis, the complex algorithms were incorporated into a software programme, CalcuSyn. This method has been used for many drug combination studies (Roscelli et al., 2016; Attia et al., 2016; Matthews et al., 2017; Zhong et al., 2018).

CalcuSyn was validated by carrying out an adapted version of two publications showing either synergy or antagonism in SKOV3 cells (Taylor-Harding et al., 2010; Hunakova et al., 2014). The difference with the original experimental designs was that cells were treated for 24 h and cytotoxicity was assessed at 96 h post-treatment, instead of being exposed to the combination for the whole duration of the experiment (72 h). As discussed in the previous chapter, treating cells for days is not physiologically relevant as any drug would have been metabolised in only a few hours in patients. Hence, cells were exposed to Acelarin and cisplatin for a relatively short period of time (2 to 24 h). Contrastingly, in most studies cells were pre-treated for 4 h to 24 h with drug A and drug B was left until the end of the experiment, usually 72 h (Zanellato et al., 2011; Tang et al., 2013).

The choice of the right model for combination studies is also crucial, as reported by Hunakova where cisplatin-sulforaphane combination was synergistic in A2780 cells but antagonistic in SKOV3 cells (Hunakova et al., 2014). Similar findings were de-

scribed by Budman and Calabro, whose combination studies of docetaxel with different compounds in breast cancer cell lines showed no universal effect (Budman and Calabro, 2002). The synergistic interaction between gemcitabine and cisplatin was investigated in a panel of human ovarian cell lines, including A2780, its cisplatin-resistant variant ADDP and gemcitabine-resistant variant AG6000 (Bergman et al., 1996; Moorsel, 1999). Although these cell lines were models of resistance to the standard chemotherapies used in the treatment of ovarian cancer, they were created by exposure to increasing concentrations of cisplatin or gemcitabine over time *in vitro* (Ruiz Van Haperen et al., 1994). PE01 and PE04 cell lines were derived from a single patient who had developed resistance to platinum treatment over time (Langdon et al., 1988). Therefore, they represented a more relevant model for this work. There is also the question of the *in vitro* system limits mentioned in the previous chapter, such as the lack of the physiological environment. The hypoxic condition of the tumour can be recreated in a laboratory setting and it would be interesting to investigate these combinations to determine how oxygen levels may affect them, especially as it was showed that it has an effect on sensitivity to Acelarin and gemcitabine.

The investigation of different sequential treatments with Acelarin-cisplatin combination in PE01 and PE04 cell lines did not show synergistic effect. This could be due to the conditions chosen, such as the range of concentrations or timing. Bergman's research highlighted the importance of sequence and timing, as a same combination can be antagonistic at shorter exposure (less than 24 h) but synergistic after 48 to 72 h drug treatment. They also found that pre-incubation with cisplatin for 4 h followed by a gemcitabine incubation for 1, 4, 24, and 72 h resulted in synergism or additivity for all the combinations.

Interestingly however, differences were observed between the different sequences and PE01/PE04 cell lines and this correlates with the platinum sensitivity of the cells. It is well established that platinum-based chemotherapies are highly efficient in platinum-sensitive cancers whereas resistance emerges from adaptation, partly associated with increased tolerance to platinum-DNA damage (Johnson et al., 1997; Rabik and Dolan, 2007). It has been shown that ovarian cancer cell lines resistant to cisplatin and carboplatin exhibited elevated levels of DNA repair proteins and repair activity as well as a decrease in apoptosis (Jung and Lippard, 2007; Stefanou et al., 2015). In addition, DNA repair proteins expression (such as BRCA1 and ERCC1) is correlated with poor survival in advanced ovarian cancer (Weberpals et al., 2009). The reverse mutation of BRCA2 in PE04 rendered them resistant to cisplatin by increasing the DNA repair activity (Sakai et al., 2009; Cooke et al., 2011). In PE01 cells pre-treated with Acelarin prior to treatment with cisplatin, the effect observed was mainly of cisplatin. Even though Acelarin had an effect on cell growth when used alone, this might be minor compared to cisplatin. If DNA damage induced by cisplatin happened before activation of Acelarin or incorporation of dFdCTP into DNA, any additional cytotoxicity may have been insufficient to potentiate the effect of cisplatin. As mentioned above, PE04 cells have an increased repair mechanism rate compared to PE01. Initial treatment with cisplatin induces DNA damage, which is being repaired. During this process, more of the faulty nucleotide is incorporated into DNA, in addition of the main pathway of incorporation during synthesis. This leads to persistence of DNA damage and a prolonged cell death. Moorsel et al. found that the synergism between gemcitabine and cisplatin appeared to be mainly due to an increase in platinum-DNA adduct formation, possibly related to conformational changes due to dFdCTP incorporation into DNA (Moorsel, 1999). In another study, it was shown that the inhibition of repair of cisplatin DNA damage by gemcitabine is critical to the cytotoxic synergy reported between the drugs (Mou-

farij, 2003). Mechanistic studies with evaluation of amount of DNA damage induced by the different combination by the mean of γ H2AX should be performed to further understand the consequences of interaction between cisplatin and Acelarin.

The different publications mentioned above used A2780 cells to assess the effect of cisplatin-gemcitabine combination in ovarian cancer. The growth characteristic of the cells is an important factor for the analysis of such studies. It was previously established that A2780 cell line is very sensitive to both gemcitabine and Acelarin. The doubling time of this cell line being relatively short, only 18 h (Beaufort et al., 2014), more dFdCTP is likely to be incorporated into new synthesised DNA. By contrast, the doubling time of PE01 and PE04 cells is about 37 h (Langdon et al., 1988). Therefore, with short drug treatments, a quickly growing cell line is more prone to accumulation of DNA strand breaks induced by platinum damage amplified by DNA distortions following dFdCTP incorporation.

CalcuSyn has a number of limitations that need to be addressed. The first one is the translation from cell survival data to synergy/antagonism status. Despite having an effect on cell growth, if there was no fraction affected for cells treated with a single drug, then no combination index could be calculated. Furthermore, there may be some divergence between the CI values and cell survival, and this can affect the interpretation of the results. Because of the model $CI < 1$ synergy, $CI = 1$ additivity and $CI > 1$ antagonism, there is no definition for a lack of difference in cell survival between single agent(s) and combinations and they may be represented as antagonist when despite this not being correct. This was illustrated with the first experiment where sulforaphane and cisplatin were used in combination in SKOV3 cells. Although the CI values were similar to the one published in Hunakova's and colleagues study, they did not present any additional data that can confirm they really had an antagonistic

response with their drug combinations.

Another issue encountered in publications on combinations studies is that the variability inherent to this kind of experiment is rarely mentioned. In this chapter only one representative experiment was shown, but similar trend was observed in repeats (Appendix). It is important to highlight that biological variability is an important factor to take into consideration, as cells respond slightly differently to one or several drugs from one experiment to another. This will affect the growth inhibition and consequently the interpretation of drug effect as the same combination repeated several times result in slightly different CI values. Therefore, the allocation of a single CI value to an interaction may be a simplification of the mechanism of the drugs and their effects and more information should be required.

This study was carried out in non-constant ratio combinations. For each experiment, one of the drug was used at fix concentration with varying concentration of the other drug. Another method consists of constant-ratio drug combinations, for which both drugs can be used at IC_{50} values to create a mixture that behaves like a third drug to the cells. This is then diluted serially, with several concentration points above and below its IC_{50} value (Chou, 2006). This method has the advantage of generating automated data for the Fa-CI plot (also called CI plot or Chou-Talalay plot) and computer simulation can be carried out, in addition to the dose-effect curves (Chou, 2010). The main difference with the non-constant ratio is that CI values can only be calculated at the specific combinations experimented. An advantage of this one is that it is possible to investigate the effect of low and high concentration of the different drugs, as one might be more toxic than the other.

Chou argued that although quantitative determination of synergism of two drugs usually takes one to two weeks *in vitro*, it can take several years to understand the mech-

anisms by which it occurs. Furthermore, *in vitro* synergy does not imply therapeutic index as the combination of a more cytotoxic regimen may still lead to enhanced toxicity in patients. When moving to clinical studies in humans, the analysis of drug combinations has to face strong practical and ethical limitations. Extensive pre-clinical studies in animals are required to justify the use of a combination therapy but those are costly, controversial and not always relevant (Shanks et al., 2009; Fouquier and Guedj, 2015). With more than 200 Food and Drug Administration (FDA)-approved cancer drugs, combining two drugs will result in at least 19,900 combinations, and this would increase exponentially if three drugs or more were to be tested (Sun et al., 2017). Therefore, there is a need to predict effectively which combinations are worth investigating. Novel technologies and methodologies, such as *in silico* approaches, have been developed to speed the rate of discovery whilst reducing the need for expensive lab work and clinical trials (Andrade et al., 2016). Computational methodologies have become a crucial component of many drug discovery programs and have improved the identification of effective drug combinations (Bulusu et al., 2016; Jaeger et al., 2016). High-throughput screening strategies, combined with mathematical models, can take into account the complexity of the signalling network as well as timing of drug perturbations. A screen with 10,000 sequential combinations of 100 FDA-approved anti-cancer therapies was performed in melanoma and pancreatic cancer cell lines. Approximately 23% of the tested combinations showed high-confidence sequential effects, either synergistic or antagonistic (Koplev et al., 2017). This demonstrated that cellular perturbations of many drug combinations have temporal aspects, which are currently both under-utilised and poorly understood. Jeon and colleagues proposed an *in silico* method that used an unbiased high-throughput drug screening to calculate and predict the synergy scores of 583 drug combinations for 31 cancer cell lines (Jeon et al., 2018). Such approaches also consider genetic information, such as mutations, expressions of genes in cancer-

related pathways, and pharmacological information when relevant. This will lead to personalised therapy as a specific drug or combination of drugs will be identified for each patient.

Paclitaxel-gemcitabine is a standard combination for patients who have a relapse of ovarian cancer with proven efficacy, but *in vitro* studies demonstrated that they induce an antagonistic effect when administered simultaneously, while sequential treatment produces additive cytotoxic effects that do not depend on the sequence of the administration (Theodossiou et al., 1998). This highlights the fact that pre-clinical data may not predict accurately the clinical relevance of some chemotherapeutic regimens and the importance of selecting appropriate models for such studies. On the other hand, even with combinations which exhibit excellent results in pre-clinical studies, there is no guarantee of effectiveness or that it may not be highly toxic for patients. Acelarin is already showing promising results *in vivo* (Blagden et al., 2018), and clinical studies of Acelarin in combination with other agents, are currently ongoing in patients with ovarian and biliary cancers. Preliminary results have shown Acelarin-carboplatin combination to be well tolerated by patients with both platinum-sensitive and platinum-resistant ovarian cancer, with one complete response (Blagden et al., 2017; Gourley et al., 2018). Acelarin is also used in combination with cisplatin in phase I for biliary cancer (McNamara et al., 2018). The findings presented in this chapter showed the importance of the order of treatment based on genetic background of the tumour and this could be applied in the clinical trials.

5 | Identification of predictive biomarkers for Acelarin

5.1 Introduction

Despite substantial advances in the treatment of various cancers, many patients still receive chemotherapeutic agents which are relatively nonspecific in targeting cancer cells and inflict considerable side effects. Often patients will experience a relapse, due to intrinsic and acquired resistance. The identification of biomarkers may help determine the most appropriate therapy and the effect of treatment. Despite numerous publications that have described new cancer biomarkers that promised to revolutionise the diagnosis of cancer and the management of patients in the last decade, very few have entered the clinic (Diamandis, 2012; Burke, 2016).

The development of loss-of-function genetic screens has been successfully used to identify genes involved in drug resistance and sensitivity for a variety of chemotherapeutic agents. These may become potential predictive biomarkers if clinical application is validated (Berns and Bernards, 2012; Gerhards and Rottenberg, 2018). The genome-scale genetic knockdown screen approach was applied to screen for candidate genes mediating cancer cell sensitivity to Acelarin. The GeCKOv2 genome-scale CRISPR/Cas9 knockdown library (Sanjana et al., 2014) was used in pancreatic MiaPaCa2 cells and sgRNA distribution was compared by next generation sequencing after 14 and 21 days

of drug treatment (Sarr et al., 2018).

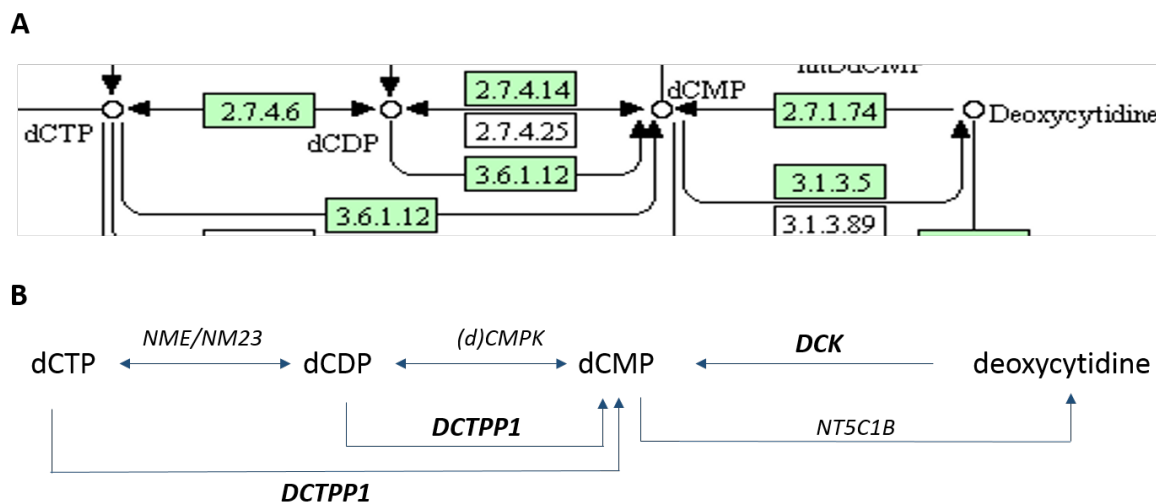


Figure 5.1: Roles of DCK and DCTPP1 in pyrimidine metabolism pathway. (A) KEGG mapping of deoxycytidine metabolism. (B) Simplified representation of deoxycytidine metabolism. Deoxycytidine is phosphorylated into its monophosphate form dCMP by DCK, whereas DCTPP1 hydrolyses dCTP and dCDP into dCMP.

The only pathway consistently selected was pyrimidine metabolism; specifically DCK and DCTPP1, involved in the regulation of the dCMP/dCTP pool (Fig.5.1). DCK phosphorylates deoxycytidine into its monophosphate form (dCMP), while DCTPP1 hydrolyses deoxycytidine di- and triphosphate into dCMP, thus converging towards the same metabolite. DCK is required for activation of gemcitabine; low DCK expression in tumour biopsies from patients treated with gemcitabine correlating with a poor prognosis (Maréchal et al., 2010). DCTPP1, dCTP pyrophosphatase 1, belongs to the all- α NTP pyrophosphohydrolase superfamily. Requena and colleagues have shown that a strong down-regulation of DCTPP1 activity in human cells induces a significant increase in the intracellular pool of dCTP (Requena et al., 2014). This could be associated with resistance to Acelarin, as dFdCTP competes with dCTP for incorporation into DNA.

Another method to identify biomarkers is by using a more targeted candidate approach, such as specific proteins involved in drug metabolism. Based on the activation pathway of Acelarin, it was hypothesised that a lack of carboxylesterase and phosphoramidase expression may interfere with Acelarin metabolism, thus preventing the release of dFdCMP metabolite.

The aim of this chapter was to validate candidate genes mediating sensitivity to Acelarin in the ovarian cell line A2780. Their clinical relevance was then investigated in a pan-cancer Phase I cohort treated with Acelarin.

5.2 Pyrimidine metabolism pathway modulates sensitivity to Acelarin and gemcitabine

5.2.1 Validation of candidate genes DCK and DCTPP1 *in vitro*

The GeCKOv2 library (Sanjana et al., 2014) comprises a list of six independent single guide RNAs for each gene. Each sgRNA targets a different region of the gene of interest and the knockdown efficacy varies amongst them. A non-targeting sequence, sgScr, was also used as a control. Independent sgRNAs were cloned into pLentiCRISPRv2 and verified by Awa Sarr. Lentiviral transduction was performed in A2780 cells according to the method described in section 2.5.1.

From the six sgRNA initially used for DCK knockdown, stably modified cell lines were successfully produced with five of them. Knockdown efficacy was assessed by western blot and DCK expression was found reduced by more than 90% in the A2780-sgDCKa cell line compared to A2780-sgScr cells (Fig.5.2A). In the other sgDCK-

transduced cell lines, DCK expression was decreased approximately 40 to 60% only (Appendix 7.16), hence they were not used for further studies.

A2780-sgDCK and A2780-sgScr cells were subsequently treated with different concentrations of Acelarin or gemcitabine (5 to 500 nM) for 24 h and SRB was performed 96 h post-treatment. A2780-sgDCK cells treated with gemcitabine were completely resistant, with 75% of cells surviving at 500 nM, compared to A2780-sgScr cells (IC_{50} : 8 nM). On the contrary, cells treated with Acelarin displayed only a 2.5-fold increase of IC_{50} compared to the control (347 nM vs 134 nM, $p < 0.005$) (Fig.5.2B).

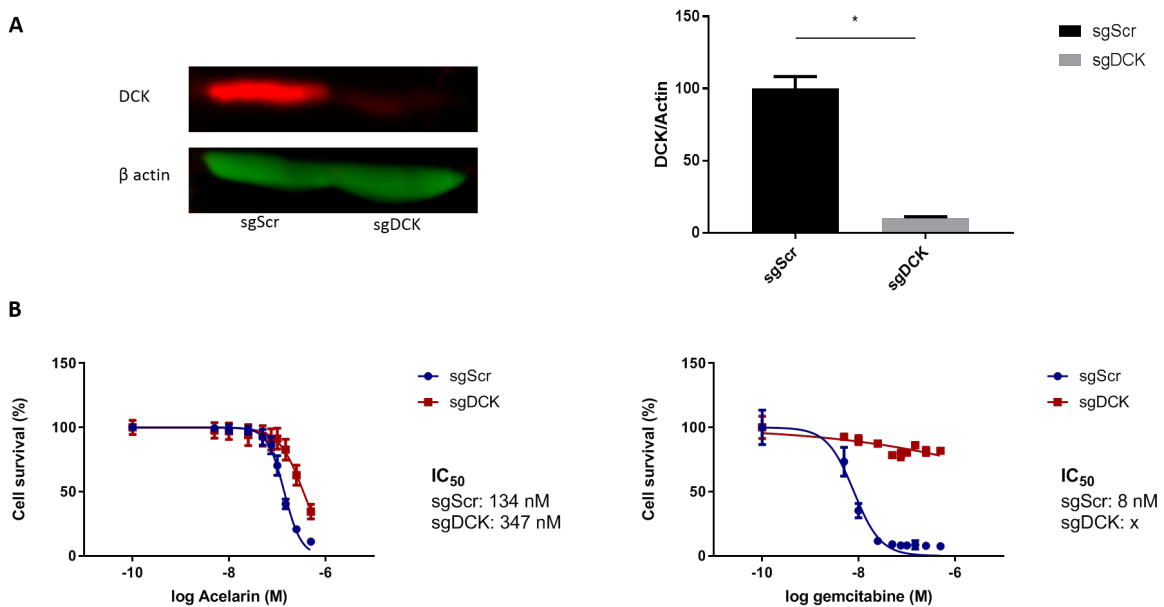


Figure 5.2: Effect of DCK knockdown on sensitivity of A2780 cells to Acelarin and gemcitabine. (A) Western blot for DCK expression in A2780-sgScr and A2780-sgDCK cell lines and quantification (* $p < 0.05$; Mann-Whitney test); error bars represent mean \pm SD (n=3). (B) Dose response curve of A2780-sgScr and A2780-sgDCK cell lines to treatment with Acelarin and gemcitabine. Data are expressed as the mean \pm SEM of three independent experiments. A2780-sgScr vs A2780-sgDCK: $p < 0.005$; Mann-Whitney test.

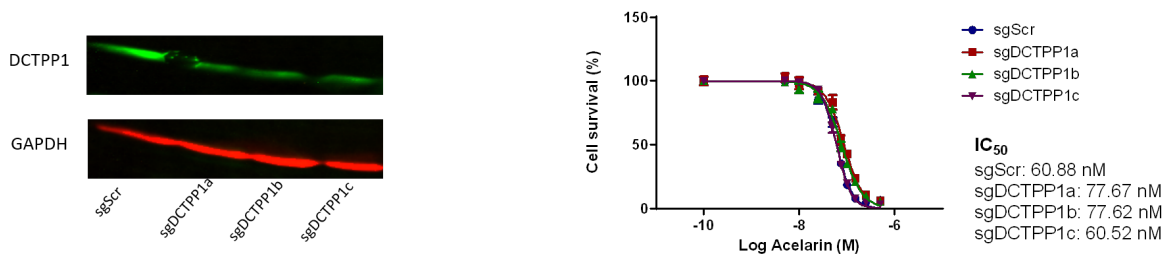


Figure 5.3: Effect of DCTPP1 knockdown on sensitivity of A2780 cells to Acelarin. Western blot for DCTPP1 expression in A2780-sgScr and A2780-transduced cell with sgDCTPP1a, sgDCTPP1b and sgDCTPP1c. Dose response curve of A2780-sgScr and A2780-sgDCTPP1 cell lines to treatment with Acelarin. IC₅₀ were determined from the average data collected with SRB assays. Data are expressed as the mean \pm SD.

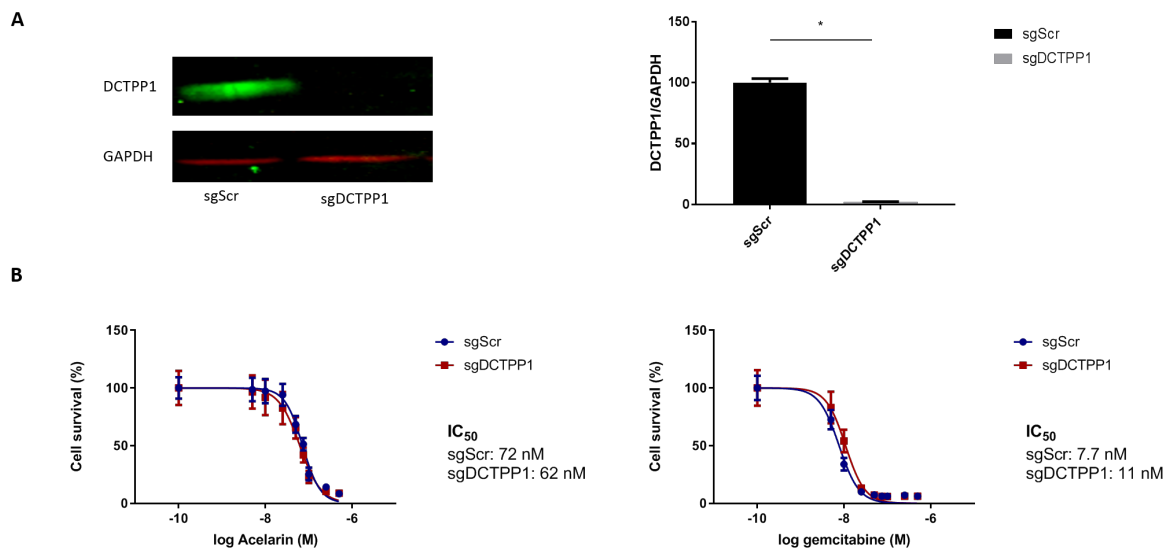


Figure 5.4: Effect of DCTPP1 knockdown on sensitivity of A2780 cells to Acelarin and gemcitabine. (A) Western blot for DCTPP1 expression in A2780-sgScr and A2780-sgDCTPP1e cell lines and quantification (* p < 0.05; Mann-Whitney test); error bars represent mean \pm SD (n=3). (B) Dose response curve of A2780-sgScr and A2780-sgDCTPP1 cell lines to treatment with Acelarin and gemcitabine. Data are expressed as the mean \pm SEM of three independent experiments. A2780-sgScr vs A2780-sgDCTPP1 treated with gemcitabine: p < 0.005; Mann-Whitney test.

For DCTPP1 knockdown, a first attempt was carried out using sgDCTPP1a, sgDCTPP1b and sgDCTPP1c only. DCTPP1 expression was found to be reduced by 80% in the three cell lines, but no significant difference in IC₅₀ was observed for cells treated with Acelarin (Fig.5.3). No conclusion could be drawn from this experiment as there could be no effect of reduction of DCTPP1 in sensitivity to Acelarin, or else, the knockdown was not significant enough and therefore a residual effect of the protein was enough to exercise its function.

Cells transduced with the other three sgRNA showed that knockdown of 98% could be achieved with sgDCTPP1e (Fig.5.4A). A2780-sgScr and A2780-sgDCTPP1 cells were treated with different concentrations of Acelarin or gemcitabine (5 to 500 nM) for 24 h and SRB was performed 96 h post-treatment. No change in sensitivity was detected in cells treated with Acelarin. Interestingly, loss of DCTPP1 conferred a 1.4-fold-increase resistance to A2780-sgDCTPP1 cells treated with gemcitabine (Fig.5.4B).

To go further in unravelling the mechanisms that modulate sensitivity to Acelarin, simultaneous inactivation of DCK and DCTPP1 was performed to assess for any synergistic effects, compared with individual knockdown. This was performed by electroporation-based transfection. Instead of using a lentiviral system, plasmids containing sgDCK-sgDCTPP1 or sgScr-sgScr were delivered directly inside the cell by nucleofection. The plasmids of interest were independently introduced in A2780 cells along with a pBabe-puro plasmid (puromycin selection plasmid) in order to select nucleofected cells with puromycin resistance. A control plasmid containing a gene coding for GFP was used to verify transfection efficacy (Fig.5.5).

Protein expression was reduced by 85% for DCK and 90% DCTPP1, compared to the control cell line A2780-sgScr-sgScr (Fig.5.6A). A2780-sgDCK-sgDCTPP1 cells displayed a 4-fold decreased sensitivity to Acelarin, compared to A2780-sgScr-sgScr

cells and were totally resistant to gemcitabine (Fig.5.6B). Interestingly, similar observations were made in other A2780 cells independently nucleofected with sgDCK-sgDCTPP1 and sgScr-sgScr. Reduction of DCK protein expression was not as significant, with approximately 65% reduction and DCTPP1 expression was reduced by 85% in A2780-sgDCK-sgDCTPP1 cells compared to A2780-sgScr-sgScr cells (Fig.5.7A). A2780-sgDCK-sgDCTPP1 cells treated with gemcitabine displayed 40% cell death when treated with 500 nM. In contrast, for cells treated with Acelarin, the difference was still 3-fold (IC_{50} sgScr-sgScr 56.7 nM vs IC_{50} sgDCK-sgDCTPP1 162 nM, $p < 0.005$) (Fig.5.7B). These data suggest there is no synergistic effect on Acelarin sensitivity by simultaneously reducing both DCK and DCTPP1 expression. Furthermore, unlike gemcitabine, the reduction of DCK expression is not proportional to the effect on sensitivity to Acelarin.

The localisation of DCK was studied 72 h post-treatment with Acelarin and gemcitabine. In control cells, DCK was expressed at very low levels and mostly in the cytoplasm. Cells exposed to gemcitabine showed an increased protein expression of DCK with both nuclear and cytoplasmic localisation, whereas in Acelarin treated cells, it was predominately perinuclear (Fig.5.8). Moreover, most cells treated with Acelarin were bigger than control cells, which is consistent with the cell cycle delay described in section 3.4.

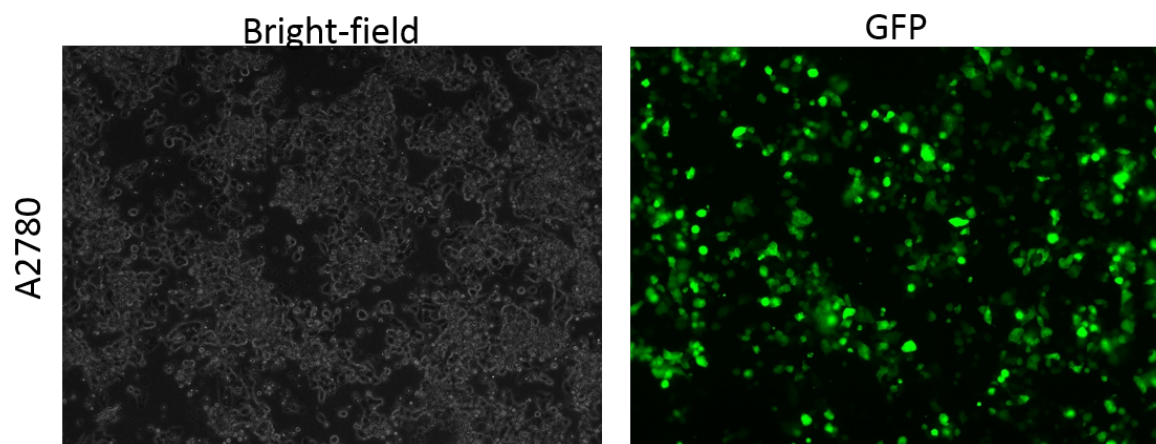


Figure 5.5: GFP signal as positive control of nucleofection.

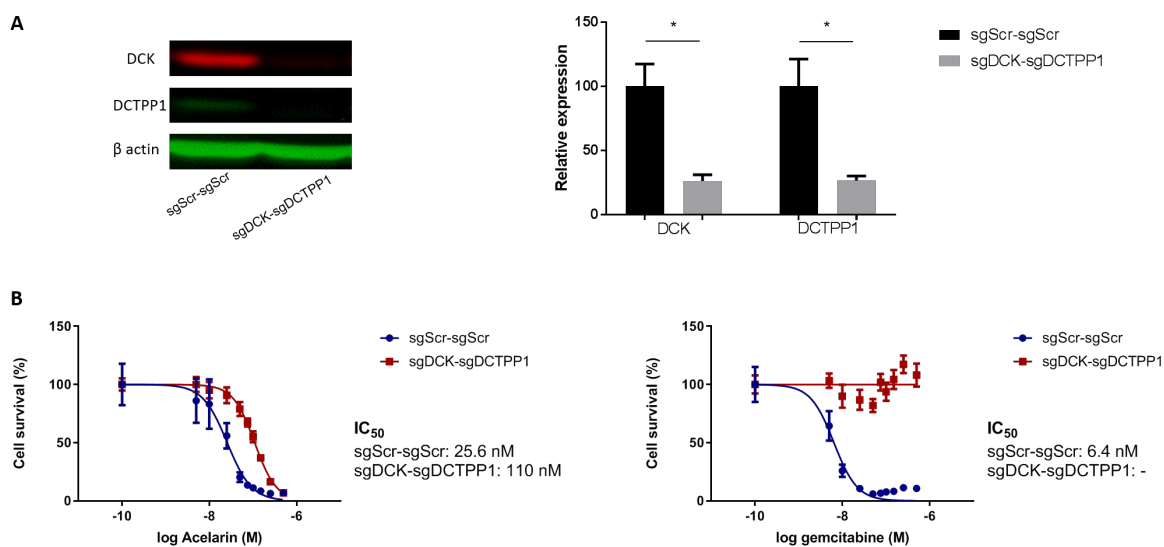


Figure 5.6: Effect of DCK-DCTPP1 double knockdown on sensitivity of A2780 cells to Acelarin and gemcitabine. (A) Western blot for expression DCK and DCTPP1 in A2780-sgScr-sgScr and A2780-sgDCK-sgDCTPP1 cell lines and quantification ($* p < 0.05$; Mann-Whitney test); error bars represent mean \pm SD ($n=3$). (B) Dose response curve of A2780-sgScr-sgScr and A2780-sgDCK-sgDCTPP1 cell lines to treatment with Acelarin and gemcitabine. Data are expressed as the mean \pm SEM of at least two independent experiments. A2780-sgScr-sgScr vs A2780-sgDCK-sgDCTPP1: $p < 0.005$; Mann-Whitney test.

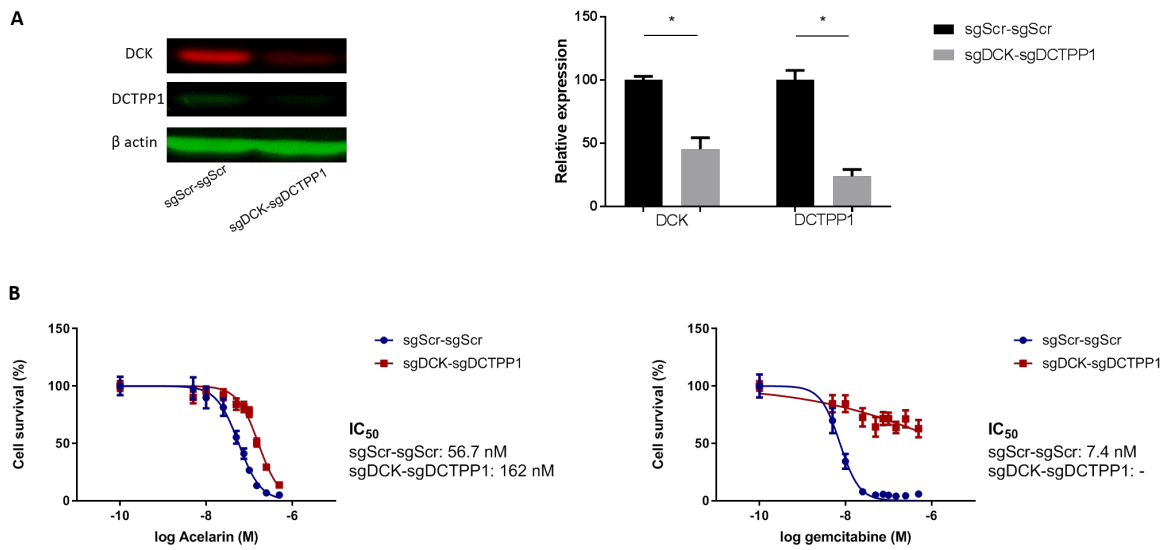


Figure 5.7: Effect of DCK-DCTPP1 double knockdown on sensitivity of A2780 cells to Acelarin and gemcitabine. (A) Western blot for expression DCK and DCTPP1 in A2780-sgScr-sgScr and A2780-sgDCK-sgDCTPP1 cell lines and quantification ($* p < 0.05$; Mann-Whitney test). (B) Dose response curve of A2780-sgScr-sgScr and A2780-sgDCK-sgDCTPP1 cell lines to treatment with Acelarin and gemcitabine. Data are expressed as the mean \pm SEM of two independent experiments. A2780-sgScr-sgScr vs A2780-sgDCK-sgDCTPP1: $p < 0.005$; Mann-Whitney test.

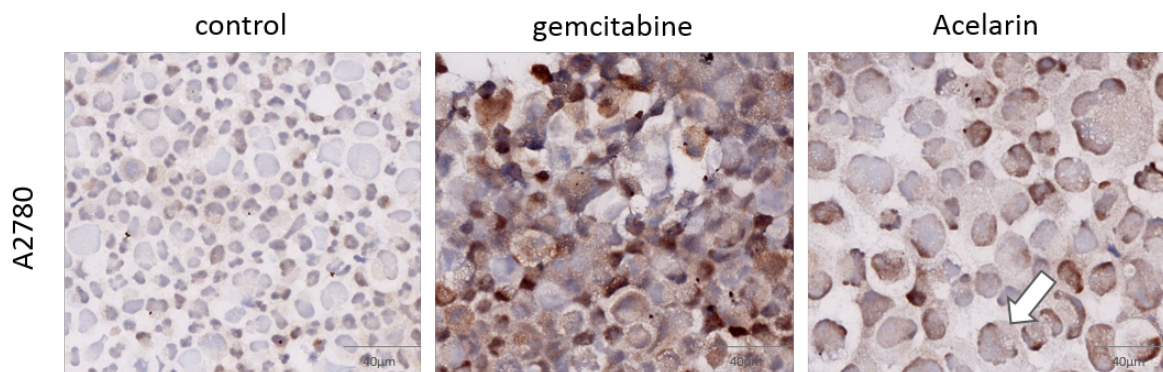


Figure 5.8: DCK expression and localisation in response to gemcitabine and Acelarin treatment. A2780 cells were treated with IC_{50} of gemcitabine or Acelarin for 24 h and harvested at 72 h. Images represent immunoperoxidase of DCK (brown). White arrow: DCK is predominately perinuclear in cells treated with Acelarin. Magnification x40.

RRM1 is involved in the maintenance of the dCDP/dCTP pool, by converting ribonucleotide into deoxyribonucleotides. It was hypothesised that in absence of DCK, RRM1 expression might be increased to replenish the pool of dCTP, as a result of compensatory mechanism. Its expression was assessed by western blot in A2780-sgScr and A2780-sgDCK cells but there was no significant change in expression between the two cell lines (Fig.5.9).

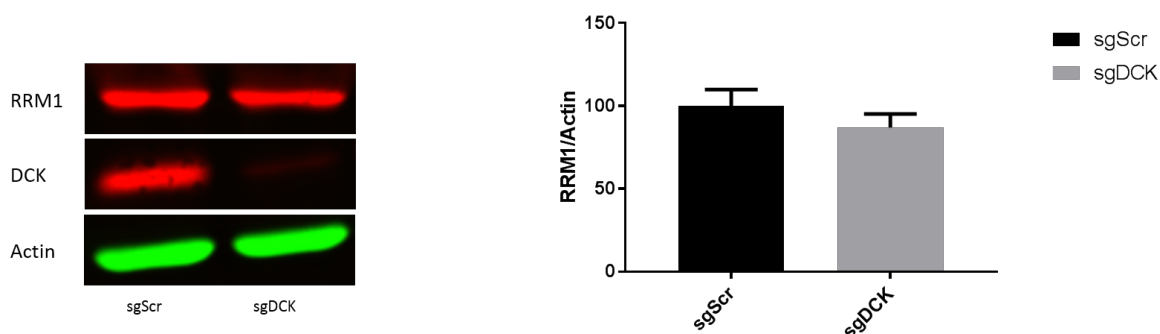


Figure 5.9: RRM1 expression in DCK knockdown cells. Protein expression of RRM1 was assessed in A2780-sgScr and A2780-sgDCK cell lines by western blot; error bars represent mean \pm SD (n=3). There was no significant difference between the two cell lines.

Role of dCMP/dCTP pool in sensitivity to Acelarin

The implication of DCK and DCTPP1 in the modulation of Acelarin sensitivity in different cancer cell lines have been demonstrated through both the genome-scale CRISPR screen and individual knockdown validation (Sarr et al., 2018). While DCK was not expected to have a direct effect on sensitivity to Acelarin, both candidates were of interest for the role they have in the pyrimidine metabolism. In order to investigate the effect of dCMP/dCTP pool regulation on Acelarin and gemcitabine sensitivity, cytotoxicity assays were carried out in A2780 cells.

The experiment was designed as follow:

- (1) cells were plated with either 50 μM or 100 μM deoxycytidine (dCyd) and left for 48h prior to any treatment with Acelarin or gemcitabine.
- (2) cells were plated and left to grow for 48h as usual, and 50 μM or 100 μM dCyd was added as a direct competitor to Acelarin and gemcitabine.

In both scenarios, cells were exposed to drugs for 24 h and SRB was performed 96 h post-treatment.

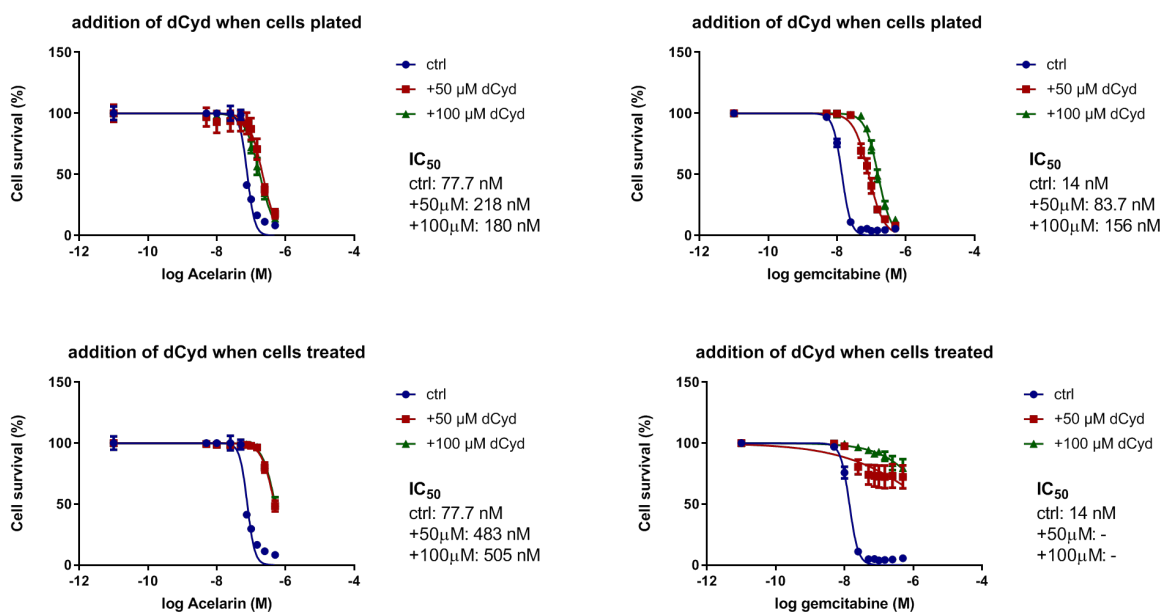


Figure 5.10: Effect of dCMP/dCTP pool on sensitivity to Acelarin and gemcitabine. Dose response curves of A2780 cells incubated with 50 or 100 μM exogenous dCyd prior to treatment with a range of concentration of Acelarin (A) or gemcitabine (B). Dose response curves of cells were treated with a range of concentration of Acelarin (C) and gemcitabine (D) simultaneously with 50 or 100 μM dCyd. Data are expressed as the mean \pm SEM of three independent experiments. A2780 vs A2780 50 μM or 100 μM dCyd: $p < 0.005$; Mann-Whitney test.

The presence of dCyd resulted in a decrease of sensitivity to Acelarin and gemcitabine. Compared to the control, the IC₅₀ of cells pre-treated with 50 μM dCyd was 2.8-fold increased and 2.3-fold for 100 μM dCyd for cells treated with Acelarin. It was 6-fold for 50 μM dCyd and 11-fold increased for 100 μM dCyd, for cells treated with gemcitabine.

When dCyd was added as a direct competitor to these drugs, the IC₅₀ was 6.2 times higher for 50 μM dCyd and 6.5 higher for 100 μM dCyd, for cells treated with Acelarin, compared to control. At 500 nM Acelarin, there was approximately 30-35% death with both 50 μM and 100 μM dCyd. Cells co-treated with both 50 μM and 100 μM dCyd were completely resistant to gemcitabine, while control cells displayed an IC₅₀ of 14 nM. The lack of cell death for cells exposed to combination of dCyd and gemcitabine is consistent with the idea that dCyd is directly competing against gemcitabine for activation by DCK.

These data suggest that dysregulation of dCMP/dCTP pool is important in the sensitivity of cells to treatment with Acelarin and gemcitabine.

5.2.2 DCK and DCTPP1 in Acelarin Phase I cohort

The results described above established the role of pyrimidine metabolism and more specifically, of DCK and DCTPP1 in modulation of sensitivity to Acelarin *in vitro*. The clinical relevance of DCK and DCTPP1 as potential predictive biomarkers was investigated in cancer biopsy tissues from patients from a pan-cancer phase I cohort treated with Acelarin.

From the Acelarin treated Phase I cohort, 39 biopsies from 37 patients were obtained. All patients had rapidly progressing disease on study entry and had exhausted

all other treatment options. Biopsies were taken prior to treatment with Acelarin and results of immunostaining were analysed with clinical follow-up. The cases represented a range of different cancers and patients had received prior gemcitabine treatment or not (Table 5.1). As part of the trial, patients received six cycles of Acelarin unless there was evidence of disease progression, unacceptable toxicity or treatment was declined (Blagden et al., 2018). Patients' response to Acelarin was evaluated based on Response Evaluation Criteria In Solid Tumours (RECIST 1.1 version) (Eisenhauer et al., 2009). A partial response is defined as a 30% or more decrease in tumour size, compared to the baseline scan. If a tumour increased by 20%, or new lesion emerged, this was considered as progressive disease. Stable disease is the stage in between, when there was neither sufficient shrinkage nor sufficient increase in size to qualify to one of the other conditions. Of the 37 patients present in this study, two achieved a partial response (unconfirmed) to Acelarin, thirteen patients achieved stable disease for six months or more and twenty-two patients achieved stable disease for less than six months, or progressive disease developed within that time.

Tissues were immunostained and scanned images were quantified using QuPath version 0.1.2, a free open source image analysis software designed for digital pathology (Bankhead et al., 2017). Allred scores for DCK and DCTPP1 expression were calculated by QuPath for each tissue, based on the protein expression in cells detected within the annotations, excluding what was considered as non-tumour cells. Allred score is the sum of the proportion of stained cells with intensity score and varies from 0 to 8. Segmentation parameters were defined so that Allred scores were obtained for nuclear and cytoplasmic expression in each tissue sample (Appendix 7.1).

Category	Subcategory	Total collective (%)
Sex	Female	27 (72.97)
	Male	10 (27.03)
Age		31 - 83 median = 56
Tumour type (carcinoma unless specified otherwise)	Ovary	10 (27.03)
	Colon	6 (16.22)
	Oesophageal	3 (8.11)
	Breast	3 (8.33)
	Lung	2 (5.4)
	Endometrium	2 (5.4)
	Pancreas	2 (5.4)
	Biliary	2 (5.4)
	Mesothelioma	2 (5.4)
	Osteosarcoma	1 (2.70)
	Cervix	1 (2.77)
	Adrenal	1 (2.77)
	Anal	1 (2.77)
Prior gemcitabine	Yes	14 (37.84)
	No	23 (62.16)
RECIST	Partial response (unconfirmed)	2 (5.4)
	Stable disease	25 (67.57)
	Progressive disease	10 (27.03)

Table 5.1: Patients information from phase I clinical study.

Both DCK and DCTPP1 were mainly localised in the nucleus (DCK $p < 0.0001$; DCTPP1 $p < 0.05$). Nuclear and cytoplasmic expression were compared in patients who had progressive disease or stable for less than 6 months (group 1; $n=22$), and those who were stable for 6 months and more and partial responders (group 2; $n=17$) (Fig.5.11). There was no significant difference between the two groups. Therefore, there was no correlation between expression of DCK or DCTPP1 and patients' response to Acelarin. In addition, the analysis of DCK and DCTPP1 combined together or as a ratio did not show any further correlation than taken separately (Appendix 7.18).

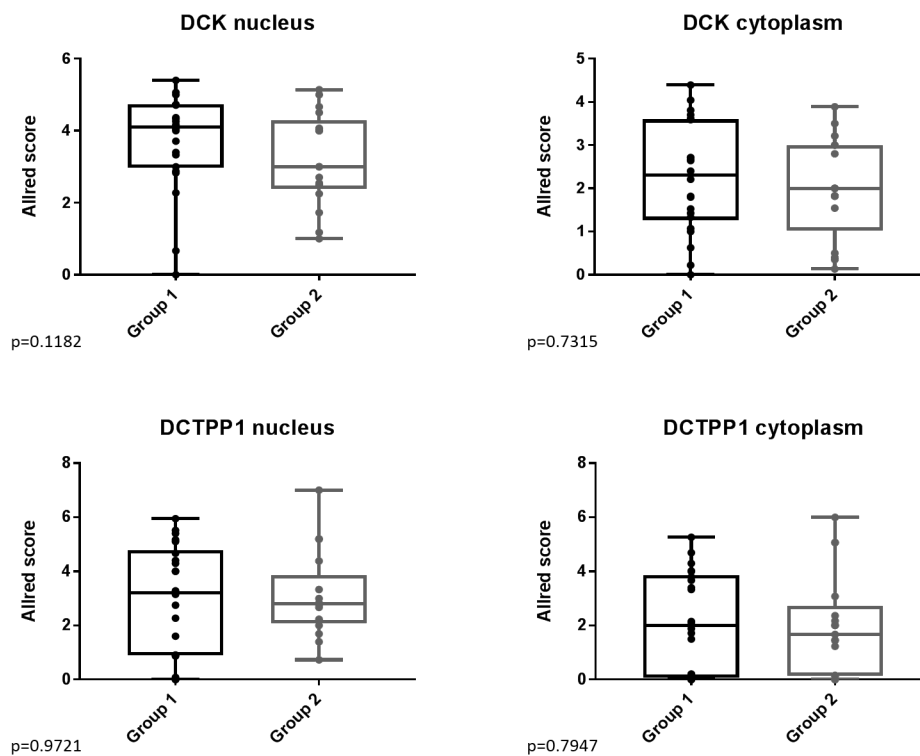


Figure 5.11: Comparison of Allred score for DCK and DCTPP1. Allred score for DCK nucleus, DCK cytoplasm, DCTPP1 nucleus and DCTPP1 cytoplasm were compared between the two groups of patients. $p > 0.05$, Mann-Whitney.

5.2.3 Case studies

DCK and DCTPP1 expression was investigated in the two patients with partial response. The first one was a 60 years old female, diagnosed with lung adenocarcinoma, who had not been previously treated with gemcitabine. She survived for 10 months while receiving Acelarin. Allred score was 4.2 for DCK and 0.9 for DCTPP1, representing a relatively high expression of DCK and a low expression of DCTPP1 (Fig.5.12A). Interestingly, for the second patient, a 70 years old female diagnosed with pancreatic cancer and who had received prior gemcitabine, the tumour displayed low DCK expression (Fig.5.12B), but size had reduced by 30% within 3 cycles of Acelarin. Allred score was 1.4 for DCK and 2.4 for DCTPP1.

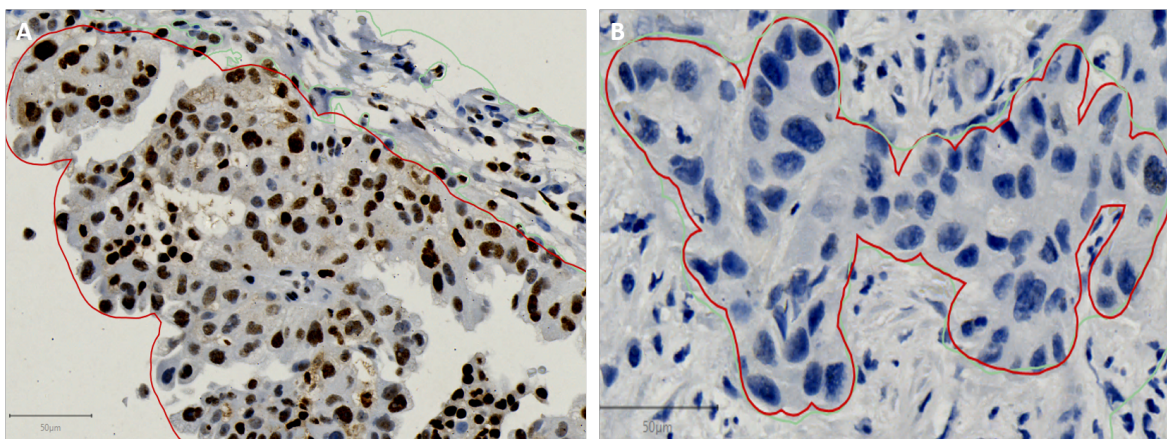


Figure 5.12: DCK expression in patients with partial response. (A) Lung carcinoma - Allred score DCK 4.2. (B) Pancreatic cancer - Allred score DCK 1.4.

For two other patients, two biopsies taken at different times were available. First patient was a 73 years old male, diagnosed with colorectal cancer and who had no prior gemcitabine treatment. A 13.5% tumour increase was observed upon treatment with Acelarin. Allred score for DCK decreased from 3.5 to 2.5 (Fig.5.13A-B) whereas

DCTPP1 increased from 2.6 to 6.5 (Fig.5.13) between the two biopsies, which were taken at 14 months interval. The second case was a 38 years old male, diagnosed with osteosarcoma and who had no prior gemcitabine treatment. He remained stable for 10 months with 1% increase in tumour size. Allred scores for DCK and DCTPP1 were 3.5 and 2.4 respectively in the first tissue. In the second biopsy which was taken 2 months later, Allred score for DCK was 4.3 and 1.5 for DCTPP1.

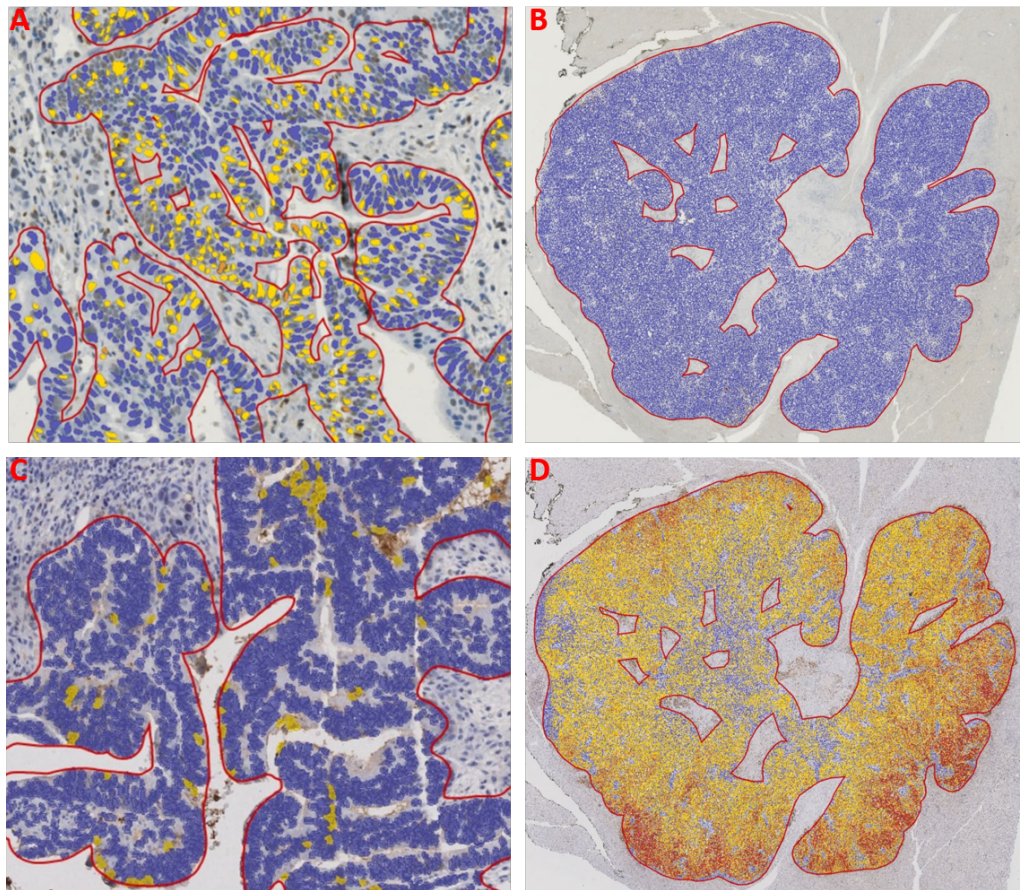


Figure 5.13: DCK and DCTPP1 expression in tumour tissues. Tissue biopsies of a patient with colorectal cancer, blue represents absence of protein in this region, orange and red are mild and high protein expression. (A) DCK staining in first biopsy; (B) DCK staining in second biopsy 14 months later; (C) DCTPP1 staining in first biopsy; (D) DCTPP1 staining in second biopsy 14 months later.

It is possible that the alteration of DCK and DCTPP1 was a consequence of treatment and a form of adaptive change in response to effect of Acelarin on cancer cells, but there was no clear trend, so all we can conclude is that tumours have heterogeneous levels of DCK and DCTPP1. These data suggest that pre-treatment DCK or DCTPP1 expression do not correlate with disease progression and are not predictive biomarkers in patients treated with Acelarin.

5.3 Candidate approach for biomarker: activation of Acelarin

Loss-of-function genetic screens have proven to be powerful tools in the identification of genes and cellular signalling pathways involved in drug resistance. However, caution should be used when performing CRISPR/Cas9 screens, since this methodology may not uncover strongly selected genes and may be dependent on factors such as *in vitro* drug metabolism effects. For this reason, other approaches should also be considered, such as targeting specific candidates that may have a role in drug metabolism. Here, I focused on the activation pathway of Acelarin, especially carboxylesterases and phosphoramidase such as Cathepsin A, CES2 and HINTs genes. They have been previously studied in the activation of a phosphoramidate pro-drug (Murakami et al., 2010).

The expression of each of these candidates was investigated by RT-qPCR to confirm their presence in A2780 and SKOV3 cell lines (Fig.5.14A), as well as western blot for protein expression of Hint1 (Fig.5.14B). The knockdown of HINT1 was performed in A2780 cells with CRISPR/Cas9 system and the efficacy was assessed by western blot. A2780-sgScr and A2780-sgHINT1 cells were treated with different concentrations of Acelarin (5 to 500 nM) for 24 h and SRB was performed 96 h post-treatment

(Fig.5.15). HINT1 expression was reduced by about 92% in both A2780-sgHINT1a and A2780-sgHINT1b compared to A2780-sgScr cells. This resulted in a 1.8-fold decrease of sensitivity to Acelarin, with IC_{50} of A2780-sgScr at 105.1 nM vs 187.1 and 180.6 nM for A2780-sgHINT1a and A2780-sgHINT1b, respectively ($p < 0.005$). For the other genes, siRNA was tentatively used without any conclusive results; more optimisation needs to be carried out.

Expression of HINT1 was assessed in the tumour biopsies from phase I clinical study previously described. Allred scores for HINT1 were compared in patients who had progressive disease or stable for less than 6 months (group 1; $n=22$), and those who were stable for 6 months and more and partial responders (group 2; $n=17$) (Fig.5.16). There was no significant difference between the two groups. Therefore, there was no correlation between HINT1 expression and patients' responses to Acelarin.

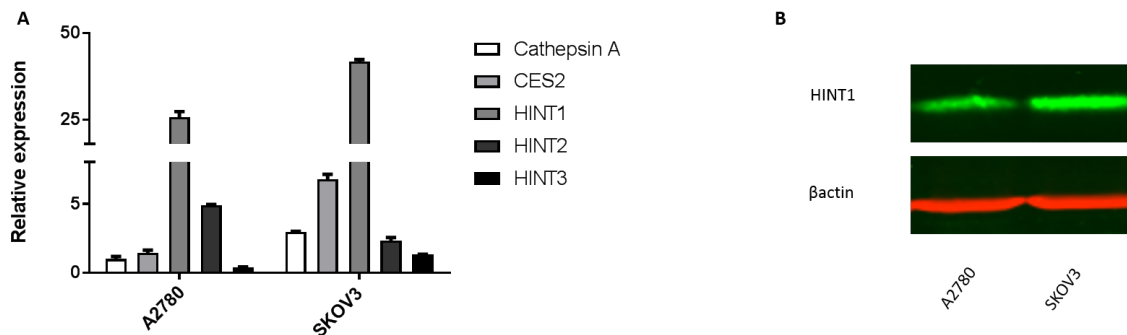


Figure 5.14: Endogenous expression of candidates in ovarian cell lines. (A) Cathepsin A, CES2, HINT1, HINT2 and HINT3 gene expression were assessed by RT-qPCR in A2780 and SKOV3 cell lines. (B) Protein expression of HINT1 in A2780 and SKOV3 cell lines.

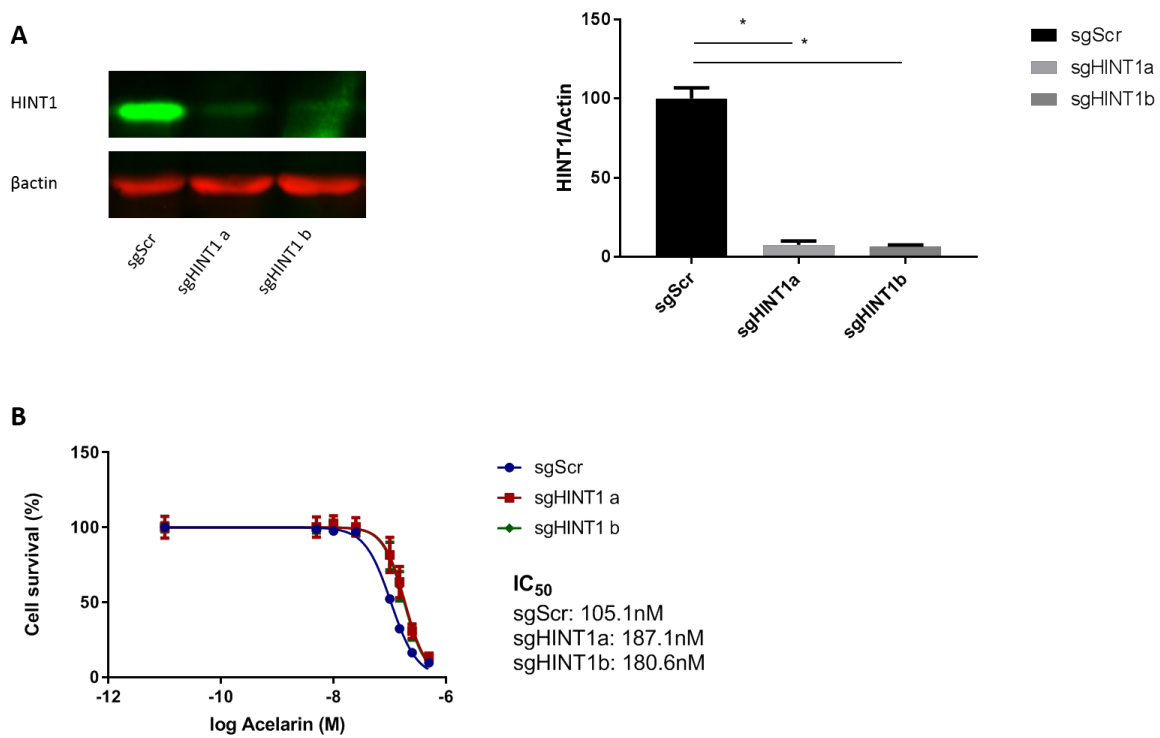


Figure 5.15: Effect of HINT1 knockdown on sensitivity of A2780 cells to Acelarin. (A) Western blot for HINT1 expression in A2780-sgScr and A2780-transduced cell with sgHINT1a and sgHINT1b. (B) Dose response curve of A2780-sgScr and A2780-sgHINT1 cell lines to treatment with Acelarin. Data are expressed as the mean \pm SEM of two independent experiments. A2780-sgScr vs A2780-sgHINT1: $p < 0.005$; Mann-Whitney test.

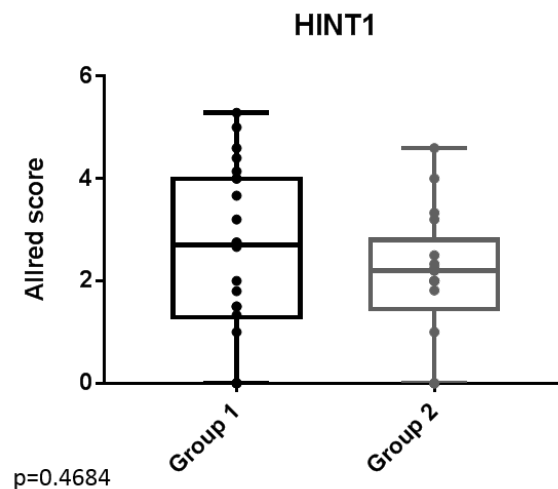


Figure 5.16: Allred score of HINT1 in patients $p > 0.05$, Mann-Whitney.

5.4 Discussion

Genome-wide loss-of-function screening has proven a useful strategy to identify genes involved in mechanisms and resistance to cancer (Berns et al., 2004; Kang et al., 2017; Sharma and Petsalaki, 2018). Yet, remains the risk of off-targets and the importance of validation of any candidate genes obtained from such screens. One method for validation consists of performing individual knockdown with CRISPR/Cas9 system and independent sgRNA targeting sequences (Shalem et al., 2014; Tzelepis et al., 2016).

A genome-scale CRISPR/Cas9 screen was used in a pancreatic cell line to identify genes involved in resistance to Acelarin (Sarr et al., 2018). Two candidates were of high interest due to their role in the regulation of dCMP/dCTP pool, dCTP being a direct competitor to Acelarin metabolite dFdCTP. To go beyond validation in the pancreatic cell line it was initially performed in, effect of DCK and DCTPP1 on sensitivity to Acelarin was investigated in an ovarian cell line.

Individual knockdown of DCK and DCTPP1 were performed in A2780 cells and cytotoxicity assays were carried out to assess the effect on sensitivity to Acelarin between knockdown and control cell lines. A2780-sgDCK cells were completely resistant when treated with gemcitabine. By contrast, it had a limited effect on sensitivity to Acelarin, with just a 2.3-fold increase in IC_{50} . These data were consistent with previous studies which have demonstrated gemcitabine resistance to be associated with loss of DCK expression in A2780 cells (Ruiz Van Haperen et al., 1994; Bergman et al., 2000). Moreover, the phosphorylated status of Acelarin, which makes it independent from DCK for activation (Slusarczyk et al., 2014), supports the hypothesis that it is the metabolism of deoxycytidine that modulates sensitivity to Acelarin.

Contrary to MiaPaCa2 cells, loss of DCTPP1 in A2780 cells had no effect on cells treated with Acelarin compared to control cells. This suggests that the modulation of sensitivity to Acelarin treatment by DCTPP1 is specific to MiaPaCa2 cells. However, it conferred a 1.5-fold increased resistance to cells treated with gemcitabine. It has been shown that 2' modified dCTP analogues, such as gemcitabine, were not substrate of DCTPP1 (Requena et al., 2016). In another study, they have reported that decreased DCTPP1 expression altered the intracellular deoxycytidine pool resulting in an increase of dCTP (Requena et al., 2014). Furthermore, Amsailale and colleagues demonstrated a negative feedback mechanism by which DCK is regulated by dCTP (Amsailale et al., 2014). Therefore, increase of dCTP pool by reduction of DCTPP1 expression may compete with dFdCTP as well as inhibit DCK. Although, resistance to gemcitabine was significant, it remained limited compared to DCK knockdown.

DCK and DCTPP1 are involved in the maintenance of dCMP/dCTP pool, their substrates converging towards the same metabolite, dCMP. dCMP is a direct competitor of gemcitabine for phosphorylation by DCK and dCTP competes with dFdCTP for incorporation into DNA. Investigations of DCK activity inhibition showed significant reduction in levels of metabolites in cells treated with gemcitabine but no change for Acelarin (Ghazaly, Slusarczyk, Mason, Gribben, McGuigan and Blagden, 2014). The role of this pathway in sensitivity to Acelarin was explored with a simultaneous knock-down in A2780 cells. The effect of DCK and DCTPP1 combined knockdown was similar as to the one of DCK single knockdown. Therefore, there was no synergistic effect on Acelarin sensitivity by simultaneously reducing both DCK and DCTPP1 expression.

It has previously been reported that compensatory mechanisms to overcome the loss of genes occur when performing genome editing with CRISPR/Cas9 (Rossi et al., 2015; Peretz et al., 2018). Considering the pyrimidine metabolism pathway,

several enzymes are involved in the regulation of the dCMP/dCTP pool, such as nucleoside diphosphate kinases NME/NM23, deoxycytidine monophosphokinase dCMPK and ribonucleotide reductase RRM1/RRM2 (Fig.5.17). Shukla and colleagues reported an increase of NME/NM23 expression in pancreatic cell line resistant to gemcitabine (Shukla et al., 2017). Their function might compensate the loss of DCTPP1, whereas there is no other enzyme directly involved in the phosphorylation of dCyd to dCMP. Ribonucleotide reductase is responsible for the conversion of CDP into dCDP. High expression of RRM1 and RRM2 proteins is correlated with resistance to gemcitabine in cell lines (Duxbury et al., 2004; Minami et al., 2015) and poor prognosis for patients (Deng et al., 2014; Aoyama et al., 2017). Despite inhibition of RRM1/RRM2 by dFdCDP (Heinemann et al., 1992), it was hypothesised that their expression was increased to maintain the cellular dCTP pool in order to enable cells to proliferate. This was based on two studies which demonstrated an increase of DCK and RRM1/RRM2 expression in MiaPaCa2 cells treated with gemcitabine. On the contrary, when cells were made resistant over time, DCK expression was largely reduced, whereas RRM1 and RRM2 were still significantly higher than in control cells (Nakano et al., 2007; Nishio et al., 2011). However, in this study, there was no significant change of RRM1 expression in DCK-knockdown cells.

One possible explanation for the decrease of sensitivity to Acelarin when low expression of DCK *in vitro* could be that a small proportion of the drug had lost its phosphoramidate moiety. Thus it would be converted into gemcitabine which is not activated in sgDCK cells. Despite this, Acelarin retained its cytotoxicity, albeit showing a modest decrease. Furthermore, mass spectrometry studies showed that less than 1% of the dose of Acelarin administered to the patient was excreted as either Acelarin or dFdC, suggesting that the drug is stable during plasma transport to the tumour cells (Blagden et al., 2018).

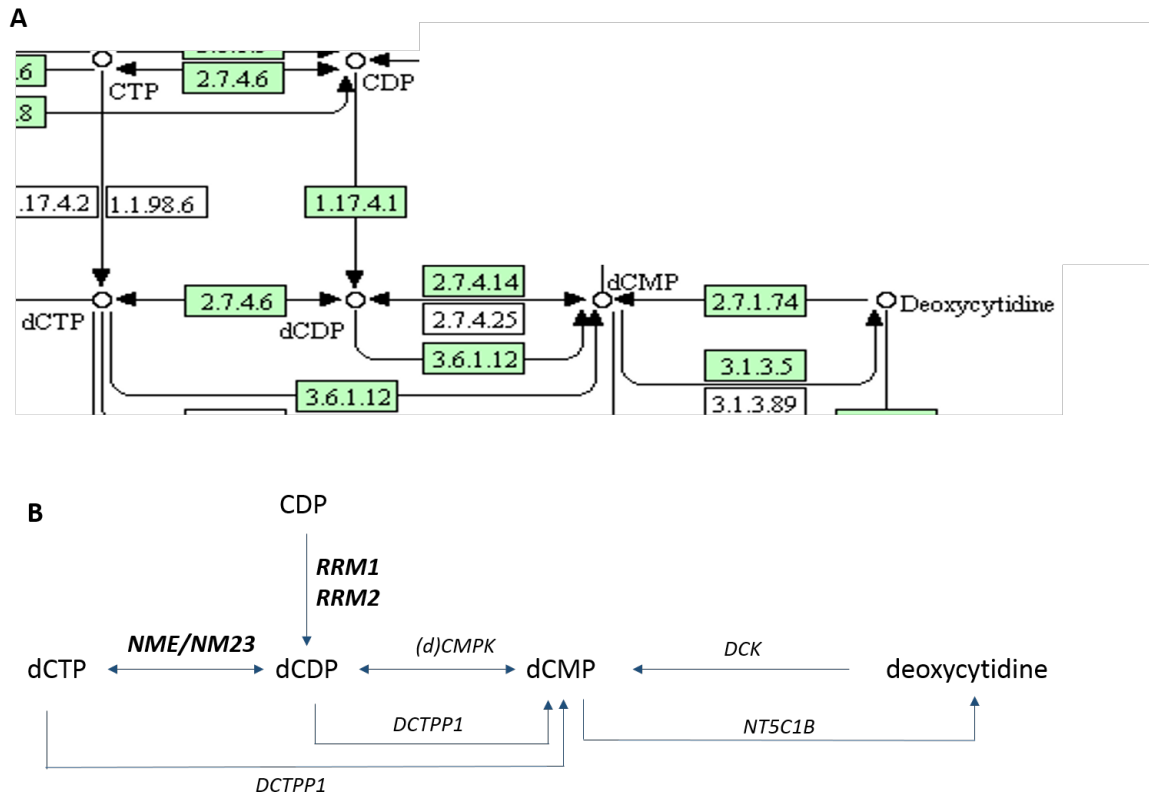


Figure 5.17: Pyrimidine metabolism pathway. (A) KEGG mapping of deoxycytidine metabolism. (B) Simplified representation of deoxycytidine metabolism. Cytidine diphosphate is converted into its deoxycytidine form dCDP by RRM1 and RRM2 and then into dCTP by NME/NM23.

Dysregulation of pyrimidine metabolism pathway results in an increase of dCTP (Requena et al., 2014), which competes directly with dFdCTP for incorporation into DNA. The effect of excess of dCyd was investigated in A2780 cells treated with gemcitabine or Acelarin. In the presence of dCyd to competitively inhibit DCK, cells were completely resistant to gemcitabine. A similar experiment was performed in a study that showed competition of gemcitabine anti-viral activity by exogenous dCyd co-treatment (Lee et al., 2017). By contrast, at equal concentrations of dCyd, Acelarin retained its cytotoxicity, albeit showing a modest decrease of cell survival. While dCyd partially impairs Acelarin activity, the effect was much less than the complete inhibi-

tion seen with gemcitabine. Another factor is timing, cells were more prone to become resistant when they were co-treated with excess of dCyd and drug than when they had been pre-treated with dCyd prior to being exposed to Acelarin or gemcitabine. Yet, exogenous deoxycytidine confers complete resistance to gemcitabine while sensitivity to Acelarin is retained. This is consistent with the idea that dCTP competes with dFdCTP for incorporation into DNA during replication but that there is more active metabolites released by Acelarin than gemcitabine. This could be confirmed by analysis of the metabolites levels by mass spectrometry.

Expression and localisation of DCK in response to gemcitabine and Acelarin treatment were assessed in A2780 cells by immunostaining. The level of DCK protein was found to be increased in cells treated with gemcitabine, as well as in those treated with Acelarin, but to a lesser extent. There is no consensus about intracellular localisation of DCK in the literature. While one group observed that DCK was mainly expressed in the cytoplasm (Hatzis et al., 1998), another found it in the nucleus (Johansson et al., 1997), whereas a different publication based on cytospin results showed it was nuclear or cytoplasmic depending on the cell line (Hubeek et al., 2005). In A2780 control cells, it was in both cellular compartments. DCK expression was largely increased in gemcitabine treated cells both nuclear and cytoplasmic. On the contrary, it was mostly perinuclear when treated with Acelarin. This is another evidence of the difference between both drugs. Furthermore, the increased size of cells treated with Acelarin, compared to control, is consistent with the results displayed in chapter 3, where Acelarin had a prolonged delayed effect on the cell cycle compared to control and gemcitabine.

After having established the importance of pyrimidine metabolism pathway in modulation of Acelarin sensitivity in ovarian and pancreatic cell lines (Sarr et al., 2018), the clinical relevance of DCK and DCTPP1 as potential predictive biomarker was investigated in biopsy tissues from Acelarin Phase I cohort. Using an Allred score system, their expression was determined based on their localisation, nuclear or cytoplasmic. DCK and DCTPP1 were found in both nucleus and cytoplasm but mainly in the tumour cell nuclei. Expression of DCTPP1 has been reported to be in both compartments, in cancer cell lines as well as cancer tissues but with nuclear accumulation of DCTPP1 in cancerous tissues including lung, breast, liver, cervical, gastric and esophagus cancer (Requena et al., 2014; Zhang et al., 2013). This is consistent with the role of DCTPP1 in the nucleotide metabolism, as it removes the non-canonical nucleotides, hence preventing their aberrant incorporation into DNA and thus might make the cancer cells more resistant to DNA damage and apoptosis. It was previously reported that DCK was highly expressed in lymphocytes (Spasokoukotskaja et al., 1995; Staub and Eriksson, 2006) and similar observation was made in these tissues. Some of the biopsies displayed lymphocyte infiltration within tumoral tissue and this could potentially introduce error in Allred score for DCK. However, to prevent this, parameters on QuPath were set as such that cells with small nuclei, more likely to be lymphocytes than cancer cells, were excluded from analysis. The main advantage of QuPath is that the same parameters are applied to all the tissues and this limits the subjectivity of the observer (Bankhead et al., 2017; Loughrey et al., 2018).

The analysis of 39 tumour tissues, from a range of different cancer types, did not show a correlation between DCK and DCTPP1 expression and efficacy of Acelarin. Although the number of patients is small, the data suggest that Acelarin achieved clinical activity even in patients with low DCK expressing tumours. This was especially clear in the patient who had a partial response with within three cycles of Acelarin while

they had low DCK and gemcitabine treatment had failed. Most biomarker studies are done at a later stage of drug development or retrospectively after the clinical trials have ended. However, analysis of information gathered from pre-treatment tissues with patients outcome can also be of interest. Sebastiani and colleagues have shown that levels of DCK in gemcitabine-naive tissues correlated with overall survival following gemcitabine treatment and were stable even after resistance to gemcitabine occurred (Sebastiani et al., 2006). In this study biopsies were pre-treatment with Acelarin, but as shown with the cases study, protein expression can vary over time.

These data suggest that DCK and DCTPP1 are not predictive biomarkers. Further clinical trials are being carried out to assess the long term efficacy of Acelarin treatment in patients, during which time levels of DCK and DCTPP1 could be analysed again in tumour tissues at a later stage. Moreover, monitoring dCMP/dCTP levels in Acelarin treated tumours may be of benefit. Although results from the screen did not prove beneficial for the patients, the robustness of the screen was validated (Sarr et al., 2018), and effect of the pyrimidine metabolism pathway on the sensitivity to Acelarin was demonstrated in ovarian cell line.

Further work is necessary to identify the relevance of the activation candidates *in vitro* and *in vivo*. First, optimisation of siRNA for Cathepsin A and CES2 or using CRISPR/Cas9 system are required to knockdown each gene separately and assess any potential effect on sensitivity to Acelarin. However, there might be redundancy, especially within the HINTs family. Although it is a mitochondrial protein, HINT2 has high-sequence homology to HINT1 (61% identical), while HINT3 is less similar with only 28% identity (Anderson et al., 2013; Chou et al., 2007). Murakami and colleagues showed that HINT1 was responsible for the activation of a pro-drug whereas HINT3 had no effect on it. Gene expression analysis showed a relatively high expression of

HINT1 and HINT2 but low HINT3 in both A2780 and SKOV3 cells.

Although each individual knockdown probably has a limited effect on sensitivity to Acelarin, there may be synergy when expression of two or several of them is low. Similar to the ratio hENT1xdCK/RRM1xRRM2 (Nakano et al., 2007) that correlates with acquired gemcitabine-resistance in pancreatic cancer cells, expression of HINTs and maybe Cathepsin A and CES2 could be predictive biomarkers for sensitivity to Acelarin, but there is no information either *in vitro* or *in vivo* as to how much of each of the enzymes is required.

HINT1 is also known as a haploinsufficient tumour suppressor and negatively regulated by epigenetic. It is silenced in a range of different cancers such as lung, gastric and liver (Wang et al., 2007; Zhang et al., 2009). Preliminary work in our group showed that HINT1 is mostly negative in lung cancer, and its expression is rather dynamic in ovarian, pancreatic and renal cancer (Appendix 7.19). Besides its role in metabolism of Acelarin, it would be of interest to study its implication as a potential prognostic biomarker.

6 | General discussion

6.1 Discussion

Major improvements have been made in the detection and management of patients with cancer in the past decades. However, despite the development of new cytotoxic drugs with initial high response rates and more recently targeted therapy, chemoresistance remains a burden. Although the first-line treatment with platinum-based chemotherapy is very effective, more than 70% of patients develop a recurrence and die from progressive disease (Matulonis et al., 2016; Pignata et al., 2017). Gemcitabine, a nucleoside analogue, is used as second line chemotherapy regimen for ovarian cancer, but it faces numerous inherent and acquired cancer resistance mechanisms that dramatically limit its effectiveness. Therefore, there is an urgent need to develop new therapeutic compounds with increased efficacy and minimal toxicity and move towards a more personalised medicine to determine which treatment will be most beneficial for individual patient.

The development of the ProTide approach addressed some of the problems encountered with nucleoside analogues and already proved increased efficacy and safety profile, with two FDA approved drugs and others in clinical trials for cancer and viral infection (Mehellou et al., 2017). Acelarin, a phosphoramidate transformation of gemcitabine, is the first anti-cancer ProTide to enter the clinic. Designed to overcome resistance associated with gemcitabine, it is supposed to have a similar way to induce

cell death, but little is known about the mechanisms by which Acelarin exerts its action and if or how it differs from gemcitabine. With its increased lipophilicity, Acelarin is thought to be independent from a transporter for cellular uptake because it was shown that, unlike gemcitabine, its sensitivity was not affected when hENT1 was inhibited (Slusarczyk et al., 2014; Mehellou et al., 2017). The addition of the phosphoramidate motif improved the pharmacokinetic/dynamic properties and made it favourable for therapy as a single agent (Blagden et al., 2018), as well as in combination with carboplatin in patients with ovarian cancer (Blagden et al., 2017; Gourley et al., 2018). Due to the nature of the ProTide, with the phosphoramidate motif composed of three different components (an aryl, an ester and an amino acid), the possibilities are vast and it is possible that another compound with a theoretical better profile was missed, due to manufacturing limitations or by not testing in the right model. Furthermore, it is not known as yet how the phosphoramidate moiety is recycled after the ProTide is activated. The amino acid is likely to be used in physiological pathways, but more investigation is required to fathom the fate of the aryl and ester and their potential effect on cells.

The work presented in this thesis showed that, although similar in structure to gemcitabine, the ProTide chemistry does alter cytotoxicity and the effects of Acelarin are prolonged over time *in vitro*, giving a potential explanation for its better efficacy and lower toxicity in patients. Although the cytotoxicity results displayed a lower potency of Acelarin compared to gemcitabine, this may be due to delayed activation of the ProTide in cancer cell lines. As the exact mechanism of activation remains unknown it was impossible to determine if the proteins required were expressed in these cells and kinetics of activation still need to be elucidated. This reflects some critical issue when screening for new anti-cancer compounds. Based solely on the cytotoxicity *in vitro* in some cell lines, it may be concluded that Acelarin was not worth further

investigation, whereas in patients, the peak concentration of the active intracellular metabolite, dFdCTP, at the end of infusion was 217-times greater than reported for equimolar doses of gemcitabine, with minimal toxic metabolite accumulation (Blagden et al., 2018). Gemcitabine is quickly degraded whereas Acelarin is more stable and more likely to exert a long term cytotoxic effect compared to gemcitabine. Here it was established that, as well as overcoming resistance associated with gemcitabine, Acelarin may have a more targeted mode of action. It can be considered as a 'cleaner' drug as at equimolar concentrations, gemcitabine would just induce cell death because of high toxicity, that is desirable "on target" effects in proliferating cancer cells, but also generalised cytotoxicity that affects both proliferating cancer cells but also host tissues too.

In addition, the fact that a higher concentration of Acelarin was required to reach comparable cell death to gemcitabine may also be a result of the limitation of two-dimensional cell culture, when it has already been proven that Acelarin is more potent than gemcitabine (Blagden et al., 2018). Development of 3D culture technologies have led to the elaboration of novel and more physiological models, called organoids (Lancaster and Knoblich, 2015). Those are cell-derived *in vitro* three-dimensional organ models which allow the study of biological processes, such as cell behaviour, tissue repair and response to drugs, in an environment that mimics endogenous cell organisation and organ structures (Drost and Clevers, 2018). In a near future, using organoids for drug screening may lead to a more personalised cancer treatment (Francies et al., 2016; Nantasanti et al., 2016).

Personalised medicine refers to the right treatment for the right patient at the right time. On the other hand, clinical trials are conventionally designed and analysed based on the concept of 'onesize-fits all', assuming that the effect of a drug is similar

for all patients with the particular disease; the drug treatment effect is evaluated by comparing mean treatment effects between treated and untreated patients (Chen et al., 2015). The role of genetic heterogeneity within patients and tumours is increasingly recognised as important to understand the dynamics of cancer progression and therapeutic resistance (Merlo and Maley, 2010). The molecular characteristics of a tumour vary between the moment of diagnosis and later on during the course of treatment. Loss of tumour suppressor, amplification of tyrosine kinase, increase of DNA repair protein expression are only a few example of variation that occur and have an impact on the prognosis and treatment efficacy (Oldenhuis et al., 2008). Many patients receive anti-cancer therapy from which they do not benefit whilst they do experience toxicity. Therefore, instead of using drugs that are nonspecific, there is a need to develop targeted therapy that could target cancer cells only and not any rapidly proliferating cells. Performing a genetic screening would allow a better selection of which patients can benefit from a given treatment, however this would come with a cost and require to be done regularly as tumours adapt over time. This variability makes biomarker studies more complex, especially as the development of chemoresistance is the consequence of a number of essential alterations in tumour cells rather than a single mutation. This is why so many initial promising results are reported for biomarker candidates *in vitro* but are often not reproducible in patients (Diamandis, 2012; Burke, 2016). This raises the following question: should we preclude patients from receiving treatment based on the lack of expression of one potential marker, when they might still have some, even limited, benefit? It is crucial to think of a wider picture with the involvement of cellular pathways in tumour biology, rather than individual genes separately.

A biomarker is defined as a characteristic that is objectively measured and evaluated as an indicator of normal biologic processes, pathogenic processes or pharmacological responses to a specified therapeutic intervention. Two main types are used to

make a decision concerning cancer treatment (Oldenhuis et al., 2008; Chen et al., 2015). Prognostic biomarkers provide information about the patients overall cancer outcome, regardless of therapy, whilst predictive biomarkers give information about the effect of a therapeutic intervention. The presence or the absence of a prognostic marker can be useful for the selection of patients for a certain treatment, but does not predict the response to this treatment. On the other hand, a predictive biomarker can be a target for therapy. The concern is that it requires invasive biopsy to sample some tumour tissue to test. Historically, the identification of markers involved in resistance to anti-cancer drugs depended on the candidate gene approach. Knowledge of the biological function of the compounds is required as the success depends upon the correct choice of genes/pathways; this increases the risk of arbitrariness. The development of genome-wide screen permitted the discovery of a number of new genes and cellular pathways involved in resistance to different drugs as it is an unbiased approach targeting the entire genome (Wilkening et al., 2009; Amos et al., 2010). However, the results of a screen have to be interpreted with some caution as there could be a number of false positive genes (Li et al., 2014), as well as a cell line specificity.

DCK and DCTPP1, two candidates selected from a genome-wide screen for resistance to Acelarin in a pancreatic cell line (Sarr et al., 2018), were validated in an ovarian cell line. DCK was an unexpected candidate since, contrary to gemcitabine, it is not required for activation of Acelarin (Slusarczyk et al., 2014). Both proteins are involved in the pyrimidine metabolism pathway. This pathway was previously shown by Shukla and colleagues to play a major role in gemcitabine resistance, by increasing the level of intracellular dCTP, which creates a negative regulation of DCK (Shukla et al., 2017). It was also established to be involved in modulation of sensitivity to Acelarin in chapter 5 section 2.1. However, the validation of the screen gave slightly different results in ovarian and pancreatic cell lines, as the loss of DCTPP1 had no effect on

the sensitivity to Acelarin in ovarian cancer cells. This proves the importance of the validation process of such genome-wide screens (Sharma and Petsalaki, 2018).

The analysis of the pre-treatment biopsies from the phase I cohort for Acelarin, representing a range of different tumours, did not show a correlation between DCK and DCTPP1 expression and efficacy of Acelarin. The data suggest that Acelarin achieved clinical activity even in patients with low DCK expressing tumours. This supports the notion that Acelarin overcomes the cancer cell resistance mechanisms that limit the clinical utility of gemcitabine. Importantly, patients who had previously relapsed on gemcitabine treatment showed clinical responses to Acelarin, further confirming the potential for Acelarin to represent a more effective treatment option for these patients. In conclusion, DCK and DCTPP1 are not negative biomarkers for Acelarin, and low expression of those proteins should not preclude patients from consideration for Acelarin treatment.

The gene candidate approach, based on the metabolism of Acelarin, determined that HINT1 was a potential candidate for resistance to Acelarin *in vitro* as it acts as a phosphoramidase releasing the nucleotide once inside the cell. However, it is unknown how much enzyme is required. No correlation was found between expression of HINT1 and clinical response to Acelarin. Although the cohort was small and would benefit from a larger number of samples, it emphasises the difficulty of biomarker studies and why thousands are published annually but very few make it through to the clinic. Interestingly, none of the candidates described in chapter 1 section 3.2 were selected in the Acelarin screen. Performing single knockdown with CRISPR/Cas9 in a panel of cancer cell lines and treating them with different ProTides would allow a robust validation of the implication of HINT1 and other candidates in resistance to the compounds. In addition, previously reported gemcitabine genetic screens did not select the known

resistance factors of gemcitabine (Azorsa et al., 2009; Fredebohm et al., 2013; Smith et al., 2014). Hence, it is hypothesised that there may be some adaptation responses to the drug selection pressure on the CRISPR/Cas9 library. Therefore, caution should be used when performing CRISPR/Cas9 screens, since this methodology may not uncover very strongly selected genes and may be dependent on factors such as *in vitro* drug metabolism effects. The ratio of Nakano and colleagues concerning resistance to gemcitabine, DCKxhENT1/RRM1xRRM2, highlights the concept that there is not one single biomarker that predicts chemotherapy efficacy. It is unlikely that it would be any different for Acelarin and further investigations are required to find a correlation between different factors potentially involved in resistance to the drug. With the development of the organoids, CRISPR/Cas9 can be used to knockdown genes of interest before the creation of these *in vitro* models and proceed to similar validation that would be more relevant than traditional two-dimensional cell culture (Zhan et al., 2018).

Combination therapy is a cornerstone of cancer treatment, in order to reduce the doses and avoid resistance. It is rather difficult to investigate combination studies *in vitro* and even more to translate these results to the clinic, especially as so many factors are not taken into account in a cell culture model. These studies are now using the well accepted definition of synergy/antagonism based on combination index as defined by Chou-Talalay (Chou et al., 2006; Chou, 2010). However, this concept suffers from limitations. Some publications claim to show an effect when it might not actually be real. This is because the combination index is a mathematical model based on algorithms and it does not take into account biological variability. Even though it should be fairly reproducible, the variability of toxicity combined with inadequate length of treatment makes it complicated to interpret the results except if there is a strong synergy or antagonism as seen in combination studies with fluvastatin and cisplatin (Taylor-Harding et al., 2010). Even then, it was shown in chapter 4 that a

given CI value does not necessarily reflect the reality of cell survival and both set of data should be used together to interpret the results, rather than just the combination index as often noticed in the literature (Budman and Calabro, 2002; Shord and Patel, 2009; Hunakova et al., 2014; Zhong et al., 2018). The complexity of this kind of study resides in the design, but to draw conclusions on the effect of a drug combination based on just a single value is a substantial simplification and is unlikely to translate to the patients. In addition, many *in vitro* studies looked at different sequences with varying lengths of treatment designed to show an effect, regardless this not being physiologically relevant because of the lack of clearance and other parameters in a laboratory setting, rather than taking into account how to predict what is possible in patients.

Another aspect to consider is the impact of the environment on drug sensitivity and how it affects the combination itself. As previously discussed, cell sensitivity to gemcitabine is affected by hypoxia, which is a main characteristic of tumour cores, and the effect of oxygen level on gemcitabine-cisplatin combination has not been investigated. One of the consequence of hypoxia on cell metabolism is an increase of pyrimidine synthesis (Shukla et al., 2017), which was shown in chapter 5 to affect mostly gemcitabine, and only to a certain extent Acelarin. It can be hypothesised that the effect will be limited on an Acelarin-cisplatin combination compared to a combination with gemcitabine. Even though no synergy between Acelarin and cisplatin was found in the ovarian cancer model used in this thesis, different patterns were observed between the platinum sensitive and resistant cell lines. This evidence supports the hypothesis that shorter treatment and in specific order could provide with useful information for future clinical trials. More work is required to fully understand the mechanisms that would explain why treating the platinum-resistant cell line with cisplatin first followed by Acelarin can potentiate the effect of both drugs.

In conclusion, there is strong evidence that the ProTide approach applied to gemcitabine alters the toxicity profile and makes Acelarin a more favourable drug for the treatment of ovarian cancer. More work is also required to unravel the interaction between cisplatin and Acelarin and this could help determine the best combination to use for the patients. This thesis supports the idea that it is important to better understand the underlying mechanisms of a given compound rather than just testing its cytotoxic efficacy. Here the focus was on pharmacodynamics but there is a need to improve the pharmacokinetic-pharmacodynamic (PKPD) modelling to quantitatively characterise the relationships between drug exposures and biological responses as a function of time (Tuntland et al., 2014).

6.2 Future work

The nucleoside analogues are relatively non-specific compounds as they are incorporated into replicating DNA of any rapidly proliferating cells, most likely cancer cells as they divide more often than most normal cells. By contrast, targeted therapy takes advantage of changes acquired in malignant cancer cells (receptors, proteins, mechanisms) by using compounds specifically targeting these and thus limiting their action on healthy cells. However, the traditional chemotherapies still represent a reliable strategy as long as they can be delivered inside the cells and be activated. Investigating the effect of Acelarin on healthy cells vs cancer cells may provide useful information to determine factors involved in resistance/sensitivity to Acelarin and better understand the effect of specific mutations and which proteins should be targeted in order to improve Acelarin efficacy.

To this date, there is still no biomarker available to determine which patients can benefit from Acelarin. The pathway most likely to provide with potential candidates is the activation of Acelarin, which remains to be elucidated. It is hypothesised that a low expression of Cathepsin A, CES2 or HINTs proteins will result in a decrease of dFdCMP/dFdCTP metabolites. The effect of HINT1 on Acelarin sensitivity in ovarian cancer cell line was shown in chapter 5 but more work is necessary to confirm the implication of the other candidates. It will also be relevant to assess their expression in current phase of the clinical study, where more patients are enrolled and further clinical data, such as overall survival, are available. Even if activation of Acelarin is a key pathway, more factors are likely to be involved in resistance to Acelarin. This was supported by the analysis of gene expression of the different candidates in SKOV3 cells. This cell line is resistant to Acelarin but expression of each candidate gene was higher than in the sensitive cell line A2780. SWATH mass spectrometry would be a useful tool to compare and analyse the differences in protein expression with untreated cells as the baseline and after treatment with Acelarin to determine which cellular pathways may be altered.

Poly (ADP-ribose) polymerase (PARP) has a well-established role in DNA repair process. PARP inhibitors are thought to augment cytotoxic therapy without increasing side effects and to kill cancer cells with DNA repair defects as a single agent in BRCA defective ovarian and breast cancer (Weil and Chen, 2012). Ovarian cancer patients with BRCA1 or BRCA2 mutation were reported to be more sensitive to Olaparib in phase II clinical trial (Gelmon et al., 2011). In 2014, the European Medicines Agency approved Olaparib to be a maintenance treatment in high-grade serous epithelial ovarian cancer patients with mutated BRCA1 or BRCA2 who have recurrent disease previously treated with platinum. PARP inhibitors have also been developed as chemotherapy sensitisers. Several publications described the positive effect of combination of gemcitabine and

platinum-based chemotherapy with a PARP inhibitor in patients (Rajan et al., 2012; Gray et al., 2018). Acelarin is already showing promising results in combination with carboplatin in ovarian cancer and this could be even more efficient if combined with a PARP inhibitor for example. Clinical trials involving gemcitabine and PARP inhibitors (+/- platinum-based therapy) are ongoing (Gray et al., 2018). As the investigation of Acelarin-cisplatin is going on to understand how both drugs interact with the other, a combination study with Olaparib might provide useful information on potential synergy and could be integrated in the current clinical trials.

Acelarin may replace gemcitabine one day, and become one of the standard chemotherapies for ovarian cancer.

7 | Appendices

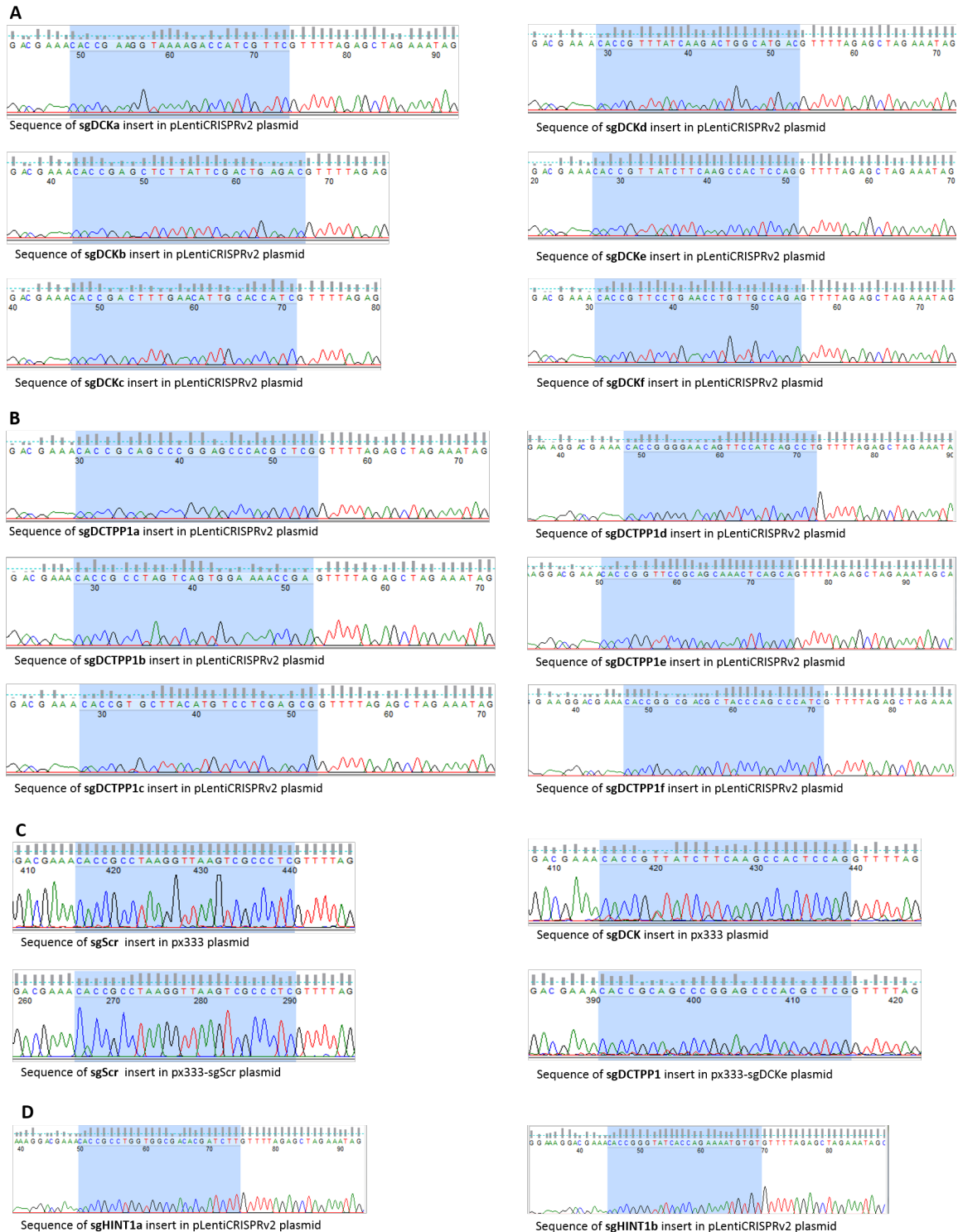


Figure 7.1: Verification of sgRNA inserts in pLentiCRISPRv2 px333 plasmids. sgDCK (A), sgDCTPP1 (B) in pLentiCRISPRv2 and sgScr, sgDCK, sgDCTPP1 (C) in px333 were cloned by Awa Sarr. (D) sgHINT1 in pLentiCRISPRv2. The plasmids were sequenced and insertion of the correct sgRNA was verified for each of them.

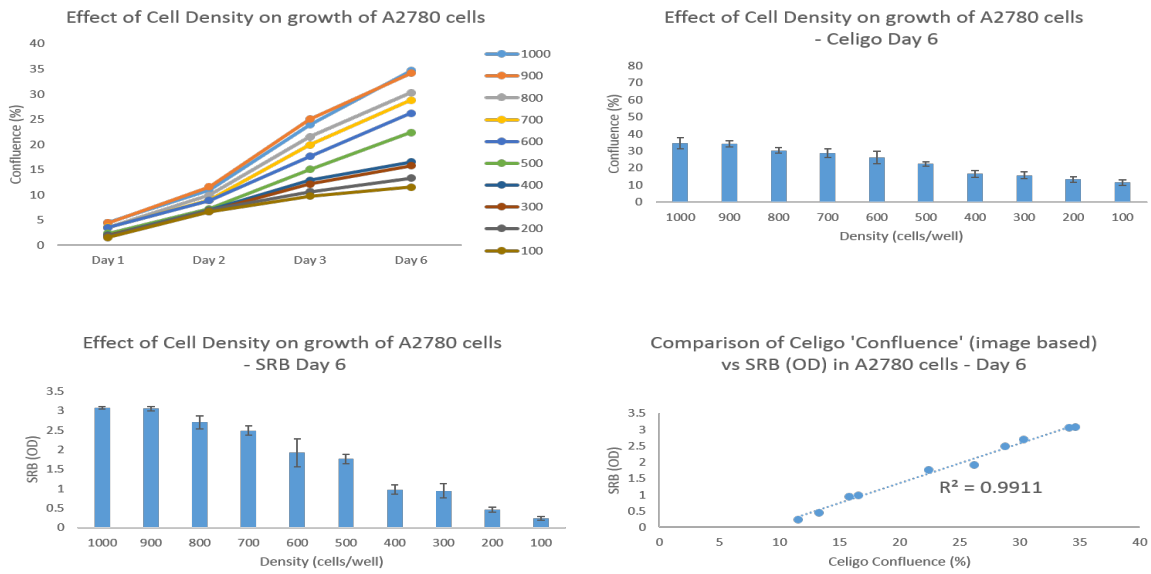


Figure 7.2: Comparison of cell confluence of A2780 cells with Celigo and SRB.

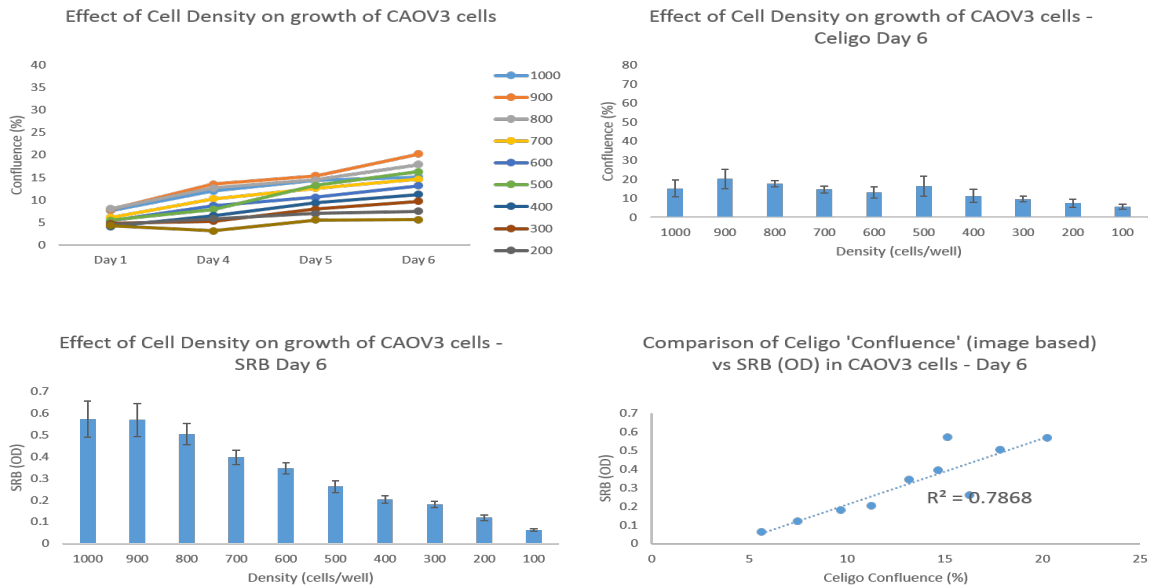


Figure 7.3: Comparison of cell confluence of CAOV3 cells with Celigo and SRB.

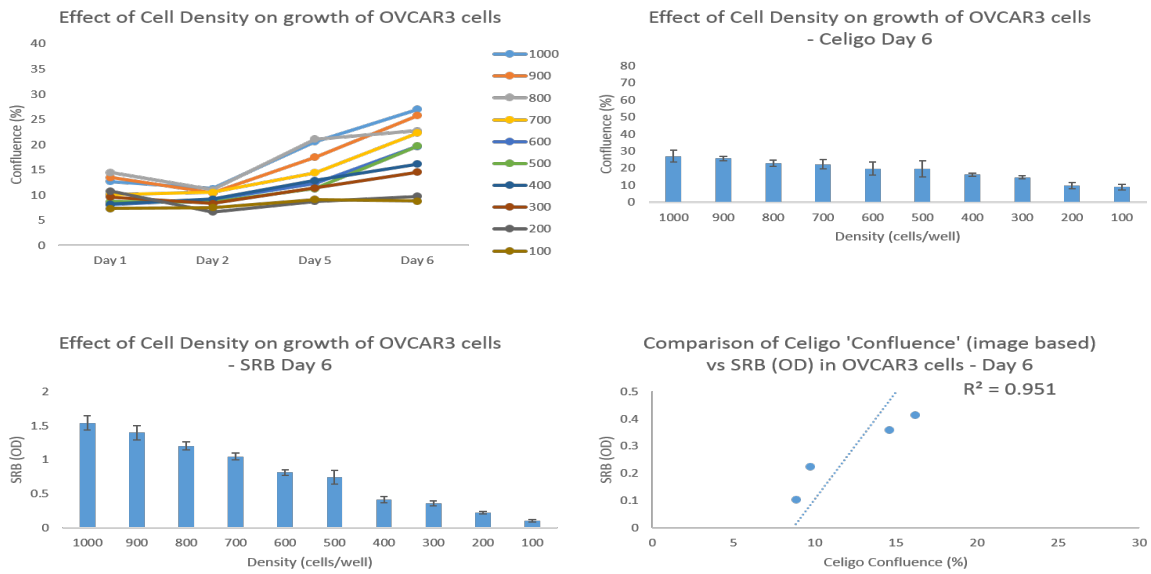


Figure 7.4: Comparison of cell confluence of OVCAR3 cells with Celigo and SRB.

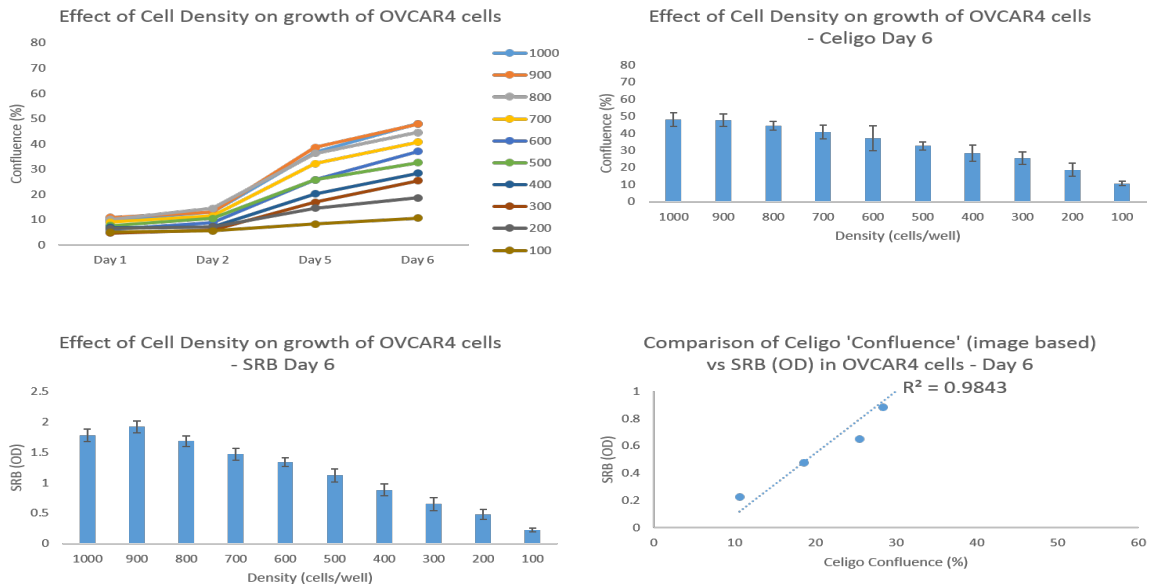


Figure 7.5: Comparison of cell confluence of OVCAR4 cells with Celigo and SRB.

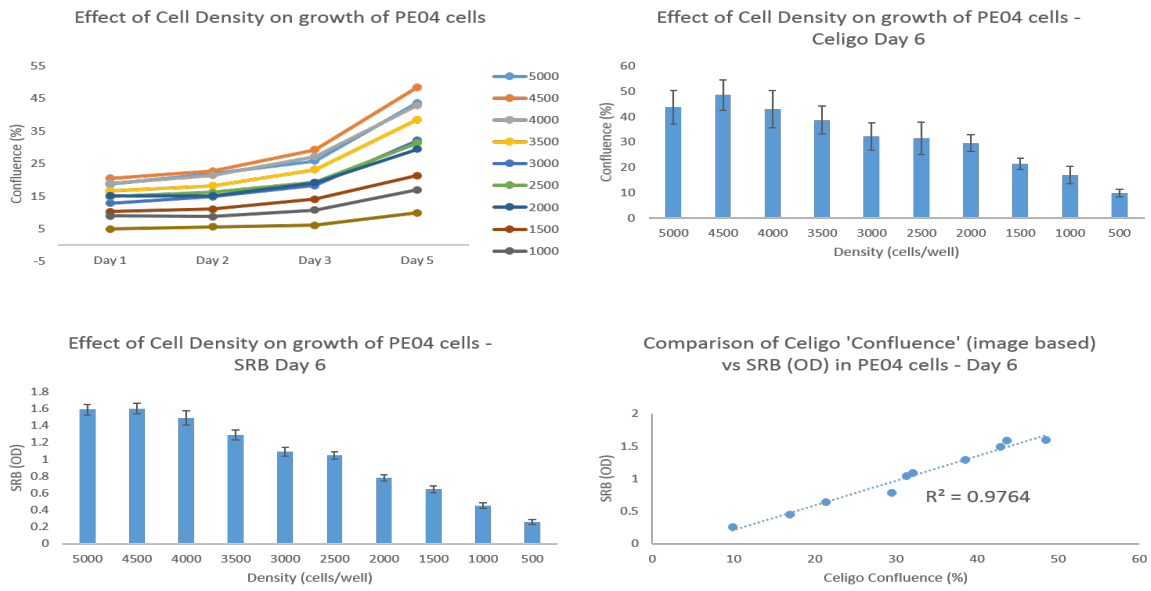


Figure 7.6: Comparison of cell confluence of PE04 cells with Celigo and SRB.

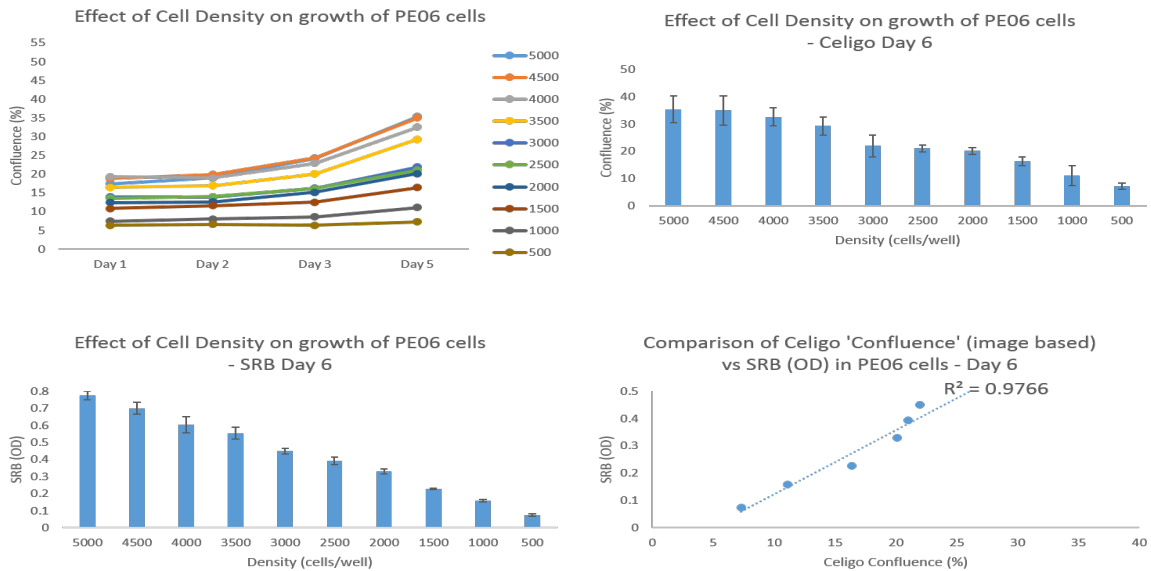


Figure 7.7: Comparison of cell confluence of PE06 cells with Celigo and SRB.

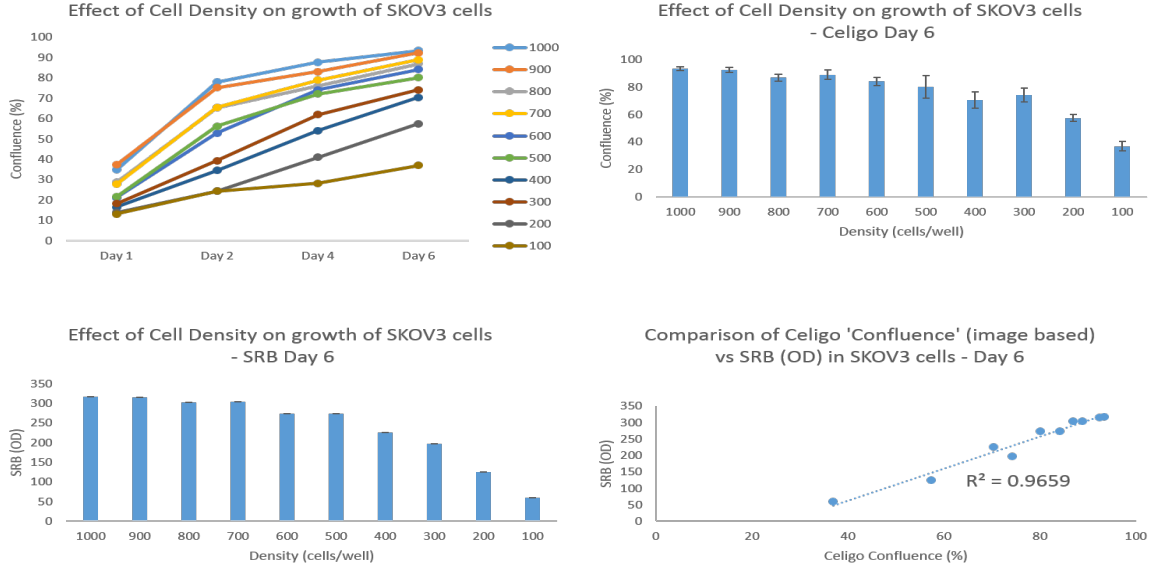
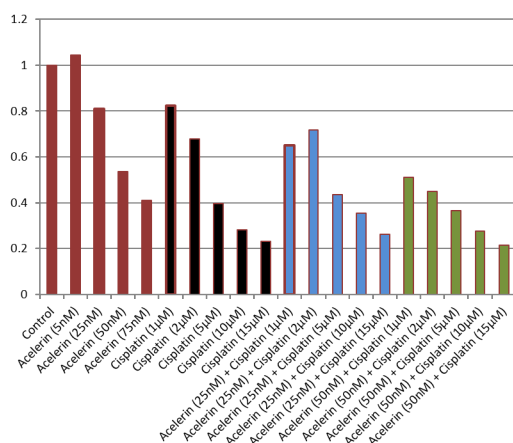


Figure 7.8: Comparison of cell confluence of SKOV3 cells with Celigo and SRB.

Group	DCK nucleus	DCK cytoplasm	DCTPP1 nucleus	DCTPP1 cytoplasm	RECIST	Prior gem	
1	4.73	4.05	5.95	5.26	Stable	3 months	yes
	4.71	3.81	2.75	2.10	Stable	4 months	no
	5.00	4.39	5.17	4.00	Progressive		no
	4.37	1.53	0.87	0.20	Stable	3 months	yes
	4.05	1.07	0.08	0.00	Progressive		yes
	2.83	1.33	4.00	3.67	Stable	3 months	no
	3.33	2.67	4.67	3.33	Stable	3 months	no
	4.73	1.82	3.29	1.71	Stable	4 months	yes
	0.67	0.22	0.90	0.10	Stable	2 months	no
	3.71	1.43	0.00	0.00	Progressive		yes
	2.28	1.80	5.11	4.02	Progressive		no
	3.00	2.71	1.60	0.20	Progressive		yes
	4.73	3.59	0.91	0.00	Stable	4 months	yes
	0.00	0.00	3.15	2.15	Progressive		yes
	4.33	1.00	0.00	0.00	Progressive		yes
	4.00	2.71	4.30	3.80	Progressive		no
	3.40	2.40	4.40	3.40	Progressive		yes
	5.40	3.70	5.40	4.30	Progressive		no
5.07	3.62	5.52	4.69	Stable 5	months	yes	
2.88	0.63	4.00	1.50	Stable 5	months	no	
4.17	2.64	2.27	1.88	Stable 5	months	no	
2	4.00	3.00	2.82	2.36	Stable	10 months	no
	4.67	3.89	5.19	5.06	Stable	15 months	no
	3.00	2.00	7.00	6.00	Stable	10 months	no
	1.18	0.35	2.83	1.44	Stable	12 months	no
	2.25	1.83	2.23	1.23	Stable	13 months	yes
	4.07	1.82	4.38	3.08	Stable	8 months	no
	2.54	1.82	2.17	2.17	Stable	8 months	no
	2.50	2.00	2.75	2.00	Stable	11 months	no
	5.14	3.21	1.69	0.15	Partial response	10 months	no
	1.73	1.55	5.20	5.07	Stable	23 months	no
	4.51	2.80	0.73	0.10	Stable	7 months	yes
	2.50	0.50	1.40	0.00	Stable	8 months	no
	2.71	0.14	3.33	1.47	Partial response	3 months	yes
	1.00	0.40	2.67	1.67	Stable	9 months	no
	4.00	3.00	2.80	2.00	Stable	10 months	no
	5.00	3.50	3.00	0.00	Stable	10 months	no
	3.00	2.00	2.00	0.00	Stable	8 months	no

Table 7.1: DCK and DCTPP1 Allred scores with RECIST and gemcitabine information.

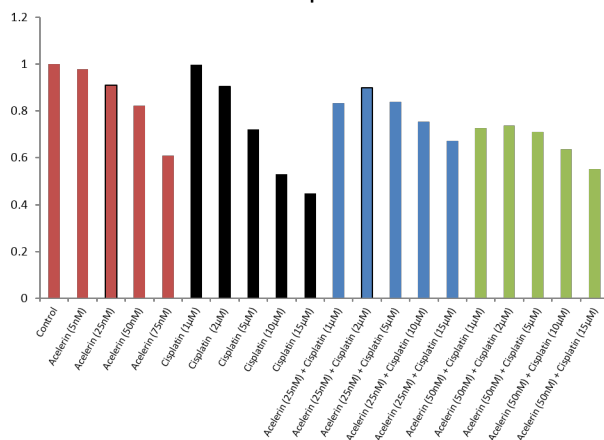
Effects of Acelarin and Cisplatin Combinations on the growth of PE01 cells



Acelarin	Cisplatin	CI value (PE01)
25nM	2µM	1.959
25nM	5µM	1.318
25nM	10µM	1.655

24hr exposure, Day 4 SRB

Effects of Acelarin and Cisplatin Combinations on the growth of PE04 cells



Acelarin	Cisplatin	CI value (PE04)
25nM	2µM	1.645
25nM	5µM	1.738
25nM	10µM	2.084

24hr exposure, Day 4 SRB

Figure 7.9: Effect of simultaneous treatment with Acelarin-cisplatin combination on PE01 and PE04 cells. Cells were treated for 24 h with different concentration of Acelarin and cisplatin as single agents or 25 nM Acelarin with 2 µM, 5 µM or 10 µM cisplatin for combination. After treatment, cells were washed out and let to grow until SRB was performed at 96 h post-treatment. CI values were obtained with CalcuSyn. Data were collected and analysed by Ateeb Khan and Peter Mullen.

PE01					
Acelarin	control	75 nM	100 nM	250 nM	500 nM
	100	86.83	95.51	76.09	74.22
Cisplat	ctrl	1 uM	4 uM	12 uM	20 uM
	100	99.89	98.36	74.24	55.59
Acelarin	control	75 nM	100 nM	250 nM	500 nM
1 uM cis	100	113.21	105.13	108.36	113.40
12 uM cis	100	70.06	69.84	71.56	70.36
Cisplat	control	1 uM	4 uM	12 uM	20 uM
75 nM Ac	100	91.82	88.91	65.77	55.68
250 nM Ac	100	102.31	93.88	69.07	48.40

Cis (uM)	Ac (nM)	CI
1.0	75.0	-
1.0	100.0	-
1.0	250.0	-
1.0	500.0	-

Cis (uM)	Ac (nM)	CI
1.0	75.0	1.08
4.0	75.0	1.09
12.0	75.0	0.85
20.0	75.0	1.10

Cis (uM)	Ac (nM)	CI
1.0	250.0	-
4.0	250.0	5.26
12.0	250.0	1.21
20.0	250.0	1.05

Cis (uM)	Ac (nM)	CI
12.0	75.0	0.95
12.0	100.0	0.99
12.0	250.0	1.32
12.0	500.0	1.71

Cis (uM)	Ac (nM)	CI
1.0	250.0	-
4.0	250.0	5.26
12.0	250.0	1.21
20.0	250.0	1.05

Cis (uM)	Ac (nM)	CI
12.0	75.0	1.34
12.0	100.0	1.45
12.0	250.0	1.76
12.0	500.0	1.84

Cis (uM)	Ac (nM)	CI
12.0	75.0	1.37
12.0	100.0	1.45
12.0	250.0	1.85
12.0	500.0	2.27

Cis (uM)	Ac (nM)	CI
1.0	75.0	-
4.0	75.0	1.95
12.0	75.0	1.37
20.0	75.0	1.63

Cis (uM)	Ac (nM)	CI
1.0	100.0	10.22
4.0	100.0	1.54
12.0	100.0	1.57
20.0	100.0	1.75

Cis (uM)	Ac (nM)	CI
1.0	75.0	NaN
1.0	100.0	NaN
1.0	250.0	NaN
1.0	500.0	NaN

Cis (uM)	Ac (nM)	CI
1.0	75.0	NaN
4.0	75.0	NaN
12.0	75.0	NaN
20.0	75.0	NaN

Cis (uM)	Ac (nM)	CI
1.0	250.0	NaN
4.0	250.0	NaN
12.0	250.0	NaN
20.0	250.0	NaN

Cis (uM)	Ac (nM)	CI
12.0	75.0	NaN
12.0	100.0	NaN
12.0	250.0	NaN
12.0	500.0	NaN

Cis (uM)	Ac (nM)	CI
1.0	250.0	NaN
4.0	250.0	NaN
12.0	250.0	NaN
20.0	250.0	NaN

Figure 7.10: Repeats of drug combinations Acelarin-cisplatin in PE01 cells (1). Cells were treated for 2 h with different concentration of Acelarin, followed by 4 h of cisplatin. SRB was performed at 96 h post-treatment and CI values were obtained with CalcuSyn.

PE01						Cis (uM)	Ac (nM)	CI	Cis (uM)	Ac (nM)	CI
Acelarin	control	75 nM	100 nM	250 nM	500 nM	1.0	75.0	1.84	1.0	75.0	2.97
	100	86.83	95.51	76.09	74.22	1.0	100.0	-	4.0	75.0	1.69
Cisplat	ctrl	1 uM	4 uM	12 uM	20 uM	1.0	250.0	3.63	12.0	75.0	1.16
	100	99.89	98.36	74.24	55.59	1.0	500.0	4.79	20.0	75.0	1.24
Acelarin	control	75 nM	100 nM	250 nM	500 nM	12.0	75.0	1.05	1.0	250.0	4.36
	1 uM cis	100	113.21	105.13	108.36	12.0	100.0	-	4.0	250.0	1.76
Cisplat	control	1 uM	4 uM	12 uM	20 uM	12.0	250.0	1.08	12.0	250.0	1.06
	100	91.82	88.91	65.77	55.68	12.0	500.0	1.04	20.0	250.0	0.90
75 nM Ac	100	102.31	93.88	69.07	48.40						
250 nM Ac	100	102.31	93.88	69.07	48.40						
						Cis (uM)	Ac (nM)	CI	Cis (uM)	Ac (nM)	CI
Acelarin	control	75 nM	100 nM	250 nM	500 nM	1.0	75.0	NaN	1.0	75.0	2.12
	100	102.20	105.34	100.48	87.87	1.0	100.0	NaN	4.0	75.0	-
Cisplat	ctrl	1 uM	4 uM	12 uM	20 uM	1.0	250.0	NaN	12.0	75.0	6.45
	100	96.90	55.46	31.60	27.60	1.0	500.0	NaN	20.0	75.0	4.77
Acelarin	control	75 nM	100 nM	250 nM	500 nM	12.0	75.0	5.78	1.0	250.0	NaN
	1 uM cis	100	88.13	54.90	35.18	12.0	100.0	1.55	4.0	250.0	NaN
Cisplat	control	1 uM	4 uM	12 uM	20 uM	12.0	250.0	0.98	12.0	250.0	0.95
	100	87.17	48.31	29.31	23.84	12.0	500.0	0.93	20.0	250.0	1.72
75 nM Ac	100	98.24	100.14	88.91	70.67						
250 nM Ac	100	27.78	30.15	28.32	32.70						

Figure 7.11: Repeats of drug combinations Acelarin-cisplatin in PE01 cells (2). Cells were treated for 2 h with different concentration of Acelarin, followed by 24 h of cisplatin. SRB was performed at 96 h post-treatment and CI values were obtained with CalcuSyn.

PE01						Cis (uM)	Ac (nM)	CI	Cis (uM)	Ac (nM)	CI
Acelarin	control	75 nM	100 nM	250 nM	500 nM	1.0	75.0	6.29	1.0	75.0	5.65
	100	86.83	95.51	76.09	74.22	1.0	100.0	-	4.0	75.0	2.49
Cisplat	ctrl	1 uM	4 uM	12 uM	20 uM	1.0	250.0	1.23	12.0	75.0	1.99
	100	99.89	98.36	74.24	55.59	1.0	500.0	1.55	20.0	75.0	1.88
Acelarin	control	75 nM	100 nM	250 nM	500 nM	12.0	75.0	1.65	1.0	250.0	1.09
	1 uM cis	100	113.21	105.13	108.36	12.0	100.0	-	4.0	250.0	1.33
Cisplat	control	1 uM	4 uM	12 uM	20 uM	12.0	250.0	1.23	12.0	250.0	1.16
	100	91.82	88.91	65.77	55.68	12.0	500.0	1.34	20.0	250.0	1.27
75 nM Ac	100	102.31	93.88	69.07	48.40						
250 nM Ac	100	102.31	93.88	69.07	48.40						
						Cis (uM)	Ac (nM)	CI	Cis (uM)	Ac (nM)	CI
Acelarin	control	75 nM	100 nM	250 nM	500 nM	1.0	75.0	2.11	1.0	75.0	2.11
	100	105.47	106.45	99.47	80.72	1.0	100.0	0.35	4.0	75.0	5.89
Cisplat	ctrl	1 uM	4 uM	12 uM	20 uM	1.0	250.0	0.43	12.0	75.0	1.38
	100	101.04	95.07	63.50	49.74	1.0	500.0	0.69	20.0	75.0	1.63
Acelarin	control	75 nM	100 nM	250 nM	500 nM	12.0	75.0	1.25	1.0	250.0	0.47
	1 uM cis	100	103.59	105.16	81.33	12.0	100.0	1.11	4.0	250.0	0.69
Cisplat	control	1 uM	4 uM	12 uM	20 uM	12.0	250.0	1.05	12.0	250.0	1.18
	100	101.25	90.18	58.76	45.54	12.0	500.0	1.23	20.0	250.0	1.55
75 nM Ac	100	76.06	66.16	46.22	37.01						
250 nM Ac	100	76.06	66.16	46.22	37.01						

Figure 7.12: Repeats of drug combinations Acelarin-cisplatin in PE01 cells (3). Cells were treated for 4 h with different concentration of cisplatin, followed by 2 h of Acelarin. SRB was performed at 96 h post-treatment and CI values were obtained with CalcuSyn.

PE04						Cis (uM)	Ac (nM)	CI	Cis (uM)	Ac (nM)	CI
Acelarin	control	75 nM	100 nM	250 nM	500 nM	1.0	75.0	NaN	1.0	75.0	NaN
		100	97.47	103.19	74.66	60.80	1.0	100.0	NaN	4.0	75.0
Cisplat	ctrl	1 uM	4 uM	12 uM	20 uM	1.0	250.0	NaN	12.0	75.0	NaN
		100	103.62	101.28	85.46	75.75	1.0	500.0	NaN	20.0	75.0
Acelarin	control	75 nM	100 nM	250 nM	500 nM	12.0	75.0	NaN	1.0	250.0	NaN
	1 uM cis	100	93.09	93.63	79.56	52.64	12.0	100.0	NaN	4.0	250.0
Cisplat	ctrl	1 uM	4 uM	12 uM	20 uM	12.0	250.0	NaN	12.0	250.0	NaN
		100	86.02	87.56	86.59	78.91	12.0	500.0	NaN	20.0	250.0
	75 nMAc	100	73.21	73.60	74.43	68.64					
	250 nMAc	100									
Acelarin	control	75 nM	100 nM	250 nM	500 nM	1.0	75.0	NaN	1.0	75.0	NaN
		100	100.63	104.76	104.43	105.97	1.0	100.0	NaN	4.0	75.0
Cisplat	ctrl	1 uM	4 uM	12 uM	20 uM	1.0	250.0	NaN	12.0	75.0	NaN
		100	104.79	105.91	98.81	82.24	1.0	500.0	NaN	20.0	75.0
Acelarin	control	75 nM	100 nM	250 nM	500 nM	12.0	75.0	NaN	1.0	250.0	NaN
	1 uM cis	100	101.23	104.31	107.55	104.92	12.0	100.0	NaN	4.0	250.0
Cisplat	ctrl	1 uM	4 uM	12 uM	20 uM	12.0	250.0	NaN	12.0	250.0	NaN
		100	99.51	101.66	100.32	93.69	12.0	500.0	NaN	20.0	250.0
	75 nMAc	100	103.38	107.89	106.72	101.12					
	250 nMAc	100	98.58	99.84	100.56	83.85					

Figure 7.13: Repeats of drug combinations Acelarin-cisplatin in PE04 cells (1). Cells were treated for 2 h with different concentration of Acelarin, followed by 4 h of cisplatin. SRB was performed at 96 h post-treatment and CI values were obtained with CalcuSyn.

PE04						Cis (uM)	Ac (nM)	CI	Cis (uM)	Ac (nM)	CI
Acelarin	control	75 nM	100 nM	250 nM	500 nM	1.0	75.0	-	1.0	75.0	-
		100	97.47	103.19	74.66	60.80	1.0	100.0	-	4.0	75.0
Cisplat	ctrl	1 uM	4 uM	12 uM	20 uM	1.0	250.0	-	12.0	75.0	1.68
		100	103.62	101.28	85.46	75.75	1.0	500.0	-	20.0	75.0
Acelarin	control	75 nM	100 nM	250 nM	500 nM	12.0	75.0	1.42	1.0	250.0	9.41
	1 uM cis	100	93.09	93.63	79.56	52.64	12.0	100.0	1.42	4.0	250.0
Cisplat	ctrl	1 uM	4 uM	12 uM	20 uM	12.0	250.0	2.04	12.0	250.0	1.73
		100	86.02	87.56	86.59	78.91	12.0	500.0	2.02	20.0	250.0
	75 nMAc	100	73.21	73.60	74.43	68.64					
	250 nMAc	100									
Acelarin	control	75 nM	100 nM	250 nM	500 nM	1.0	75.0	NaN	1.0	75.0	NaN
		100	101.26	104.83	106.57	108.21	1.0	100.0	NaN	4.0	75.0
Cisplat	ctrl	1 uM	4 uM	12 uM	20 uM	1.0	250.0	NaN	12.0	75.0	NaN
		100	108.59	85.89	51.85	39.41	1.0	500.0	NaN	20.0	75.0
Acelarin	control	75 nM	100 nM	250 nM	500 nM	12.0	75.0	NaN	1.0	250.0	NaN
	1 uM cis	100	106.40	110.73	113.22	109.56	12.0	100.0	NaN	4.0	250.0
Cisplat	ctrl	1 uM	4 uM	12 uM	20 uM	12.0	250.0	NaN	12.0	250.0	NaN
		100	57.61	58.60	58.24	51.65	12.0	500.0	NaN	20.0	250.0
	75 nMAc	100	119.43	102.18	65.20	50.60					
	250 nMAc	100	101.42	86.57	56.89	46.25					

Figure 7.14: Repeats of drug combinations Acelarin-cisplatin in PE04 cells (2). Cells were treated for 2 h with different concentration of Acelarin, followed by 24 h of cisplatin. SRB was performed at 96 h post-treatment and CI values were obtained with CalcuSyn.

PE04											
Acelarin	control	75 nM	100 nM	250 nM	500 nM	Cis (uM)	Ac (nM)	CI	Cis (uM)	Ac (nM)	CI
	100	97.47	103.19	74.66	60.80	1.0	75.0	0.45	1.0	75.0	0.33
Cisplatin	ctrl	1 uM	4 uM	12 uM	20 uM	1.0	100.0	0.60	4.0	75.0	0.54
	100	103.62	101.28	85.46	75.75	1.0	250.0	0.82	12.0	75.0	1.01
Acelarin	control	75 nM	100 nM	250 nM	500 nM	1.0	500.0	1.00	20.0	75.0	1.18
1 uM cis	100	93.09	93.63	79.56	52.64	Cis (uM)	Ac (nM)	CI	Cis (uM)	Ac (nM)	CI
12 uM cis	100	90.37	84.77	77.68	54.45	12.0	75.0	1.19	1.0	250.0	0.72
Cisplatin	ctrl	1 uM	4 uM	12 uM	20 uM	12.0	100.0	1.04	4.0	250.0	0.85
75 nM Ac	100	86.02	87.56	86.59	78.91	12.0	250.0	1.29	12.0	250.0	1.20
250 nM Ac	100	73.21	73.60	74.43	68.64	12.0	500.0	1.33	20.0	250.0	1.36
Acelarin	control	75 nM	100 nM	250 nM	500 nM	Cis (uM)	Ac (nM)	CI	Cis (uM)	Ac (nM)	CI
	100	100.31	99.76	81.88	59.10	1.0	75.0	5.67	4.0	75.0	1.09
Cisplatin	ctrl	1 uM	4 uM	12 uM	20 uM	1.0	100.0	1.00	4.0	100.0	1.12
	100	90.85	75.05	59.97	48.43	1.0	250.0	1.05	4.0	250.0	0.81
Acelarin	control	75 nM	100 nM	250 nM	500 nM	1.0	500.0	1.16	4.0	500.0	0.93
1 uM cis	100	97.11	87.23	79.39	54.61	Cis (uM)	Ac (nM)	CI	Cis (uM)	Ac (nM)	CI
4 uM cis	100	74.99	74.22	53.96	31.85	1.0	75.0	-	1.0	75.0	-
Acelarin	control	75 nM	100 nM	250 nM	500 nM	1.0	100.0	-	4.0	75.0	-
	100	102.51	103.69	100.60	94.38	1.0	250.0	-	12.0	75.0	4.94
Cisplatin	ctrl	1 uM	4 uM	12 uM	20 uM	1.0	500.0	0.92	20.0	75.0	2.46
	100	97.31	93.03	82.85	70.36	Cis (uM)	Ac (nM)	CI	Cis (uM)	Ac (nM)	CI
Acelarin	control	75 nM	100 nM	250 nM	500 nM	4.0	75.0	2.28	1.0	250.0	-
1 uM cis	100	102.00	106.00	103.66	94.13	4.0	100.0	2.09	4.0	250.0	1.09
4 uM cis	100	95.86	95.46	91.45	86.33	4.0	250.0	1.16	12.0	250.0	1.17
Cisplatin	ctrl	1 uM	4 uM	12 uM	20 uM	4.0	500.0	0.92	20.0	250.0	0.97
75 nM Ac	100	106.62	100.46	94.69	85.78	Cis (uM)	Ac (nM)	CI	Cis (uM)	Ac (nM)	CI
250 nM Ac	100	97.86	90.98	81.25	69.92	1.0	75.0	-	1.0	75.0	-
Acelarin	control	75 nM	100 nM	250 nM	500 nM	1.0	100.0	-	4.0	75.0	-
	100	94.09	102.40	97.78	89.81	1.0	250.0	-	12.0	75.0	-
Cisplatin	ctrl	1 uM	4 uM	12 uM	20 uM	1.0	500.0	1.41	20.0	75.0	-
	100	99.34	92.47	76.25	65.87	Cis (uM)	Ac (nM)	CI	Cis (uM)	Ac (nM)	CI
Acelarin	control	75 nM	100 nM	250 nM	500 nM	12.0	75.0	1.56	1.0	250.0	-
1 uM cis	100	101.31	111.02	101.25	91.10	12.0	100.0	1.58	4.0	250.0	1.36
12 uM cis	100	84.44	83.93	80.33	77.33	12.0	250.0	1.71	12.0	250.0	2.09
Cisplatin	ctrl	1 uM	4 uM	12 uM	20 uM	12.0	500.0	2.12	20.0	250.0	1.97
75 nM Ac	100	104.69	93.73	104.89	74.01	Cis (uM)	Ac (nM)	CI	Cis (uM)	Ac (nM)	CI
250 nM Ac	100	102.42	91.51	85.91	72.96	1.0	75.0	-	1.0	75.0	-

Figure 7.15: Repeats of drug combinations Acelarin-cisplatin in PE04 cells (3). Cells were treated for 4 h with different concentration of cisplatin, followed by 2 h of Acelarin. SRB was performed at 96 h post-treatment and CI values were obtained with CalcuSyn.

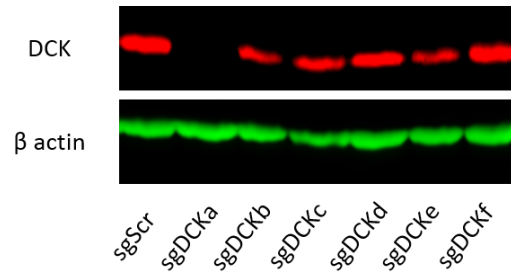


Figure 7.16: DCK knockdown in A2780 ovarian cancer cell line. Results of DCK knockdown with the different sgRNA.

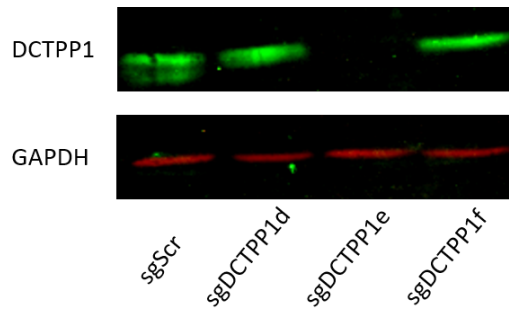


Figure 7.17: DCTPP1 knockdown in A2780 ovarian cancer cell line. Results of DCTPP1 knockdown with the different sgRNA.

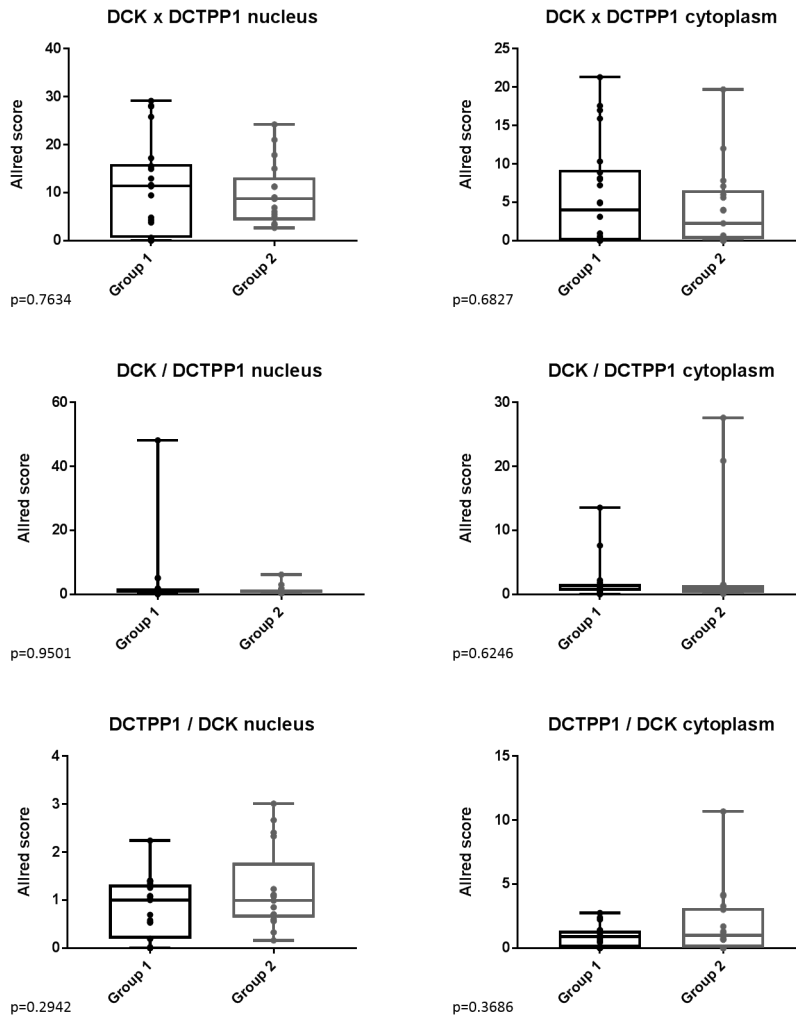


Figure 7.18: Allred score ratio of DCK and DCTPP1. Multiplication and ratio of Allred score of DCK and DCTPP1 were compared between the two groups of patients. $p > 0.05$, Mann-Whitney.

Ovarian cancer tissue

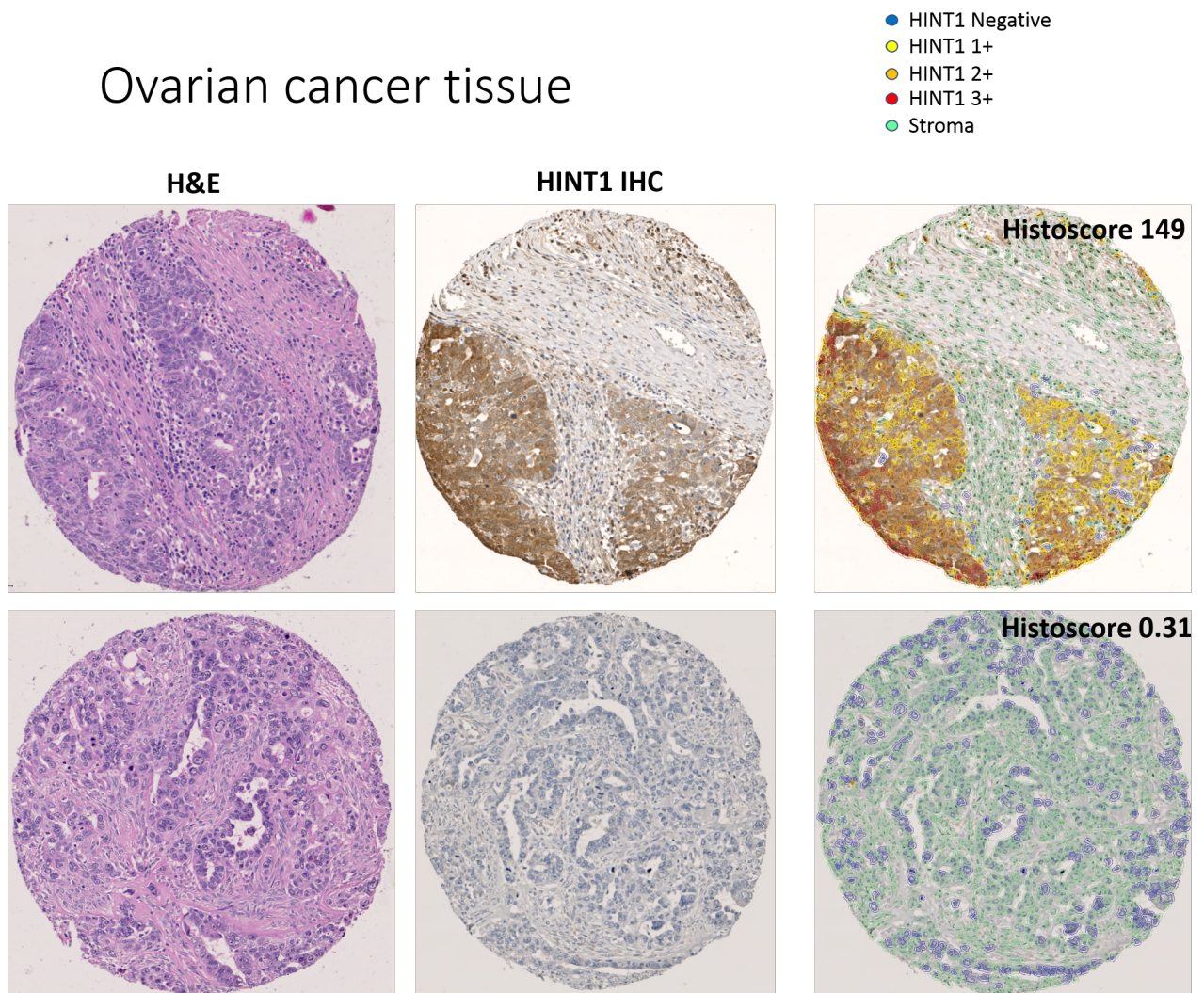


Figure 7.19: HINT1 expression in ovarian cancer. The protein expression of HINT1 is dynamic in ovarian cancer. Histoscore were obtained with QuPath.



University Teaching and Research Ethics Committee

15th January 2018

Professor David Harrison
School of Medicine

Dear Professor Harrison

Thank you for submitting your amendment application which comprised the following documents:

1. Ethical Amendment Application Form

The School of Medicine Ethics Committee is delegated to act on behalf of the University Teaching and Research Ethics Committee (UTREC) and has approved this ethical amendment application. The particulars of this approval are as follows –


Original Approval Code:	MD9202	Approved on:	16/10/2012
Amendment 5 Approval Date:	15/01/18	Approval Expiry Date:	16/10/2022
Term of Approval	10 YEARS		
Project Title:	Systems pathology of disease		
Researcher(s):	David Harrison, Fiona McKissock, Jennifer Bre, Peter Caie, In Hwa Um, Oliver Read, Ines Nearchou, Christos Gavriel, Neofytos Dimitriou, Hannah Williams, Mustafa Elshani, Raffaele De Filippis, Mary Kudsy, Mark Bates, Romina Briffa, Nourjahan Khafaga, Sophie Rao, Tsz Chan, Matthew Scott, Beth Gwyther	Supervisor(s):	David Harrison

Ethical amendment approval does not extend the originally granted approval period, rather it validates the changes you have made to the originally approved ethical application. If you are unable to complete your research within the original validation period, you are required to write to your School Ethics Committee Convener to request a discretionary extension of no greater than 6 months or to re-apply if directed to do so, and you should inform your School Ethics Committee when your project reaches completion.

Any serious adverse events or significant change which occurs in connection with this study and/or which may alter its ethical consideration, must be reported immediately to the School Ethics Committee, and an Ethical Amendment Form submitted where appropriate.

Approval is given on the understanding that you adhere to the 'Guidelines for Ethical Research Practice' (<http://www.st-andrews.ac.uk/media/UTRECguidelines%20Feb%2008.pdf>).

Yours sincerely

 Dr Morven Shearer, Convener School of Medicine Ethics Committee

School of Medicine Ethics Committee
Medical and Biological Sciences Building, North Haugh, St Andrews, Fife, KY16 9TF, Scotland, UK
Email: medethic@st-andrews.ac.uk Tel No: 01334 463585
The University of St Andrews is a charity registered in Scotland: No SC013532

Figure 7.20: Ethics approval.
193

8 | Publication

SCIENTIFIC REPORTS

OPEN

Genome-scale CRISPR/Cas9 screen determines factors modulating sensitivity to ProTide NUC-1031

Awa Sarr^{1,2}, Jennifer Bré¹, In Hwa Um¹, Tsz Huen Chan¹, Peter Mullen¹, David J. Harrison¹ & Paul A. Reynolds^{1,2}

Received: 30 January 2019

Accepted: 8 May 2019

Published online: 21 May 2019

Gemcitabine is a fluoropyrimidine analogue that is used as a mainstay of chemotherapy treatment for pancreatic and ovarian cancers, amongst others. Despite its widespread use, gemcitabine achieves responses in less than 10% of patients with metastatic pancreatic cancer and has a very limited impact on overall survival due to intrinsic and acquired resistance. NUC-1031 (Acelarin), a phosphoramidate transformation of gemcitabine, was the first anti-cancer ProTide to enter the clinic. We find it displays important *in vitro* cytotoxicity differences to gemcitabine, and a genome-wide CRISPR/Cas9 genetic screening approach identified only the pyrimidine metabolism pathway as modifying cancer cell sensitivity to NUC-1031. Low deoxycytidine kinase expression in tumour biopsies from patients treated with gemcitabine, assessed by immunostaining and image analysis, correlates with a poor prognosis, but there is no such correlation in tumour biopsies from a Phase I cohort treated with NUC-1031.

NUC-1031 (Acelarin), a phosphoramidate transformation of gemcitabine, is the first anti-cancer ProTide to enter the clinic¹. Analogues of cytidine are the backbone of many therapeutic regimens in oncology. Historically, Ara-C (Cytarabine) and more recently, gemcitabine², are first-line chemotherapy agents used in patients with pancreatic cancer³ and in combination treatments for ovarian, breast, biliary tract, lung, and bladder cancers^{4,5}. Gemcitabine acts as a cytotoxic agent primarily by blocking DNA synthesis in cancer cells^{6–8}. It is imported into cells through membrane transporters, including human Equilibrative Nucleotide Transporter 1 (hENT1), decreased expression of which in pancreatic cancer may be associated with poor overall survival⁹. Once inside the cell, gemcitabine requires phosphorylation to difluorodeoxycytidine monophosphate (dFdCMP) by deoxycytidine kinase (DCK), which represents the rate-limiting step for further phosphorylation to the active diphosphate (dFdCDP) and triphosphate (dFdCTP) metabolites². Of these, dFdCTP is the more active and incorporates into DNA to inhibit its synthesis. Subsequent failure of DNA repair triggers apoptosis and inhibits tumour growth^{10,11}. dFdCDP inactivates ribonucleotide reductase, depleting the deoxyribonucleotide pools necessary for DNA synthesis, potentiating the effects of dFdCTP^{12,13}. Gemcitabine is also rapidly catabolized by cytidine deaminase (CDA) generating difluorodeoxyuridine (dFdU)¹⁴.

Despite its widespread use, gemcitabine achieves responses in less than 10% of patients with metastatic pancreatic cancer and has very limited impact on overall survival¹⁵. Many cancers have an innate resistance to gemcitabine or, once exposed to gemcitabine, develop resistance, often within weeks of treatment initiation, markedly limiting its efficacy and clinical benefit^{8,16}. Three key cancer cell resistance mechanisms have been associated with a poor survival prognosis for gemcitabine: transport, activation, and breakdown. Cells deficient in the nucleoside transporter hENT1 are highly resistant to gemcitabine¹⁷ and patients with pancreatic cancer who express low or undetectable levels of hENT1 have significantly lower median survival times than those with detectable levels¹⁸. Deficiency of the activating enzyme DCK led to acquired gemcitabine resistance in a human ovarian carcinoma cell line exposed to increasing levels of gemcitabine *in vitro*¹⁹ and patients with pancreatic cancer who express low levels of DCK have significantly poorer overall survival than those with high levels²⁰. Finally, increased levels of the catabolising enzyme CDA have been associated with reduced median survival times in gemcitabine-treated patients with pancreatic cancer²¹.

The ProTide drug NUC-1031 is comprised of a pre-activated nucleotide analogue (gemcitabine monophosphate) and a protective phosphoramidate moiety, which is a specific combination of aryl, ester, and amino

¹School of Medicine, University of St Andrews, St Andrews, KY16 9TF, UK. ²Biomedical Sciences Research Complex, University of St. Andrews, St. Andrews, UK. Awa Sarr and Jennifer Bré contributed equally. Correspondence and requests for materials should be addressed to P.A.R. (email: par10@st-andrews.ac.uk)

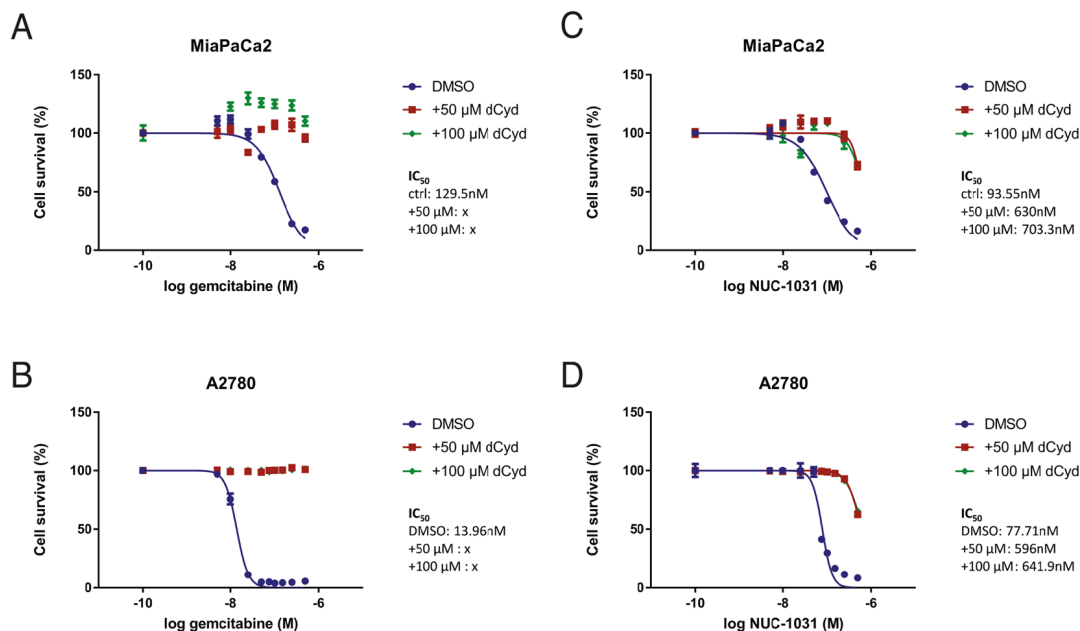


Figure 1. Exogenous dCyd negates efficacy of gemcitabine but not NUC-1031. (A,B) Dose-response curves for MiaPaCa2 or A2780 cells 4d after treatment with gemcitabine or (C,D) NUC-1031 and simultaneous addition of either DMSO, 50 μM or 100 μM of deoxycytidine (dCyd). Values represent mean \pm SEM (n = 6). A2780 vs A2780 + 50 μM dCyd vs A2780 + 100 μM dCyd: p = 0.0022; Mann-Whitney test).

acid groupings. Pre-clinical data show the increased lipophilicity of NUC-1031 enables it to circumvent hENT1-mediated transmembrane transport and, once inside the cell, the phosphoramidate protective group is cleaved off by esterases, releasing dFdCMP which is then rapidly converted to dFdCDP and dFdCTP, bypassing the rate-limiting step of phosphorylation by DCK. Furthermore, NUC-1031 avoids CDA-mediated catabolism, thus preventing dFdU accumulation^{22–24}. Both nucleotide synthesis and degradation are important in maintaining the dNTP pool and substrate cycling by 5'-nucleotidases and nucleoside kinases represent points of control²⁵.

Genome-scale genetic knockdown screens have been successfully used to identify genes involved in drug resistance/sensitivity for a variety of chemotherapeutic agents²⁶ and we employed this approach to screen for candidate genes mediating cancer cell sensitivity to NUC-1031. Surprisingly, the only pathway consistently selected was pyrimidine metabolism; specifically, multiple sgRNAs targeting two genes, DCK and deoxycytidine triphosphate pyrophosphate 1 (DCTPP1), involved in the maintenance of the dCMP/dCTP pool. In contrast, there were no consistent hits selected from the gemcitabine screen. We show that, although similar in structure, NUC-1031 displays important *in vitro* cytotoxicity differences to gemcitabine. While we find low DCK expression in tumour biopsies from patients treated with gemcitabine, assessed by immunostaining and image analysis, correlates with a poor prognosis, we find no such correlation in tumour biopsies from a Phase I cohort treated with NUC-1031. These data suggest that in contrast to gemcitabine, low DCK expression should not preclude patients from consideration for NUC-1031 treatment and that DCK is not a predictive marker of clinical response to NUC-1031.

Results

Exogenous dCyd confers complete resistance to gemcitabine while sensitivity to NUC-1031 is retained.

In order to investigate the effect of NUC-1031 and gemcitabine on dCMP/dCTP pool regulation, cytotoxicity assays for NUC-1031 and gemcitabine were carried out on MiaPaCa2 pancreatic cancer cells and A2780 ovarian cancer cells. In the presence of deoxycytidine (dCyd) to competitively inhibit DCK, MiaPaCa2 and A2780 cells (Fig. 1A,B) were completely resistant to gemcitabine, confirming the requirement of DCK for gemcitabine activation. By contrast, at equal concentrations of dCyd, NUC-1031 retained its cytotoxicity (Fig. 1C,D), albeit showing a modest decrease (30–35% reduction at equimolar doses). While dCyd does partially impair NUC-1031 activity, the effect was much less than the complete inhibition seen with gemcitabine. Pre-treatment of cells with dCyd before the addition of NUC-1031 also showed similar results (Fig. S1). These data are consistent with the phosphorylated status of NUC-1031, compared to gemcitabine.

To further elucidate these differences, cell cycle analysis was performed on A2780 cells treated at the IC₅₀ dose of NUC-1031 or gemcitabine for 2 h, followed by media washout. At 24 h after washout, more A2780 cells were in S phase after treatment with gemcitabine (62.1%) or NUC-1031 (57.85%) compared to DMSO-treated control (36.85%) (Fig. S2). However, at 48 h after washout, more A2780 cells were arrested in S phase after treatment with NUC-1031 (50.65%) than after treatment with gemcitabine (40.05%) or DMSO (36.55%) (Fig. S2). At 72 h after washout, more A2780 cells were in G2/M phase after treatment with NUC-1031 (18.95%) than after treatment with gemcitabine (12.6%) or DMSO (8.13%) (Fig. S2). Taken together, these data suggest that NUC-1031 and gemcitabine display important *in vitro* cytotoxicity differences and that the effects of NUC-1031 persist for longer *in vitro*, compared to gemcitabine.

Genome-Scale CRISPR/Cas9 screen implicates pyrimidine metabolism in NUC-1031 sensitivity. To identify genes involved in modulating resistance/sensitivity to NUC-1031 or gemcitabine, the GeCKOv2 genome-scale CRISPR/Cas9 knockdown library^{27,28} was used in pancreatic MiaPaCa2 cells and sgRNA distribution compared by next generation sequencing after 14d and 21d of drug treatment (Fig. 2A; Fig. S3). Exposure to either NUC-1031 or gemcitabine resulted in retarded population growth of transduced MiaPaCa2 cells (Fig. 2B), therefore enabling the enrichment of a small group of cells that were rendered more drug-resistant by Cas9:sgRNA-mediated modification. After 14d and 21d of NUC-1031 treatment, the sgRNA distribution was significantly different when compared to DMSO (vehicle)-treated cells, particularly after 21d, as well as an increased variability, illustrated by a larger interquartile range, indicating the selection of specific sgRNAs in response to the treatment (Fig. 2C; $p < 2.2 \times 10^{-16}$, Mann-Whitney/Wilcoxon rank sum test). Interestingly, gemcitabine treatment induced a smaller but statistically significantly different sgRNA distribution, compared to DMSO-treated cells (Fig. 2C; $p = 0.001117$ at d14, $p < 2.2 \times 10^{-16}$ at d21; Mann-Whitney/Wilcoxon rank sum test). For a subset of genes, there was enrichment of multiple sgRNAs that target each gene after 14d and 21d of NUC-1031 treatment (Fig. 2D), suggesting that loss of these particular genes contributes to increased NUC-1031 resistance. In contrast, there were no consistent hits from the gemcitabine screen (Fig. 2E, Table S1). The MAGeCK algorithm²⁹ was used to rank screening hits by the consistent enrichment among multiple sgRNAs targeting the same gene (Fig. 2F,G). The highest-ranking genes included the previously reported gemcitabine resistance factor DCK³⁰ and also several other genes, including DCTPP1, implicated in modulating intracellular dCTP³¹ (Table 1). These hits were also identified through a second independent library transduction (Fig. S4, Table S1).

Validation of candidate genes. Top-ranking genes from the GeCKOv2 screen were validated individually using independent sgRNAs cloned into pLentiCRISPRv2 and transduced into MiaPaCa2 cells in order to generate distinct knockdown cell lines for each gene. For DCK, knockdown efficiency was assessed by Western blot and DCK expression was found reduced by more than 70% in the MiaPaCa2 knockdown cell lines compared to MiaPaCa2-sgScr cells (Fig. 3A). Interestingly, the sgRNAs conferred a 4.5 to 7-fold increased resistance to NUC-1031 in MiaPaCa2-sgDCK cells, compared to MiaPaCa2-sgScr cells (Fig. 3B). However, at NUC-1031 concentrations of 250 nM, there was approximately 34% death (range of 21–47% for the 3 sgRNAs), compared to MiaPaCa2-sgDCK cells treated with gemcitabine that survived and were completely resistant to 250 nM gemcitabine (Fig. 3B). Likewise, ovarian A2780-sgDCK cells treated with gemcitabine were completely resistant to 500 nM gemcitabine, whereas A2780-sgDCK cells treated with NUC-1031 were 2-fold more resistant (IC_{50} sgDCK 242 nM vs IC_{50} sgScr 103 nM; $p = 0.0022$), compared to A2780-sgScr cells (Fig. 3B).

For DCTPP1, knockdown efficiency was assessed by Western blot analysis and DCTPP1 expression was found to be reduced by more than 90% in the MiaPaCa2 knockdown cell lines compared to MiaPaCa2-sgScr cells (Fig. 4A). Interestingly, the DCTPP1 sgRNAs conferred a 1.5-fold decreased sensitivity to NUC-1031 in MiaPaCa2-sgDCTPP1 cells, compared to MiaPaCa2-sgScr cells, indicating a small but consistent decrease in MiaPaCa2 cells sensitivity to NUC-1031 in the absence of DCTPP1 (Fig. 4B). On the contrary, no change in sensitivity was detected in MiaPaCa2-sgDCTPP1 cells compared to MiaPaCa2-sgScr cells in response to gemcitabine treatment (Fig. 4B). No change in sensitivity was detected for NUC-1031 or gemcitabine in pancreatic PSN1-sgDCTPP1 cells, compared to PSN1-sgScr cells (Fig. 4B). These data suggest that the modulatory effect of DCTPP1 on NUC-1031 sensitivity is specific to MiaPaCa2 cells.

Simultaneous knockdown of DCTPP1 and DCK shows no synergy. Since both DCK and DCTPP1 are involved in pyrimidine metabolism and maintenance of the dCMP pool, simultaneous inactivation of DCK and DCTPP1 was performed to assess for any synergistic effects, compared with individual knockdown. One guide RNA targeting DCK (sgDCK) and one targeting DCTPP1 (sgDCTPP1) or two non-targeting guide RNAs (sgScr), were cloned into pX333. Control (pX333 sgScr-sgScr) and double knockdown (pX333 sgDCK-sgDCTPP1) plasmids were introduced independently into MiaPaCa2 and A2780 cells by nucleofection. DCK protein expression was reduced by approximately 86% and DCTPP1 by approximately 72% in MiaPaCa2-sgDCK-sgDCTPP1 cells (Fig. 5A). MiaPaCa2-sgDCK-sgDCTPP1 cells displayed a 5-fold decreased sensitivity to NUC-1031, compared to MiaPaCa2-sgScr-sgScr cells, while MiaPaCa2-sgDCK-sgDCTPP1 cells were completely resistant to gemcitabine (Fig. 5B). Similar results were observed in A2780 cells with decrease of protein expression by 85% and 90% for DCK and DCTPP1, respectively. A2780-sgDCK-sgDCTPP1 cells displayed a 3-fold decreased sensitivity to NUC-1031, compared to A2780-sgScr-sgScr cells, while A2780-sgDCK-sgDCTPP1 cells were completely resistant to gemcitabine (Fig. 5B). These data suggest there is no synergistic effect on NUC-1031 sensitivity by simultaneously reducing both DCK and DCTPP1 expression.

DCK expression is not predictive in patients treated with NUC-1031. In order to assess the clinical relevance of DCK and DCTPP1 expression, cancer biopsy tissues from either pancreatic cancer patients who received gemcitabine/did not receive chemotherapy or from patients from a pan-cancer Phase I cohort treated with NUC-1031 were immunostained using antibodies to DCK and DCTPP1, and scanned images obtained from Zeiss AxioScan were quantified using QuPath³². After review by a pathologist (DJH), 60 pancreatic cancer tissue microarray (TMA) cores were identified as containing tumours, and these had associated survival data. DCTPP1 was expressed in 50 out of 60 pancreatic cancer cores, mainly in tumour cells that displayed mostly nuclear localization but also in cells in the tumour microenvironment, where DCTPP1 was localized in both the cytoplasm and nucleus. DCK was expressed in 55 out of 60 pancreatic cancer cores, in the cytoplasm and strongly in the nucleus, not only in tumour cells, but also in stromal and immune cells in the tumour microenvironment (Fig. 6A). To determine whether DCTPP1 and DCK expression levels were associated with patient outcome, Kaplan-Meier (KM) analyses were performed on histoscores using TMA navigator (www.tmanavigator.org)³³. KM analysis

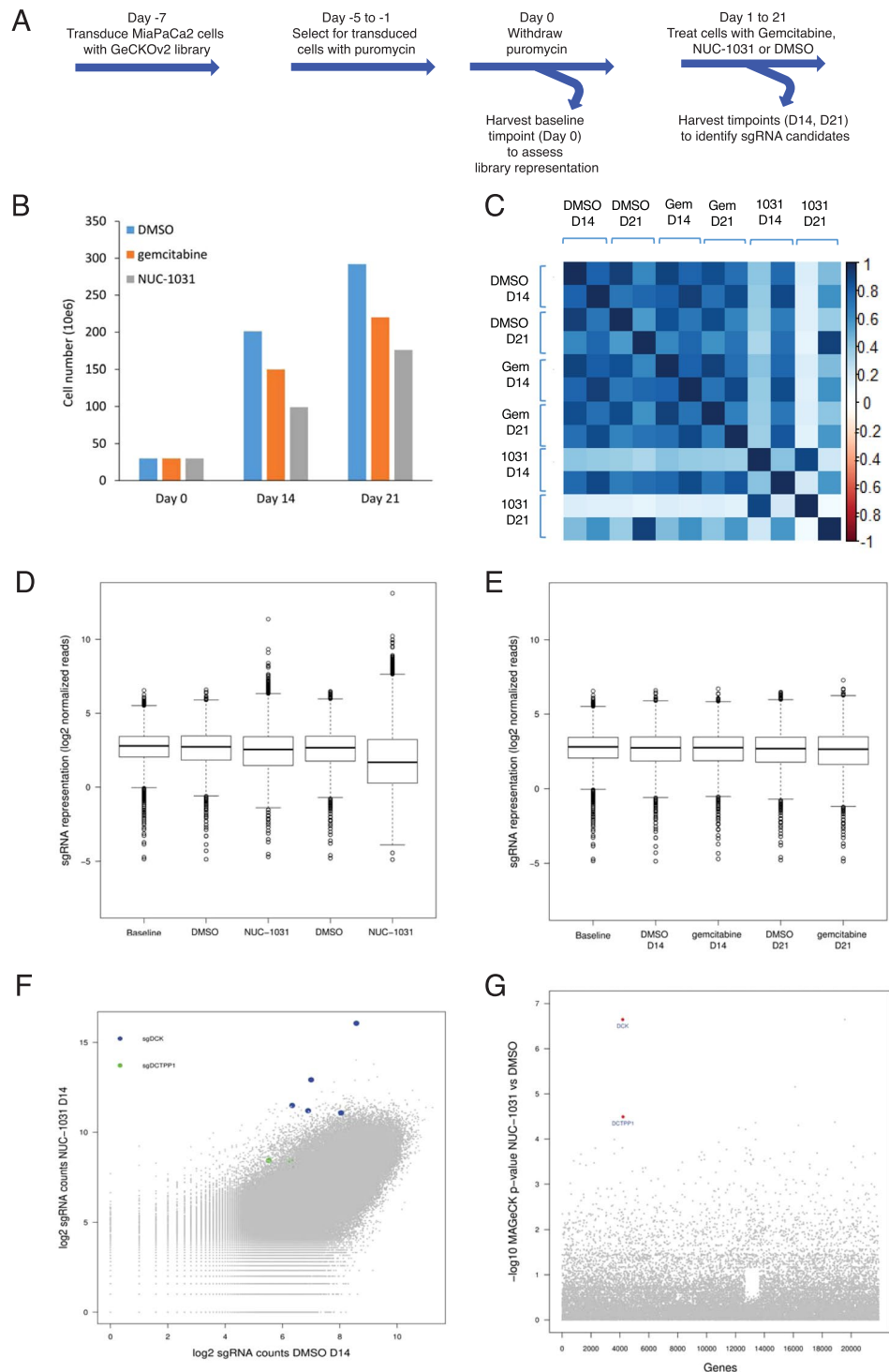


Figure 2. Genome-Scale CRISPR/Cas9 Screen Implicates DCK and DCTPP1 in NUC-1031 sensitivity. (A) Experimental design of the GECKOv2 screen for gemcitabine and NUC-1031 resistance, performed in MiaPaCa2 cells, in 2 biological replicates. (B) MiaPaCa2 cell number at d0, d14 and d21 after treatment with either dimethyl sulfoxide (DMSO) as control, gemcitabine or NUC-1031. (C) Heat map of sgRNA abundance comparing biological replicates and treatment conditions. (D,E) Distribution of sgRNA reads frequency before treatment (Baseline), in DMSO (Control), NUC-1031 or gemcitabine treated cells after d14 and d21 of exposure. The box extends from the first to the third quartile with the whiskers denoting 1.5 times the interquartile range and show an increased variability of sgRNA frequency in cells treated with NUC-1031 compared DMSO treated cells. (F) Scatterplot of sgRNA read counts in NUC-1031 treated cells compared to control (DMSO) cells showing enrichment of DCK and DCTPP1 sgRNAs after 14d exposure. (G) Identification of candidate genes, targeted by enriched sgRNAs, in NUC-1031 treated cells compared to control cells, using MAGeCK p-value analysis.

MAGeCK rank	gemcitabine				NUC-1031			
	Negative selection		Positive selection		Negative selection		Positive selection	
	Day 14	Day 21	Day 14	Day 21	Day 14	Day 21	Day 14	Day 21
1	CSF3R	NAA10	PP1R32	TSC2	TSC2	hsa-mir-555	TMEM165	TMEM165
2	LRRC24	POLR2D	hsa-mir-4711	CRYGC	ZBTB46	TSC2	DCK	DCK
3	POLB	PELO	NCOA3	ATRNL1	TSC1	DMPK	PYCR2	NTC_0397
4	MBLAC2	RPL14	CENPE	SH3BP4	ZNF281	PCOLCE	DCTPP1	SIRPD
5	NPBWR1	HPS5	UGGT2	hsa-mir-6727	COL4A1	OR10A5	SYNCRIP	TSPAN12
6	COG7	HM13	ARL1	MAP4K5	DDIT4	RUFY1	NTC_0731	HCN3
7	CTTNBP2	WDR43	hsa-mir-548h-5	hsa-mir-1254-2	OR51E2	hsa-mir-185	RASSF7	POMP
8	TNFRSF1A	COX5A	UBXN2A	NTC_0555	PHTF1	OR1M1	NACC2	NTC_0203
9	WWP2	XRCC5	NADK2	hsa-mir-1265	ERBB2IP	CCDC42B	NTC_0040	NTC_0045
10	ATP6V1B1	KIAA1239	CLEC19A	CDH29	LHPP	KCNA3	COQ4	DDO

Table 1. Top ranked genes from MAGeCK analysis. Genes ranked by MAGeCK by either negative selection or positive selection in gemcitabine or NUC-1031 treated cells after d14 and d21 of exposure.

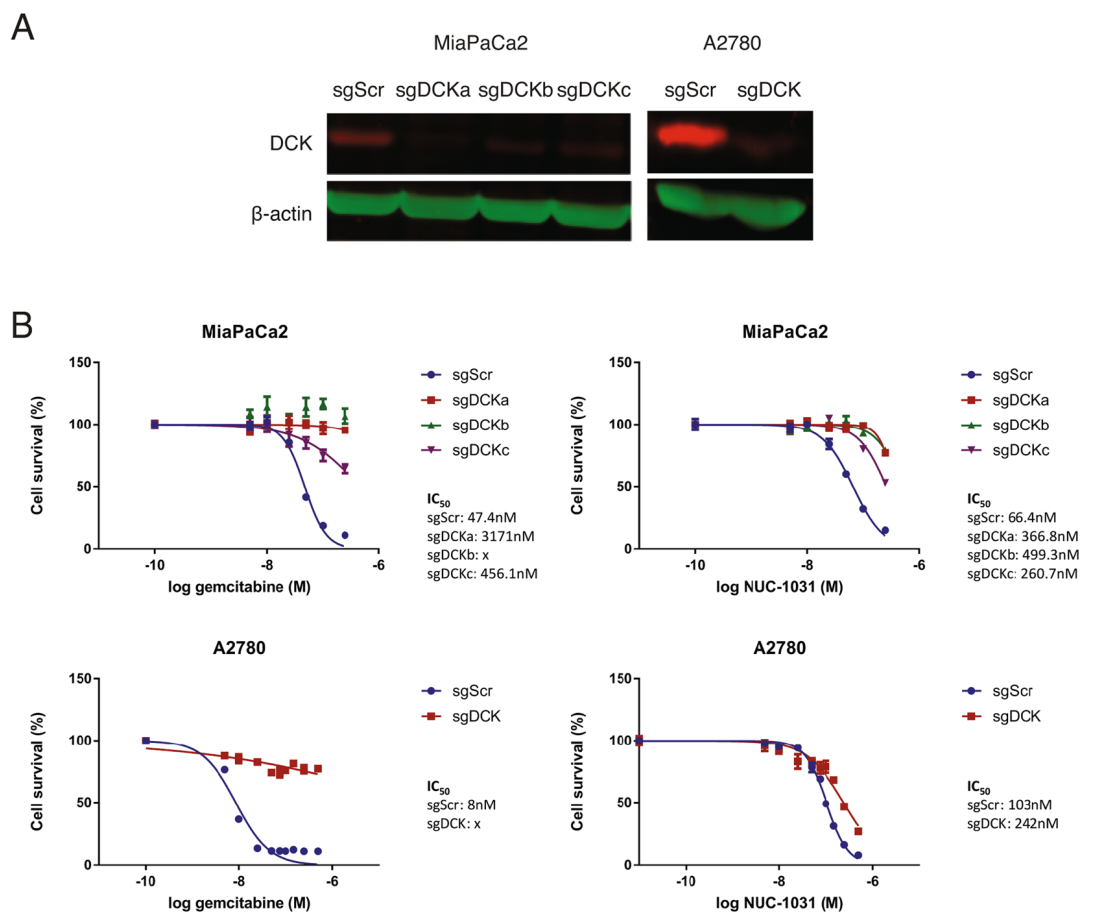


Figure 3. DCK mediates NUC-1031 sensitivity in pancreatic and ovarian cancer cells. **(A)** DCK protein expression analyzed by Western blot in MiaPaCa2 and A2780 cells transduced with independent sgRNAs targeting DCK (sgDCK) or a non-targeting scrambled control sgRNA (sgScr). **(B)** Dose-response curves for MiaPaCa2 and A2780 cells transduced with individual sgRNAs targeting DCK or a non-targeting scrambled control sgRNA (sgScr) and treated with NUC-1031 or gemcitabine ($n = 6$, \pm SEM). MiaPaCa2 sgScr vs MiaPaCa2 sgDCK: $p = 0.0022$, A2780 sgScr vs A2780 sgDCK: $p = 0.0022$ for NUC-1031 and $p = 0.0043$ for gemcitabine; Mann-Whitney test).

showed that there was no significant difference in survival (FDR corrected p -value = 0.3595) between those patients with low DCTPP1 expression (histoscores 0 to 15.68), those with medium DCTPP1 expression (histoscores 15.83 to 51.98) and those with high DCTPP1 expression (histoscores 52.31 to 149.38) (Fig. 6B). However, as expected from previous studies, KM analysis showed that patients with low DCK expression (histoscores 0 to

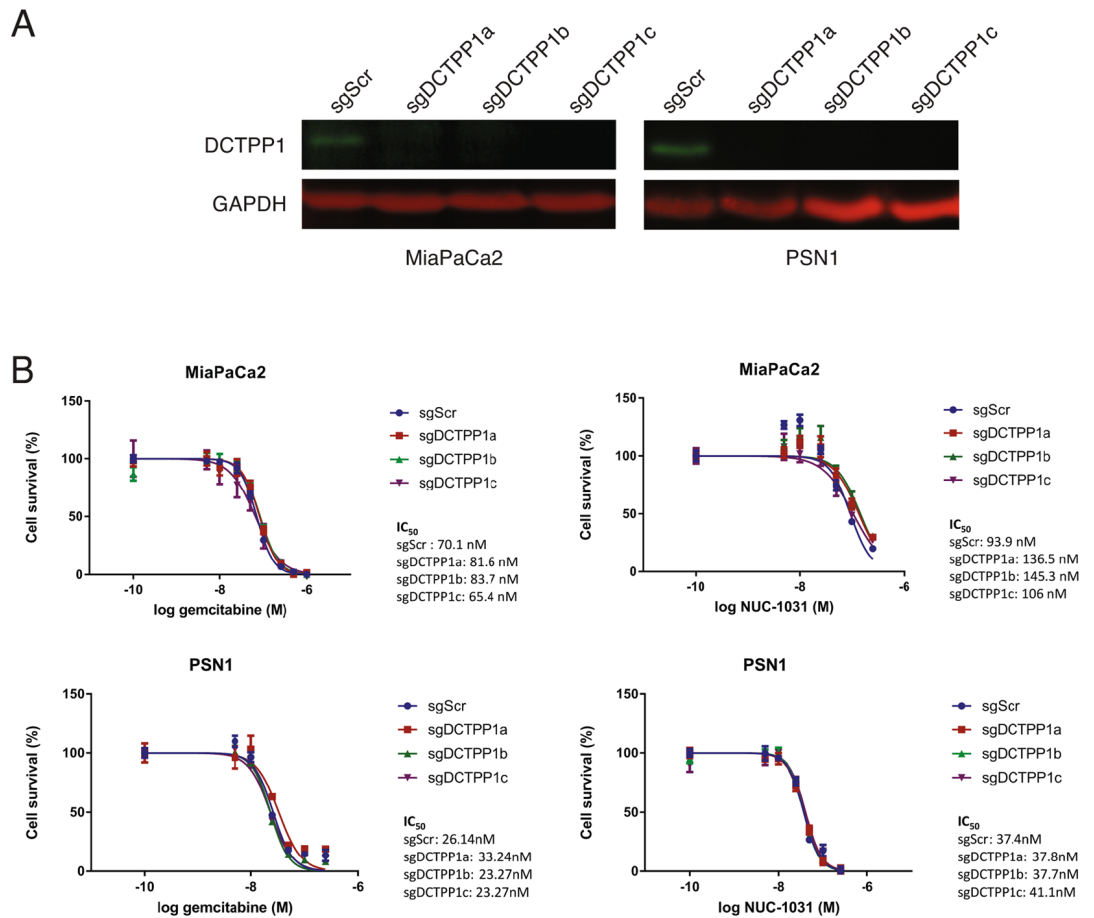


Figure 4. DCTPP1 mediates NUC-1031 sensitivity in pancreatic cancer cells. (A) DCTPP1 protein expression analyzed by Western blot in MiaPaCa2 and PSN1 cells transduced with independent sgRNAs targeting DCTPP1 (sgDCTPP1) or a non-targeting scrambled control sgRNA (sgScr). (B) Dose-response curves for MiaPaCa2 and PSN1 cells transduced with individual sgRNAs targeting DCTPP1 or a non-targeting scrambled control sgRNA (sgScr) and treated NUC-1031 or gemcitabine ($n = 6$, \pm SEM). For NUC-1031: MiaPaCa2 sgScr vs MiaPaCa2 sgDCTPP1a: $p = 0.0022$; MiaPaCa2 sgScr vs MiaPaCa2 sgDCTPP1b: $p = 0.0087$; MiaPaCa2 sgScr vs MiaPaCa2 sgDCTPP1c: $p = 0.0152$; for gemcitabine: MiaPaCa2 sgScr vs MiaPaCa2 sgDCTPP1a: $p = 0.0649$; MiaPaCa2 sgScr vs MiaPaCa2 sgDCTPP1b: $p = 0.3939$; MiaPaCa2 sgScr vs MiaPaCa2 sgDCTPP1c: $p = 0.8182$ and PSN1 sgScr vs PSN1 sgDCTPP1a: $p = 0.1797$; PSN1 sgScr vs PSN1 sgDCTPP1b: $p = 0.8182$; PSN1 sgScr vs PSN1 sgDCTPP1c: $p = 0.3939$; Mann-Whitney test).

30.19), had a significantly shorter survival (FDR corrected p -value = 8.63×10^{-6}) than those with medium DCK expression (histoscores 30.77 to 57.64) or high DCK expression (histoscores 58.33 to 96.88) (Fig. 6B).

From the NUC-1031 treated Phase I cohort, 39 biopsies from 37 patients with clinical follow-up were analyzed¹. All patients had rapidly progressing disease on study entry and had exhausted all other treatment options. Of these, two patients achieved a partial response (unconfirmed) to NUC-1031 according to RECIST 1.1 criteria, thirteen patients achieved stable disease for six months or more and twenty-two patients achieved stable disease for less than six months, or progressive disease developed within that time. Patients with progressive or stable disease for less than 6 months showed no significant difference in DCK or DCTPP1 expression by histoscore, compared to those who had stable disease for more than 6 months or had a partial response (Fig. 7A, Fig. S5). Interestingly, a lung cancer from a partial responder, who had not been previously treated with gemcitabine and survived for 10 months while receiving NUC-1031, displayed high DCK expression. A pancreatic cancer from a second patient who had relapsed on prior gemcitabine treatment but achieved a 30% reduction in tumour volume (partial response) within 3 cycles of NUC-1031 treatment, displayed low DCK expression (Fig. 7B). These data suggest that in tumours from NUC-1031 treated patients, DCK expression does not strongly correlate with disease progression.

Discussion

Despite its widespread use as a mainstay of chemotherapy in patients with pancreatic, ovarian, lung, breast and biliary tract cancers, amongst others, the fluoropyrimidine gemcitabine achieves responses in less than 10% of patients with metastatic pancreatic cancer and has a very limited impact on overall survival due to intrinsic and acquired resistance. NUC-1031, a phosphoramidate transformation of gemcitabine, was the first anti-cancer

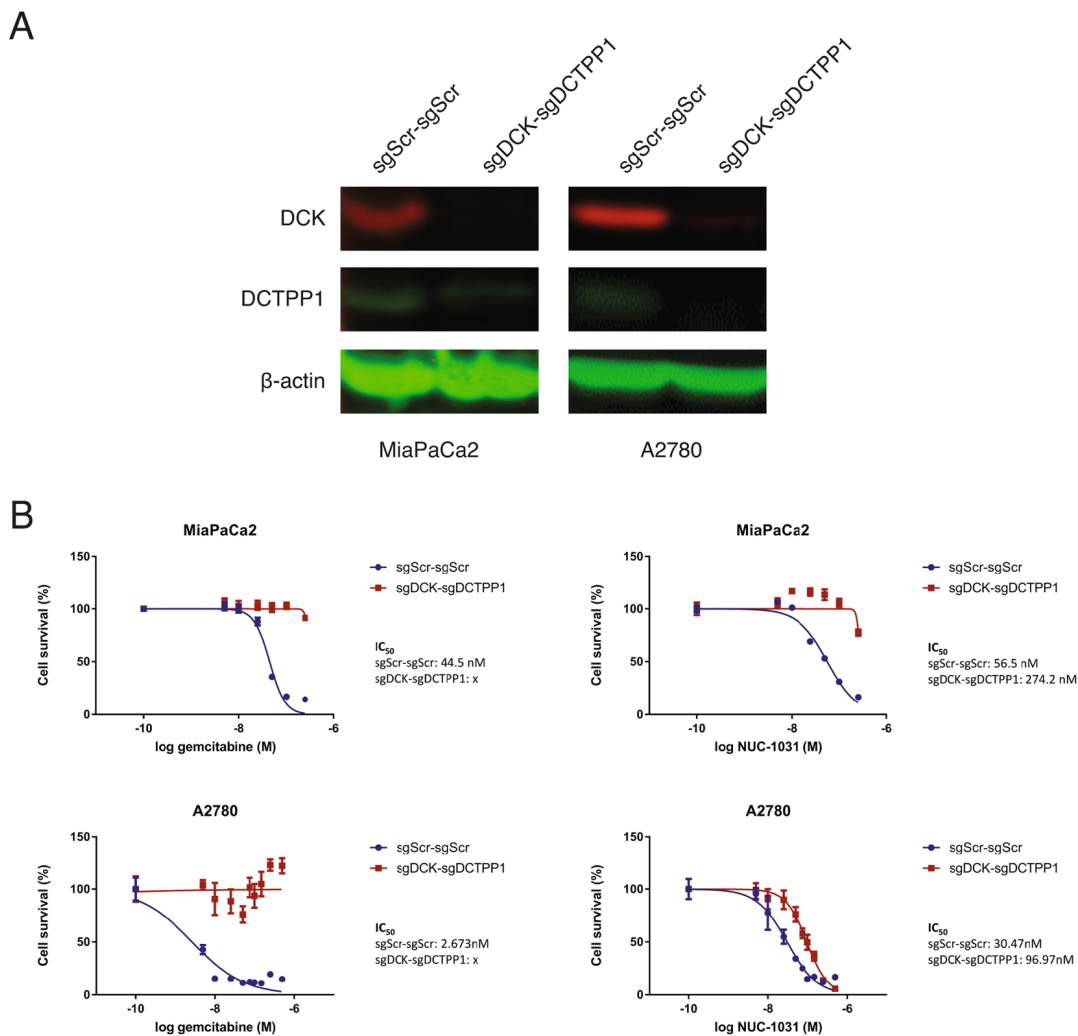


Figure 5. DCK and DCTPP1 simultaneous knockdown induced no synergistic effect in pancreatic and ovarian cancer cells to NUC-1031. **(A)** DCK and DCTPP1 protein expression analyzed by Western blot in MiaPaCa2 and A2780 cells transfected with a pX333 plasmid containing sgRNA sequences targeting DCK (sgDCK) and DCTPP1 (sgDCTPP1) or a non-targeting scrambled control sgRNA (sgScr). **(B)** Dose response curves for MiaPaCa2 and A2780 sgDCK-sgDCTPP1 cells and sgScr-sgScr cells (control), 4d after treatment with NUC-1031 or gemcitabine ($n = 6$, \pm SEM). MiaPaCa2 sgScr-sgScr vs MiaPaCa2 sgDCK-sgDCTPP1a: $p = 0.0022$, A2780 sgScr vs A2780 sgDCK-sgDCTPP1: $p = 0.0022$; Mann-Whitney test).

ProTide to enter the clinic. We find that: (1) NUC-1031 and gemcitabine display important *in vitro* cytotoxicity differences; (2) the only pathway consistently selected with NUC-1031 in our CRISPR/Cas9 screen was pyrimidine metabolism, while there were no hits consistently selected with gemcitabine under our selection conditions; (3) low DCK expression in tumour biopsies from patients treated with gemcitabine correlates with a poor prognosis, but there is no such correlation in tumour biopsies from a Phase I cohort treated with NUC-1031.

Although similar in structure to gemcitabine²⁴, these data demonstrate that ProTide chemistry does alter cytotoxicity and the effects of NUC-1031 are prolonged over time. These properties allowed for on-target, long-term *in vitro* selection with NUC-1031 in our genetic screening approach that consistently selected pyrimidine metabolism through the identification of DCK and DCTPP1, both of which regulate the dCMP/dCTP pool. The screening process was sufficiently sensitive to uncover DCTPP1 displaying a 1.5-fold change in sensitivity to NUC-1031. No major resistance factors to NUC-1031 were identified in this screen, since no other genes, except DCK, validated with more than a 2-fold change and the effects of DCK loss on NUC-1031 resistance were very modest compared to those of gemcitabine, with a minimal loss of NUC-1031 sensitivity in cancer cell lines.

Contrary to NUC-1031, no consistent candidates were selected from the gemcitabine screen. This may be explained by the pleiotropic effects of gemcitabine and the long exposure time to gemcitabine in our study, which generates off-target toxicity especially through the production of dFdU metabolites. There are multiple resistance-associated genes for gemcitabine, including DCK, hENT1, CDA, RRM1, and RRM2 that all converge on a common mechanism^{17,34}. Previously reported gemcitabine genetic screens used shorter exposure times, when compared to our study and none of these screens selected these known resistance factors^{35–37}. Since DCK, hENT1, CDA, RRM1 and RRM2 were not selected in our gemcitabine screen, although they were present in the

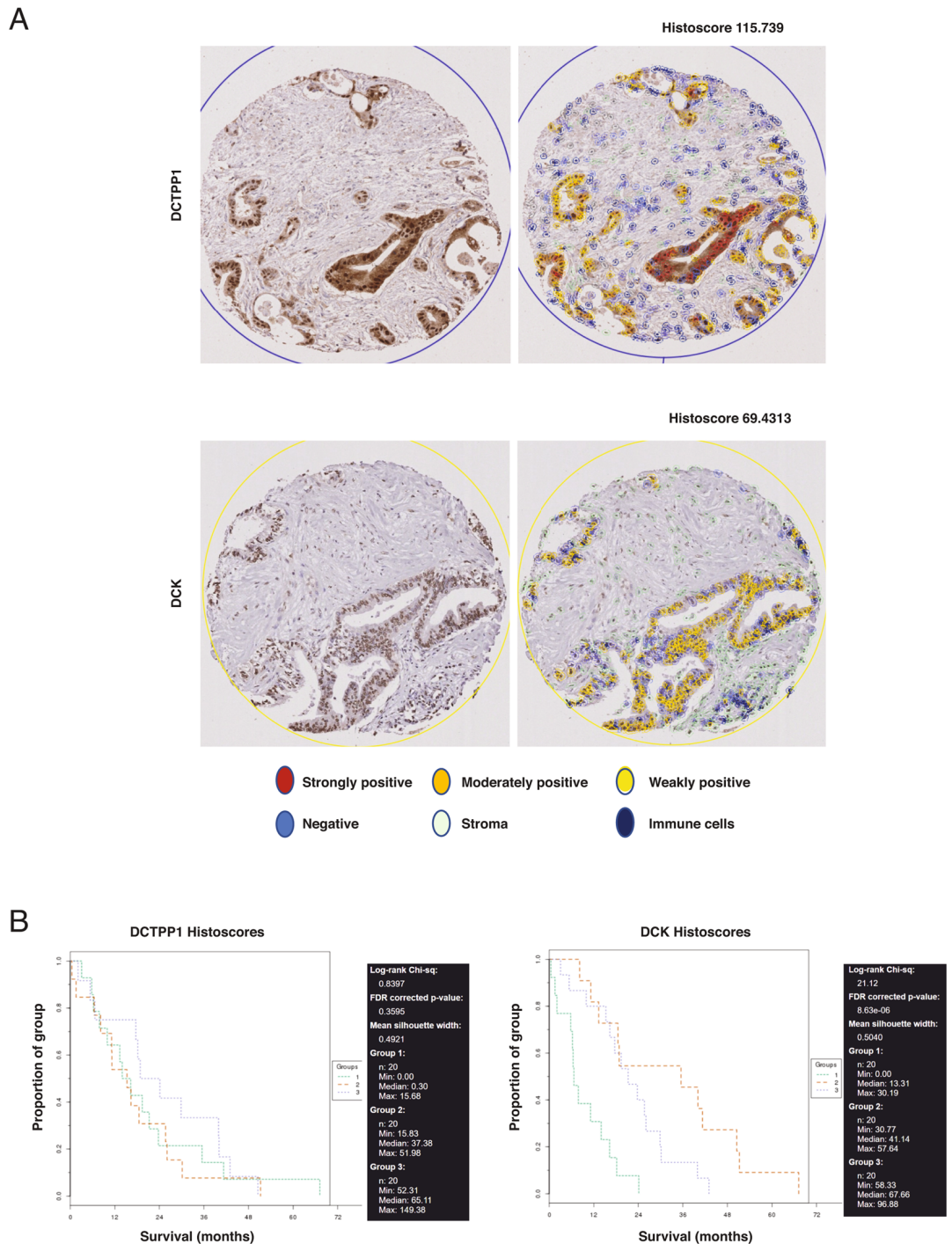
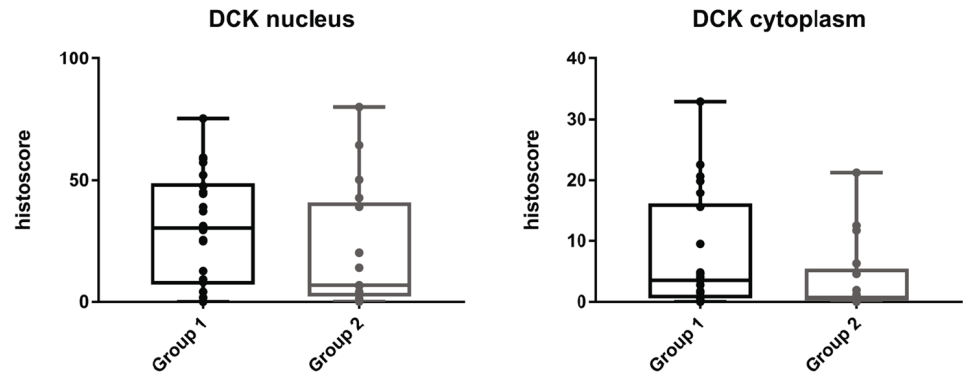


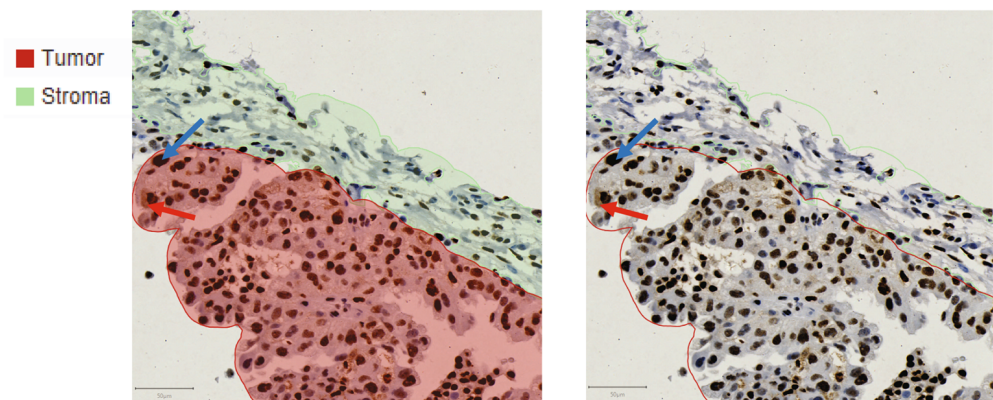
Figure 6. DCK expression is associated with outcome in gemcitabine-treated patients. **(A)** DCTPP1 expression in one tissue core before (left panel) and after (right panel) QuPath analysis based on staining intensity in tumour cells. A histoscore of 115.739 was calculated based on the proportion of positive cells and their staining intensity. DCK expression in a second tissue core before (left panel) and after (right panel) QuPath analysis based on staining intensity in tumour cells. A histoscore of 69.4313 was calculated based on the proportion of positive cells and their staining intensity. **(B)** KM survival curves for DCTPP1 and DCK expression generated using TMA Navigator. All of the tissue cores were divided in three groups according to their histoscore. Each group was composed of 20 samples presenting histoscores in the indicated ranges. Survival of patients is presented in months.

library representation (rank position DCK >1951, hENT1 >1999, CDA >1241, RRM1 >1541, RRM2 >593, respectively), we hypothesize that there may have been adaptation responses to the gemcitabine selection pressure on the CRISPR/Cas9 library. Therefore, caution should be used when performing CRISPR/Cas9 screens, since

A



B



C

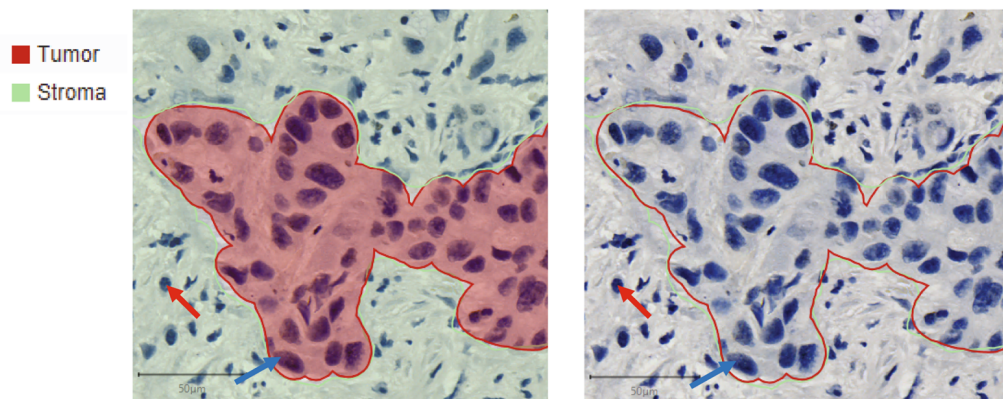


Figure 7. DCK expression in archival tissue does not correlate with outcome in patients treated with NUC-1031. **(A)** Nucleus and cytoplasm DCK histoscores in tissue from patients who achieved stable disease for less than six months, or progressive disease developed within that time (group 1, $n = 22$), or who achieved stable disease for six months or more (group 2, $n = 17$). Tissues were immunostained for DCK and scanned images were quantified using QuPath and histoscores compared between groups (DCK nucleus p -value = 0.2102; DCK cytoplasm p -value = 0.1461; Mann-Whitney test). **(B)** Lung cancer from a partial responder, who had not been previously treated with gemcitabine and survived for 10 months while receiving NUC-1031, displayed high DCK expression. QuPath segmentation of tumour (red) and stroma (green) (left panel) or unsegmented image (right panel). Blue arrow, DCK nuclear expression. Red arrow, DCK cytoplasmic expression. **(C)** Pancreatic cancer from a patient who had relapsed on prior gemcitabine treatment but achieved a 30% reduction in tumour volume (partial response) within 3 cycles of NUC-1031 treatment, displayed low DCK expression. QuPath segmentation of tumour (red) and stroma (green) (left panel) or unsegmented image (right panel). Blue arrow, DCK negative cancer cell. Red arrow, DCK negative immune cell.

this methodology may not uncover very strongly selected genes and may be dependent on factors such as *in vitro* drug metabolism effects.

We have used QuPath³² quantitative image analysis of DCK and DCTPP1 expression in tumour tissue biopsies from a Phase I patient cohort treated with NUC-1031 (ref. ¹), involving the fast and interactive training of object classifiers using machine learning techniques. The analysis of 39 biopsies, from a range of different tumours, did not show a correlation between DCK and DCTPP1 expression and efficacy of NUC-1031. Although the number of patients is small, the data suggest that NUC-1031 achieved clinical activity even in patients with low DCK expressing tumours. Further clinical studies are warranted to assess the long-term efficacy of NUC-1031 treatment in patients and monitoring dCMP/dCTP levels in NUC-1031 treated tumours may be of benefit. In conclusion, these experiments support the notion that NUC-1031 overcomes the cancer cell resistance mechanisms that limit the clinical utility of gemcitabine. Importantly, patients who had previously relapsed on gemcitabine treatment show clinical responses to NUC-1031, further confirming the potential for NUC-1031 to represent a more effective treatment option for these patients.

Materials and Methods

Cell culture and reagents. MiaPaCa2 and HEK293T cell lines were cultured in Dulbecco's modified Eagle medium (DMEM) supplemented with 10% (v/v) Fetal bovine serum and 1% (v/v) Penicillin/Streptomycin. A2780 and PSN1 cell lines were cultured in RPMI 1640 supplemented with 10% (v/v) Fetal bovine serum and 1% (v/v) Penicillin/Streptomycin. Cells were routinely tested negative for Mycoplasma using the Minerva Biolabs 'Venor GeM One Step' PCR kit.

Human GeCKOv2 CRISPR knockout pooled library was a gift from Feng Zhang (Addgene #1000000048). Pooled lentiCRISPRv2 expression vectors containing GeCKOv2 library were provided as two half-libraries A and B, at a concentration of 50 ng/ μ l. plentiCRISPRv2 was a gift from Feng Zhang (Addgene #52961) and pX333 was a gift from Andrea Ventura (Addgene #64073). Gemcitabine (Sigma-Aldrich, UK) and NUC-1031 (provided by NuCana plc), were dissolved in dimethyl sulfoxide (DMSO; Sigma-Aldrich, UK) at a stock concentration of 10 mM. 2'-deoxycytidine (Sigma-Aldrich, UK) was dissolved in DMSO at a stock concentration of 100 mM. Nucleofection (Amaxa) was performed on MiaPaCa2 and A2780 cells using standard methods to introduce pX333.

Cytotoxicity assays. MiaPaCa2 and PSN1 cells were seeded in 96-well plates at a density of 500 cells per well. After 48 h, cells were incubated with culture media containing either 0.1% (v/v) DMSO or increasing concentrations of drug (gemcitabine or NUC-1031) from 5 nM to 250 nM in six experimental replicates. Cells treated with gemcitabine were washed out after 24 h and incubated with fresh media. A2780 cells were seeded in 96-well plates at a density of 750 cells per well. After 48 h, cells were incubated with culture media containing either 0.1% (v/v) DMSO or increasing concentrations of drug (gemcitabine or NUC-1031) from 5 nM to 500 nM in six experimental replicates. Cells were washed out after 2 h and incubated with fresh media. The number of drug-treated cells at d4 post-treatment was assessed by Celigo cytometer (Nexcelom Bioscience) for MiaPaCa2 and PSN1 cells or Sulforodamine B (SRB) assay for A2780 cells and normalized to the count of DMSO-treated cells (control). Cell numbers obtained from Celigo or SRB analysis, were used to generate dose response curves and to calculate the concentration to get 50% of drug effect (IC_{50}) for gemcitabine and NUC-1031, using Graphpad Prism software.

Flow cytometry. 5×10^5 A2780 cells were plated in 6 cm dishes and left to grow for 48 h. Cells were treated with IC_{50} of either NUC-1031 or gemcitabine or culture media containing 0.1% (v/v) DMSO for 2 h. After incubation with BrdU (10 μ M) for 30 mins prior to being collected, cells were trypsinized and centrifuged at 1200 rpm for 5 min, washed with PBS and centrifuged again before being re-suspended in 1 mL of ice-cold 70% ethanol and stored at 4 °C until staining for analysis on the flow cytometer. Cells were digested with pepsin (0.4 mg/mL in 100 mM HCl - Sigma P6887) for 45 min at 37 °C after which DNA was denatured with 2N HCL/0.5% Triton X-100 for 30 min at RT and then neutralized with 0.1M sodium tetraborate pH8.5. DNA staining was performed using an anti-BrdU antibody (Beckton Dickinson, clone B44) at a 1:100 dilution in PBS/0.5% BSA/0.5% Tween20 and anti-mouse FITC (Alexa Fluor 488, Invitrogen A1101). Samples were incubated with RNase A (Qiagen 103130) and propidium iodide. They were run on a BD FACSJazzTM and data analysis was performed using FlowJo software v10.

Lentivirus production. Both half-libraries (A and B) were used and viral particles produced independently from A and B before being combined and used to infect recipient cells. 4×10^6 HEK293T cells were plated for each 10 cm dish and co-transfected the next day with 4 μ g library A or B plasmids (lentiCRISPRv2), 2 μ g pVSVg and 3 μ g psPAX2 lentiviral packaging plasmids, using 27 μ l of Trans-iT LT1 reagent (Mirus). Viral supernatant was collected 48 h and 72 h after transfection. Viral collections at 48 h and 72 h were pooled together, passed through a 0.45 μ m filter in the presence of 8 μ g/ml polybrene (Sigma-Aldrich) and then used to infect recipient cells. A total of 2×10^8 MiaPaCa2 cells were infected with lentiviral particles containing GeCKOv2 library at a MOI of 0.3 (aiming for ~300X coverage per sgRNA). Transduced cells were then selected for 7d with 2 μ g/ml puromycin (Sigma-Aldrich).

GeCKOv2 screen for gemcitabine and NUC-1031 resistance/sensitivity. 6×10^7 transduced cells were collected as a baseline for sgRNA distribution at the start of the screen. Remaining MiaPaCa2 cells were divided into three conditions with a minimum of 2.6×10^7 cells for each. They were either treated with DMSO as a control, 15 nM gemcitabine or 65 nM NUC-1031. Cells were maintained for four weeks and cell pellets consisting of 6×10^7 cells were collected 14d and 21d after the start of the treatment. Genomic DNA was extracted from these cells using Blood and cell Midi kit (Qiagen) and sgRNA sequences isolated by PCR. A second PCR reaction was carried out on the resulting amplicons to add adapter sequences for the sequencing system and barcodes

to discriminate each sample after multiplex NGS^{27,28} (Table S2). Quantification and purity of the resulting PCR products were evaluated using QubiT fluorometer, qPCR using KAPA Library Quantification Kit for Illumina platforms and Agilent 2100 Bioanalyzer system. Barcoded sgRNAs were then sequenced using the Illumina HiSeq 2500 system by Edinburgh Genomics, The University of Edinburgh.

Sequencing data analysis. Raw sequencing reads from NGS were demultiplexed then, 5' Illumina adapter sequences were trimmed using Cutadapt 1.3. Trimmed reads were then aligned to the reference GeCKOv2 library using Bowtie 0.12.9. The number of reads uniquely mapped to each reference sgRNA sequence was calculated and read count per sgRNA was normalized as follows: (read count per reference sequence/total of uniquely aligned reads for all sgRNAs in sample) $\times 10^6$. Graphic representations of sgRNA counts were generated using R Studio software. Read counts from each sample were then analyzed using the MAGeCK algorithm²⁹ to rank and prioritize sgRNAs and genes affecting MiaPaCa2 cells sensitivity or resistance to gemcitabine and NUC-1031.

Western Blotting analysis. 1×10^6 cells were plated onto 10 cm petri dishes and left to grow for 48 h. Cells were washed with ice-cold PBS and lysed in a lysis buffer composed of: 10 mM Tris pH 8.0, 150 mM NaCl, 1% sodium deoxycholate, 1% Nonidet P-40 (NP40), 1% Sodium dodecyl sulfate (SDS), 1 mM EDTA and supplemented with 1X protease inhibitor (AMV Roche), phosphatase inhibitor cocktail 2 and 3 (Sigma-Aldrich), 2 mM phenylmethylsulfonyl fluoride (PMSF) (SigmaAldrich). 200 μ L of supplemented lysis buffer were added to each plate, then protein extracts were collected and quantified by Bicinchoninic Acid (BCA) assay using Pierce BCA protein assay kit (Thermo Scientific, UK). 30 μ g of lysates were resolved by SDS Polyacrylamide Gel Electrophoresis, then transferred on a PVDF membrane. Immunoblotting was carried out at 4 °C overnight using the following antibodies: XTP3TPA/DCTPP1 (B-6) (Santa Cruz #sc-398501), DCK (Genetex #GTX102800), GAPDH (Sigma-Aldrich #G8795), β actin (Cell Signaling Technology #8H10D10). GAPDH and β actin were used as loading controls.

Immunohistochemistry and machine learning analysis. Tissue microarray (TMA) samples were obtained from a cohort of patients with pancreatic cancer (Table S3). Ethical approval was granted by Scotland A REC (10/S1402/33) for the generic use of pathology archive tissue for research. Whole section slides from a pan-cancer Phase I cohort were also obtained (Table S4) where all biopsies were taken prior to NUC-1031 treatment¹. Corresponding clinical data was also obtained from clinical records including tumour diagnosis, sex, and details on previous chemotherapy, and response if any to NUC-1031. Since ORR was not a primary focus, routine scans were conducted every 8 weeks. Patients did not receive confirmatory scans, i.e., 4 weeks after initial documentation of response, as per RECIST 1.1. All data was rendered patient non-identifiable prior to receipt. All methods were carried out in accordance with relevant guidelines and regulations and informed consent was obtained from all subjects. All experimental protocols were approved by University of St Andrews Teaching and Research Ethics Committee.

Slides were immersed three times in Xylene for 5 min and rehydrated in graded concentrations of alcohol (100, 100, 80 and 50%) for 2 min each and then rinsed in running water. Heat-induced antigen retrieval was performed in boiling Citrate buffer (10 mM, pH 6.0) at 99 °C in an automatic pressure cooker for 5 min. Endogenous peroxidase activity was blocked by incubation of the slides with 3% hydrogen peroxide, for 5 min followed by a 5 min wash in 0.1% PBS-T. Serum-free block solution (DAKO, Agilent, UK) was added on the TMA for 10 min. DCTPP1 and DCK primary antibodies (XTP3TPA/DCTPP1 (B-6) (Santa Cruz #sc-398501), DCK (Genetex #GTX102800)), were diluted in DAKO diluent to 1:500 and 1:1500 respectively. EnVision HRP-conjugated anti-Mouse or anti-Rabbit secondary antibody were added to the appropriate TMA. DAB chromogen (DAKO, Agilent, UK) was added to each slide for 10 min. Tissues were dehydrated, cleared in Xylene and then mounted with DPX mounting medium (Sigma-Aldrich, UK) and left to dry overnight. Slides were scanned and imaged using a Leica SCN400 brightfield microscope. The analysis of stained tissues images was carried out using QuPath software. Four categories of staining intensity were then created using three different thresholds to classify cells according to their staining intensity: cells with an optical density (OD) below 0.2 were considered negative, OD between 0.2 and 0.4 were weakly positive (1+), between 0.4 and 0.6 were moderately positive (2+) and above 0.6 were strongly positive (3+). QuPath was then trained to distinguish different tissue areas and cellular types within tissue cores (including non-neoplastic cells, tumour cells, immune cells, stroma, red blood cells, necrosis), by drawing around representative areas or cells and annotating them. The set parameters were then applied to analyze all tissue cores. Each tissue core was then controlled to ensure that only tumour cells were analysed, and all areas analysed outside tumour cells were removed. QuPath calculated histoscores of each case, based on the staining intensity within tumour cells and their proportion.

Statistical analysis. Statistical analysis of sgRNA count were performed using R studio software and MAGeCK program. All other statistical analyses were conducted using Graphpad Prism software. Mann Whitney U test was used when at least four replicates were available. P value < 0.05 was considered statistically significant.

References

1. Blagden, S. P. *et al.* Anti-tumour activity of a first-in-class agent NUC-1031 in patients with advanced cancer: results of a phase I study. *British journal of cancer* **119**, 815–822 (2018).
2. Mini, E., Nobili, S., Caciagli, B., Landini, I. & Mazzei, T. Cellular pharmacology of gemcitabine. *Annals of oncology* **17**(Suppl 5), v7–12 (2006).
3. Burris, H. A. *et al.* Improvements in survival and clinical benefit with gemcitabine as first-line therapy for patients with advanced pancreas cancer: a randomized trial. *Journal of Clinical Oncology* **15**, 2403–2413 (1997).
4. Kose, M. F. *et al.* A phase II study of gemcitabine plus carboplatin in platinum-sensitive, recurrent ovarian carcinoma. *Gynecologic Oncology* **96**, 374–380 (2005).

5. Eisenhauer, E. L. *et al.* A phase II study of gemcitabine, carboplatin and bevacizumab for the treatment of platinum-sensitive recurrent ovarian cancer. *Gynecologic Oncology* **134**, 262–266 (2014).
6. Huang, P., Chubb, S., Hertel, L. W., Grindey, G. B. & Plunkett, W. Action of 2',2'-Difluorodeoxycytidine on DNA Synthesis. *Cancer Research* **51**, 6110–6117 (1991).
7. Cappella, P. *et al.* Cell cycle effects of gemcitabine. *International Journal of Cancer* **93**, 401–408 (2001).
8. de Sousa Cavalcante, L. & Monteiro, G. Gemcitabine: Metabolism and molecular mechanisms of action, sensitivity and chemoresistance in pancreatic cancer. *European Journal of Pharmacology* **741**, 8–16 (2014).
9. Spratlin, J. *et al.* The absence of human equilibrative nucleoside transporter 1 is associated with reduced survival in patients with gemcitabine-treated pancreas adenocarcinoma. *Clin Cancer Res* **10**, 6956–6961 (2004).
10. Lorusso, D., Di Stefano, A., Fanfani, F. & Scambia, G. Role of gemcitabine in ovarian cancer treatment. *Annals of Oncology* **17**, v188–v194 (2006).
11. Jordheim, L. P., Durantel, D., Zoulim, F. & Dumontet, C. Advances in the development of nucleoside and nucleotide analogues for cancer and viral diseases. *Nature Reviews Drug Discovery* **12**, 447 (2013).
12. Galmarini, C. M., Mackey, J. R. & Dumontet, C. Nucleoside analogues: mechanisms of drug resistance and reversal strategies. *Leukemia* **15**, 875–890 (2001).
13. Davidson, J. D. *et al.* An Increase in the Expression of Ribonucleotide Reductase Large Subunit 1 Is Associated with Gemcitabine Resistance in Non-Small Cell Lung Cancer Cell Lines. *Cancer Research* **64**, 3761–3766 (2004).
14. Heinemann, V. *et al.* Cellular Elimination of 2',2'-Difluorodeoxycytidine 5'-Triphosphate: A Mechanism of Self-Potential. *Cancer Research* **52**, 533–539 (1992).
15. Conroy, T. *et al.* FOLFIRINOX versus Gemcitabine for Metastatic Pancreatic Cancer. *New England Journal of Medicine* **364**, 1817–1825 (2011).
16. Kim, M. P. & Gallick, G. E. Gemcitabine resistance in pancreatic cancer: picking the key players. *Clin Cancer Res* **14**, 1284–1285 (2008).
17. Mackey, J. R. *et al.* Functional Nucleoside Transporters Are Required for Gemcitabine Influx and Manifestation of Toxicity in Cancer Cell Lines. *Cancer Research* **58**, 4349–4357 (1998).
18. Greenhalf, W. *et al.* Pancreatic cancer hENT1 expression and survival from gemcitabine in patients from the ESPAC-3 trial. *J Natl Cancer Inst* **106**, djt347 (2014).
19. Ruiz van Haperen, V. W. *et al.* Development and molecular characterization of a 2',2'-difluorodeoxycytidine-resistant variant of the human ovarian carcinoma cell line A2780. *Cancer Res* **54**, 4138–4143 (1994).
20. Sebastiani, V. *et al.* Immunohistochemical and genetic evaluation of deoxycytidine kinase in pancreatic cancer: relationship to molecular mechanisms of gemcitabine resistance and survival. *Clin Cancer Res* **12**, 2492–2497 (2006).
21. Bengala, C. *et al.* Prolonged fixed dose rate infusion of gemcitabine with autologous haemopoietic support in advanced pancreatic adenocarcinoma. *British journal of cancer* **93**, 35–40 (2005).
22. McGuigan, C., Shackleton, J. M., Tollerfield, S. M. & Riley, P. A. Synthesis and evaluation of some novel phosphate and phosphinate derivatives of araA. Studies on the mechanism of action of phosphate triesters. *Nucleic Acids Res* **17**, 10171–10177 (1989).
23. Saif, M. W., Lee, Y. & Kim, R. Harnessing gemcitabine metabolism: a step towards personalized medicine for pancreatic cancer. *Ther Adv Med Oncol* **4**, 341–346 (2012).
24. Slusarczyk, M. *et al.* Application of ProTide Technology to Gemcitabine: A Successful Approach to Overcome the Key Cancer Resistance Mechanisms Leads to a New Agent (NUC-1031) in Clinical Development. *Journal of Medicinal Chemistry* **57**, 1531–1542 (2014).
25. Mathews, C. K. Deoxyribonucleotide metabolism, mutagenesis and cancer. *Nat Rev Cancer* **15**, 528–539 (2015).
26. Berns, K. & Bernards, R. Understanding resistance to targeted cancer drugs through loss of function genetic screens. *Drug resistance updates* **15**, 268–275 (2012).
27. Sanjana, N. E., Shalem, O. & Zhang, F. Improved vectors and genome-wide libraries for CRISPR screening. *Nat Methods* **11**, 783–784 (2014).
28. Shalem, O. *et al.* Genome-scale CRISPR-Cas9 knockout screening in human cells. *Science* **343**, 84–87 (2014).
29. Li, W. *et al.* MAGeCK enables robust identification of essential genes from genome-scale CRISPR/Cas9 knockout screens. *Genome Biology* **15**, 554 (2014).
30. Saiki, Y. *et al.* DCK is frequently inactivated in acquired gemcitabine-resistant human cancer cells. *Biochemical and Biophysical Research Communications* **421**, 98–104 (2012).
31. Requena, C. E., Perez-Moreno, G., Ruiz-Perez, L. M., Vidal, A. E. & Gonzalez-Pacanowska, D. The NTP pyrophosphatase DCTPPI1 contributes to the homeostasis and cleansing of the dNTP pool in human cells. *Biochem J* **459**, 171–180 (2014).
32. Bankhead, P. *et al.* QuPath: Open source software for digital pathology image analysis. *Sci Rep* **7**, 16878 (2017).
33. Lubbock, A. L., Katz, E., Harrison, D. J. & Overton, I. M. TMA Navigator: Network inference, patient stratification and survival analysis with tissue microarray data. *Nucleic Acids Res* **41**, W562–568 (2013).
34. Nakano, Y. *et al.* Gemcitabine chemoresistance and molecular markers associated with gemcitabine transport and metabolism in human pancreatic cancer cells. *British journal of cancer* **96**, 457–463 (2007).
35. Fredebohm, J., Wolf, J., Hoheisel, J. D. & Boettcher, M. Depletion of RAD17 sensitizes pancreatic cancer cells to gemcitabine. *Journal of Cell Science* **126**, 3380–3389 (2013).
36. Azorsa, D. O. *et al.* Synthetic lethal RNAi screening identifies sensitizing targets for gemcitabine therapy in pancreatic cancer. *Journal of Translational Medicine* **7**, 43 (2009).
37. Smith, S. C. *et al.* A gemcitabine sensitivity screen identifies a role for NEK9 in the replication stress response. *Nucleic Acids Research* **42**, 11517–11527 (2014).

Acknowledgements

A.S. is the recipient of a Medical Research Scotland PhD Studentship awarded to P.A.R. Edinburgh Genomics is partly supported through core grants from Natural Environment Research Council (R8/H10/56), Medical Research Council (MR/K001744/1) and Biotechnological and Biological Research Council (BB/J004243/1). Publication of this article was funded in part by the University of St Andrews Open Access Publishing Fund.

Author Contributions

A.S., J.B., D.J.H., P.A.R., conception and design of research; A.S., J.B., I.U., T.C. and P.M. performed experiments; A.S. and J.B., analyzed data; A.S., J.B., I.U., D.J.H. and P.A.R. interpreted results of experiments; A.S., J.B. and I.U. prepared figures; P.A.R. drafted manuscript; A.S., J.B., P.M., D.J.H., P.A.R., edited and revised manuscript; all authors read and approved the final version of the manuscript.

Additional Information

Supplementary information accompanies this paper at <https://doi.org/10.1038/s41598-019-44089-3>.

Competing Interests: A.S. is the recipient of a Medical Research Scotland PhD Studentship awarded to P.A.R. that is part-funded by NuCana plc. J.B. is part-funded by NuCana plc. D.J.H. is employed part-time by NuCana plc. No competing interests were disclosed by the other authors. The funders had no role in study design, data collection and analysis, decision to publish, or preparation of the manuscript.

Publisher's note: Springer Nature remains neutral with regard to jurisdictional claims in published maps and institutional affiliations.



Open Access This article is licensed under a Creative Commons Attribution 4.0 International License, which permits use, sharing, adaptation, distribution and reproduction in any medium or format, as long as you give appropriate credit to the original author(s) and the source, provide a link to the Creative Commons license, and indicate if changes were made. The images or other third party material in this article are included in the article's Creative Commons license, unless indicated otherwise in a credit line to the material. If material is not included in the article's Creative Commons license and your intended use is not permitted by statutory regulation or exceeds the permitted use, you will need to obtain permission directly from the copyright holder. To view a copy of this license, visit <http://creativecommons.org/licenses/by/4.0/>.

© The Author(s) 2019

References

- Achiwa, H., Oguri, T., Sato, S., Maeda, H., Niimi, T. and Ueda, R. (2004), ‘Determinants of sensitivity and resistance to gemcitabine: The roles of human equilibrative nucleoside transporter 1 and deoxycytidine kinase in non-small cell lung cancer’, *Cancer Science* **95**(9), 753–757.
- Ahmed, A. A., Etemadmoghadam, D., Temple, J., Lynch, A. G., Riad, M., Cancer, O., Group, S., Sharma, R., Stewart, C., Fereday, S., Caldas, C., Defazio, A., Bowtell, D. and Brenton, J. D. (2010), ‘Driver mutations in TP53 are ubiquitous in high grade serous carcinoma of the ovary’, *Journal of Pathology J Pathol* **221**, 49–56.
- Alsop, K., Fereday, S., Meldrum, C., Defazio, A., Emmanuel, C., George, J., Dobrovic, A., Birrer, M. J., Webb, P. M., Stewart, C., Friedlander, M., Fox, S., Bowtell, D. and Mitchell, G. (2012), ‘BRCA Mutation Frequency and Patterns of Treatment Response in BRCA Mutation-Positive Women With Ovarian Cancer: A Report From the Australian Ovarian Cancer Study Group’, *J Clin Oncol* **30**, 2654–2663.
- Amos, W., Driscoll, E. and Hoffman, J. I. (2010), ‘Candidate genes versus genome-wide associations: which are better for detecting genetic susceptibility to infectious disease?’, *The Royal Society* **278**, 1183–1188.
- Amsailale, R., Beyaert, M., Smal, C., Janssens, V., Van Den Neste, E. and Bontemps, F. (2014), ‘Protein phosphatase 2A regulates deoxycytidine kinase activity via Ser-74 dephosphorylation Deoxycytidine kinase Nucleoside analog Ser-74 phosphorylation Protein phosphatase Ser/Thr protein phosphatase 2A’, *FEBS Letters* **588**, 727–732.
- Anderson, K. A., Wang, D., Hirschey, M. D. and Stedman, S. W. (2013), ‘HINT2 and Fatty Liver Disease: Mitochondrial Protein Hyperacetylation Gives a Hint? NIH Public Access’, *Hepatology* **57**(5), 1681–1683.
- Andrade, E. L., Bento, A. F., Cavalli, J., Oliveira, S. K., Freitas, C. S., Marcon, R., Schwanke, R. C., Siqueira, J. M. and Calixto, J. B. (2016), ‘Non-clinical studies required for new drug development-Part I: early in silico and in vitro studies, new target discovery and validation, proof of principles and robustness of animal studies’, *Brazilian Journal of Medical and Biological Research* **49**(11).
- Antoniou, A., Pharoah, P. D. P., Narod, S., Risch, H. A., Eyfjord, J. E., Hopper, J. L., Loman, N., Olsson, H., Johannsson, O., Borg, A., Pasini, B., Radice, P., Manoukian, S., Eccles, D. M., Tang, N., Olah, E., Anton-Culver, H., Warner, E., Lubinski, J., Gronwald, J., Gorski, B., Tulinius, H., Thorlacius, S., Eerola, H., Nevanlinna, H.,

- Syrjäkoski, K., Kallioniemi, O.-P., Thompson, D., Evans, C., Peto, J., Lalloo, F., Evans, D. G. and Easton, D. F. (2003), ‘Departments of 16 Obstetrics and Gynecology and 17 Oncology’, *American Journal of Human Genetics* **72**, 1117–1130.
- Aoyama, T., Miyagi, Y., Murakawa, M., Yamaoku, K., Atsumi, Y., Shiozawa, M., Ueno, M., Morimoto, M., Oshima, T., Yukawa, N., Yoshikawa, T., Rino, Y., Masuda, M. and Morinaga, S. (2017), ‘Clinical implications of ribonucleotide reductase subunit M1 in patients with pancreatic cancer who undergo curative resection followed by adjuvant chemotherapy with gemcitabine’, *Oncology Letters* **13**, 3423–3430.
- Attia, R. T., Tolba, M. F., Trivedi, R., Tadros, M. G., Arafa, H. M. M. and Abdel-Naim, A. B. (2016), ‘Distributed under Creative Commons CC-BY 4.0 The chemomodulatory effects of glufosfamide on docetaxel cytotoxicity in prostate cancer cells’, *Journal of Life and Environmental Sciences* .
- Azorsa, D. O., Gonzales, I. M., Basu, G. D., Choudhary, A., Arora, S., Bisanz, K. M., Kiefer, J. A., Henderson, M. C., Trent, J. M., Hoff, D. D. and Mousses, S. (2009), ‘Synthetic lethal RNAi screening identifies sensitizing targets for gemcitabine therapy in pancreatic cancer’, *Journal of Translational Medicine* **7**(43).
- Banáth, J. P. and Olive, P. L. (2003), ‘Expression of Phosphorylated Histone H2AX as a Surrogate of Cell Killing by Drugs That Create DNA Double-Strand Breaks’, *Cancer Research* **63**, 4347–4350.
- Bankhead, C. R., Collins, C., Stokes-Lampard, H., Rose, P., Wilson, S., Clements, A., Mant, D., Kehoe, S. T. and Austoker, J. (2008), ‘Identifying symptoms of ovarian cancer: a qualitative and quantitative study.’, *BJOG : an international journal of obstetrics and gynaecology* **115**(8), 1008–14.
- Bankhead, P., Fernández, J. A., Mcart, D. G., Boyle, D. P., Li, G., Loughrey, M. B., Irwin, G. W., Harkin, P., James, J. A., Mcquaid, S., Salto-Tellez, M. and Hamilton, P. W. (2018), ‘Integrated tumor identification and automated scoring minimizes pathologist involvement and provides new insights to key biomarkers in breast cancer’, *Nature Publishing Group* **98**.
- Bankhead, P., Loughrey, M. B., Fernández, J. A., Dombrowski, Y., Mcart, D. G., Dunne, P. D., Mcquaid, S., Gray, R. T., Murray, L. J., Coleman, H. G., James, J. A., Salto-Tellez, M. and Hamilton, P. W. (2017), ‘QuPath: Open source software for digital pathology image analysis’, *Scientific Reports* .
- Basel, M. T., Narayanan, S., Ganta, C., Shreshta, T. B., Marquez, A., Pyle, M., Hill, J., Bossmann, S. H. and Troyer, D. L. (2018), ‘Developing a xenograft human tumor model in immunocompetent mice’, *Cancer Letters* **412**, 256–263.
- Bast, R. C., Feeney, M., Lazarus, H., Nadler, L. M., Colvin, R. B. and Knapp, R. C. (1981), ‘Reactivity of a Monoclonal Antibody with Human Ovarian Carcinoma’, *Clinical Investigation* **68**, 1331–1337.

- Bast, R. C., Hennessy, B. and Mills, G. B. (2009), ‘The biology of ovarian cancer: new opportunities for translation.’, *Nature reviews. Cancer* **9**(6), 415–28.
- Beaufort, C. M., Helmijr, J. C. A., Piskorz, A. M., Hoogstraat, M., Ruigrok-Ritstier, K., Besselink, N., Murtaza, M., van IJcken, W. F. J., Heine, A. A. J., Smid, M., Koudijs, M. J., Brenton, J. D., Berns, E. M. J. J. and Helleman, J. (2014), ‘Ovarian Cancer Cell Line Panel (OCCP): Clinical Importance of In Vitro Morphological Subtypes’, *PLoS ONE* **9**(9), e103988.
- Bell, D. a. (2005), ‘Origins and molecular pathology of ovarian cancer.’, *Modern pathology : an official journal of the United States and Canadian Academy of Pathology, Inc* **18 Suppl 2**(August 2004), S19–S32.
- Berek, J. S., Kehoe, S. T., Kumar, L. and Friedlander, M. (2018), ‘Cancer of the ovary, fallopian tube, and peritoneum’, *International Journal of Gynecology and Obstetrics* **143**, 59–78.
- Bergman, A. M., Giaccone, G., Van Moorsel, J. A., Mauritz, R., Noordhuis, P., Pinedo, H. M. and Peters, G. J. (2000), ‘Cross-resistance in the 2 H ,2 H-di⁻uorodeoxycytidine (gemcitabine)-resistant human ovarian cancer cell line AG6000 to standard and investigational drugs’, *European Journal of Cancer* **36**, 1974±1983.
- Bergman, A. M., Ruiz Van Haperen, V. W., Veerman, G., Kuiper, C. M. and Peters, G. J. (1996), ‘Synergistic interaction between cisplatin and gemcitabine in vitro’, *Clinical Cancer Research* **2**(3), 521–530.
- Berns, K. and Bernards, R. (2012), ‘Understanding resistance to targeted cancer drugs through loss of function genetic screens’, *Drug Resistance Updates* **15**, 268–275.
- Berns, K., Hijmans, E. M., Mullenders, J., Brummelkamp, T. R., Velds, A., Heimerikx, M., Kerkhoven, R. M., Madiredjo, M., Nijkamp, W., Weigelt, B., Agami, R., Ge, W., Cavet, G., Linsley, P. S., Beijersbergen, R. L. and Bernards, R. (2004), ‘A large-scale RNAi screen in human cells identifies new components of the p53 pathway’, *Nature* **428**(6981), 431–437.
- Beumer, J. H., Eiseman, J. L., Parise, R. A., Joseph, E., Covey, J. M. and Egorin, M. J. (2008), ‘Modulation of Gemcitabine (2',2'-Difluoro-2'-Deoxycytidine) Pharmacokinetics, Metabolism, and Bioavailability in Mice by 3,4,5,6-Tetrahydrouridine’, *Cancer Therapy: Preclinical* **14**(11).
- Bevis, K. S., Erwin, J. L., Barnes, M. N. and Straughn, J. M. (2011), ‘The Efficacy and Toxicity of Bevacizumab in Combination With Gemcitabine in Patients With Recurrent Ovarian Cancer’, *Clinical Ovarian Cancer* **4**(1).
- Bieganski, P., Garrison, P. N., Hodawadekar, S. C., Faye, G., Barnes, L. D. and Brenner, C. (2002), ‘Adenosine monophosphoramidase activity of Hint and Hnt1

- supports function of Kin28, Ccl1, and Tfb3.’, *The Journal of biological chemistry* **277**(13), 10852–60.
- Bijnsdorp, I. V., Giovannetti, E. and Peters, G. J. (2011), Analysis of Drug Interactions, *in* ‘Cancer Cell Culture: Methods and Protocols’, Humana Press, pp. 421–434.
- Birkus, G., Kutty, N., Frey, C. R., Shribata, R., Chou, T., Wagner, C., McDermott, M. and Cihlar, T. (2011), ‘Role of cathepsin A and lysosomes in the intracellular activation of novel antipapillomavirus agent GS-9191.’, *Antimicrobial agents and chemotherapy* **55**(5), 2166–73.
- Birkus, G., Wang, R., Liu, X., Kutty, N., MacArthur, H., Cihlar, T., Gibbs, C., Swaminathan, S., Lee, W. and McDermott, M. (2007), ‘Cathepsin A is the major hydrolyase catalyzing the intracellular hydrolysis of the antiretroviral nucleotide phosphonoamidate prodrugs GS-7340 and GS-9131.’, *Antimicrobial agents and chemotherapy* **51**(2), 543–50.
- Blagden, S. P., O’Shea, D., Rizzuto, I., Stavrika, C., Patel, M., Loyse, N., Sukumaran, A., Bharwani, N., Rockall, A., El-Bahrawy, M., Gabra, H., Wasan, H., Leonard, R., Habib, N., McGuigan, C., Gribben, J. and Ghazaly, E. (2015), First in human Phase I/II study of NUC-1031 in patients with advanced gynecological cancers, *in* ‘ASCO Meeting Abstracts’.
- Blagden, S. P., Rizzuto, I., Suppiah, P., O’Shea, D., Patel, M., Spiers, L., Sukumaran, A., Bharwani, N., Rockall, A., Gabra, H., El-Bahrawy, M., Wasan, H., Leonard, R., Habib, N. and Ghazaly, E. (2018), ‘Anti-tumour activity of a first-in-class agent NUC-1031 in patients with advanced cancer: results of a phase I study.’, *British journal of cancer* .
- Blagden, S. P., Sukumaran, A., Spiers, L., Woodcock, K., Lipplaa, A., Nicum, S., Gnanaranjan, C., Harrison, D. J. and Ghazaly, E. (2017), PRO-002: A phase Ib dose-escalation study of NUC-1031 with carboplatin for recurrent ovarian cancer, *in* ‘AACR’.
- Bobbs, A. S., Cole, J. M. and Cowden Dahl, K. D. (2015), ‘Emerging and Evolving Ovarian Cancer Animal Models Supplementary Issue: Animal Models of Cancer Biology’, *CanCER Growth and Metastasis* **8**(s1), 29–36.
- Bonadona, V., Bonai“ti, B. B., Olschwang, S., Grandjouan, S., Huiart, L., Longy, M., Guimbaud, R., Buecher, B., Bignon, Y.-J., Caron, O., Colas, C., Noguès, C., Lejeune-Dumoulin, S., Olivier-Faivre, L., Polycarpe-Osaer, F., Nguyen, T. D., Desseigne, F., Saurin, J.-C., Berthet, P., Leroux, D., Duffour, J., Manouvrier, S., Frébourg, T., Sobol, H., Lasset, C. and Bonai“tibonai“ti-Pellié, C. (2011), ‘Cancer Risks Associated With Germline Mutations in MLH1, MSH2, and MSH6 Genes in Lynch Syndrome’, *JAMA* **305**(22).

- Boone, J. D., Dobbin, Z. C., Michael Straughn Jr, J. and Buchsbaum, D. J. (2015), 'Ovarian and cervical cancer patient derived xenografts: The past, present, and future', *Gynecologic Oncology* **138**, 486–491.
- Booth, M., Beral, V. and Smith, P. (1989), 'Risk factors for ovarian cancer: a case-control study', *British journal of cancer* **60**(4), 592–598.
- Boswell-Casteel, R. C. and Hays, F. A. (2017), 'Equilibrative Nucleoside Transporters-A Review', *Nucleosides Nucleotides Nucleic Acids* **36**(1), 7–30.
- Boven, E., Schipper, H., Erkelens, C. a., Hatty, S. a. and Pinedo, H. M. (1993), 'The influence of the schedule and the dose of gemcitabine on the anti-tumour efficacy in experimental human cancer.', *British journal of cancer* **68**(1), 52–6.
- Brabander, M. D., De Brabander, M., Geuens, G., Nuydens, R., Willebrords, R. and De Mey, J. (1981), 'Taxol induces the assembly of free microtubules in living cells and blocks the organizing capacity of the centrosomes and kinetochores.', *Proceedings of the National Academy of Sciences* **78**(9), 5608–5612.
- Bray, F., Ferlay, J. and Soerjomataram, I. (2018), 'Global Cancer Statistics 2018 : GLOBOCAN Estimates of Incidence and Mortality Worldwide for 36 Cancers in 185 Countries', *CA Cancer J Clin* **68**, 394–424.
- Budman, D. R. and Calabro, A. (2002), 'In vitro search for synergy and antagonism: evaluation of docetaxel combinations in breast cancer cell lines', *Breast Cancer Research and Treatment* **74**, 41–46.
- Bulusu, K. C., Guha, R., Mason, D. J., Lewis, R. P. I., Muratov, E., Motamedi, Y. K., Cokol, M. and Bender, A. (2016), 'Modelling of compound combination effects and applications to efficacy and toxicity: state-of-the-art, challenges and perspectives', *Drug Discovery Today* **21**(2).
- Burke, H. B. (2016), 'Predicting Clinical Outcomes Using Molecular Biomarkers', *Biomarkers in CanCer* **8**(8), 89–99.
- Cai, L., Tang, X., Guo, L., An, Y., Wang, Y. and Zheng, J. (2009), 'Decreased serum levels of carboxylesterase-2 in patients with ovarian cancer.', *Tumori* **95**(4), 473–8.
- Caltová, K. and Červinka, M. (2012), 'Antiproliferative effects of selected chemotherapeutics in human ovarian cancer cell line A2780', *Acta Medica* **55**, 116–124.
- Cannistra, S. A. (2004), 'Cancer of the Ovary', *N Engl J Med* **351**24351, 2519–29.
- Cappella, P., Tomasoni, D., Faretta, M., Lupi, M., Montalenti, F., Viale, F., Banzato, F., D'Incalci, M. and Ubezio, P. (2001), 'Cell cycle effects of gemcitabine', *Int J Cancer* **93**(May), 401–408.

- Carpinelli, G., Bucci, B., D'Agnano, I., Canese, R., Caroli, F., Raus, L., Brunetti, E., Giannarelli, D., Podo, F. and Carapella, C. M. (2006), 'Gemcitabine treatment of experimental C6 glioma: The effects on cell cycle and apoptotic rate', *Anticancer Research* **26**(4 B), 3017–3024.
- Casagrande, J. T., Pike, M. C., Ross, R. K., Louie, E. W., Roy, S. and Henderson, B. E. (1979), "Incessant Ovulation" and Ovarian Cancer', *The Lancet* **314**(8135), 170–173.
- Chabner, B. A. and Roberts, T. G. J. (2005), 'Chemotherapy and the war on cancer', *Nature Reviews Cancer* **5**.
- Chen, Lu Tzu-Pin, Chen Yu-Chuan and Lin Wei-Jiun (2015), 'Predictive biomarkers for treatment selection: statistical considerations', *Biomarkers in Medicine* **9**(11), 1121–1135.
- Chen, V. W., Ruiz, B., Killeen, J. L., Coté, T. R., Wu, X. C. and Correa, C. N. (2003), 'Pathology and classification of ovarian tumors.', *Cancer* **97**(10 Suppl), 2631–2642.
- Chen, X., Jorgenson, E. and Cheung, S. T. (2009), 'New tools for functional genomic analysis', *Drug Discovery Today* **14**, 754–760.
- Chen, Z., Zhou, J., Zhang, Y. and Bepler, G. (2011), 'Modulation of the Ribonucleotide Reductase M1 – Gemcitabine Interaction in vivo by N-ethylmaleimide', *Biochem Biophys Res Commun* **8**(24), 383–388.
- Chi, D. S., Eisenhauer, E. L., Lang, J., Huh, J., Haddad, L., Abu-Rustum, N. R., Sonoda, Y., Levine, D. A., Hensley, M. and Barakat, R. R. (2006), 'What is the optimal goal of primary cytoreductive surgery for bulky stage IIIC epithelial ovarian carcinoma (EOC)?', *Gynecologic Oncology* **103**, 559–564.
- Chibaudel, B., Tournigand, C., Bonnetain, F., Maindrault-Goebel, F., Lledo, G., André, T., Larsen, A. K., Bengrine-Lefevre, L., Louvet, C. and De Gramont, A. (2013), 'Platinum-sensitivity in metastatic colorectal cancer: Towards a definition', *European Journal of Cancer* **49**, 3813–3820.
- Chou, T.-C. (2006), 'Theoretical Basis, Experimental Design, and Computerized Simulation of Synergism and Antagonism in Drug Combination Studies', *Pharmalogical reviews* **58**(3).
- Chou, T. C. (2010), 'Drug combination studies and their synergy quantification using the chou-talalay method', *Cancer Research* **70**(2), 440–446.
- Chou, T. C. and Talalay, P. (1983), 'Analysis of combined drug effects: a new look at a very old problem', *Trends in Pharmacological Sciences* **4**, 450–454.
- Chou, T.-c. and Talalay, P. (1984), 'Quantitative Dose-Effect Relationships : the Combined Effects of Multiple', *Advances in Enzyme Regulation* **22**, 27–55.

- Chou, T. F., Baraniak, J., Kaczmarek, R., Zhou, X., Cheng, J., Ghosh, B. and Wagner, C. R. (2006), 'Phosphoramidate pronucleotides: A comparison of the phosphoramidase substrate specificity of human and Escherichia coli histidine triad nucleotide binding proteins', *Molecular Pharmaceutics* **4**(2), 208–217.
- Chou, T.-F., Cheng, J., Tikh, I. B. and Wagner, C. R. (2007), 'Evidence that Human Histidine Triad Nucleotide Binding Protein 3 (Hint3) is a Distinct Branch of the Histidine Triad (HIT) Superfamily', *J. Mol. Biol* **373**, 978–989.
- Clarke, S. J. and Rivory, L. P. (1999), 'Clinical Pharmacokinetics of Docetaxel', *Clinical Pharmacokinetics* **36**(2), 99–114.
- Collins, A. R. (2004), 'The Comet Assay for DNA Damage and Repair', *Molecular biotechnology* **26**.
- Congiattu, C., Brancale, A. and Mcguigan, C. (2007), 'Nucleosides, Nucleotides and Nucleic Acids Molecular Modelling Studies on the Binding of Some Protides to the Putative Human Phosphoramidase Hint1', *Nucleosides, Nucleotides and Nucleic Acids ISSN: 26*, 1121–1124.
- Cooke, S. L., Ng, C. K., Melnyk, N., Garcia, M. J., Hardcastle, T., Temple, J., Langdon, S., Huntsman, D. and Brenton, J. D. (2011), 'Genomic analysis of genetic heterogeneity and evolution in high-grade serous ovarian carcinoma', *Oncogene* **29**, 4905–4913.
- Damiani, E., Solorio, J. A., Doyle, A. P. and Wallace, H. M. (2019), 'How reliable are in vitro IC50 values? Values vary with cytotoxicity assays in human glioblastoma cells', *Toxicology Letters* **302**, 28–34.
- De Clercq, E. (2012), 'Milestones in the discovery of antiviral agents: nucleosides and nucleotides', *Acta Pharmaceutica Sinica B* **2**(6), 535–548.
- De Clercq, E. and Li, G. (2016), 'Approved Antiviral Drugs over the Past 50 Years', *Clinical Microbiology Review* **29**(3).
- Della Pepa, C., Tonini, G., Santini, D., Losito, S., Pisano, C., Di Napoli, M., Chiara Cere, S., Gargiulo, P. and Pignata, S. (2015), 'Laboratory-Clinic Interface Low Grade Serous Ovarian Carcinoma: From the molecular characterization to the best therapeutic strategy', *Cancer Treatment Reviews* **41**, 136–143.
- Deng, T., Pan, H., Han, R., Huang, D., Li, H., Zhou, L., Wang, X., Bai, M., Li, X., Liu, R., Ge, S., Ning, T., Zhang, L. and Ba, Y. (2014), 'Gemcitabine sensitivity factors, hENT1 and RRM1 as potential prognostic biomarker for advanced biliary tract cancer', *Int J Clin Exp Med* **7**(12), 5041–5049.
- Derudas, M., Brancale, A., Naesens, L., Neyts, J., Balzarini, J. and McGuigan, C. (2010), 'Application of the phosphoramidate ProTide approach to the antiviral drug ribavirin.', *Bioorganic & medicinal chemistry* **18**(7), 2748–55.

- Dhillon, K. K., Swisher, E. M. and Taniguchi, T. (2011), ‘Secondary mutations of BRCA1/2 and drug resistance’, *Cancer Science* **102**(4), 663–669.
- Diamandis, E. P. (2012), ‘The failure of protein cancer biomarkers to reach the clinic: why, and what can be done to address the problem?’, *BMC Medicine* **10**.
- Domcke, S., Sinha, R., Levine, D. A., Sander, C. and Schultz, N. (2013), ‘Evaluating cell lines as tumour models by comparison of genomic profiles’, *Nature Communications* **4**(2126).
- Dorum, A., Kristensen, G. B., Abeler, V. M., Tropc, C. G. and Mailer, P. (1996), ‘Early Detection of Familial Ovarian Cancer’, *European Journal of Cancer* **32**(10), 1645–1651.
- Drost, J. and Clevers, H. (2018), ‘Organoids in cancer research’, *Nature Reviews Cancer* **18**.
- du Bois, A., Lück, H.-J., Meier, W., Adams, H.-P., Möbus, V., Costa, S., Bauknecht, T., Richter, B., Warm, M., Schröder, W., Olbricht, S., Nitz, U., Jackisch, C., Emons, G., Wagner, U., Kuhn, W. and Pfisterer, J. (2003), ‘A Randomized Clinical Trial of Cisplatin/Paclitaxel Versus Carboplatin/Paclitaxel as First-Line Treatment of Ovarian Cancer’, *Journal of the National Cancer Institute* **95**(17).
- du Bois, A., Reuss, A., Pujade-Lauraine, E., Harter, P., Ray-Coquard, I. and Pfisterer, J. (2009), ‘Role of surgical outcome as prognostic factor in advanced epithelial ovarian cancer: A combined exploratory analysis of 3 prospectively randomized phase 3 multicenter trials: by the arbeitgemeinschaft gynaekologische onkologie studiengruppe ovarialkarzin’, *Cancer* **115**(6), 1234–1244.
- Duxbury, M. S., Ito, H., Zinner, M. J., Ashley, S. W. and Whang, E. E. (2004), ‘RNA interference targeting the M2 subunit of ribonucleotide reductase enhances pancreatic adenocarcinoma chemosensitivity to gemcitabine’, *Oncogene* **23**(8), 1539–1548.
- D’Agostino, G., Amant, F., Berteloot, P., Scambia, G. and Vergote, I. (2003), ‘Phase II study of gemcitabine in recurrent platinum- and paclitaxel-resistant ovarian cancer’, *Gynecologic Oncology* **88**(3), 266–269.
- Einzig, A. I., Wiernik, P. H., Sasloff, J., Runowicz, C. D. and Goldberg, G. L. (1992), ‘Phase II study and long-term follow-up of patients treated with taxol for advanced ovarian adenocarcinoma.’, *Journal of clinical oncology : official journal of the American Society of Clinical Oncology* **10**(11), 1748–53.
- Eisenhauer, E. A., Therasse, P., Bogaerts, J., Schwartz, L. H., Sargent, D., Ford, R., Dancey, J., Arbuck, S., Gwyther, S., Mooney, M., Rubinstein, L., Shankar, L., Dodd, L., Kaplan, R., Lacombe, D., Verweij, J. and Biologicals, G. (2009), ‘New response evaluation criteria in solid tumours: Revised RECIST guideline (version 1.1)’, *European Journal of Cancer* **45**, 228–247.

- Eisenhauer, E. L., Zanagnolo, V., Cohn, D. E., Salani, R., O'Malley, D. M., Sutton, G., Callahan, M. J., Cobb, B., Fowler, J. M. and Copeland, L. J. (2014), 'A phase II study of gemcitabine, carboplatin and bevacizumab for the treatment of platinum-sensitive recurrent ovarian cancer', *Gynecologic Oncology* **134**(2), 262–266.
- Eltabbakh, G. H., Donovan, E. and Eltabbakh, G. (2016), 'Efficacy of a modified regimen of gemcitabine and cisplatin among women with recurrent epithelial ovarian cancer', *Journal of Solid Tumors* **6**(2).
- Eto, K., Kawakami, H., Kuwatani, M., Kudo, T., Abe, Y., Kawahata, S., Takasawa, A., Fukuoka, M., Matsuno, Y., Asaka, M. and Sakamoto, N. (2013), 'Human equilibrative nucleoside transporter 1 and Notch3 can predict gemcitabine effects in patients with unresectable pancreatic cancer', *British Journal of Cancer* **108**, 1488–1494.
- Ewald, B., Sampath, D. and Plunkett, W. (2008), 'Nucleoside analogs: molecular mechanisms signaling cell death.', *Oncogene* **27**(50), 6522–6537.
- Farrell, J. J., Moughan, J., Wong, J. L., Regine, W. F., Schaefer, P., Benson, A. B., Macdonald, J. S., Liu, X., Yen, Y., Lai, R., Zheng, Z., Bepler, G., Guha, C. and Elsaleh, H. (2016), 'Precision Medicine and Pancreatic Cancer', *Pancreas* **45**(10), 1485–1493.
- Ferrandina, G., Mey, V., Nannizzi, S., Ricciardi, S., Petrillo, M., Ferlini, C., Danesi, R., Scambia, G. and Tacca, M. D. (2010), 'Expression of nucleoside transporters, deoxycytidine kinase, ribonucleotide reductase regulatory subunits, and gemcitabine catabolic enzymes in primary ovarian cancer', *Cancer Chemother Pharmacol* **65**, 679–686.
- Ferreira, D., Adegá, F. and Chaves, R. (2013), 'The Importance of Cancer Cell Lines as in vitro Models in Cancer Methyloome Analysis and Anticancer Drugs Testing', *Intech*.
- Florento, L., Matias, R., Tuaño, E., Santiago, K., dela Cruz, F., Tuazon, A. and Florento, L. M. (2012), 'Comparison of Cytotoxic Activity of Anticancer Drugs against Various Human Tumor Cell Lines Using In Vitro Cell-Based Approach', *Int J Biomed Sci InternatIonal journal of BIomedIcal science* **8**(1).
- Ford, D., Easton, D. F., Bishop, D. T., Narod, S. A. and Goldgar, D. E. (1994), 'Risks of cancer in BRCA1-mutation carriers', *The Lancet* **343**(8899), 692–695.
- Fouquier, J. and Guedj, M. (2015), 'Analysis of drug combinations: current methodological landscape', *Pharmacology research and perspectives* **3**(3), 149.
- Francies, H. E., Barthorpe, A., McLaren-Douglas, A., Barendt, W. J. and Garnett, M. J. (2016), 'Drug Sensitivity Assays of Human Cancer Organoid Cultures', *Methods in Molecular Biology*.

- Fredebohm, J., Wolf, J., Hoheisel, D. and Boettcher, M. (2013), ‘Depletion of RAD17 sensitizes pancreatic cancer cells to gemcitabine’, *Journal of Cell Science* **126**, 3380–3389.
- Galluzzi, L., Senovilla, L., Vitale, I., Michels, J., Martins, I., Kepp, O., Castedo, M. and Kroemer, G. (2012), ‘Molecular mechanisms of cisplatin resistance’, *Oncogene* **31**(15), 1869–1883.
- Galmarini, C. M., Mackey, J. R. and Dumontet, C. (2001), ‘Nucleoside analogues: mechanisms of drug resistance and reversal strategies’, *Leukemia* **15**, 875–890.
- Garcia-Cremades, M., Pitou, C., Iversen, P. W. and Troconiz, I. F. (2017), ‘Characterizing Gemcitabine Effects Administered as Single Agent or Combined with Carboplatin in Mice Pancreatic and Ovarian Cancer Xenografts: A Semimechanistic Pharmacokinetic/Pharmacodynamics Tumor Growth-Response Model s’, *The Journal of Pharmacology and Experimental Therapeutics* **360**, 445–456.
- Garnett, M. J. (2012), ‘Systematic identification of genomic markers of drug sensitivity in cancer cells’, *Nature* **483**(7391), 570–575.
- Gelmon, K. A., Tischkowitz, M., Mackay, H., Swenerton, K., Robidoux, A., Tonkin, K., Hirte, H., Huntsman, D., Clemons, M., Gilks, B., Yerushalmi, R., Macpherson, E., Carmichael, J. and Oza, A. (2011), ‘Olaparib in patients with recurrent high-grade serous or poorly differentiated ovarian carcinoma or triple-negative breast cancer: a phase 2, multicentre, open-label, non-randomised study’, *Lancet Oncology* **12**, 852–861.
- Gerhards, N. M. and Rottenberg, S. (2018), ‘New tools for old drugs: Functional genetic screens to optimize current chemotherapy’, *Drug Resistance Updates* **36**, 30–46.
- Ghazaly, E. A., Slusarczyk, M., Mason, M., Gribben, J., McGuigan, C. and Blagden, S. (2014), Abstract CT401: NUC-1031: A novel ProTide that overcomes the key cancer resistance mechanisms associated with poor survival, *in* ‘AACR’.
- Ghazaly, E., Rizzuto, I., Gabra, H., Habib, N., Leonard, R., Wasan, H., McGuigan, C. and Blagden, S. (2014), PRO GEM1 : A Phase I / II study of a first-in-class nucleotide analogue Acelarin (NUC-1031) in patients with advanced solid tumours Barts, *in* ‘ASCO Meeting Abstracts’.
- Giovannetti, E., Tacca, M. D., Mey, V., Funel, N., Nannizzi, S., Ricci, S., Orlandini, C., Boggi, U., Campani, D., Chiaro, M. D., Iannopollo, M., Bevilacqua, G., Mosca, F. and Danesi, R. (2006), ‘Transcription Analysis of Human Equilibrative Nucleoside Transporter-1 Predicts Survival in Pancreas Cancer Patients Treated with Gemcitabine’, *Cancer Research* **66**(7), 3928–3963.

- Gmeiner, W. H., Yu, S., Pon, R. T., Pourquier, P. and Pommier, Y. (2003), ‘Structural basis for topoisomerase I inhibition by nucleoside analogs’, *Nucleosides, Nucleotides and Nucleic Acids* **22**(5-8), 653–658.
- Goff, B. A., Mandel, L., Muntz, H. G. and Melancon, C. H. (2000), ‘Ovarian Carcinoma Diagnosis’, *Cancer* **89**(10), 2068–2075.
- Goldin, A. and Nathan, M. (1957), ‘The Employment of Combinations of Drugs in the Chemotherapy of Neoplasia: A Review’, *Cancer Research* **17**(7).
- Goodspeed, A., Heiser, L. M., Gray, J. W. and Costello, J. C. (2016), ‘Tumor-Derived Cell Lines as Molecular Models of Cancer Pharmacogenomics.’, *Molecular cancer research : MCR* **14**(1), 3–13.
- Gourley, C., Dalton, H. J., Banerjee, S. N., Buscema, J. and Lockley, M. (2018), PRO-105 , a phase II open-label study of NUC-1031 in patients with platinum- resistant ovarian cancer ., in ‘ASCO Meeting Abstracts’, pp. 1–2.
- Gray, H. J., Bell-McGuinn, K., Fleming, G. F., Cristea, M., Xiong, H., Sullivan, D., Luo, Y., McKee, M. D., Munasinghe, W. and Martin, L. P. (2018), ‘Phase I combination study of the PARP inhibitor veliparib plus carboplatin and gemcitabine in patients with advanced ovarian cancer and other solid malignancies’, *Gynecologic Oncology* **148**(3), 507–514.
- Greco, W. R., Bravo, G. and Parsons, J. C. (1995), ‘The Search for Synergy: A Critical Review Response Surface Perspective’, *Pharmacology* **47**(2).
- Guénard, D., Guéritte-Voegelein, F. and Potier, P. (1993), ‘Taxol and Taxotere: Discovery, Chemistry, and Structure-Activity Relationships’, *C. S. Org. Prep. Proced. Int* **26**(2), 665–667.
- Gyori, B. M., Venkatachalam, G., Thiagarajan, P. S., Hsu, D. and Clement, M.-V. (2014), ‘OpenComet: An automated tool for comet assay image analysis’, *Redox Biology* **2**, 457–465.
- Hainsworth, B. J. D., Erland, J. B., Kalman, L. a., Schreeder, M. T. and Greco, F. A. (1997), ‘Carcinoma of Unknown Primary Site: Treatment With 1-Hour Paclitaxel, Carboplatin, and Extended- Schedule Etoposide’, *Society* **15**(6), 2385–2393.
- Harder, N., Athelougou, M., Hessel, H., Brieu, N., Yigitsoy, M., Zimmermann, J., Baatz, M., Buchner, A., Stief, C. G., Kirchner, T., Binnig, G., Schmidt, G. and Huss, R. (2018), ‘Tissue Phenomics for prognostic biomarker discovery in low- and intermediate-risk prostate cancer’, *Scientific Reports* **8**(1), 1–19.
- Harrap, K. R. (1985), ‘Preclinical studies identifying carboplatin as a viable cisplatin alternative’, *Cancer Treatment Reviews* **12**(SUPPL. A), 21–33.

- Hasan, N., Ohman, A. W. and Dinulescu, D. M. (2015), ‘The promise and challenge of ovarian cancer models HHS Public Access’, *Transl Cancer Res* **4**(1), 14–28.
- Hatzis, P., Al-Madhoon, A. S., Jüllig, M., Petrakis, T. G., Eriksson, S. and Talianidis, I. (1998), ‘The intracellular localization of deoxycytidine kinase’, *Journal of Biological Chemistry* **273**(46), 30239–30243.
- Havrilesky, L., Darcy, K. M., Hamdan, H., Priore, R. L., Leon, J., Bell, J. and Berchuck, A. (2003), ‘Prognostic significance of p53 mutation and p53 overexpression in advanced epithelial ovarian cancer: A Gynecologic Oncology Group Study’, *Journal of Clinical Oncology* **21**(20), 3814–3825.
- He, Y., Zhu, Q., Chen, M., Huang, Q., Wang, W., Li, Q., Huang, Y. and Di, W. (2016), ‘The changing 50% inhibitory concentration (IC₅₀) of cisplatin: a pilot study on the artifacts of the MTT assay and the precise measurement of density-dependent chemoresistance in ovarian cancer’, *Oncotarget* **7**(43).
- Heinemann, V., Hertel, L. W., Grindey, G. B. and Plunkett, W. (1988), ‘Comparison of the Cellular Pharmacokinetics and Toxicity of 2’, 2’ -Difluorodeoxycytidine and 1- β -d-Arabinofuranosylcytosine’, *Cancer Research* **48**, 4024–4031.
- Heinemann, V., Xu, Y.-Z., Chubb, S., Sen, A., Hertel, L. W., Grindey, G. B. and Plunkett, W. (1992), ‘Cellular Elimination of 2’, 2’-Difluorodeoxycytidine 5’-Triphosphate: A Mechanism of Self-Potentialion’, *Cancer Research* **52**, 533–539.
- Hendel, A., Bak, R. O., Clark, J. T., Kennedy, A. B., Ryan, D. E., Roy, S., Steinfeld, I., Lunstad, B. D., Kaiser, R. J., Wilkens, A. B., Bacchetta, R., Tsalenko, A., Dellinger, D., Bruhn, L. and Porteus, M. H. (2015), ‘Chemically modified guide RNAs enhance CRISPR-Cas genome editing in human primary cells’, *Nature biotechnology* **33**(9), 985–989.
- Hernandez, L., Kim, M. K., Lyle, L. T., Bunch, K. P., House, C. D., Ning, F., Noonan, A. M. and Annunziata, C. M. (2016), ‘Characterization of ovarian cancer cell lines as in vivo models for preclinical studies HHS Public Access’, *Gynecol Oncol* **142**(2), 332–340.
- Hertel, L. W., Boder, G. B., Kroin, J. S., Rinzel, S. M., Poore, G. a., Todd, G. C. and Grindey, G. B. (1990), ‘Evaluation of the Antitumor Activity of Gemcitabine (2’ , 2’ Evaluation of the Antitumor Activity of Gemcitabine’, *Cancer Research* **50**(14), 4417–4422.
- Herzog, T. J. (2002), ‘Update on the role of topotecan in the treatment of recurrent ovarian cancer’, *Oncologist* **7 Suppl 5**(suppl 5), 3–10.

- Hodge, L. S., Taub, M. E. and Tracy, T. S. (2011), 'The Deaminated Metabolite of Gemcitabine, 2',2'-Difluorodeoxyuridine, Modulates the Rate of Gemcitabine Transport and Intracellular Phosphorylation via Deoxycytidine Kinase', *Drug Metabolism and Disposition* **39**(11), 2013–2016.
- Holton, R. a., Somoza, C., Kim, H.-b., Liang, F., Biediger, R. J., Boatman, P. D., Shindo, M., Smith, C. C., Kim, S., Nadizadeh, H., Suzuki, Y., Tao, C., Vu, P., Tang, S., Zhang, P., Murthi, K. K., Gentile, L. N. and Liu, J. H. (1994), 'First Total Synthesis of Taxol. 1. Functionalization of the B Ring', *Journal of the American Chemical Society* **116**(2), 1597–1598.
- Honeywell, R. J., Ruiz van Haperen, V. W., Veerman, G., Smid, K. and Peters, G. J. (2015), 'Inhibition of thymidylate synthase by 2',2'-difluoro-2'-deoxycytidine (Gemcitabine) and its metabolite 2',2'-difluoro-2'-deoxyuridine', *The International Journal of Biochemistry & Cell Biology* **60**, 73–81.
- Howlander, N., Noone, A., Krapcho, M., Miller, D., Bishop, K., Altekruse, S., Kosary, C., Yu, M., Ruhl, J., Tatalovich, Z., Mariotto, A., Lewis, D., Chen, H., Feuer, E. and Cronin, K. (2016), SEER Cancer Statistics Review, 1975-2013, National Cancer Institute. Bethesda, MD, https://seer.cancer.gov/archive/csr/1975_2013/, based on November 2015 SEER data submission, posted to the SEER web site, Technical report.
- Howlander, N., Noone, A., Krapcho, M., Miller, D., Bishop, K., Kosary, C., Yu, M., Ruhl, J., Tatalovich, Z., Mariotto, A., Lewis, D., Chen, H., Feuer, E. and Cronin, K. (2017), SEER Cancer Statistics Review, 1975-2014. Bethesda, MD: National Cancer Institute, https://seer.cancer.gov/csr/1975_2014/, based on November 2016 SEER data submission, posted to the SEER web site, Technical report.
- Hubeek, I., Peters, G. J., Broekhuizen, A. J. F., Talianidis, I., Sigmond, J., Gibson, B. E. S., Creutzig, U., Giaccone, G. and Kaspers, J. L. (2005), 'Immunocytochemical detection of deoxycytidine kinase in haematological malignancies and solid tumours', *J Clin Pathol* **58**, 695–699.
- Hunakova, L., Gronesova, P., Horvathova, E., Chalupa, I., Cholujovala, D., Duraj, J. and Sedlak, J. (2014), 'Modulation of cisplatin sensitivity in human ovarian carcinoma A2780 and SKOV3 cell lines by sulforaphane.', *Toxicology letters* **230**(3), 479–86.
- ICON and AGO, T. (2003), 'Paclitaxel plus platinum-based chemotherapy versus conventional platinum-based chemotherapy in women with relapsed ovarian cancer: the ICON4/AGO-OVAR-2.2 trial', *The Lancet* **361**(9375), 2099–2106.
- Ikediobi, O. N., Davies, H., Bignell, G., Edkins, S., Stevens, C., O'meara, S., Santarius, T., Avis, T., Barthorpe, S., Brackenbury, L., Buck, G., Butler, A., Clements, J., Cole, J., Dicks, E., Forbes, S., Gray, K., Halliday, K., Harrison, R., Hills, K., Hinton, J., Hunter, C., Jenkinson, A., Jones, D., Kosmidou, V., Lugg, R., Menzies, A.,

Mironenko, T., Parker, A., Perry, J., Raine, K., Richardson, D., Shepherd, R., Small, A., Smith, R., Solomon, H., Stephens, P., Teague, J., Tofts, C., Varian, J., Webb, T., West, S., Widaa, S., Yates, A., Reinhold, W., Weinstein, J. N., Stratton, M. R., Futreal, P. A. and Wooster, R. (2006), ‘Mutation analysis of 24 known cancer genes in the NCI-60 cell line set’.

URL: <http://www.sanger.ac.uk/genetics/CGP/Census/>.

Jaeger, S., Igea, A., Arroyo, R., Alcalde, V., Canovas, N., Orozco, M., Nebreda, A. R. and Aloy, P. (2016), ‘Therapeutics, Targets, and Chemical Biology Quantification of Pathway Cross-talk Reveals Novel Synergistic Drug Combinations for Breast Cancer’, *Cancer Research* .

Jelovac, D. and Armstrong, D. K. (2011), ‘Recent progress in the diagnosis and treatment of ovarian cancer.’, *CA: a cancer journal for clinicians* **61**(3), 183–203.

Jeon, M., Kim, S., Park, S., Lee, H. and Kang, J. (2018), ‘In silico drug combination discovery for personalized cancer therapy’, *BMC Systems Biology* **12**(2), 16.

Ji, J., Zhang, Y., Redon, C. E., Reinhold, W. C., Chen, A. P., Fogli, L. K., Holbeck, S. L., Parchment, R. E., Hollingshead, M., Tomaszewski, J. E., Dudon, Q., Pommier, Y., Doroshow, J. H. and Bonner, W. M. (2017), ‘Phosphorylated fraction of H2AX as a measurement for DNA damage in cancer cells and potential applications of a novel assay’, *PLoS ONE* .

Jinek, M., Chylinski, K., Fonfara, I., Hauer, M., Doudna, J. A., Charpentier, E., Wiedenheft, B., Sternberg, S. H., Doudna, J. A., Bhaya, D., Davison, M., Barrangou, R., Terns, M. P., Terns, R. M., Deltcheva, E., Carte, J., Wang, R., Li, H., Terns, R. M., Terns, M. P., Haurwitz, R. E., Jinek, M., Wiedenheft, B., Zhou, K., Doudna, J. A., Wang, R., Preamplume, G., Terns, M. P., Terns, R. M., Li, H., Gesner, E. M., Schellenberg, M. J., Garside, E. L., George, M. M., Macmillan, A. M., Hatoum-Aslan, A., Maniv, I., Marraffini, L. A., Brouns, S. J. J., Sashital, D. G., Jinek, M., Doudna, J. A., Lintner, N. G., Semenova, E., Wiedenheft, B., Wiedenheft, B., Hale, C. R., Howard, J. A. L., Delmas, S., Ivančić-Baće, I., Bolt, E. L., Westra, E. R., Hale, C. R., Zhang, J., Makarova, K. S., Makarova, K. S., Grishin, N. V., Shabalina, S. A., Wolf, Y. I., Koonin, E. V., Makarova, K. S., Aravind, L., Wolf, Y. I., Koonin, E. V., Gottesman, S., Barrangou, R., Garneau, J. E., Sapranauskas, R., Taylor, G. K., Heiter, D. F., Pietrokovski, S., Stoddard, B. L., Deveau, H., Lewis, B. P., Burge, C. B., Bartel, D. P., Hutvagner, G., Simard, M. J., Mojica, F. J. M., Díez-Villaseñor, C., García-Martínez, J., Almendros, C., Marraffini, L. A., Sontheimer, E. J., Sashital, D. G., Wiedenheft, B., Doudna, J. A., Christian, M., Miller, J. C., Urnov, F. D., Rebar, E. J., Holmes, M. C., Zhang, H. S., Gregory, P. D., Carroll, D., Caparon, M. G., Scott, J. R., Frøkjær-Jensen, C., Denman, R. B., Hofacker, I. L., Stadler, P. F., Darty, K., Denise, A., Ponty, Y., Zebala, J. A., Choi, J., Barany, F., Pingoud, V., Wright, D. J., Jack, W. E. and Modrich, P. (2012), ‘A programmable

- dual-RNA-guided DNA endonuclease in adaptive bacterial immunity.’, *Science (New York, N. Y.)* **337**(6096), 816–21.
- Johansson, M., Brismar, S. and Karlsson, A. (1997), ‘Human deoxycytidine kinase is located in the cell nucleus’, *Proceedings of the National Academy of Sciences* **94**, 11941–11945.
- Johansson, P., Fasth, A., Ek, T. and Hammarsten, O. (2017), ‘Validation of a flow cytometry-based detection of γ -H2AX, to measure DNA damage for clinical applications’, *Cytometry Part B: Clinical Cytometry* **92**(6), 534–540.
- Johnson, S. W., Laub, P. B., Beesley, J. S., Ozols, R. F. and Hamilton, T. C. (1997), ‘Increased platinum-DNA damage tolerance is associated with cisplatin resistance and cross-resistance to various chemotherapeutic agents in unrelated human ovarian cancer cell lines’, *Cancer Research* **57**(5), 850–856.
- Jones, R. M., Kotsantis, P., Stewart, G. S., Groth, P. and Petermann, E. (2014), ‘BRCA2 and RAD51 promote double-strand break formation and cell death in response to Gemcitabine’, *Molecular cancer therapeutics* **13**, 2412–2421.
- Jordan, S. J., Whiteman, D. C., Purdie, D. M., Green, A. C. and Webb, P. M. (2006), ‘Does smoking increase risk of ovarian cancer? A systematic review’, *Gynecologic Oncology* **103**, 1122–1129.
- Jordheim, L. P., Durantel, D., Zoulim, F. and Dumontet, C. (2013), ‘Advances in the development of nucleoside and nucleotide analogues for cancer and viral diseases.’, *Nature reviews. Drug discovery* **12**(6), 447–64.
- Jung, Y. and Lippard, S. J. (2007), ‘Direct Cellular Responses to Platinum-Induced DNA Damage’, *Chemical Reviews* **107**(5).
- Kamisawa, T., Wood, L. D., Itoi, T. and Takaori, K. (2016), ‘Pancreatic cancer’, *The Lancet* **388**, 73–85.
- Kang, S. M., Rosales, J. L., Meier-Stephenson, V., Kim, S., Lee, K. Y. and Narendran, A. (2017), ‘Genome-wide loss-of-function genetic screening identifies opioid receptor μ 1 as a key regulator of L-asparaginase resistance in pediatric acute lymphoblastic leukemia’, *Oncogene* **36**, 5910–5913.
- Karst, A. M. and Drapkin, R. (2010), ‘Ovarian cancer pathogenesis: a model in evolution.’, *Journal of oncology* **2010**, 932371.
- Kasinski, A. L., Kelnar, K., Stahlhut, C., Orellana, E., Zhao, J., Shimer, E., Dysart, S., Chen, X., Bader, A. G. and Slack, F. J. (2015), ‘A combinatorial microRNA therapeutics approach to suppressing non-small cell lung cancer’, *Oncogene* **34**, 3547–3555.

- Keating, G. M. (2014), 'Sofosbuvir: A Review of its Use in Patients with Chronic Hepatitis C', *Drugs* **74**, 1127–1146.
- Khan, K., Tewari, S., Awasthi, N. P., Mishra, S. P., Agarwal, G. R., Rastogi, M. and Husain, N. (2018), 'Flow cytometric detection of gamma-H2AX to evaluate DNA damage by low dose diagnostic irradiation', *Medical Hypotheses* **115**, 22–28.
- King, M.-C., Marks, J. H., Mandell, J. B., Ben-Yishay, M., Dutcher, J. P., Gross, S. J., Runowicz, C. D., Venkatraj, U., Israel Medical Center Katherine Daley, B., Havens, G., Penschaszadeh, V.-t. B., Petersen, B., Pressman, P., Antman, K. H., Cancer Center Robin Camhi Baum, S.-K., Borgen, P., Brown, K. L., Glogowski, E., Haas, B. R., Hampel, H., McDer-mott, D. A., Norton, L., Hanson Pierce, H., Pinto, M., Robson, M., Scheuer, L., Schulz, C. J., Bialer, M., Green-berg, L., Kemel, Y., Lundberg, J., McKenna, C. A., Mehta, L., Sastry, S., Practitioners Ernest Greenberg, P. J., C Greenberg, P. A., Kolb, T., Lichy, J., Lawrence College Jessica Benjoya Mandell, S., Berliner, J. L., Rosenthal, G., Gilbert, F., Oliveria, S., Hale Coats, K., Hull, J., Lee, M. K., Morrow, J. E., Owens, K. N., Shiovitz, S., Stray, S., Walsh, T., Walsh, V. L., Plains Hospital Center Robert Burk, W. D., Demsky, R., Duffy, K., Fialk, M. A., Mank-Seymour, A. R. and Shappell, H. L. (2003), 'Breast and Ovarian Cancer Risks Due to Inherited Mutations in BRCA1 and BRCA2 Downloaded from', *Science* **302**.
- Klotz, D. M. and Wimberger, P. (2017), 'Cells of origin of ovarian cancer: ovarian surface epithelium or fallopian tube?', *Archives of Gynecology and Obstetrics* **296**, 1055–1062.
- Komiyama, S., Kugimiya, T., Takeya, C., Takahashi, R. and Kubushiro, K. (2018), 'Platinum-resistant recurrent ovarian cancer with long survival on bevacizumab and gemcitabine', *Journal of Obstetrics and Gynaecology Research* pp. 1–5.
- Koplev, S., Longden, J., Ferkinghoff-Borg, J., Voellmy, F., Sommer, M. O. A., Linding Correspondence, R., Bjerregå, M. B., Cox, T. R., Erler, J. T., Pedersen, J. T. and Linding, R. (2017), 'Dynamic Rearrangement of Cell States Detected by Systematic Screening of Sequential Anticancer Treatments', *Cell Reports* **20**.
- Koshiyama, M., Matsumura, N. and Konishi, I. (2014), 'Recent concepts of ovarian carcinogenesis: Type I and type II', *BioMed Research International* **2014**.
- Kuo, K.-T., Mao, T.-L., Jones, S., Veras, E., Ayhan, A., Wang, T.-L., Glas, R., Slamon, D., Velculescu, V. E., Kuman, R. J. and Shih, I.-M. (2009), 'Short Communication Frequent Activating Mutations of PIK3CA in Ovarian Clear Cell Carcinoma', *Am J Pathol* **174**, 1597–1601.
- Kuo, L. J. and Yang, L.-X. (2008), 'Gamma-H2AX - a novel biomarker for DNA double-strand breaks.'

- Kurman, R. J. and Shih, I.-M. (2008), ‘Pathogenesis of ovarian cancer: lessons from morphology and molecular biology and their clinical implications.’, *International journal of gynecological pathology : official journal of the International Society of Gynecological Pathologists* **27**(2), 151–60.
- Kurman, R. J. and Shih, I.-M. (2010), ‘The Origin and Pathogenesis of Epithelial Ovarian Cancer-a Proposed Unifying Theory’, *Am J Surg Pathol* **34**(3), 433–443.
- Lancaster, M. A. and Knoblich, J. A. (2015), ‘Generation of Cerebral Organoids from Human Pluripotent Stem Cells’, *Nature Protocols* p. 2329–2340.
- Langdon, S. P., Lawrie, S. S., Hay, F. G., Hawkes, M. M., McDonald, A., Hayward, I. P., Schol, D. J., Hilgers, J., Leonard, R. C. F. and Smyth, J. F. (1988), ‘Characterization and properties of nine human ovarian adenocarcinoma cell lines’, *Cancer Research* **48**, 6166–6172.
- Lebwohl, D. and Canetta, R. (1998), ‘Clinical Oncology Update Clinical Development of Platinum Complexes in Cancer Therapy: an Historical Perspective and an Update’, *European Journal of Cancer* **34**(10), 1522–1534.
- Lee, K., Kim, D.-E., Jang, K.-S., Kim, S.-J., Cho, S. and Kim, C. (2017), ‘Gemcitabine, a broad-spectrum antiviral drug, suppresses enterovirus infections through innate immunity induced by the inhibition of pyrimidine biosynthesis and nucleotide depletion’, *Oncotarget* **8**(70), 115315–115325.
- Lengyel, E., Burdette, J. E., Kenny, H. A., Matei, D., Pilrose, J., Haluska, P., Nephew, K. P., Hales, D. B. and Stack, M. S. (2014), ‘Epithelial Ovarian Cancer Experimental Models’, *Oncogene* **33**(28), 3619–3633.
- Li, H., Balajee, A. S., Su, T., Cen, B., Hei, T. K. and Weinstein, I. B. (2008), ‘The HINT1 tumor suppressor regulates both gamma-H2AX and ATM in response to DNA damage.’, *The Journal of cell biology* **183**(2), 253–65.
- Li, W., Xu, H., Xiao, T., Love, M., Zhang, F., Irizarry, R., Liu, J., Brown, M. and Liu, X. (2014), ‘MAGeCK enables robust identification of essential genes from genome-scale CRISPR/Cas9 knockout screens’, *Genome Biology* **12**(9).
- Lokich, J. and Anderson, N. (1998), ‘Carboplatin versus cisplatin in solid tumors: An analysis of the literature’, *Annals of Oncology* **9**(1), 13–21.
- Longuespée, R., Boyon, C., Desmons, A., Vinatier, D., Leblanc, E., Farré, I., Wistorski, M., Ly, K., D’Anjou, F., Day, R., Fournier, I. and Salzet, M. (2012), ‘Ovarian cancer molecular pathology.’, *Cancer metastasis reviews* **31**(3-4), 713–32.
- Lorusso, A., Di Stefano, A., Fanfani, F. and Scambia, G. (2006), ‘Role of gemcitabine in ovarian cancer treatment’, *Annals of Oncology* **17**(SUPPL. 5), 188–194.

- Loughrey, M. B., Bankhead, P., Coleman, H. G., Hagan, R. S., Craig, S., McCorry, A. M., Gray, R. T., McQuaid, S., Dunne, P. D., Hamilton, P. W., James, J. A. and Salto-Tellez, M. (2018), 'Validation of the systematic scoring of immunohistochemically stained tumour tissue microarrays using QuPath digital image analysis', *Histopathology* **73**(2), 327–338.
- Lovell, D. P. and Omori, T. (2008), 'Statistical issues in the use of the comet assay', *Mutagenesis* **23**(3), 171–182.
- Lund, B., Hansen, O. P., Theilade, K., Hansen, M. and Neijt, J. P. (1994), 'Phase II Study of Gemcitabine (2',2'-Difluorodeoxycytidine) in Previously Treated Ovarian Cancer Patients', *JNCI Journal of the National Cancer Institute* **86**(20), 1530–1533.
- Lynch, H. T., Casey, M. J., Snyder, C. L., Bewtra, C., Lynch, J. F., Butts, M. and Godwin, A. K. (2009), 'Hereditary ovarian carcinoma: Heterogeneity, molecular genetics, pathology, and management', *Molecular oncology* **3**, 97–137.
- Mackey, J. R., Mani, R. S., Selner, M., Mowles, D., Young, J. D., Belt, J. A., Crawford, C. R. and Cass, C. E. (1998), 'Functional nucleoside transporters are required for gemcitabine influx and manifestation of toxicity in cancer cell lines', *Cancer Research* **58**(19), 4349–4357.
- Maréchal, R., Bachet, J.-b., Mackey, J. R., Dalban, C., Demetter, P., Graham, K., Couvelard, A., Svrcek, M., Bardier-dupas, A., Hammel, P., Sauvanet, A., Louvet, C., Paye, F., Rougier, P., Penna, C., André, T., Dumontet, C., Cass, C. E., Peter Jordheim, L., Matera, E.-l., Closset, J., Salmon, I., Devière, J., Emile, J.-f. and Van Laethem, J.-l. (2012), 'Levels of Gemcitabine Transport and Metabolism Proteins Predict Survival Times of Patients Treated With Gemcitabine for Pancreatic Adenocarcinoma', *GASTROENTEROLOGY* **143**, 664–6746.
- Maréchal, R., MacKey, J. R., Lai, R., Demetter, P., Peeters, M., Polus, M., Cass, C. E., Salmon, I., Devière, J. and Van Laethem, J. L. (2010), 'Deoxycytidine kinase is associated with prolonged survival after adjuvant gemcitabine for resected pancreatic adenocarcinoma', *Cancer* **116**(22), 5200–5206.
- Matthews, H., Deakin, J., Rajab, M., Idris-Usman, M. and Nirmalan, N. J. (2017), 'Investigating antimalarial drug interactions of emetine dihydrochloride hydrate using CalcuSyn-based interactivity calculations', *PLoS ONE*.
- Matulonis, U. A., Sood, A. K., Fallowfield, L., Howitt, B. E., Sehouli, J. and Karlan, B. Y. (2016), 'Ovarian cancer', *Nature Reviews Disease Primers* **2**, 1–22.
- McCluggage, W. G. (2011), 'Morphological subtypes of ovarian carcinoma: a review with emphasis on new developments and pathogenesis.', *Pathology* **43**(5), 420–32.

- McGuigan, C., Habib, N. A., Wasan, H. S., Gabra, H., Jiao, L. R., Slusarczyk, M., Chabot, J. A. and Saif, M. W. (2011), 'A phosphoramidate ProTide (NUC-1031) and acquired and intrinsic resistance to gemcitabine.', *ASCO Meeting Abstracts* **29**(15_suppl), e13540.
- McGuigan, C., Pathirana, R. N., Mahmood, N. and Hay, A. J. (1992), 'Aryl phosphate derivatives of AZT inhibit HIV replication in cells where the nucleoside is poorly active', *Bioorganic & Medicinal Chemistry Letters* **2**(7), 701–704.
- McGuire, W. P., Hoskins, W. J., Brady, M. F., Kucera, PAUL R. Partridge, E. E., Look, K. Y., Clarke-Pearson, D. L. and Davidson, M. (1996), 'Cyclophosphamide and cisplatin compared with paclitaxel and cisplatin in patients with stage III and stage IV ovarian cancer', *The New England Journal of Medicine* **334**, 1–6.
- McNamara, M., Bridgewater, J., Palmer, D., Wasan, H., Ryder, W., Gnanaranjan, C., Ghazaly, E., Evans, T. and Valle, J. (2018), Poster ASCO GI 2018 biliary tract cancer.pdf, in 'ASCO GI Meeting Abstracts', Chicago.
- Mehellou, M. Y., Rattan, H. S. and Balzarini, J. (2017), 'The ProTide Prodrug Technology: From the Concept to the Clinic', *Journal of Medicinal Chemistry* **61**, 22112226.
- Merlo, L. M. F. and Maley, C. C. (2010), 'The role of genetic diversity in cancer', *The Journal of Clinical Investigation* **120**(2), 401.
- Minami, K., Shinsato, Y., Yamamoto, M., Takahashi, H., Zhang, S., Nishizawa, Y., Tabata, S., Ikeda, R., Kawahara, K., Tsujikawa, K., Chijiwa, K., Yamada, K., Akiyama, S.-I., P Erez-Torras, S., Pastor-Anglada, M., Furukawa, T. and Yasuo, T. (2015), 'Ribonucleotide reductase is an effective target to overcome gemcitabine resistance in gemcitabine-resistant pancreatic cancer cells with dual resistant factors-NC-ND license (<http://creativecommons.org/licenses/by-nc-nd/4.0/>)', *Journal of Pharmaceutical Sciences* **127**, 319–325.
- Mini, E., Nobili, S., Caciagli, B, Landini, I. and Mazzei, T. (2006), 'Cellular pharmacology of gemcitabine', *Annals of Oncology* **17**(SUPPL. 5), 7–12.
- Miyagawa, K. (2008), 'Clinical relevance of the homologous recombination machinery in cancer therapy', *Cancer Science* **99**(2), 187–194.
- Moorsel, V. (1999), 'Mechanisms of synergism between cisplatin and gemcitabine in ovarian and non-small-cell lung cancer cell lines.', *British journal of cancer* **80**(7), 981–90.
- Moufarij, M. A. (2003), 'Gemcitabine Potentiates Cisplatin Cytotoxicity and Inhibits Repair of Cisplatin-DNA Damage in Ovarian Cancer Cell Lines', *Molecular Pharmacology* **63**(4), 862–869.

- Murakami, E., Tolstykh, T., Bao, H., Niu, C., Micolochick Steuer, H. M., Bao, D., Chang, W., Espiritu, C., Bansal, S., Lam, A. M., Otto, M. J., Sofia, M. J. and Furman, P. A. (2010), 'Mechanism of Activation of PSI-7851 and Its Diastereoisomer PSI-7977', *The Journal of biological chemistry* **285**(45), 34337–34347.
- Nagourney, R. A., Brewer, C. A., Radecki, S., Kidder, W. A., Sommers, B. L., Evans, S. S., Minor, D. R. and DiSaia, P. J. (2003), 'Phase II trial of gemcitabine plus cisplatin repeating doublet therapy in previously treated, relapsed ovarian cancer patients', *Gynecologic Oncology* **88**(1), 35–39.
- Nakano, Y., Tanno, S., Koizumi, K., Nishikawa, T., Nakamura, K., Minoguchi, M., Izawa, T., Mizukami, Y., Okumura, T. and Kohgo, Y. (2007), 'Gemcitabine chemoresistance and molecular markers associated with gemcitabine transport and metabolism in human pancreatic cancer cells.', *British journal of cancer* **96**(3), 457–63.
- Nantasanti, S., De Bruin, A., Rothuizen, J., Penning, L. C. and Schotanus, B. A. (2016), 'Enabling Technologies for Cell-Based Clinical Translation Concise Review: Organoids Are a Powerful Tool for the Study of Liver Disease and Personalized Treatment Design in Humans and Animals'.
- Nikolova, T., Dvorak, M., Jung, F., Adam, I., Krämer, E., Gerhold-Ay, A. and Kaina, B. (2014), 'The H2AX Assay for Genotoxic and Nongenotoxic Agents: Comparison of H2AX Phosphorylation with Cell Death Response', *Toxicological Sciences* **140**(1), 103–117.
- Nishio, R., Tsuchiya, H., Yasui, T., Matsuura, S., Kanki, K., Kurimasa, A., Hisatome, I. and Shiota, G. (2011), 'Disrupted plasma membrane localization of equilibrative nucleoside transporter 2 in the chemoresistance of human pancreatic cells to gemcitabine (dFdCyd)', *Cancer Science* **102**(3), 622–629.
- Norouzi-Barough, L., Sarookhani, M. R., Sharifi, M., Moghbelinejad, S., Jangjoo, S. and Salehi, R. (2018), 'Molecular mechanisms of drug resistance in ovarian cancer', *Journal of Cellular Physiology* **233**(6), 4546–4562.
- Okon, A., Matos De Souza, M. R., Shah, R., Amorim, R., Da Costa, L. J. and Wagner, C. R. (2017), 'Anchimerically Activatable Antiviral ProTides', *ACS Medicinal Chemistry Letters* **8**(9), 958–962.
- Olaussen, K. A., Dunant, A., Fouret, P., Brambilla, E., André, F., Haddad, V., Taranchon, E., Filipits, M., Pirker, R., Popper, H. H., Stahel, R., Sabatier, L., Pignon, J.-P., Tursz, T., Le Chevalier, T. and Soria, J.-C. (2006), 'DNA Repair by ERCC1 in Non-Small-Cell Lung Cancer and Cisplatin-Based Adjuvant Chemotherapy', *The New England Journal of Medicine* **10**, 355.

- Oldenhuis, C. N. A. M., Oosting, S. F., Gietema, J. A. and De Vries, E. G. E. (2008), 'Prognostic versus predictive value of biomarkers in oncology', *European Journal of Cancer* **44**, 946–953.
- Olive, P. L. and Banáth, J. P. (2006), 'The comet assay: a method to measure DNA damage in individual cells', *NATURE PROTOCOLS* **1**(23).
- Olive, P. L., Wlodek, D. and Banáth, J. P. (1991), 'DNA Double-Strand Breaks Measured in Individual Cells Subjected to Gel Electrophoresis', *Cancer Research* **51**, 4671–4676.
- Olivier, R. I., Lubsen-Brandsma, M. A. C., Verhoef, S. and Van Beurden, M. (2005), 'CA125 and transvaginal ultrasound monitoring in high-risk women cannot prevent the diagnosis of advanced ovarian cancer', *Gynecologic Oncology* **100**, 20–26.
- Orellana, E. A. and Kasinski, A. L. (2016), 'Sulforhodamine B (SRB) Assay in Cell Culture to Investigate Cell Proliferation', *Biology protocol* .
- Ozols, R. F., Bundy, B. N., Greer, B. E., Fowler, J. M., Clarke-Pearson, D., Burger, R. A., Mannel, R. S., DeGeest, K., Hartenbach, E. M., Baergen, R. and Mackey, D. (2003), 'Phase III trial of carboplatin and paclitaxel compared with cisplatin and paclitaxel in patients with optimally resected stage III ovarian cancer: A Gynecologic Oncology Group study', *Journal of Clinical Oncology* **21**(17), 3194–3200.
- Peretz, L., Besser, E., Hajbi, R., Casden, N., Ziv, D., Kronenberg, N., Gigi, L. B., Sweetat, S., Khawaled, S., Aqeilan, R. and Oded Behar, . (2018), 'Combined shRNA over CRISPR/ cas9 as a methodology to detect off-target effects and a potential compensatory mechanism OPEN', *Scientific Reports* .
- Permeth-Wey, J. and Sellers, T. A. (2009), *Epidemiology of Ovarian Cancer*.
- Pfisterer, J., Plante, M., Vergote, I., Du Bois, A., Hirte, H., Lacave, A. J., Wagner, U., Stähle, A., Stuart, G., Kimmig, R., Olbricht, S., Le, T., Emerich, J., Kuhn, W., Bentley, J., Jackisch, C., Lück, H. J., Rochon, J., Zimmermann, A. H. and Eisenhauer, E. (2006), 'Gemcitabine plus carboplatin compared with carboplatin in patients with platinum-sensitive recurrent ovarian cancer: An intergroup trial of the AGO-OVAR, the NCIC CTG, and the EORTC GCG', *Journal of Clinical Oncology* **24**(29), 4699–4707.
- Piccart, M. J., Bertelsen, K., James, K., Cassidy, J., Mangioni, C., Simonsen, E., Stuart, G., Kaye, S., Vergote, I., Blom, R., Grimshaw, R., Atkinson, R. J., Swenerton, K. D., Trope, C., Nardi, M., Kaern, J., Tumolo, S., Timmers, P., Roy, J.-A., Lhoas, F., Lindvall, B., Bacon, M., Birt, A., Andersen, J. E., Zee, B., Paul, J., Baron, B. and Pecorelli, S. (2000), 'Randomized Intergroup Trial of Cisplatin-Paclitaxel Versus Cisplatin-Cyclophosphamide in Women With Advanced Epithelial Ovarian Cancer: Three-Year Results', *Journal of the National Cancer Institute* **92**(9).

- Piccart, M. J., Bertelsen, K., Stuart, G., Cassidy, J., Mangioni, C., Simonsen, E., James, K., Kaye, S., Vergote, I., Blom, R., Grimshaw, R., Atkinson, R., Swenerton, K., Trope, C., Nardi, M., Kaern, J., Tumolo, S., Timmers, P., Roy, J. A., Lhoas, F., Lidvall, B., Bacon, M., Birt, A., Andersen, J., Zee, B., Paul, J., Pecorelli, S., Baron, B. and McGuire, W. (2003), 'Long-term follow-up confirms a survival advantage of the paclitaxel-cisplatin regimen over the cyclophosphamide-cisplatin combination in advanced ovarian cancer', *International Journal of Gynecological Cancer* **13**(SUPPL. 2), 144–148.
- Piek, J. M., Van Diest, P. J., Zweemer, R. P., Jansen, J. W., Poort-Keesom, R. J., Menko, F. H., Gille, J. J., Jongsma, A. P., Pals, G., Kenemans, P. and Verheijen, R. H. (2001), 'Dysplastic changes in prophylactically removed Fallopian tubes of women predisposed to developing ovarian cancer', *Journal of Pathology* **195**(4), 451–456.
- Pignata, S., C Cecere, S., Du Bois, A., Harter, P. and Heitz, F. (2017), 'Treatment of recurrent ovarian cancer', *Annals of Oncology* **28**(suppl_8), viii51–viii56.
- Polley, M.-Y. C., Leung, S. C. Y., Mcshane, L. M., Gao, D., Hugh, J. C., Mastropasqua, M. G., Viale, G., Zabaglo, L. A., Penault-Llorca, F., Bartlett, J. M. S., Gown, A. M., Symmans, W. F., Piper, T., Mehl, E., Enos, R. A., Hayes, D. F., Dowsett, M., Nielsen, T. O. and Nielsen, T. (2013), 'An international Ki67 reproducibility Study', *Journal of the National Cancer Institute* **105**, 1897–1906.
- Pommier, Y. (2006), 'Topoisomerase I inhibitors: Camptothecins and beyond', *Nature Reviews Cancer* **6**(10), 789–802.
- Pourquier, P., Gioffre, C., Kohlhagen, G., Urasaki, Y., Goldwasser, F., Hertel, L. W., Yu, S., Pon, R. T., Gmeiner, W. H. and Pommier, Y. (2002), 'Gemcitabine (2',2'-difluoro-2'-deoxycytidine), an antimetabolite that poisons topoisomerase I.', *Clinical cancer research : an official journal of the American Association for Cancer Research* **8**(8), 2499–504.
- Prat, J. (2012), 'New insights into ovarian cancer pathology', *Annals of Oncology* **23**(SUPPL. 10).
- Pratt, S. E., Durland-Busbice, S., Shepard, R. L., Heinz-Taheny, K., Iversen, P. W. and Dantzig, A. H. (2013), 'Human carboxylesterase-2 hydrolyzes the prodrug of gemcitabine (LY2334737) and confers prodrug sensitivity to cancer cells.', *Clinical cancer research : an official journal of the American Association for Cancer Research* **19**(5), 1159–68.
- Prestayko, A. W., D'Aoust, J. C., Issell, B. F. and Crooke, S. T. (1979), 'Cisplatin (cis-diamminedichloroplatinum II)', *Cancer Treatment Reviews* **6**(1), 17–39.

- Rabik, C. A. and Dolan, M. E. (2007), ‘Molecular mechanisms of resistance and toxicity associated with platinating agents’, *Cancer Treatment Reviews* **33**(1), 9–23.
- Rajan, A., Carter, C. A., Kelly, R. J., Gutierrez, M., Kummar, S., Szabo, E., Yancey, M. A., Ji, J., Mannargudi, B., Woo, S., Spencer, S., Douglas Figg, W. and Giaccone, G. (2012), ‘A Phase I Combination Study of Olaparib with Cisplatin and Gemcitabine in Adults with Solid Tumors’.
- Rath, D., Amlinger, L., Rath, A. and Lundgren, M. (2015), ‘The CRISPR-Cas immune system: Biology, mechanisms and applications’, *Biochimie* **117**, 119–128.
- Redinbo, M. R. and Potter, P. M. (2005), ‘Mammalian carboxylesterases: From drug targets to protein therapeutics’, *Drug Discovery Today* **10**(5), 313–325.
- Reichman, B. S., Seidman, A. D., Crown, J. P., Heelan, R., Hakes, T. B., Lebwohl, D. E., Gilewski, T. A., Surbone, A., Currie, V., Hudis, C. A. and et al. (1993), ‘Paclitaxel and recombinant human granulocyte colony-stimulating factor as initial chemotherapy for metastatic breast cancer’, *J Clin Oncol* **11**(10), 1943–1951.
- Reid, B. M., Permuth, J. B. and Sellers, T. A. (2017), ‘Epidemiology of ovarian cancer: a review’, *Cancer Biology & Medicine* .
- Reis, A., Hornblower, B., Robb, B. and Tzertzinis, G. (2014), ‘CRISPR/Cas9 and Targeted Genome Editing: A New Era in Molecular Biology | NEB’.
- Requena, C. E., Erez-Moreno, G., Ruiz-Erez, L. M., Vidal, A. E. and Gon Alez-Pacanowska, D. (2014), ‘The NTP pyrophosphatase DCTPP1 contributes to the homeostasis and cleansing of the dNTP pool in human cells’, *Biochem. J* **459**, 171–180.
- Requena, C. E., Pérez-Moreno, G., Horváth, A., Vértessy, B. G., Ruiz-Pérez, L. M., González-Pacanowska, D. and Vidal, A. E. (2016), ‘The nucleotidohydrolases DCTPP1 and dUTPase are involved in the cellular response to decitabine’, *Biochem. J* **473**, 2635–2643.
- Ries, L., Harkins, D., Krapcho, M., Mariotto, A., Miller, B., Feuer, E., Clegg, L., Eisner, M., Horner, M., Howlader, N., Hayat, M., Hankey, B. and Edwards, B. (2006), SEER Cancer Statistics Review, 1975–2003, National Cancer Institute. Bethesda, MD, https://seer.cancer.gov/csr/1975_2003/, based on November 2005 SEER data submission, posted to the SEER web site, Technical report.
- Ritzel, M. W. L., Ng, A. M. L., Yao, S. Y. M., Graham, K., Loewen, S. K., Smith, K. M., Ritzel, R. G., Mowles, D. A., Carpenter, P., Chen, X. Z., Karpinski, E., Hyde, R. J., Baldwin, S. A., Cass, C. E. and Young, J. D. (2001), ‘Molecular Identification and Characterization of Novel Human and Mouse Concentrative Na⁺-Nucleoside Co-transporter Proteins (hCNT3 and mCNT3) Broadly Selective for Purine and Pyrimidine Nucleosides (System cib)’, *Journal of Biological Chemistry* **276**(4), 2914–2927.

- Romero, I. and Bast, R. C. (2012), 'Minireview: Human Ovarian Cancer: Biology, Current Management, and Paths to Personalizing Therapy', *Endocrinology* **153**(4), 1593–1602.
- Roscilli, G., De Vitis, C., Ferrara, F. F., Noto, A., Cherubini, E., Ricci, A., Mariotta, S., Giarnieri, E., Giovagnoli, M. R., Torrisi, M. R., Bergantino, F., Costantini, S., Fenizia, F., Lambiase, M., Aurisicchio, L., Normanno, N., Ciliberto, G. and Mancini, R. (2016), 'Human lung adenocarcinoma cell cultures derived from malignant pleural effusions as model system to predict patients chemosensitivity.', *Journal of translational medicine* **14**, 61.
- Rose, P. G. (2016), 'First-Line Chemotherapy for Ovarian Cancer: Inferences From Recent Studies', *The Oncologist* **21**(11), 1286–1290.
- Rose, P. G., Mossbrugger, K., Fusco, N., Smrekar, M., Eaton, S. and Rodriguez, M. (2003), 'Gemcitabine reverses cisplatin resistance: Demonstration of activity in platinum- and multidrug-resistant ovarian and peritoneal carcinoma', *Gynecologic Oncology* **88**(1), 17–21.
- Rossi, A., Kontarakis, Z., Gerri, C., Nolte, H., Hölper, S., Krüger, M. and Didier, and Stainier, Y R, v. . . d. . n. (2015), 'Genetic compensation induced by deleterious mutations but not gene knockdowns', *Nature* .
- Roy, R., Chun, J. and Powell, S. N. (n.d.), 'BRCA1 and BRCA2: different roles in a common pathway of genome protection HHS Public Access'.
- Rubin, S. C., Blackwood, M. A., Bandera, C., Behbakht, K., Benjamin, I., Rebbeck, T. R. and Boyd, J. (1998), 'BRCA1, BRCA2, and hereditary nonpolyposis colorectal cancer gene mutations in an unselected ovarian cancer population: Relationship to family history and implications for genetic testing', *Journal of Obstetrics and Gynaecology* **178**(4).
- Rudin, D., Li, L., Niu, N., Kalari, K. R., Gilbert, J. A., Ames, M. M. and Wang, L. (2011), 'Gemcitabine Cytotoxicity: Interaction of Efflux and Deamination.', *Journal of drug metabolism & toxicology* **2**(107), 1–10.
- Ruiz Van Haperen, V., Eriksson, S., Boven, E., Stegmann, A. P. A., Hermsen, M., Vermorken, J. B., Pinedo, H. M. and Peters, G. J. (1994), 'Development and Molecular Characterization of a 2', 2'-difluorodeoxycytidine I This study was supported by the ICRET1 @ from the', *Cancer research* **54**, 4138–4143.
- Russo, A., Calò, V., Bruno, L., Rizzo, S., Bazan, V. and Fede, G. D. (2009), 'Hereditary ovarian cancer', *Critical Reviews in Oncology/Hematology* **69**, 28–44.

- Saboulard, D., Naesens, L., Cahard, D., Salgado, A., Pathirana, R., Velazquez, S., McGuigan, C., De Clercq, E. and Balzarini, J. (1999), 'Characterization of the activation pathway of phosphoramidate triester prodrugs of stavudine and zidovudine.', *Molecular Pharmacology* **56**(4), 693–704.
- Saiki, Y., Yoshino, Y., Fujimura, H., Manabe, T., Kudo, Y., Shimada, M., Mano, N., Nakano, T., Lee, Y., Shimizu, S., Oba, S., Fujiwara, S., Shimizu, H., Chen, N., Nezhad, Z. K., Jin, G., Fukushige, S., Sunamura, M., Ishida, M., Motoi, F., Egawa, S., Unno, M. and Horii, A. (2012), 'DCK is frequently inactivated in acquired gemcitabine-resistant human cancer cells', *Biochemical and Biophysical Research Communications* **421**, 98–104.
- Sakai, W., Swisher, E. M., Jacquemont, C., Chandramohan, K. V., Couch, F. J., Langdon, S. P., Wurz, K., Higgins, J., Villegas, E. and Taniguchi, T. (2009), 'Functional restoration of BRCA2 protein by secondary BRCA2 mutations in BRCA2-mutated ovarian carcinoma', *Cancer Research* **69**(16), 6381–6386.
- Sakai, W., Swisher, E. M., Karlan, B. Y., Agarwal, M. K., Higgins, J., Friedman, C., Villegas, E., Jacquemont, C., Farrugia, D. J., Couch, F. J., Urban, N. and Taniguchi, T. (2008), 'Secondary mutations as a mechanism of cisplatin resistance in BRCA2-mutated cancers', *Nature* **451**(7182), 1116–1120.
- Sanjana, N. E., Shalem, O. and Zhang, F. (2014), 'Improved vectors and genome-wide libraries for CRISPR screening HHS Public Access Supplementary Material', *Nat Methods* **11**(8), 783–784.
- Sarosy, G., Kohn, E., Stone, D. A., Rothenberg, M. L., Jacob, J., Adamo, D. O., Ognibene, F. P., Cunnion, R. E. and Reed, E. (1992), 'Phase I study of taxol and granulocyte colony-stimulating factor in patients with refractory ovarian cancer.', *J. Clin. Oncol.* **10**(7), 1165–70.
- Sarr, A., Bré, J., Mullen, P., Blagden, S., Um, I. H., Harrison, D. J. and Reynolds, P. A. (2018), Genome-wide CRISPR / Cas9 screen identifies factors required for sensitivity to pyrimidine nucleotide analogs, *in* 'American Association for Cancer Research Annual Meeting', Chicago.
- Schiller, J. H., Harrington, D., Belani, C. P., Langer, C., Sandler, A., Krook, J., Zhu, J. and Johnson, D. H. (2002), 'Comparison of four chemotherapy regimens for advanced non-small-cell lung cancer', *The New England Journal of Medicine* **346**(2).
- Schulz, M., Lahmann, P. H., Riboli, E. and Boeing, H. (2004), 'Dietary Determinants of Epithelial Ovarian Cancer: A Review of the Epidemiologic Literature', *Nutrition and Cancer* **50**(2), 120–140.
- Sebastiani, V., Ricci, F., Rubio-Viquiera, B., Kulesza, P., Yeo, C. J., Hidalgo, M., Klein, A., Laheru, D. and Iacobuzio-Donahue, C. A. (2006), 'Immunohistochemical

- and Genetic Evaluation of Deoxycytidine Kinase in Pancreatic Cancer: Relationship to Molecular Mechanisms of Gemcitabine Resistance and Survival', *Clin Cancer Res* **12**(8), 2492–2497.
- Shah, R., Maize, K. M., Zhou, X., Finzel, B. C. and Wagner, C. R. (2017), 'Caught before Released: Structural Mapping of the Reaction Trajectory for the Sofosbuvir Activating Enzyme, Human Histidine Triad Nucleotide Binding Protein 1 (hHint1)', *Biochemistry* **56**, 35593570.
- Shalem, O., Sanjana, N. E., Hartenian, E., Shi, X., Scott, D. A., Heckl, D., Ebert, B. L., Root, D. E. and Doench, J. G. (2014), 'Genome - scale CRISPR - Cas9 knockout screening in human cells', *Science* **343**(6166), 84–87.
- Shanks, N., Greek, R. and Greek, J. (2009), 'Are animal models predictive for humans?', *Philosophy, Ethics, and Humanities in Medicine* .
- Sharma, S. and Petsalaki, E. (2018), 'Molecular Sciences Application of CRISPR-Cas9 Based Genome-Wide Screening Approaches to Study Cellular Signalling Mechanisms', *International Journal of Molecular Sciences* **19**.
- Shaw, T. J., Senterman, M. K., Dawson, K., Crane, C. A. and Vanderhyden, B. C. (2004), 'Characterization of intraperitoneal, orthotopic, and metastatic xenograft models of human ovarian cancer', *Molecular Therapy* **10**(6), 1032–1042.
- Shih, I.-M. and Kurman, R. J. (2004), 'Ovarian tumorigenesis: a proposed model based on morphological and molecular genetic analysis.', *The American journal of pathology* **164**(5), 1511–1518.
- Shord, S. S. and Patel, S. R. (2009), 'Paclitaxel alters the expression and specific activity of deoxycytidine kinase and cytidine deaminase in non-small cell lung cancer cell lines', *Journal of Experimental & Clinical Cancer Research* **28**(28).
- Shukla, S., Purohit, V., Mehla, K., Gunda, V., Chaika, N., Vernucci, E., King, R. J., Abrego, J., Goode, G. D., Dasgupt, A., Illies, A. L., Gebregiworgis, Teklab Bingbing, D., Augustine, J. J., Murthy, D., Attri, K. S., Mashadova, O., Grandgenett, P. M., Powers, R., Ly, Q. P., Lazenby, A. J., Grem, J. L., Yu, F., Matés, J. M., Asara, J. M., Kim, J.-w., Hankins, J. H., Weekes, C., Hollingsworth, M. A., Sarkova, N. J., Sasson, A. R., Fleming, J. B., Oliveto, J. M., Lyssiotis, C. A., Cantley, L. C., Berim, L. and Singh, P. K. (2017), 'MUC1 and HIF-1 α Signaling Crosstalk Induces Anabolic Glucose Metabolism to Impart Gemcitabine Resistance to Pancreatic Cancer', *Cancer cell* **32**(1), 71–87.
- Siddik, Z. H. (2003), 'Cisplatin: mode of cytotoxic action and molecular basis of resistance.', *Oncogene* **22**(47), 7265–79.

- Singer, G., Iii, R. O., Cohen, Y., Wang, B. G., Sidransky, D., Kurman, R. J. and Shih, I.-M. (2003), 'Mutations in BRAF and KRAS Characterize the Development of Low-Grade Ovarian Serous Carcinoma', *Journal of the National Cancer Institute* **95**(6).
- Singer, G., Kurman, R. J., Chang, H.-W., Cho, S. K. R. and Shih, M. (2002), 'Diverse Tumorigenic Pathways in Ovarian Serous Carcinoma', *American Journal of Pathology* **160**(4).
- Skehan, P., Storeng, R., Scudiero, D., Monks, A., McMahon, J., Vistica, D., Warren, J. T., Bokesch, H., Kenney, S. and Boyd, M. R. (1990), 'New Colorimetric Cytotoxicity Assay for Anticancer-Drug Screening', *Journal of the National Cancer Institute* **82**, 1107–1112.
- Slusarczyk, M., Ferla, S., Brancale, A. and Mcguigan, C. (2018), 'Synthesis and biological evaluation of 6-substituted-5-fluorouridine ProTides', *Bioorganic & Medicinal Chemistry Letters* **26**, 551–565.
- Slusarczyk, M., Lopez, M. H., Balzarini, J., Mason, M., Jiang, W. G., Blagden, S., Thompson, E., Ghazaly, E. and McGuigan, C. (2014), 'Application of ProTide technology to gemcitabine: A successful approach to overcome the key cancer resistance mechanisms leads to a new agent (NUC-1031) in clinical development', *Journal of Medicinal Chemistry* **57**(4), 1531–1542.
- Smith, S. C., Petrova, A. V., Madden, M. Z., Wang, H., Pan, Y., Warren, M. D., Hardy, C. W., Liang, D., Liu, E. A., Robinson, M. H., Rudra, S., Wang, J., Ehdaivand, S., Torres, M. A., Wang, Y. and Yu, D. S. (2014), 'A gemcitabine sensitivity screen identifies a role for NEK9 in the replication stress response', *Nucleic Acids Research* **42**(18), 11517–11527.
- Spasokoukotskaja, T., Arnér, E. S., Brosjö, O., Gunvén, P., Juliusson, G., Liliemark, J. and Eriksson, S. (1995), 'Expression of deoxycytidine kinase and phosphorylation of 2-chlorodeoxyadenosine in human normal and tumour cells and tissues', *European Journal of Cancer* **31**(2), 202–208.
- Spratlin, J., Sangha, R., Glubrecht, D., Dabbagh, L., Young, J. D., Dumontet, C., Cass, C., Lai, R. and Mackey, J. R. (2004), 'The Absence of Human Equilibrative Nucleoside Transporter 1 Is Associated with Reduced Survival in Patients With Gemcitabine-Treated Pancreas Adenocarcinoma', *Clinical Cancer Research* **10**(780), 6956–6961.
- Spratlin, J. and Sawyer, M. B. (2007), 'Pharmacogenetics of paclitaxel metabolism', *Critical Reviews in Oncology/Hematology* **61**, 222–229.
- Staub, M. and Eriksson, S. (2006), 'The role of deoxycytidine kinase in DNA synthesis and nucleoside analog activation', *Cancer Drug Discovery and Development: Deoxynucleoside Analogs in Cancer Therapy*, pp. 29–52.

- Stefanou, D. T., Bamias, A., Episkopou, H., Kyrtopoulos, S. A., Likka, M., Kalampokas, T., Photiou, S., Gavalas, N., Sfikakis, P. P., Dimopoulos, M. A. and Souliotis, V. L. (2015), ‘Aberrant dna damage response pathways may predict the outcome of platinum chemotherapy in ovarian cancer’, *PLoS ONE* **10**(2), 1–19.
- Strese, S., Fryknäs, M., Larsson, R. and Gullbo, J. (2013), Effects of hypoxia on human cancer cell line chemosensitivity, Technical report.
- Sun, J., Wei, Q., Zhou, Y., Wang, J., Liu, Q. and Xu, H. (2017), ‘A systematic analysis of FDA-approved anticancer drugs’, *BMC Systems Biology* **11**.
- Swisher, E. M., Sakai, W., Karlan, B. Y., Wurz, K., Urban, N. and Taniguchi, T. (2008), ‘Secondary BRCA1 mutations in BRCA1-mutated ovarian carcinomas with platinum resistance’, *Cancer Research* **68**(8), 2581–2586.
- Takasaki, K., Miyamoto, M., Takano, M., Soyama, H., Aoyama, T., Matsuura, H., Kato, K., Sakamoto, T., Kuwahara, M., Iwahashi, H., Ishibashi, H., Yoshikawa, T. and Furuya, K. (2018), ‘Addition of bevacizumab to gemcitabine for platinum-resistant recurrent ovarian cancer: a retrospective analysis’, *Cancer Chemotherapy and Pharmacology* **81**, 809–814.
- Tang, Y., Wang, Y. and Teng, X. (2013), ‘Sequence-dependent effect of gemcitabine and cisplatin on A549 non-small-cell lung cancer cells’, *Molecular Medicine Reports* **8**(1), 221–226.
- Taylor-Harding, B., Orsulic, S., Karlan, B. Y. and Li, A. J. (2010), ‘Fluvastatin and cisplatin demonstrate synergistic cytotoxicity in epithelial ovarian cancer cells’, *Gynecologic Oncology* **119**(3), 549–556.
- The Cancer Genome Atlas Research, T. (2011), ‘Integrated genomic analyses of ovarian carcinoma.’, *Nature* **474**(7353), 609–15.
- Theodossiou, C., Cook, J. A., Fisher, J., Teague, D., Liebmann, J. E., Russo, A. and Mitchell, J. B. (1998), ‘Interaction of gemcitabine with paclitaxel and cisplatin in human tumor cell lines’, *International Journal of Oncology* **12**(4), 825–832.
- Torre, L. A., Trabert, B., DeSantis, C. E., Miller, K. D., Samimi, G., Runowicz, C. D., Gaudet, M. M., Jemal, A. and Siegel, R. L. (2018), ‘Ovarian cancer statistics, 2018’, *CA: A Cancer Journal for Clinicians* pp. 284–296.
- Toyooka, T., Ishihama, M. and Ibuki, Y. (2011), ‘Phosphorylation of Histone H2AX Is a Powerful Tool for Detecting Chemical Photogenotoxicity’, *Journal of Investigative Dermatology* **131**, 1313–1321.
- Tuntland, T., Ethell, B., Kosaka, T., Blasco, F., Zang, R. X., Jain, M., Gould, T., Hoffmaster, K., Macchiarulo, A., Mukhopadhyay, B. and Johnson, J. . (2014), ‘Implementation of pharmacokinetic and pharmacodynamic strategies in early research

- phases of drug discovery and development at Novartis Institute of Biomedical Research', *Frontiers in Pharmacology* .
- Tzelepis, K., Koike-Yusa, H., De Braekeleer, E., Li, Y., Metzakopian, E., Dovey, O. M., Mupo, A., Grinkevich, V., Li, M., Mazan, M., Gozdecka, M., Ohnishi, S., Cooper, J., Patel, M., McKerrell, T., Chen, B., Domingues, A. F., Gallipoli, P., Teichmann, S., Ponstingl, H., McDermott, U., Saez-Rodriguez, J., Huntly, B. J., Iorio, F., Pina, C., Vassiliou, G. S. and Yusa, K. (2016), 'A CRISPR Dropout Screen Identifies Genetic Vulnerabilities and Therapeutic Targets in Acute Myeloid Leukemia', *Cell Reports* **17**(4), 1193–1205.
- Ulker, M., Duman, B. B., Sahin, B. and Gumurdulu, D. (2015), 'ERCC1 and RRM1 as a predictive parameter for non-small cell lung, ovarian or pancreas cancer treated with cisplatin and/or gemcitabine', *Współczesna Onkologia* **3**, 207–213.
- Varga, Z., Diebold, J., Dommann-Scherrer, C., Frick, H., Kaup, D., Noske, A., Obermann, E., Ohlschlegel, C., Padberg, B., Rakozy, C., Oliver, S. S., Schobinger-Clement, S., Schreiber-Facklam, H., Singer, G., Tapia, C., Wagner, U., Mastropasqua, M. G., Viale, G. and Lehr, H.-A. (2012), 'How Reliable Is Ki-67 Immunohistochemistry in Grade 2 Breast Carcinomas? A QA Study of the Swiss Working Group of Breast-and Gynecopathologists', *PLoS ONE* **7**(5).
- Veltkamp, S. A., Plum, D., Van Tellingen, O., Beijnen, J. H. and Schellens, J. H. M. (2008), 'Extensive Metabolism and Hepatic Accumulation of Gemcitabine After Multiple Oral and Intravenous Administration in Mice', *Drug Metabolism and Disposition* **36**(8), 1606–1615.
- Vichai, V. and Kirtikara, K. (2006), 'Sulforhodamine B colorimetric assay for cytotoxicity screening', *Nature Protocols* **1**(3), 1112–1116.
- Walsh, T., Casadei, S., Lee, M. K., Pennil, C. C., Nord, A. S., Thornton, A. M., Roeb, W., Agnew, K. J., Stray, S. M., Wickramanayake, A., Norquist, B., Pennington, K. P., Garcia, R. L., King, M.-C. and Swisher, E. M. (2011), 'Mutations in 12 genes for inherited ovarian, fallopian tube, and peritoneal carcinoma identified by massively parallel sequencing', *Proceedings of the National Academy of Sciences* **108**(44).
- Walsh, V. and Goodman, J. (1999), 'Cancer chemotherapy, biodiversity, public and private property: the case of the anti-cancer drug Taxol', *Social Science and Medicine* **49**, 1215–1225.
- Walsh, V. and Goodman, J. (2002), 'From taxol to taxol®: The changing identities and ownership of an anti-cancer drug', *Medical Anthropology* **21**, 307–336.
- Wang, L., Zhang, Y., Li, H., Xu, Z., Santella, R. M. and Weinstein, I. B. (2007), 'Hint1 Inhibits Growth and Activator Protein-1 Activity in Human Colon Cancer Cells', *Cancer Research* **67**(10), 4700–4708.

- Wani, M. C., Taylor, H. L., Wall, M. E., Coggon, P. and McPhail, A. T. (1971), 'Plant Antitumor Agents. VI. The Isolation and Structure of Taxol, a Novel Antileukemic and Antitumor Agent from *Taxus brevifolia*', *Journal of the American Chemical Society* **93**(9), 2325–2327.
- Weberpals, J., Garbuio, K., O'Brien, A., Clark-Knewks, K., Doucette, S., Antoniouk, O., Gess, G. and Dimitreulakos, J. (2009), 'The DNA repair proteins BECA1 and EEECC1 as predictive markers In sporadic ovarian cancer', *International Journal of Cancer* **124**(4), 806–815.
- Weil, M. K. and Chen, A. (2012), 'PARP Inhibitor Treatment in Ovarian and Breast Cancer', *Current Problems in Cancer* **35**(1), 7–50.
- Whittemore, A. S., Harris, R., Itnyre, J. and Halpern, J. (1992), 'Characteristics relating to ovarian cancer risk: collaborative analysis of 12 US case-control studies. I. Methods. Collaborative Ovarian Cancer Group', *Am J Epidemiol* **136**(10), 1175–1183.
- Wilkening, S., Chen, B., Bermejo, L. and Canzian, F. (2009), 'Is there still a need for candidate gene approaches in the era of genome-wide association studies?'
- Wong, C. C., Cheng, K.-W. and Rigas, B. (2012), 'Preclinical Predictors of Anticancer Drug Efficacy: Critical Assessment with Emphasis on Whether Nanomolar Potency Should Be Required of Candidate Agents', *Journal of Pharmacology and Experimental Therapeutics* **341**, 572–578.
- Wong, K.-K., Tsang, Y. T. M., Deavers, M. T., Mok, S. C., Zu, Z., Sun, C., Malpica, A., Wolf, J. K., Lu, K. H. and Gershenson, D. M. (2010), 'BRAF Mutation Is Rare in Advanced-Stage Low-Grade Ovarian Serous Carcinomas', *Am J Pathol* **177**, 1611–1617.
- Yin, B. W. T. and Lloyd, K. O. (2001), 'Molecular cloning of the CA125 ovarian cancer antigen: Identification as a new mucin, MUC16', *Journal of Biological Chemistry* **276**(29), 27371–27375.
- Zanellato, I., Boidi, C. D., Lingua, G., Betta, P.-G., Orecchia, S., Monti, E. and Osella, D. (2011), 'In vitro anti-mesothelioma activity of cisplatin-gemcitabine combinations: evidence for sequence-dependent eVects', *Cancer Chemother Pharmacol* **67**, 265–273.
- Zhan, T., Rindtorff, N., Betge, J., Ebert, M. P. and Boutros, M. (2018), 'CRISPR/Cas9 for cancer research and therapy'.
- Zhang, S., Royer, R., Li, S., Mclaughlin, J. R., Rosen, B., Risch, H. A., Fan, I., Bradley, L., Shaw, P. A. and Narod, S. A. (2011), 'Frequencies of BRCA1 and BRCA2 mutations among 1,342 unselected patients with invasive ovarian cancer', *Gynecologic Oncology* **121**, 353–357.

- Zhang, Y.-J., Wu, H.-C., Shen, J., Li, H., Wang, L., Yu, M.-W., Lee, P.-H., Weinstein, I. B. and Santella, R. M. (2009), 'Silencing of Hint1, a novel tumor suppressor gene, by promoter hypermethylation in hepatocellular carcinoma', *Cancer Letters* **275**(2), 277–284.
- Zhang, Y., Ye, W. Y., Wang, J. Q., Wang, S. J., Ji, P., Zhou, G. Y., Zhao, G. P., Ge, H. L. and Wang, Y. (2013), 'dCTP pyrophosphohydrolase exhibits nucleic acid accumulation in multiple carcinomas', *European Journal of Histochemistry* **57**(29).
- Zhong, Z., Yu, H., Wang, S., Wang, Y. and Cui, L. (2018), 'Anti-cancer effects of Rhizoma Curcumae against doxorubicin-resistant breast cancer cells', *Chinese Medicine* **13**, 44.